

Promoters: Prof. Dr. Sarah BAATOUT

Radiobiology Unit,
Molecular and Cellular Expert Group,
Institute for Environment, Health and Safety
Belgian Nuclear Research Center (SCK•CEN)

& Department of Molecular Biotechnology
Faculty of Bioscience Engineering
Ghent University

Em. Prof. Dr. Patrick VAN OOSTVELDT

Department of Molecular Biotechnology
Faculty of Bioscience Engineering
Ghent University

Co-promoter: Dr. Ir. An AERTS

Radiobiology Unit,
Molecular and Cellular Expert Group,
Institute for Environment, Health and Safety
Belgian Nuclear Research Center (SCK•CEN)

Mentor: Dr. Mohammed Abderrafi BENOTMANE

Radiobiology Unit,
Molecular and Cellular Expert Group,
Institute for Environment, Health and Safety
Belgian Nuclear Research Center (SCK•CEN)

Dean: Prof. Dr. Ir. Guido VAN HUYLENBROECK

Rector: Prof. Dr. Anne DE PAEPE



The vascular endothelial cell response following exposure to low doses of ionizing radiation

Charlotte Rombouts

Thesis submitted in fulfillment of the requirements for the degree of Doctor (PhD) in Applied
Biological Sciences: cell and gene biotechnology

"The vascular endothelial cell response following exposure to low doses of ionizing radiation"

"Respons van vasculaire endotheelcellen na blootstelling aan lage dosissen ioniserende straling"

Rombouts Charlotte (2014). The vascular endothelial cell response following exposure to low doses of ionizing radiation. PhD thesis. Ghent University (Ghent, Belgium).

ISBN: 978-90-5989-692-5

The author and the promoters give the authorization to consult and to copy parts of this work for personal use only. Any other use is limited by the Laws of Copyright. Permission to reproduce any material contained in this work should be obtained from the author.

Members of the Examination Committee

Prof. Dr. Sarah Baatout (promoter)

Radiobiology Unit, Molecular and Cellular Expert Group, Institute for Environment, Health and Safety, Belgian Nuclear Research Center (SCK•CEN)

Department of Molecular Biotechnology, Faculty of Bioscience Engineering, Ghent University

Em. Prof. Dr. Patrick Van Oostveldt (promoter)

Department of Molecular Biotechnology, Faculty of Bioscience Engineering, Ghent University

Dr. Ir. An Aerts (co-promoter)

Radiobiology Unit, Molecular and Cellular Expert Group, Institute for Environment, Health and Safety, Belgian Nuclear Research Center (SCK•CEN)

Prof. Dr. Ir. Pascal Boeckx (chairman)

Department of Applied Analytical and Physical Chemistry · Isotope Bioscience Laboratory, Faculty of Bioscience Engineering, Ghent University

Prof. Dr. Ir. Tom Van de Wiele (secretary)

Biochemical and Microbial Technology, Faculty of Bioscience Engineering, Ghent University

Prof. Dr. Ir. Sofie Bekaert

Clinical Research Center, Faculty of Medicine and Health Sciences, Ghent University

Prof. Dr. Evelyne Meyer

Department of Pharmacology, Toxicology and Biochemistry, Faculty of Veterinary Medicine, Ghent University

Prof. Dr. Ir. Tim De Meyer

Department of Mathematical Modelling, Statistics and Bio-informatics, Faculty of Bioscience Engineering, Ghent University

Prof. Dr. Ir. Winnok De Vos

Department of Molecular Biotechnology, Faculty of Bioscience Engineering, Ghent University

Prof. Dr. Luc Leybaert

Department of Basic Medical Sciences, Faculty of Medicine and Health Sciences, Ghent University

Prof. Dr. Jan Philippé

Department of Clinical Chemistry, Microbiology and Immunology, Faculty of Medicine and Health Sciences, Ghent University

Prof. Dr. Dietrich Averbeck

Institut de Radioprotection et de Sûreté Nucléaire, IRSN-DRH/PRP-HOM (France)

Table of contents

Table of contents	vii
List of figures	xii
List of tables	xiv
List of abbreviations	xv
Chapter 1: General introduction	1
1.1 Radiation protection: coming to a justified and optimized use of ionizing radiation.	3
1.1.1 What is ionizing radiation?	3
1.1.2 The notion of dose	3
1.1.3 Brief history of radiation protection	4
1.1.4 The current issue of low doses in radiation protection	7
1.1.4.1 Use of the LNT model for radiation protection purposes.....	7
1.1.4.2 Radiobiological findings that question the LNT model.....	9
1.1.4.3 Non-cancer disease risks and radiation protection	11
1.2 Cardiovascular disease risk related to low doses of ionizing radiation.....	13
1.2.1 Recognition of radiation-related cardiovascular disease risk	13
1.2.2 Low dose exposed epidemiological cohorts	14
1.2.2.1 Classification of cardiovascular diseases in epidemiology	14
1.2.2.2 Survivors of the atomic bombings of Hiroshima and Nagasaki	14
1.2.2.3 Occupational exposure	17
1.2.2.4 Meta-analysis	18
1.2.3 Epidemiology alone is not the answer	19
1.2.4 Societal concern	20
1.3 Clinical manifestation and pathology of radiation-induced cardiovascular diseases	23
1.3.1 Overview.....	23
1.3.2 Pericarditis.....	24

1.3.3	Coronary artery disease	24
1.3.4	Congestive heart failure	27
1.3.5	Hypotheses for underlying molecular and cellular mechanisms	28
1.3.5.1	The role of inflammation	30
1.3.5.2	What about low doses?	30
1.4	Endothelium as a critical target in radiation-related cardiovascular disease	32
1.4.1	Endothelium is the safeguard of normal vascular functioning	32
1.4.2	Endothelial dysfunction: molecular and cellular mechanisms	33
1.4.2.1	Decreased NO bioavailability	34
1.4.2.2	Premature senescence.....	35
1.4.2.3	Mitochondrial dysfunction.....	37
1.4.3	<i>In vitro</i> endothelial models	38
1.4.4	The effect of ionizing radiation on the endothelium	40
1.4.4.1	DNA-targeted effects	40
1.4.4.2	Radiation-induced mitochondrial dysfunction	41
1.4.4.3	Radiation-induced premature senescence	42
1.4.5	High throughput transcriptomic profiling.....	43
1.4.5.1	Microarray data analysis.....	44
Chapter 2:	Thesis aims	45
Chapter 3:	Differential response to acute low dose radiation in primary and immortalized endothelial cells	49
3.1	Abstract.....	51
3.2	Introduction.....	52
3.3	Material and methods	55
3.3.1	Cell culture and irradiation.....	55
3.3.2	Immunocytochemistry for phosphorylated H2AX histone (γ -H2AX) analysis ...	55

3.3.3	Automated fluorescence microscopy and image analysis.....	56
3.3.4	Cell cycle analysis	57
3.3.5	Annexin-V/PI costaining for apoptosis analysis	57
3.3.6	Cytospin and May-Grünwald Giemsa staining for determination of cell morphology	57
3.3.7	Statistical analysis.....	58
3.4	Results.....	59
3.4.1	Acute low dose X-irradiation causes DNA damage in HUVEC and EA.hy926 cells	59
3.4.2	Acute X-irradiation induces cell cycle arrest in HUVEC and EA.hy926 cells.....	63
3.4.3	Acute low dose X-irradiation induces apoptosis in HUVEC and EA.hy926 cells	64
3.4.4	Acute X-irradiation induces morphological changes in HUVEC and EA.hy926 cells	66
3.5	Discussion	68
3.6	Conclusion	73
3.7	Acknowledgements	73
Chapter 4:	Oxidative stress and mitochondrial DNA damage in endothelial cells following acute low dose radiation exposure.....	76
4.1	Abstract.....	78
4.2	Introduction	79
4.3	Material and methods	82
4.3.1	Cell culture and irradiation.....	82
4.3.2	Fluorometric CM-H ₂ DCFDA assay for measurement of intracellular ROS levels	82
4.3.3	DNA extraction	83
4.3.4	PCR detection of the CD	83
4.4	Results.....	86
4.4.1	Intracellular ROS levels.....	86

4.4.2	Mitochondrial DNA damage.....	87
4.5	Discussion	89
4.5.1	CM-H ₂ DCFDA assay for the measurement of intracellular ROS levels	89
4.5.2	PCR for the assessment of the CD, a marker for mtDNA damage	91
4.6	Conclusion and perspectives	93
Chapter 5: Transcriptomic profiling suggests a role for IGFBP5 in premature senescence of human umbilical vein endothelial cells (HUVEC) after chronic low dose rate irradiation		95
5.1	Abstract.....	97
5.2	Introduction.....	98
5.3	Materials and methods.....	102
5.3.1	Cell culture conditions.....	102
5.3.2	Chronic gamma radiation exposure	102
5.3.3	RNA extraction	102
5.3.4	Microarray assay	103
5.3.5	Microarray data analysis	103
5.3.6	Principal component analysis (PCA).....	104
5.3.7	Analysis of senescence-related differential gene expression	106
5.3.8	Gene Set Enrichment Analysis (GSEA).....	106
5.3.9	Quantitative real-time PCR validation.....	107
5.4	Results.....	108
5.4.1	Chronic LDR radiation-induced differential gene expression in HUVEC	108
5.4.2	GSEA and Enrichment Map	110
5.4.3	Senescence-related differential gene expression in HUVEC.....	120
5.5	Discussion	124
5.5.1	One week of chronic LDR radiation exposure induces an early stress response	

5.5.2	The stress response disappears after three and six weeks of chronic LDR radiation exposure	126
5.5.3	Development of an inflammation-related profile starts after three weeks of exposure to 4.1 mGy/h.....	127
5.5.4	Early stress response leads to premature senescence, associated with inflammation, after six weeks of exposure to 4.1 mGy/h.....	128
5.5.5	Candidate genes involved in radiation-induced premature senescence following exposure to 4.1 mGy/h.....	130
5.5.6	Remarks on the study.....	133
5.6	Conclusion	135
5.7	Acknowledgments	136
Chapter 6:	General discussion and perspectives	137
Summary	153
Samenvatting	159
References	165
Acknowledgments	191
Curriculum Vitae	197

List of figures

Figure 1: Schematic representation of different possible extrapolations to estimate radiation risks of cancer down to very low doses (< 100 mSv)	9
Figure 2: Radiation dose-response relationship (ERR/Gy) in the LSS cohort for death from stroke (left panel) and death from heart disease (right panel), showing linear-quadratic and linear functions.....	16
Figure 3: Average annual effective dose per person received in 1980 (left panel) and 2006 (right panel) in the United States.....	21
Figure 4: Overview of the heart anatomy.....	24
Figure 5: Schematic overview of the development of an atherosclerotic lesion	26
Figure 6: Overview of the major steps in the pathogenesis of coronary artery disease on the local and systemic level.....	30
Figure 7: A theoretical overview of how radiation-induced macrovascular and microvascular pathologies can interact to cause myocardial ischemia, which may ultimately develop into clinical heart disease	30
Figure 8: Overview of the major physiological functions of the arterial endothelium.	33
Figure 9: Electron structures of common ROS. Below each structure, its name and chemical formula are given	35
Figure 10: Simplified overview of two major senescence-inducing molecular pathways, the p53 and the p16-pRB pathway.....	37
Figure 11: Schematic overview of the human mitochondrial genome	39
Figure 12: Detection of DSB by immunostaining of γ -H2AX spots followed by fluorescence microscopy	61
Figure 13: Quantification of γ -H2AX spot number.....	62
Figure 14: Quantification of γ -H2AX spot occupancy	63
Figure 15: Dissapearance of γ -H2AX spot number over time.....	64
Figure 16: Cell cycle distribution assessed by PI staining and flow cytometry.....	65
Figure 17: Apoptosis assessed by the Annexin-V/PI assay and flow cytometry.....	67
Figure 18: Morphological analysis of HUVEC and EA.hy926 cells.....	68
Figure 19: Overview of the CM-H ₂ DCFDA assay	84
Figure 20: Schematic representation of mtDNA that consists of 16 569 bp	85

Figure 21: Intracellular ROS levels measured in EA.hy926 cells and HUVEC using the CM-H ₂ DCFDA assay..	87
Figure 22: Electrophoresis gels of PCR products obtained after amplification with primer pair F1/R1 for control (lanes 1-3), 0.1 Gy (lanes 4-6), 5 Gy (lanes 7-9) and H ₂ O ₂ treated samples (lanes 10-12) from EA.hy926 cells.....	88
Figure 23: Electrophoresis gels of PCR products obtained after amplification with primers pairs F2/R2, F3/R3 and F4/R4	89
Figure 24: Chronic γ -radiation (¹³⁷ Cs) of HUVEC.....	101
Figure 25: Bar chart of the sources of variation, after batch removal, which gives an overview of the relative contribution of each factor in the 5-way ANOVA.....	104
Figure 26: PCA plots which give a visualization of the variation in intensity values across the probesets on the whole chip (genome) between the different samples	106
Figure 27: Venn diagrams representing differentially expressed genes (including non-annotated genes) with a p-value < 0.05 and a FC > 1.5	110
Figure 28: Enrichment Maps for HUVECs exposed to 1.4 mGy/h (A, B, C) and 4.1 mGy/h (D, E, F) at week 1, 3 and 6 based on GSEA results using GO BP.....	121
Figure 29: Venn diagram representing differentially expressed genes (including non-annotated genes) between week six and week one for 4.1 mGy/h and control with an unadjusted p-value < 0.001.....	122
Figure 30: Comparison of Affymetrix Human 1.0 ST arrays data (A) to quantitative real-time PCR (B) for IGFBP5.....	123
Figure 31: Schematic overview of the possible role of IGFBP5 in radiation-induced premature senescence.	134

List of tables

Table 1: Overview of typical ionizing radiation doses in cardiac imaging procedures.....	22
Table 2: Morphological analysis of HUVEC and EA.hy926 cells.	69
Table 3: Overview of primer oligonucleotide sequences used for the assessment of mtDNA damage.....	85
Table 4: Overview of the PCR programs used for the assessment of mtDNA damage.	86
Table 5: Differentially expressed annotated genes with a p-value < 0.05 and a FC > 1.5..	111
Table 6: Overview of up- and down-regulated pathways in irradiated HUVEC (1.4 and 4.1 mGy/h) compared to control conditions, defined by GSEA using Kegg PATHWAY as a gene set database, and with an FDR-value < 0.05.....	114
Table 7: Differentially expressed ($p < 0.001$; $ FC > 2$) annotated genes between week six and week one specific for irradiated cells (4.1 mGy/h).	122
Table 8: Gene list created based on the genes that were differentially expressed between week six and week one with a p-value < 0.001 and that were in common between control and irradiated (4.1 mGy/h) HUVEC..	122
Table 9: Top-10 genes of which the expression profile was most similar to that of IGFBP5..	124

List of abbreviations

Numbers and symbols

8-oxo-dG	8-oxo-7,8-dihydro-2-deoxyguanosine
γ -H2AX	phosphorylated H2AX histone

A

ABI3BP	ABI Family, Member 3 (NESH) Binding Protein
ACOT7	acyl-CoA thioesterase 7
ADP	adenosine-diphosphate
AHS	Adult Health Study
ALARA	as low as reasonable achievable
ANOVA	analysis of variance
AP-1	activator protein
APoE	apolipoprotein E
ARE	antioxidant response element
ARF	ADP-ribosylation factor
ASNS	asparagine synthetase
ATM	ataxia telangiectasia mutated
ATP	adenosine-triphosphate
ATR	ataxia telangiectasia and Rad3-related protein

B

BNP	B-type natriuretic peptide
BSA	bovine serum albumin
Bq	Becquerel

C

CD	common deletion
CDK	cyclin-dependent kinase
CI	confidence intervals
CM-H ₂ DCFDA	chloromethylated derivate of 2',7'-dichlorofluorescein
CNOT6L	CCR4-NOT Transcription Complex, Subunit 6-Like
CRP	C-reactive protein
CST1	cystatin SN
CT	computed tomography
CVA	cerebrovascular disease
CVD	cardiovascular disease

D

DAF-FM	4-amino-5-methylamino-2',7'-difluorofluorescein
DAPI	4',6'-diamidino-2-phenylindole
DCF	2',7'-dichlorofluorescein
DDREF	dose and dose rate effectiveness factor
DMEM	Dulbecco's Modified Eagle Medium
DMSO	dimethyl sulfoxide
DSB	double strand breaks

E

E2F	E2F transcription factor
EC	endothelial cell

ECM	extracellular matrix
EDHF	endothelium-derived hyperpolarizing factor
EFNBB2	ephrin B2
eNOS	endothelial NO synthase
ERK	extracellular signal regulated kinase
ERR	excess relative risk
ET-1	endothelin 1
F	
FAM TM	6-carboxyfluorescein
FBS	fetal bovine serum
FC	fold change
FDG	fluorodeoxyglucose
FERMT3	fermitin family member 3
FITC	fluorescein isothiocyanate
G	
GCLM	glutamate cysteine ligase modifier subunit
GO BP	Gene Ontology biological process
GSEA	gene set enrichment analysis
GSH	glutathione
Gy	Gray
H	
HDM2	E3-ubiquitin-protein ligase
HR	homologous recombination
hTERT	human telomerase reverse transcriptase
HUVEC	human umbilical vein endothelial cells
I	
ICAM-1	intercellular adhesion molecule 1
ICRP	International Commission on Radiological Protection
IGF	insulin-like growth factor
IGFBP5	insulin-like growth factor binding protein
IHD	ischemic heart disease
IL-6	interleukin 6
IL-8	interleukin 8
iNOS	inducible NO synthase
IPA	Ingenuity Pathway Analysis
L	
LDL	low-density lipoproteins
LDR	low dose rate
LET	linear energy transfer
LNT	linear non-threshold
LSS	Life Span Study
M	
MGB	minor groove binder
mNOS	mitochondrial NO synthase
mtDNA	mitochondrial DNA

N

NADPH	nicotinamide adenine dinucleotide phosphate
NCRP	US National Committee on Radiation Protection
NF- κ B	nuclear factor kappaB
NHEJ	non-homologous DNA end-joining
Nrf2	nuclear factor erythroid 2-related factor 2
nNOS	neuronal NO synthase
NO	nitric oxide
Non-IHD	non-ischemic heart disease
NOS	NO synthase
NT-proBNP	N-terminal pro-B-type natriuretic peptide

P

p.i.	post irradiation
PAPPA2	pappalysin 2
PCA	principal component analysis
PCR	polymerase chain reaction
PDT	population doubling time
pen/strep	penicillin/streptomycin
PET	positron emission tomography
PHGDH	phosphoglycerate dehydrogenase
PI	propidium iodide
PI3K	phosphatidylinositol 3-kinase
PIR	pirin
PLAT	plasminogen activator tissue-type
PLAU	urokinase-type plasminogen activator
PLIN3	perilipin 3
PPAR	peroxisome proliferators-activated receptor
pRB	retinoblastoma protein
PSAT1	phosphoserine aminotransferase 1
PYGL	phosphorylase, Glycogen, Liver

R

RASSF2	Ras Association (RalGDS/AF-6) Domain Family Member 2
RERF	Radiation Effects Research Foundation
RIN	RNA integrity number
RNS	reactive nitrogen species
ROS	reactive oxygen species
rRNA	ribosomal RNA

S

SA- β -gal	senescence-associated β -galactosidase
SELP	selectin P
SERPIND1	serin peptidase inhibitor, clade D, member 1
SMURF2	SMAD Specific E3 Ubiquitin Protein Ligase 2
SOD	superoxide dismutase
SPECT	single-photon emission computed tomography
Sv	Sievert

T

tBHP	tert-butylhydroperoxide
TCA	tricarboxylic acid cycle
TGF- β	transforming growth factor β
TNF- α	tumor necrosis factor α
tRNA	transfer RNA

U

UNSCEAR	United Nations Scientific Committee on the Effects of Atomic Radiation
---------	--

V

VCAM-1	vascular cellular adhesion molecule 1
VSMC	vascular smooth muscle cells
VWF	von Willebrand factor

Chapter 1: General introduction

1.1 Radiation protection: coming to a justified and optimized use of ionizing radiation

1.1.1 What is ionizing radiation?

Ionizing radiation is everywhere, from Earth to space. It is a type of energy, in the form of particles or waves, which is characterized by its ability to ionize, i.e. the ejection of one or more electrons of an atom [1]. Naturally occurring substances with unstable nuclei undergo spontaneous transformation to become stable. These substances are radioactive and the transformation is called radioactive decay. Radioactive decay is accompanied with the release of ionizing radiation in the form of electromagnetic γ -rays and charged particles such as α - and β -particles [2]. Another sort of electromagnetic ionizing radiation is X-radiation, which is extensively used for medical applications. X-rays, although in most aspects identical to γ -rays, differ in their origin. Whereas γ -rays result from the natural decay of a radioactive element, X-rays are produced artificially in X-ray generators [3]. Electrons are accelerated to a high energy after which they interact with a specific material such as gold or tungsten, knocking electrons from the inner shell of the metal atom. To replace the loss an electron passes from a high to a lower energy state while emitting X-rays [1]. Besides α - and β -particles, other charged particles exist such as neutrons, accelerated ions and fission fragments [4]. For instance, the novel hadrontherapy for cancer treatment uses proton or carbon ion beams produced by proton or ion accelerators, respectively [5]. Also, in space a heterogeneous mixture of charged particles is present [6].

1.1.2 The notion of dose

To assess the impact of ionizing radiation on human health and to set guidelines in radioprotection, units to measure dose and its biological effects are required. Biological effects are related to the energy deposition by ionizing radiation in the matter of concern.

The *absorbed energy dose* is defined as the amount of energy delivered by ionizing radiation to a unit of mass and is measured in Gray (Gy), with $1 \text{ Gy} = 1 \text{ Joule (J)} / 1 \text{ kilogram (kg)}^1$. The absorbed dose is, however, a pure physical description of absorbed energy and does not consider the quality of the ionizing radiation type and the extent of biological damage it

¹ To note, Gy corresponds to the old unit rad (= radiation absorbed dose) as follows: $1 \text{ Gy} = 100 \text{ rad}$.

inflicts in a certain type of tissue or organ. Therefore, the terms equivalent and effective dose have been introduced [4, 7].

The *equivalent dose* takes into account the ability of a particular kind of ionizing radiation to cause damage and is obtained by multiplying the absorbed dose with a radiation weighting factor (w_r). This factor is based on the linear energy transfer (LET) which represents the average energy loss of an ionizing particle per unit length of its trajectory in the matter [1]. For example, the w_r for low-LET electromagnetic ionizing radiation (X- and γ -rays) is assigned 1 whereas for high-LET α -particles it is assigned 20.

Since tissues and organs have different sensitivities to ionizing radiation, tissue weighting factors (w_t) are established to determine the *effective dose* for the whole human body. The effective dose is obtained by summing the equivalent doses to all tissues and organs multiplied by their respective w_t . This measure of radiation exposure is also assigned a different unit, Sievert (Sv), and expresses the biological effect that a certain type of ionizing radiation has on the human body [2]. It should be stressed that the used w_t are averaged over both genders and all adult ages, making effective dose a reflection of the radiation burden of an average human adult [8]. Furthermore, Sv can only be used for stochastic effects and not for deterministic tissue reactions [9].

The focus in this PhD will be on cardiovascular effects related to low-LET X- and γ -radiation. As radiation-induced cardiovascular disease (CVD) is, thus far, assumed not to be stochastic in nature, one should use absorbed dose (Gy) [10]. Nevertheless, many epidemiological studies use effective dose (Sv) for a variety of reasons [10]. In this PhD, we will use both Gy and Sv depending on the original formulation in the study cited.

1.1.3 Brief history of radiation protection

The first discoveries of ionizing radiation were made in the 1890s. X-rays were detected by Wilhelm Konrad Roentgen [11]. Natural emanating radiation from uranium was identified by Henri Becquerel which was explored further by Pierre and Marie Curie who managed to purify radium from uranium. Intertwined with the discovery of ionizing radiation and the development of its applications, the field of radiation protection progressed.

The development of X-ray machines, resulting from the first discovery of X-rays in 1895, was embraced in the field of medicine as they were, and still are, very useful in imaging internal

structures of the human body and in treating health conditions. In the beginning, X-rays were praised for their beneficial effects and extensively used for the treatment of a wide range of diseases, from birthmarks to syphilis, but without consideration of possible hazards for human health. Though, from the early 20th century, there were already various cases in which adverse health effects related to the use of ionizing radiation became apparent. A text-book example concerns Clarence Dally whose death is considered the first to be associated with man-made radiation [11, 12]. Dally worked at Thomas Edison's lab developing an X-ray-powered light bulb. Edison put a stop on his work as he explained later *'I soon found that the X-ray had affected poisonously my assistant, Mr. Dally, so that his hair came out and his flesh commenced to ulcerate'*. Dally developed a degenerative skin disease that progressed into a carcinoma leading to his death in 1904 [12]. The extensive use of X-rays at the turn of the century manifested itself as a wave of deaths in the 1920s, due to blood diseases and cancers with long latency, amongst the pioneering radiologists and their patients [12]. Another insidious danger for human health was the use of radium which was originally also thought to have only beneficial health effects. Doctors prescribed radium solutions or injected radium intravenously for a wide range of health disorders. The recognition of adverse health effects of radium started in the 1920s with the so-called "radium girls". Young women who had worked in factories painting radium dials on watches and clocks became seriously ill. Further investigation attributed the ingestion of large cumulative doses of radium, upon licking the painting brushes, to the illnesses and death [13, 14].

Progressively, awareness of adverse (late) health effects of ionizing radiation started to sink in and national and international conferences were held to discuss possible protection measures against ionizing radiation. The Second International Congress of Radiology in 1928 led to the establishment of the International X-ray and Radium Protection Committee who issued their first protection guidelines, although only for professionals in the medical field. The American counterpart, the Advisory Committee on X-ray and Radium Protection, also found its origin in this epoch [13].

At the same time, progress was made in experimental physics leading to the discovery of nuclear fission in 1939 [15]. This led soon to the use of nuclear power in the military field with, as an example, the notorious atomic explosions in Hiroshima and Nagasaki in 1945 which remains one of the most controversial events in the 20th century [16]. It ended the Second World War, but in such a deadly and destructive manner that it unleashed the threat of

more deadly wars to come. Nevertheless, following these bombings, more nuclear weapons were developed and stored in many countries over the world creating a fragile situation of continuous fear for destruction of civilizations. Next to this fear of nuclear destruction, the large amount of nuclear tests and the construction of nuclear reactors (for both peaceful and warlike purposes) in the 1950s and 60s led to uncontrolled releases of radioactive waste in the environment. Furthermore, the use of X-rays and radio-isotopes for medical and industrial purposes increased as well, adding to the contamination of soil and water [13, 15]. This raised new questions for radiation protection of human health and also the environment. In particular, since nuclear fission created new radioactive substances for which health and environmental effects were unknown. Also, while before radiation protection only concerned those exposed in their profession, and mainly in the medical field, now, the whole population became of concern. In addition, the public became aware of, and started to worry about, health risks related to exposure to ionizing radiation.

In the early beginnings of radiation biology research it was already apparent that ionizing radiation caused damage to cells [17]. The conventional biological understanding is that ionizing radiation damages biological molecules, and in particular DNA, ultimately leading to cell death or transformation [18]. From the 1950s onwards, radiation protection philosophy started to change. Whereas before it was believed there was a threshold dose below which no biological harm was caused, radiobiological advances soon pointed out that even small doses of radiation could damage cells. Progressively radiation protection bodies acknowledged these findings and abandoned the use of "*tolerance dose*" and replaced it with "*maximum permissible dose*". This dose, based on the available knowledge, is expected not to cause appreciable health effects to a person during his lifetime [13]. The question "*How much exposure should a human be allowed?*" which is preceded with the question "*How much is harmful?*" became the foundation of radiation protection guidelines. The two major committees established in the 1920s adopted new names to reflect the change in philosophy and were renamed the International Commission on Radiological Protection (ICRP) and the US National Committee on Radiation Protection (NCRP) [13]. New organizations were formed as well, such as the United Nations Scientific Committee on the Effects of Atomic Radiation (UNSCEAR) established in 1955 which was assigned the task to study the effects of atomic radiations on human and environment [15].

1.1.4 The current issue of low doses in radiation protection

1.1.4.1 Use of the LNT model for radiation protection purposes

Nowadays, radiation protection bodies still struggle with the question '*How much is harmful?*', in particular in the low dose range. Even though a large number of epidemiological and radiobiological studies are dedicated to investigate the effects of low doses of ionizing radiation their health impact is not yet fully elucidated, thus hampering an accurate risk assessment.

Health effects of ionizing radiation can be divided into so-called deterministic and stochastic effects. *Deterministic effects*, these days also referred to as tissue reactions, prevail with high doses of radiation, whereas *stochastic effects* prevail with low doses. In brief, high dose irradiation causes a substantial amount of cell killing leading to clinical detectable tissue reactions. These tissue reactions are characterized by a threshold-dose and an increase in their severity with increasing dose above this threshold. With stochastic effects it is not the severity but the probability that increases with dose. Two diseases of concern, which are stochastic in nature, are cancer and hereditary disease [19, 20]. Hereditary disease manifests itself in the offspring of exposed humans when radiation-induced mutations occur in the reproductive cells (eggs and sperm) of the body [11].

Current radiation protection guidelines for low dose exposures are based on cancer and hereditary disease risk estimates. For clarity, the current consensus is to define a low dose as 100 mSv or less and a low dose rate as 0.1 mGy/min or less [11, 21, 22]. Epidemiological findings form the basis for risk estimation. Epidemiological cohorts include the Japanese atomic bomb survivors, occupationally exposed groups (radiologists, nuclear industry workers, etc.), patients exposed during treatment or diagnostic procedures, and groups exposed to environmental sources of radiation [23]. The most informative cohort is formed by the Japanese atomic bomb survivors for whom an excess cancer risk was statistically evidenced for doses above 100 mSv. Below 100 mSv, however, epidemiological data are inconclusive. This is mainly because of practical limits of epidemiological studies. Indeed, larger, and practically not feasible, cohorts would be needed to quantify excess cancer risks due to radiation at these lower doses with sufficient statistical power [24]. Risk assessment in the low dose region (< 100 mSv) is therefore based on extrapolations made from high dose risk estimates. The high dose risk estimates are reduced by a dose and dose rate effectiveness

factor (DDREF) to account for the more efficient biological repair mechanisms with low dose and low dose rate exposure [11, 22]. Additional risk-modulating factors such as gender, age at exposure, radiation quality, dose rate, genetic background and lifestyle factors of the exposed individual also have an influence on risk estimates.

Currently it is agreed to consider the extrapolation from high to low dose based on the assumption that the risk of developing cancer increases with dose and without the presence of a threshold dose. This is referred to as the *linear non-threshold* (LNT) model and implies that no dose can be considered absolutely safe, although risks are considered negligible below a certain dose [25]. The use of the LNT model for radiation protection purposes at low doses is in agreement with the "*as low as reasonable achievable*" (ALARA) principle that is commonly used to protect human health from harmful agents. In recent years, radiobiological and epidemiological findings have questioned the validity of the LNT model as a basis for radiation protection guidelines, although evidence is insufficient [26]. Other possible high to low dose risk extrapolations that have been proposed include the linear threshold model, the linear quadratic model, the hormetic model, and a downward curving model (Figure 1). However, until proven otherwise it is not advised to discard the implementation of the LNT model in radiation protection guidelines for cancer and hereditary risks.

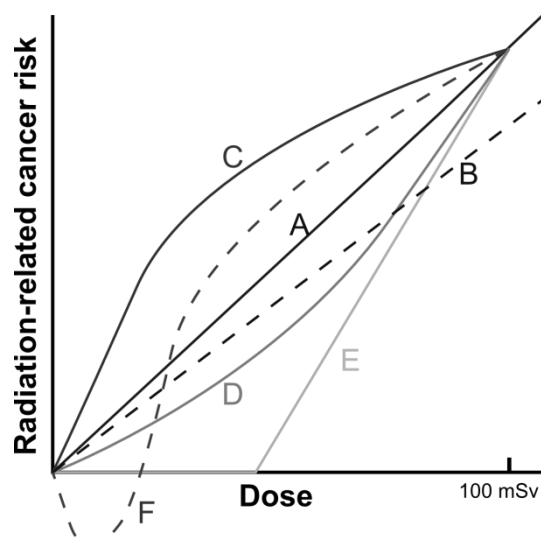


Figure 1: Schematic representation of different possible extrapolations to estimate radiation risks of cancer down to very low doses (< 100 mSv). In principle all the proposed extrapolations could be consistent with the known high dose risks estimates from epidemiological studies, although some models are less credible than others. The LNT model has been adopted as radiation protection standard for radiation-induced cancer and as long there is insufficient scientific credibility for the other models, it is not advised to discard the LNT model as radiation protection standard. **A.** linear non-threshold (LNT) model for high dose rate, **B.** LNT model for low dose rate (after adjustment with DDREF) **C.** downward curving (decreasing slope), **D.** linear quadratic model (increasing slope), **E.** linear threshold model, **F.** hormetic model. Figure based on [11, 24].

Based on the LNT model, ICRP has set current effective dose limits, for protection against stochastic effects, to 20 mSv/year for occupational exposures and to 1 mSv/year for the general public [22]. It should be mentioned that these dose limits are not valid for patients exposed to ionizing radiation for medical purposes. In this case, exposure is not restricted in terms of dose but is based on the principle of justification. Exposure to ionizing radiation should be justified in term of health benefit for the patient and requires a sound judgment to decide whether the expected benefits will outweigh the likely radiation risks [27].

1.1.4.2 Radiobiological findings that question the LNT model

The classical radiobiological paradigm considers DNA as the critical cellular target of ionizing radiation, the so-called "*target theory*". In this theory, biological effects are considered the consequence of the cellular response to radiation-induced DNA damage. This damage can be inflicted directly but also indirectly by the action of free radicals which are formed upon interaction of ionizing radiation with water [28]. The target theory forms the

radiobiological basis of the LNT model. Indeed, at the tissue level, this theory presumes that with exposure to higher doses of ionizing radiation more cells are hit and deleterious effects consequently increase proportionally. At the cellular level, the yield of DNA damage is assumed to increase in proportion to dose and as a consequence the probability of mutagenic damage in the irradiated cell increases linearly with dose [29, 30].

Since cancer is considered the major health risk of low doses of radiation, the current radiation protection system is aimed at limiting the incidence of radiation-induced cancer. In general, the LNT model, based on the target theory, is used for cancer risk estimation in the low dose region. However, cancer development is not a single cell event but a complex process modulated by various factors such as genetics, environment and the target organ. Cancer may be initiated by a radiation-induced mutagenic event in a single cell, but several other steps need to be overtaken for full cancer development [31]. How low doses of ionizing radiation influences cancer development is not fully known but more and more attention is given to the role of so-called "*non-targeted effects*" comprising bystander effects and genomic instability. Non-targeted effects are defined as biological responses to ionizing radiation observed in cells that were not directly hit [29, 30, 32]. These effects question thus the target theory on which the LNT model is based.

Bystander effects describe biological effects of ionizing radiation which are found in cells that were not irradiated, but which are in close proximity of those that were [29]. They are proposed to be mediated by some sort of communication between irradiated and non-irradiated cells, most likely by means of secreted soluble factors which are diffused through the culture medium or by cell-to-cell gap junction communication [30]. Bystander effects manifest themselves as a wide range of biological endpoints including, but not limited to, DNA damage, cell killing, chromosomal aberrations and transformation. Another non-targeted effect is genomic instability which describes the increasing rate of genetic alterations in the progeny of irradiated cells, multiple generations after the initial insult. Many biological endpoints of genomic instability are in common with those of the bystander effect and it has been proposed that the two are interlinked [29]. The mechanisms leading to both bystander effects and genomic instability, and their interrelationship, are not yet fully understood. Experimental findings suggest a role for a wide range of factors including reactive oxygen and nitrogen species (ROS/RNS), cytokines, mitochondrial dysfunction, deficient DNA damage repair system, changes in gene expression, perturbations in cellular homeostasis and epigenetic mechanisms [29, 31-33].

Another phenomenon is the *adaptive response* in which a low dose of ionizing radiation (adaptive dose) given prior to a higher (challenging) dose attenuates the deleterious effects of the challenging dose. The excess risk of the challenging dose is reduced by the prior adapting dose, but is still generally increased. The priming dose should be capable of inducing effective protective signaling mechanisms, such as up-regulation of DNA repair mechanisms, and is usually between 0.01-0.2 Gy of low LET radiation [34]. The protective effects of the priming dose ahead of a higher dose are transitory and last usually between 4 and 48 h [35]. The adaptive response has been considered as a component of non-targeted effects, although this remains under discussion [29].

Non-targeted effects could have implications for the current evaluation of cancer risk at low doses. It is very likely that they challenge the linearity of cancer risk in the low dose region but it is not clear in which way. For example, bystander effects may lead to an increased number of mutagenic cells and thus an increased risk. On the other hand, they may decrease risk when lethal effects are propagated to other cells [36]. So far, most experimental work on non-targeted effects is performed *in vitro* and the relevance *in vivo* and ultimately their impact on radiation-induced detrimental health outcome are even less understood. Therefore, the significance of non-targeted effects on radiation risk assessment is still under discussion.

1.1.4.3 Non-cancer disease risks and radiation protection

Traditionally, non-cancer diseases are not considered as health risks following exposure to low doses of radiation. Indeed, non-cancer diseases are classified as deterministic tissue reactions which are characterized by a threshold dose [37]. The ICRP has judged that below an absorbed dose of 100 mGy no clinical relevant tissue damage occurs [22]. Recent epidemiological findings point, however, to an excess risk of non-cancer diseases following exposure to lower doses as previously thought [37]. The evidence is the most sound for *cardiovascular diseases* (CVD) and *cataract*. At present, an excess risk of CVD mortality above 0.5 Gy has been evidenced by epidemiological studies (more detailed explanation in section 1.2.). The dose-risk relationship is undetermined below 0.5 Gy, but if this relationship proves to be without a threshold it may have considerable impact on current low dose health risk estimates. The overall excess risk of mortality following low dose exposures may then be about twice the risk currently assumed, based on radiation-induced cancers alone [38].

In the next chapter, a more detailed overview is given of epidemiological findings. Furthermore the societal concern of a possible excess risk of CVD mortality, and also morbidity, following low dose exposures is discussed.

For the definition of low and high dose radiation in this thesis we followed the definitions set by the Health Protection Agency in the following report "*Circulatory disease risk. Report of the independent Advisory Group on Ionising Radiation. 2010*". In this report low doses of radiation are defined as being below 0.5 Gy (since epidemiological findings concerning CVD are inconclusive for doses below 0.5 Gy), and high doses as 5 Gy and above [10].

1.2 Cardiovascular disease risk related to low doses of ionizing radiation

1.2.1 Recognition of radiation-related cardiovascular disease risk

The recognition that exposure of the heart and the vasculature to high doses of ionizing radiation can cause CVD started in the late 1960s [39]. This was mainly related to the clinical observation of cardiovascular complications in radiation-treated survivors of Hodgkin's lymphoma and other childhood cancers. Later, larger-scale epidemiological studies have found a clear association between therapeutic doses of thoracic irradiation and an increased risk of cardiovascular disease in these long-term cancer survivors, confirming the earlier observations [40].

An excess risk of CVD was also observed after postoperative radiotherapy for breast cancer. In these patients, a part of the heart received accumulated doses of ≥ 40 Gy (fractionated 20 x 2 Gy). After correction for fractionation effects using the linear quadratic model and an α/β ratio of 1–3 Gy, determined in experimental studies in the rat heart, Schultz-Hector and Trott have calculated that this corresponds to equivalent single doses to the total heart of about 1-2 Gy [41]. The Early Breast Cancer Trialists' Collaborative Group has performed a meta-analysis on mortality data of more than 30.000 breast cancer patients 15 years after treatment. The mortality of heart disease was increased with 27 % in patients treated with surgery and subsequent radiotherapy compared to patients treated with surgery alone [42]. Evaluation of long-term mortality in breast cancer survivors may however be influenced by the varying prognosis of the different treatment regimes (surgery versus radiotherapy). This can be circumvented by comparing women irradiated for left-sided tumors with women irradiated for right-sided tumors. Cardiac radiation doses are larger in radiotherapy patients with left-sided tumors than in radiotherapy patients with right-sided tumors [43]. Analysis of 308 861 women with breast cancer registered in the Surveillance, Epidemiology and End-Results cancer registries database from the United States has revealed an increased heart disease mortality ratio for women irradiated for left-sided breast cancer compared to right-sided breast cancer [44]. A study related to 72 134 women diagnosed with breast cancer in Denmark and Sweden during 1976-2006 and followed-up for 30 years revealed an increased risk of ischemic heart disease, pericarditis and valvular disease in irradiated women with left-sided tumors (mean cardiac dose 6.3 Gy) compared to right-sided tumors (mean cardiac dose 2.7 Gy) [45].

Also, radiotherapy patients with benign diseases such as the peptic ulcer patients form interesting study cohorts. For instance, coronary heart disease mortality was compared between peptic ulcer patients treated with radiotherapy (n = 1859) and treated by other means (n = 1860) [46]. The calculated received volume-weighted cardiac doses ranged from 1.6 to 3.9 Gy and the portion of the heart directly in the field received doses of 7.6-18.4 Gy. A significantly increased risk of coronary heart disease mortality was observed with increasing dose. Only recently, various epidemiological findings, in particular from the Japanese atomic bomb survivors, have raised awareness of possible CVD risk following exposure to low and moderate doses of radiation [41]. Below an overview is given of the major epidemiological findings related to CVD risk following low dose exposure.

1.2.2 Low dose exposed epidemiological cohorts

1.2.2.1 Classification of cardiovascular diseases in epidemiology

Reviewing the epidemiological literature related to CVD and low dose ionizing radiation is complicated by the different classifications of CVD, also referred to as heart disease. Moreover, all CVD are often pooled in one diagnosis in epidemiological studies. However, this hampers thorough understanding of radiation-related CVD risk, and distinction should be made between the different clinical manifestations (see detailed explanation of the different clinical manifestations in section 1.3.) [47]. In addition, many epidemiological studies face the problem of misclassification of the cause of death, except for stroke, for which the diagnosis tends to be reasonably good [10]. In fact, stroke is not considered a CVD, but a circulatory disease since it involves the blood circulation in the brain and is unrelated to the heart. It is defined by brain injury which occurs when a blood vessel in the brain ruptures or is blocked leading to loss of blood supply in the brain area of concern.

1.2.2.2 Survivors of the atomic bombings of Hiroshima and Nagasaki

The most informative cohort is the Life Span Study (LSS), consisting of 120 321 exposed and non-exposed individuals selected from respondents to the national census of Japan in 1950 calling for survivors exposed to the bombings in Hiroshima and Nagasaki, and from residential surveys in the cities after the national census. Mortality in this population has been investigated since 1950 by collecting information through the national population registry (*koseki*) and death certificates obtained throughout Japan. Cancer incidence data was available

from population-based cancer registries since 1957 in Hiroshima and since 1958 in Nagasaki [48]. Next to the availability of these data, the large size, the presence of both sexes and all ages, and well-characterized individual dose estimates² makes this cohort a valuable source for risk estimation. Another cohort, the Adult Health Study (AHS), was established in 1958 and consists of 19 961 subjects from the LSS cohort. These survivors undergo biennial health examinations which provide additional clinical and sub-clinical information to the death and cancer registries data. In this way, disease morbidity for a variety of conditions can be investigated [50].

Preston and coworkers have evaluated non-cancer mortality based on the LSS report 13 published by the Radiation Effects Research Foundation (RERF), which spans the time period 1950-1997 [51]. In this study, the weighted colon doses from the DS86 dosimetry system was used for individual dose estimates. Only the period 1968-1997 was included to account for the "healthy survivor" selection effect. Individuals had to be alive in 1950 to enter the LSS cohort and have thus survived the difficult conditions after the bombing, which means that the health experience of this cohort may not be typical for a normal population. This is reflected as a decrease in non-cancer mortality during 1950-1960 in the LSS members that received doses below 2 Sv, as shown by Shimizu and coworkers [52]. This "healthy survivor" selection effect had largely disappeared by the mid-1960s. To exclude this confounding effect, Preston and coworkers advised to restrict the analyses to proximal survivors who were within 3 km of the hypocenter of the bombing, and to a follow-up period starting from 1968 [51]. Based on the LNT model, excess relative risk (ERR)³ estimates were calculated to be 0.17 with 90% confidence intervals (CI) (0.08;0.26) for heart disease and 0.12 (90% CI 0.02;0.22) for stroke, for the period 1968-1997 [51].

Shimizu and coworkers have evaluated ERR of mortality from heart disease and stroke in the LSS cohort with a follow-up of 53 years (1950-2003) [53]. For individual dose estimates,

² Since 1957, the Radiation Effects Research Foundation has developed several dosimetry systems to determine neutron and gamma doses received by the atomic bomb survivors. The DS86 system represents the calculated organ doses (active marrow, bladder, bone, brain, female breast, eye, foetus/uterus, large intestine, liver, lung, ovary, pancreas, stomach, testes and thyroid) taking shielding, provided by structures and the human body, into account. The DS86 was implemented in 1986. The most recent dosimetry system is the DS02 system implemented in 2003, which has tackled the discrepancies between the measured and calculated values for neutron activation in Hiroshima observed in the DS86 system [49].

³ The excess relative risk (ERR) is an epidemiological risk measure that quantifies how much the level of risk among persons with a given level of exposure, in this case of ionizing radiation exposure, exceeds the risk of non-exposed persons [10].

weighted colon doses (Gy) from the DS02 dosimetry system were used. In addition, they have obtained, by a mail survey, information regarding sociodemographic (education, occupation type), lifestyle (smoking, alcohol intake) and health variables (obesity, diabetes mellitus) from 36 468 members of the LSS cohort. This allowed them to evaluate the effect of these confounding factors on ERR estimates. It should be noted that they included the full follow-up period from 1950-2003 and all survivors, thus not taking into account the "healthy survivor" selection effect. They found an ERR of 0.14 (95% CI 0.06;0.23) for heart disease and an ERR of 0.09 (95% CI 0.01;0.17) for stroke based on the LNT model. Whereas the LNT model fitted best the data for heart disease, the quadratic model was best to fit the data for stroke (Figure 2). The latter model implies relatively little risk at lower doses. Indeed calculation of ERR for stroke over restricted dose ranges revealed a ERR of 0.03 (95% CI -0.10;0.16) for 0-1 Gy and -0.07 (95% CI -0.28;0.16) for 0-0.5 Gy. Furthermore, they showed that the association of dose with CVD risk in the LSS cohort is unlikely to be an artifact from confounding by sociodemographic, lifestyle or disease risk factors.

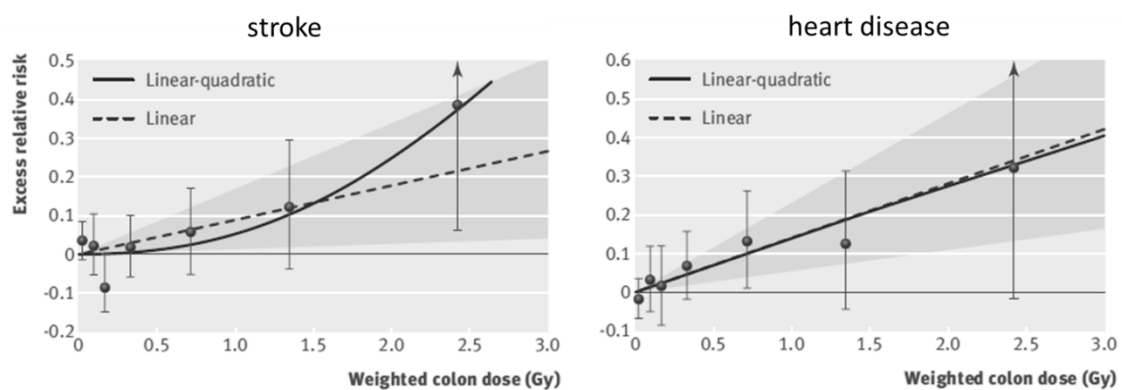


Figure 2: Radiation dose-response relationship (ERR/Gy) in the LSS cohort for death from stroke (left panel) and death from heart disease (right panel), showing linear-quadratic and linear functions. Shaded areas represent 95% confidence region for the fitted linear line. Error bars represent 95% CI for each dose category risks and the bullet represents the point estimate of risk for each dose category. The participants were divided in several dose categories according to their weighted colon dose (in Gy = γ dose plus 10 times neutron dose) [53].

The abovementioned studies have used the LSS cohort for CVD risk estimations. Takahashi and coworkers have examined the association with dose and the incidence of stroke in the AHS cohort [50]. For their study, information of health examinations from the follow-up from 1980 onwards has been used, resulting in 9515 AHS participants. For individual dose

estimates, weighted colon doses (Gy) from the DS02 dosimetry system were used. In this study population, risk for hemorrhagic stroke was observed to increase with dose. This was across the full range of doses for men, while in women there seems to be a threshold of about 1.3 Gy.

1.2.2.3 Occupational exposure

Studies in radiation workers are of interest since they generally involve relatively low doses received over repeated exposures, although in some cases accumulated doses may be high. Various studies have been performed, of which the most important will be discussed. The largest studied cohort consists of 275 000 nuclear industry workers from 15 countries, referred to as the 15-country study [54]. The average cumulative dose received was 20.7 mSv. An overall increasing trend, although not significant, for circulatory disease mortality was observed. It was concluded that their findings are compatible with both no increased risk and with an increased risk comparable to that observed in A-bomb survivors. A more recent study by Muirhead and coworkers has revealed an increasing circulatory disease mortality risk with dose, which was borderline significant, in the UK National Registry of Radiation Workers in the industrial and medical field [55]. The average cumulative dose received was 24.9 mSv. This finding should, however, be interpreted with caution seeing the lack of information on confounding factors. Another large cohort consists of 206 620 radiation workers in the industrial and medical field, registered in the National Dose Registry of Canada [56]. Average exposure of all workers was 6.3 mSv, with large differences between males (10.6 mSv) and females (1.7 mSv). A significant increasing trend of circulatory disease mortality with dose was observed in males. Again, there is a lack of information on confounding factors and there is also incompleteness of dose records. The Chernobyl liquidator cohort consists of 61 017 individuals with an average cumulative dose of 0.109 Gy. An ERR/Gy of 0.41 (95% CI 0.05;0.78) was found for ischemic heart disease morbidity and stroke, though not adjusted for recognized risk factors such as excessive weight, hypercholesterolemia, smoking, alcohol consumption, and others [57].

The Mayak cohort is of particular interest since it includes information both on mortality and morbidity, and information on confounding factors [58]. In 1948, the first nuclear energy enterprise in Russia, Mayak Plutonium Association, was put in operation. Since 1948 the Mayak personnel undergo regular routine medical examinations. In addition, every 3-5 years a more detailed examination is carried out in a specialized hospital. This examination system

led to a unique archive of medical data which was used to create the 'Clinic' medical-dosimetric database. Also, from a dosimetric point of view, the database is sound. Individual dosimetry for external gamma exposure was introduced in 1948 and for internal exposure during the 1960s [58]. Complete data are available for 12 585 Mayak workers employed during 1948-1958 and followed-up until December 2000. The mean cumulated external dose was 0.91 ± 0.95 Gy (99% percentile 3.9 Gy) for men and 0.65 ± 0.75 Gy (99% percentile 2.99 Gy) for women. In this cohort, a significant increasing trend in ischemic heart disease morbidity was observed with increasing total external dose (ERR/Gy = 0.11 (95% CI 0.049;0.168)). Influence of confounding factors on this trend was minimal [59]. The most recent analysis of the Mayak cohort includes 18 763 workers with an additional follow-up of 5 years [60]. Overall, risk estimates for ischemic heart disease are similar to the earlier study (ERR/Gy = 0.10 (95% CI 0.045;0.153)). Remarkable though, a statistically significant decrease in ischemic heart disease incidence was found among workers exposed to external doses of 0.2-0.5 Gy compared to workers exposed to external doses below 0.2 Gy. This decreased risk is heavily influenced by the observations in female workers. The authors remark that this finding should be interpreted with caution since it has never been reported in other studies.

It must be noted that besides the classical CVD-related confounding factors, occupational studies have to deal with the "healthy worker" selection effect, similar to the "healthy survivor" selection effect in A-bomb survivors. The "healthy worker" selection effect occurs when workers who are healthier and have lower mortality and morbidity rates are selectively retained in the workplace, as such accumulating higher doses. One can adjust for this confounding by considering duration of employment as a confounding factor in the analysis, as done in the 15-country study [54].

1.2.2.4 Meta-analysis

The Advisory Group on Ionising Radiation has reviewed the available epidemiological data for low and moderate dose exposure in 2010. Taking all the studies together, they reported a small but statistically significant overall ERR/Gy of 0.09 (95% CI 0.07;0.12). They remarked, however, that there was a lot of heterogeneity in risk estimates of the different studies included in their meta-analysis [10]. Little and coworkers have recently extended this meta-analysis [38]. They estimated excess risks for four subgroups of circulatory disease, classified

according to the *'International Classification of Diseases, 10th revision'*: ischemic⁴ heart disease (IHD), non-ischemic heart disease (non-IHD), cerebrovascular disease (CVA), and all other circulatory diseases. Significant effect of heterogeneity between the different studies was found for CVA and other circulatory diseases, but not for IHD and non-IHD. ERR were calculated based on the LNT model, which implicitly assumes a linear association of CVD risk at low doses and dose rates. They noted that this assumption is reasonable since there is little evidence for non-linearity in the Japanese atomic bomb survivors and Mayak workers data. Furthermore, at least for IHD and non-IHD, the ERR/Sv was consistent between the Japanese atomic bomb survivors, Mayak workers and other occupational cohorts [38]. Although it should be noted that Schollnberger and coworkers advocate for, at least in the LSS data, the consideration and testing of other dose-response models for non-cancer effects [61]. To conclude, the overall consensus of the abovementioned reports is that there is a significant elevated CVD risk for doses above 0.5 Gy [10, 62].

1.2.3 Epidemiology alone is not the answer

CVD are the leading cause of mortality and morbidity and account for 30-50% of all deaths in most developed countries. It is a multifactorial disease with many risk factors such as lifestyle and other personal factors [63]. The most established risk factors include male sex, elevated low-density lipoproteins (LDL), smoking, hypertension, family history of premature coronary disease, and diabetes mellitus [64]. Epidemiological studies, as presented above, have limited statistical power to detect a possible excess risk of CVD following low dose exposure (0.5 Gy), due to the high background level of CVD in the population as a whole and many potentially confounding risk factors [10]. For example, it has been calculated that, if excess risk is in proportion to dose, a cohort of 5 million people would be needed to quantify the excess risk of a 10 mSv dose [24]. Other factors that have an influence on epidemiological results are the distribution of the dose range, accuracy of dosimetry, the duration of follow-up after exposure and correct assignment of cause of mortality [65].

Although epidemiological studies have led to a better insight in radiation-related CVD risk, there are still many uncertainties that need to be clarified. Is there a threshold dose? Does the latency of CVD development depend on the dose? What are the sensitive targets in the heart and vasculature? Does exposure has an impact on CVD incidence or progression, or both?

⁴ Ischemia describes the phenomenon when tissues are deprived of oxygen due to restricted blood supply.

What is the impact of acute, fractionated or chronic exposure on risk estimates? For an accurate dose risk assessment, these questions need to be answered.

Classical epidemiological studies, as described above, will not provide all the needed insight to answer these questions. A more targeted approach such as the integration of epidemiology and biology is required. For example, the assessment of subclinical endpoints and other cardiovascular biomarkers by functional imaging in patients receiving radiotherapy will offer insight into the development and progression of CVD following radiation exposure [63, 65]. Single-photon emission computed tomography (SPECT) or positron emission tomography (PET) imaging of micro-vascular perfusion has already been applied in breast cancer studies. The outcome differed between the studies. For instance, whereas in one study perfusion defects were observed within 6-12 months after radiotherapy, no significant differences in perfusion defects were found in another study [66, 67]. Also, the evaluation of cardiovascular biomarkers in radiotherapy patients may be useful. For instance, elevated levels of N-terminal pro-B-type natriuretic peptide (NT-proBNP)⁵ have been shown to be predictive for heart failure and/or CVD mortality across a broad range of individuals [70]. Higher values of NT-proBNP were found in patients treated with radiotherapy for left-sided breast cancer compared to patients treated with other means [71].

Next to epidemiology, radiobiological research is essential for understanding CVD risk in the low dose region. Since epidemiological findings for low and moderate doses are suggestive and not persuasive, their use in dose risk assessment is limited. A thorough understanding of the biological mechanisms is thus needed to complement the epidemiological findings. And once there is a comprehensive biological understanding, the inclusion of biologically based dose-response models will be of benefit for accurate risk estimation in the low dose region [72].

1.2.4 Societal concern

The possible excess risk of CVD following exposure to low doses is of great societal concern. According to the ICRP, a dose of 0.5 Sv may lead to approximately 1% of exposed individuals developing cardiovascular or cerebrovascular disease, more than 10 years after the

⁵ As a result of wall stress, induced by amongst others IHD, pulmonary thromboembolism and congestive heart failure, the B-type natriuretic peptide (BNP) gene is upregulated in cardiomyocytes. The propeptide proBNP is cleaved into the physiologically active BNP and the biologically inactive N-terminal fragment (NT-proBNP). The BNP hormone has various natriuretic vasodilatory effects on the heart and the vascular system [68, 69].

exposure, in addition to the 30-50% suffering from disease without being exposed to ionizing radiation [73]. Although the assumed risk is rather small, it may have serious implications for public health. Indeed, seeing the high background rate of CVD, the absolute number of excess cases would be substantial [65].

Various issues such as occupational radiation exposures, future of nuclear power, manned space flights, and threat of radiological terrorism, call for a thorough understanding of low dose health risks [24]. The main concern is, however, the increasing use of ionizing radiation for diagnostic medical purposes (Figure 3). For instance, since 1993 the number of computed tomography (CT) scans has quadrupled in the US and similar trends are observed in Europe [74].

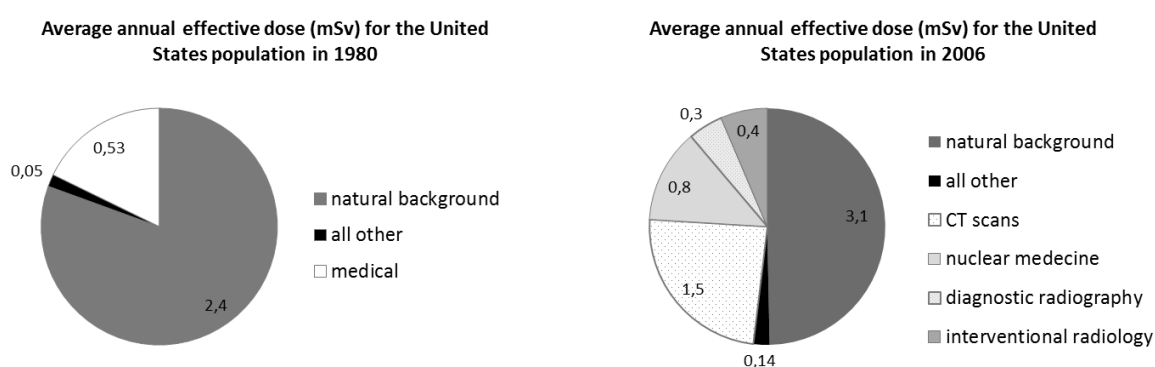


Figure 3: Average annual effective dose per person received in 1980 (left panel) and 2006 (right panel) in the United States. The large increase in the use of ionizing radiation for medical purposes, in the period 1980-2006, contributed to a total increase from 3.0 mSv in 1980 to 6.2 mSv in 2006. Similar trends are observed in other industrialized countries [75].

In particular, the increased use of non-invasive cardiovascular imaging techniques such as cardiac CT scans and myocardial perfusion imaging with radionuclides, are of importance. Indeed, effective doses range from 1 to 20 mSv depending on the procedure (Table 1) [9]. Although one cannot deny the huge health benefits of these improved diagnostic procedures, concerns are raised regarding the 'overuse' and potential associated health risks [76]. For example, it has been observed that 14-22% of cardiac imaging tests were inappropriate in the US [77, 78].

Examination	Representative Effective Dose Value (mSv)	Range of Reported Effective Dose Values (mSv)	Administered Activity (MBq)
Chest X-ray posteroanterior and lateral	0.1	0.05-0.24	N/A
Diagnostic invasive coronary angiogram	7	2-16	N/A
<u>Coronary CT angiogram</u>			
– 64-slice multidetector, retrospective gating	12	9-19	N/A
– 64-slice multidetector, reduced tube voltage (100 kVp)	6	3-8	N/A
– 64-slice multidetector, prospective triggering	3	2-4	N/A
– Dual-source high pitch	< 1	< 1	N/A
– 264 or 320 multidetector row CT	4	2-8	N/A
<u>Nuclear medicine studies</u>			
<i>Myocardial perfusion</i>			
– Sestamibi (1-day) stress/rest	12	N/A	1480
– Tetrofosmin (1-day) stress/rest	10	N/A	1480
– Thallium stress/redistribution	29	N/A	130
– Rubidium-82 rest/stress	10	N/A	2960
<i>Myocardial viability</i>			
– PET F-18 FDG	14	N/A	740
– Thallium stress/reinjection	41	N/A	185

Table 1: Overview of typical ionizing radiation doses in cardiac imaging procedures [79]. CT = computed tomography, FDG = fluorodeoxyglucose, N/A = not applicable, PET = positron emission photography.

As mentioned before, radiation protection of patients is not based on dose limits but on the principle of justification which states that the benefits and risks from the use of ionizing radiation should be carefully evaluated. However, this risk/benefit balance is highly patient-dependent and the decision for the use of a specific imaging test relies on the physician's judgment. Several guidelines have been published by various societies such as the European Society of Cardiology and the American College of Cardiology Foundation, to aid in this decision [9, 80]. These guidelines offer information regarding the accuracy of the tests, the usefulness of the information obtained from the test, but also regarding the risks of the tests including those related to radiation adverse health effects. Also, the implementation of informed consent, in which the patient is informed of possible risks and decides if he will give his consent, will stimulate physicians to more carefully balance benefits and risks of a specific imaging procedure [76, 79]. Furthermore, the development and implementation of dose-lowering techniques will be of benefit not only for the patient [81], but also for the physician. Also, the identification of biomarkers of susceptibility allows screening for sensitive patients, aiding in the evaluation of the risk/benefit balance [82].

1.3 Clinical manifestation and pathology of radiation-induced cardiovascular diseases

1.3.1 Overview

As mentioned above, radiotherapy patients who received doses above 40 Gy to part of the heart may develop cardiovascular complications later in life [43]. More recently, epidemiological findings also point to an excess risk of CVD following exposure to lower doses. CVD, also commonly referred to as heart disease, comprise a broad range of different clinical manifestations. Radiation-induced clinical manifestation of CVD is dependent on various factors such as dose, the volume of the heart exposed, age at exposure, latency of disease, length of follow-up and other confounding factors (e.g. smoking and diet) [83]. The major clinical manifestations of radiation-related CVD, pericarditis, congestive heart failure and coronary artery disease, will be discussed below. Ionizing radiation may also cause valvular disease, arrhythmias and conduction abnormalities, but the evidence for a direct causal relationship is not strong [43, 84].

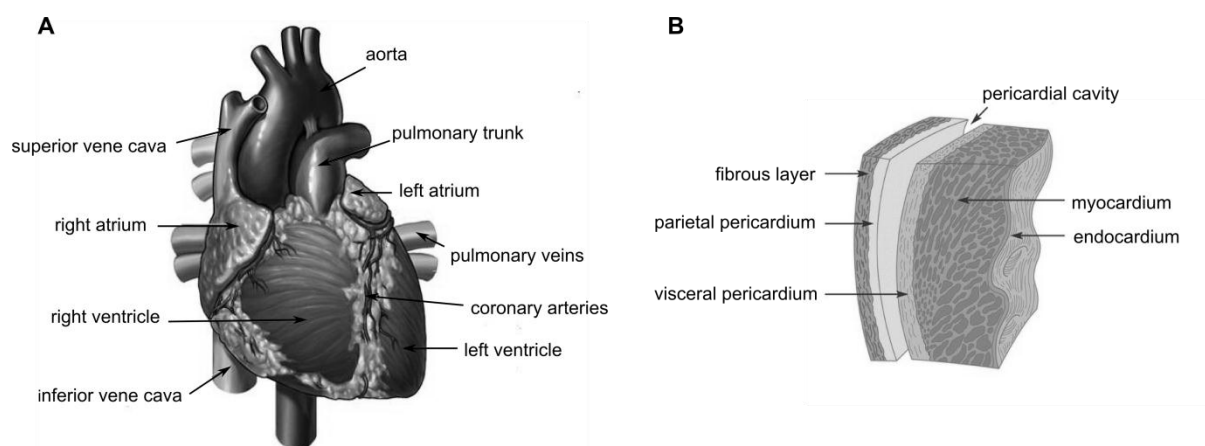


Figure 4: Overview of the heart anatomy. **A.** Illustration of the external anatomy with the major cardiac veins and arteries. **B.** More detailed illustration of the pericardial sac that surrounds the heart. Figure adapted from <http://cnx.org/content/m46676/latest/> and http://medtech1.com/attack/heart_anatomy.cfm.

1.3.2 Pericarditis

The earliest sign of radiation-related heart disease is acute pericarditis which occurs already months after high dose irradiation of the heart (> 40 Gy). Since 1970, advances in radiotherapy treatments have led to significant reduction of both the dose and the volume of the heart exposed [41]. Therefore, radiation-induced pericarditis is not common anymore these days. Acute pericarditis is inflammation of the pericardium, the membrane that surrounds the heart (Figure 4), and is characterized by the exudation of protein-rich fluid in the pericardial sac. On longer term, this can lead to chronic constrictive pericarditis due to fibrin deposition causing a thickened, rigid pericardial sac [40, 85]. The development of acute pericarditis was also observed in rabbits, rats and dogs after single doses to the heart of 16 to 20 Gy [86-88]. These experimental studies showed a threshold dose of about 15 Gy with a steep dose-response relationship (incidence of 100 % at 20 Gy).

1.3.3 Coronary artery disease

Obstruction of the blood flow in coronary arteries, responsible for blood supply to the heart, is referred to as coronary artery disease [10]. Mild obstruction due to narrowing of the coronary arteries leads to angina (discomfort due to ischemia of the heart muscle) whereas severe blockage leads to myocardial infarction (heart attack) which on its turn leads to acute heart failure. Atherosclerosis is the major underlying pathogenesis causing coronary artery disease. It can be described as a chronic inflammatory disease of the arterial wall in which the buildup of plaques in the intima impairs normal vascular functioning (Figure 5). These plaques are characterized by accumulation of lipids and fibrous elements [89]. The development and progression of atherosclerosis is a complex process with many players. The presence of plaques leads to narrowing of the artery and, upon rupture of a plaque, even to blockage of the artery [90].

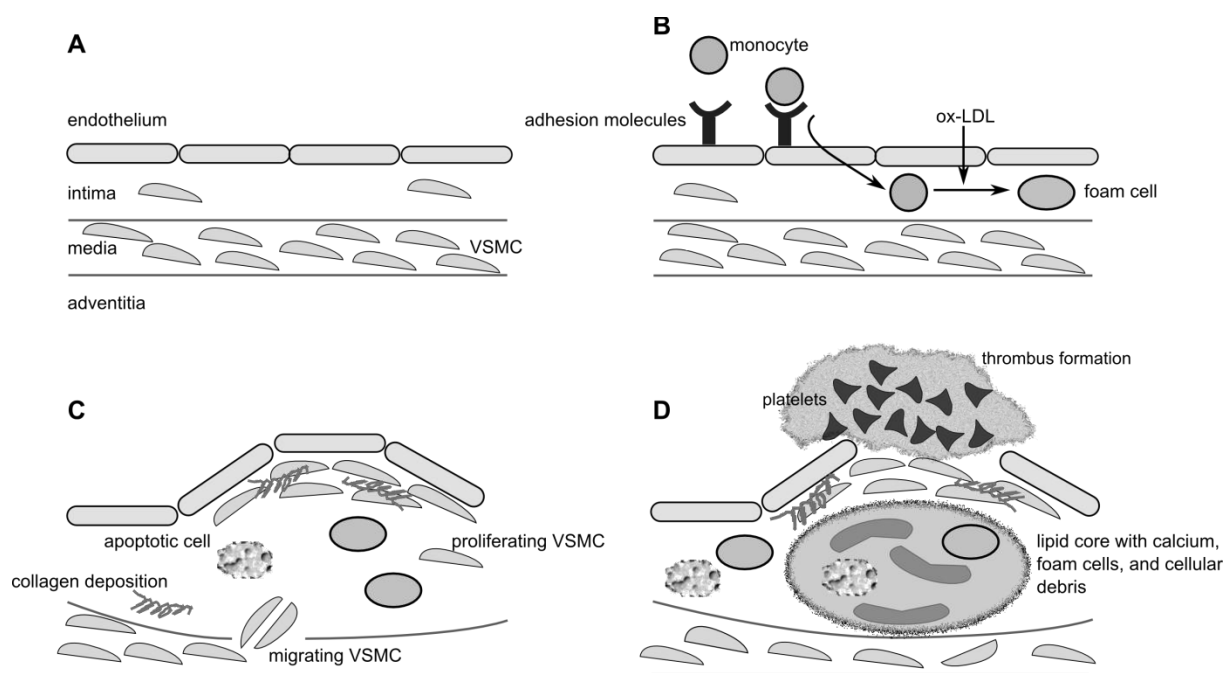


Figure 5: Schematic overview of the development of an atherosclerotic lesion. In all steps, inflammation plays an important role. **A.** A healthy artery with a well-functioning intact endothelium, a tunica intima, media and adventitia. Vascular smooth muscle cells (VSMC) are mainly found in the tunica media but also in the tunica intima. **B.** One of the initiating steps is the expression of adhesion molecules on the endothelium and the subsequent attraction of inflammatory blood cells (mainly monocytes). These monocytes will transmigrate to the intima where they will mature to macrophages which will then transform to foam cells upon the uptake of ox-LDL. **C.** Further progression to an atherosclerotic plaque includes the transmigration of VSMC from the tunica media into the intima and the proliferation of VSMC in the intima. There is also an enhanced production of extracellular matrix molecules such as collagen, elastin and proteoglycans. Macrophages, foam cells and VSMC can die, and released lipids will accumulate in the central region of the plaque, also denoted the lipid or necrotic core. **D.** When a plaque ruptures it will induce thrombosis which is the major complication. The blood component will get in contact with the tissue factors present in the interior of the plaque triggering the formation of a thrombus which will hamper or even obstruct blood flow. Figure based on [91]. VSCM = vascular smooth muscle cell, ox-LDL = oxidized low density lipoprotein

Normal rodents are resistant to atherosclerosis since they have low plasma levels of pro-atherosclerotic low-density lipoprotein (LDL). Therefore, atherosclerosis-prone animal models were developed. For example, ApoE $-/-$ and LDL receptor $-/-$ mouse models are commonly used [92, 93]. Apolipoprotein E (ApoE) is an important glycoprotein in the transport and metabolism of lipids and lack of a functional ApoE gene leads to an altered plasma lipid profile, and the rapid development of atherosclerotic lesions. Mice that lack a functional LDL receptor gene also have an altered plasma lipid profile, with elevated LDL

levels. LDL receptor deficient mice will develop atherosclerosis when fed with a lipid-rich diet.

The effect of ionizing radiation on the development and progression of atherosclerosis has been investigated in various animal models, which has been reviewed in [10]. For example, Stewart and coworkers have examined the development and progression of atherosclerotic lesions in ApoE $-/-$ mice after single dose irradiation (14 Gy) of the neck region [94]. There was no major increase in the total plaque burden in the exposed carotid arteries but the quality of the plaques was changed, having inflammatory characteristics. Indeed, plaques showed a macrophage-rich core, low collagen content and intraplaque hemorrhage, which are known to render human atherosclerotic plaques unstable and prone to rupture. They also observed the presence of atypical swollen endothelial cells. It is hypothesized that radiation-induced changes of endothelial function together with radiation-induced endothelial cell death and exposure of thrombotic elements of the underlying subendothelium leads to chronic inflammation and the development of a vulnerable plaque [94]. Gene expression profiling of ApoE $-/-$ mice exposed to an acute dose of 16 Gy also revealed the up-regulation of inflammation-related pathways [95]. Further research in the lab of Stewart showed that a more clinically relevant fractionated irradiation scheme (20 x 2 Gy in 4 weeks) also predisposes to the formation of an inflammatory plaque [96]. Remarkable, acute lower dose irradiation (8 Gy) of ApoE $-/-$ mice did not predispose to an inflammatory plaque, but did accelerate the development of atherosclerosis, as demonstrated by an increased number of plaques. Overall, they concluded that exposure to high dose ionizing radiation accelerates the atherosclerotic process in the presence of other risk factors (e.g. high fat diet), and predisposes to the development of a vulnerable inflammatory plaque prone to rupture [10].

With low doses and dose rates of radiation, the picture is different. Mitchel and coworkers have exposed ApoE $-/-$ mice to low doses of radiation (0.025 – 0.5 Gy) at either high (150 mGy/min) or low (1 mGy/min) dose rate [97]. The mice were exposed at an early stage of atherosclerotic disease (2 months old) or at a late stage of atherosclerotic disease (8 months old). Doses of 0.025 to 0.050 Gy, given in both low and high dose rate, induced a protective effect by slowing the formation of new lesions and the increase in the size of existing lesions, in mice exposed at an early stage. High dose rate exposure increased, however, the progression of lesion severity. The effect for mice exposed at a late stage of atherosclerotic disease with low dose rate was similar as that for mice exposed at an early stage. On the other hand, high dose rate exposures protected against progression of lesion severity, opposite to

what was observed in mice exposed at an early stage. Additional experiments with ApoE $-/-$ mice with reduced p53 functionality (Trp53 $+/-$) revealed an important role for p53 in atherosclerosis progression [98]. For example, protective effects of low dose radiation delivered at both low and high dose rate were observed in Trp53 normal mice exposed at a late stage of atherosclerotic disease. On the other hand, with the same irradiation procedure, detrimental effects were observed in Trp53 $+/-$ mice exposed at a late stage of atherosclerotic disease. Overall, these findings raised the importance of dose rate effects and p53 functionality on the development of atherosclerosis. Furthermore, their findings point out that a linear extrapolation of the effects at high doses to low doses is not appropriate.

1.3.4 Congestive heart failure

Congestive heart failure is described by a compromised blood pumping function of the heart, due to a reduced capacity of the heart muscles, causing under-perfusion of the body tissues. The underlying pathologies are various and include IHD, hypertension, valvular heart disease, cardiomyopathies, and congenital heart disease [99]. Rats that received single doses of at least 15 Gy to the heart developed congestive heart failure within their normal lifespan [88]. Further radiobiological research has revealed an important role for radiation-induced decrease in capillary density. Areas of decreased capillary density in the heart are characterized by focal loss of the endothelial cell marker alkaline phosphatase [100]. Progressive reduction of capillary density leads to ischemic necrosis, fibrosis and death of cardiac myocytes (muscle cells) in these areas. This myocardial degeneration is associated with the first symptomatic signs of congestive heart failure, a slight drop in left ventricle ejection fraction [40]. This reduced cardiac function is maintained in a steady-state for a certain period, due to *in vivo* compensatory mechanisms, and fatal congestive heart failure is only observed on the long-term [101]. Indeed, with *ex vivo* experiments, cardiac function deteriorated more rapidly [102].

Also with lower doses, myocardial damage has been observed. For instance, mild alterations in cardiac function in ApoE $-/-$ mice after exposure to 2 Gy was observed, which was however not deteriorated over time [103]. Histological examination revealed functional damage to the microvasculature as indicated by a focal loss of alkaline phosphatase. More recently, Monceau and coworkers have exposed the heart of ApoE $-/-$ and wild-type mice to doses of 0.2 Gy [104]. Mild but significant alterations in cardiac function were observed in

both mouse strains after exposure to 0.2 Gy. The progression of cardiac dysfunction remained, however, stable over the whole study period (60 weeks) suggesting the occurrence of compensatory mechanisms. Whereas in ApoE $-/-$ mice cardiac damage was the consequence of reactive fibrosis in response of inflammatory signaling, this was the consequence of reparative fibrosis induced by the loss of cardiac myocytes in wild-type mice. Overall, ApoE $-/-$ mice were more radiosensitive. This implies that atherosclerosis predisposition enhances and accelerates the structural deterioration of the heart after exposure to low doses of ionizing radiation, and can thus be considered as a risk factor.

1.3.5 Hypotheses for underlying molecular and cellular mechanisms

Nowadays, coronary artery disease is considered the major cardiovascular complication in patients that have received radiotherapy for thoracic malignancies [98]. Schultz-Hector and Trott have created a schematic representation of the most important steps in coronary artery disease (consequence of atherosclerosis in the coronary arteries), and the interaction with radiation effects (Figure 6) [43]. There are two hypotheses for the molecular and cellular mechanisms that increase the morbidity and mortality of coronary artery disease following high to moderate dose radiation exposure. The first hypothesis states that radiation interacts with the pathogenesis of age-related atherosclerosis, as such accelerating atherosclerosis development.

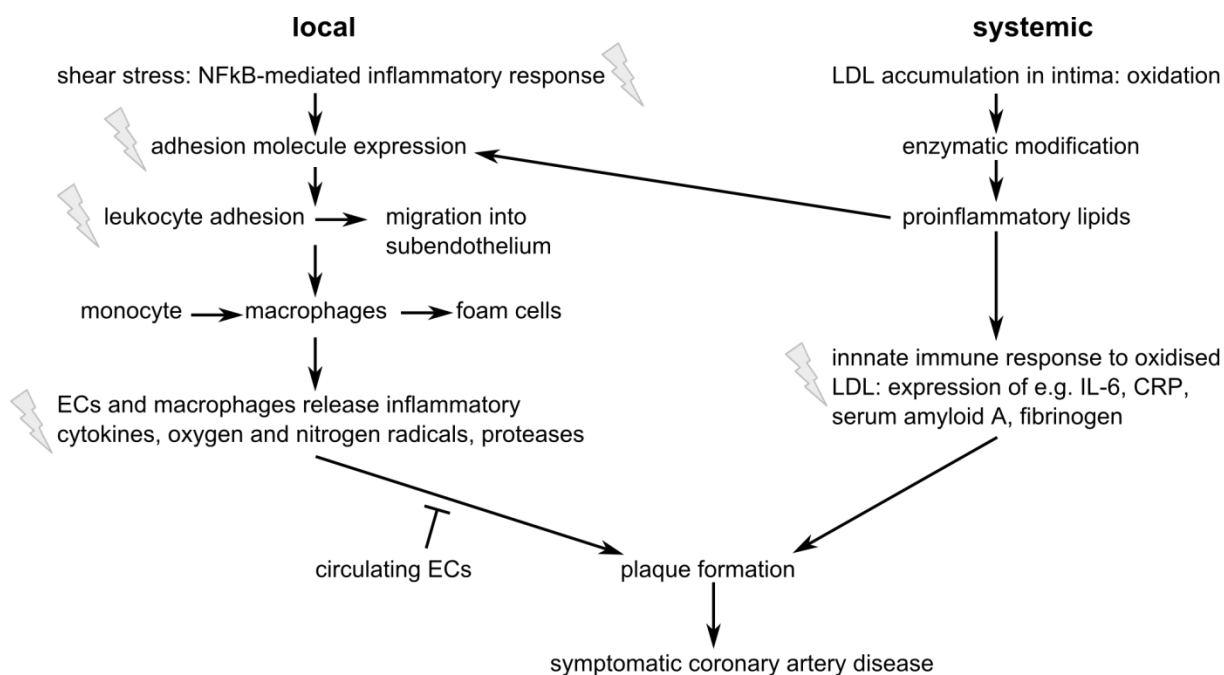


Figure 6: Overview of the major steps in the pathogenesis of coronary artery disease on the local and systemic level. Flashes indicate events that were also observed after radiation exposure, and which are mainly related to inflammation [41]. ECs: endothelial cells, LDL: low density lipoprotein, IL-6: interleukin 6, CRP: C-reactive protein

The second hypothesis is that radiation increases the lethality of age-related myocardial infarction by decreasing the heart tolerance to acute infarctions as a result of microvascular damage in the myocardium. These hypotheses do not stand alone, and both macro- and microvascular effects will most likely act together to produce clinical heart disease (Figure 7).

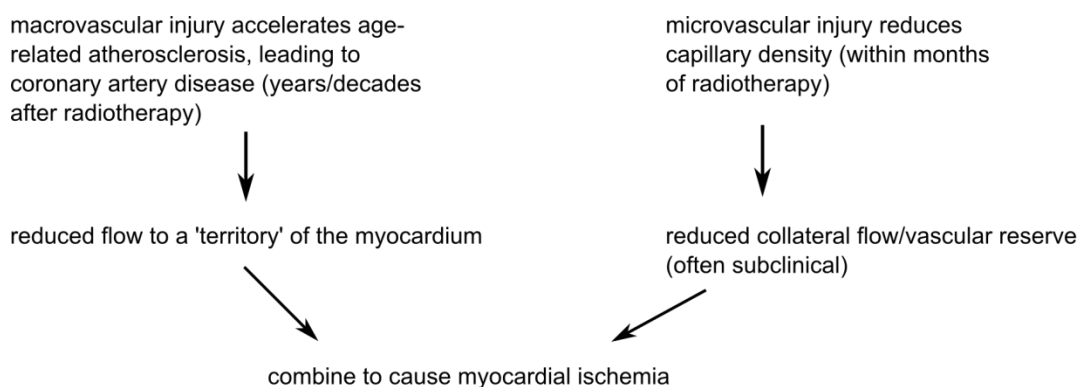


Figure 7: A theoretical overview of how radiation-induced macrovascular and microvascular pathologies can interact to cause myocardial ischemia, which may ultimately develop into clinical heart disease [43].

1.3.5.1 The role of inflammation

As indicated in Figure 6, ionizing radiation acts on the atherosclerotic process by enhancing pro-inflammatory signaling [37, 41]. Atherosclerotic plaques are formed by the migration of inflammatory cells from the bloodstream into the intima where they transform to foam cells. Endothelial expression of adhesion molecules plays an important role in this process. Radiation has been shown to up-regulate E-selectin, intercellular adhesion molecule 1 (ICAM-1) and vascular cellular adhesion molecule 1 (VCAM-1) following irradiation of endothelial cells, in a time- and dose-dependent manner [41]. For instance, exposure of endothelial cells with 5 Gy induced an increase in ICAM-1 and E-selectin expression 6 h after irradiation [105]. The transcription factor NF- κ B is involved in radiation-induced up-regulation of adhesion molecules [106]. Besides induction of adhesion molecules, cytokines such as IL-6 and IL-8, and other inflammatory molecules such as TGF- β , were shown to increase after high and moderate irradiation [107, 108]. Also, the Japanese atomic bomb survivors' cohort showed signs of a general increased state of inflammation, with increased levels of IL-6 and C-reactive protein (CRP) [109]. In addition to pro-inflammatory responses, there is evidence of pro-thrombotic changes after irradiation of the endothelium. For example, several *in vitro* and *in vivo* studies demonstrated increased levels of von Willebrand factor (VWF) and decreased levels of the anticoagulant thrombomodulin [41, 110].

1.3.5.2 What about low doses?

Although epidemiological findings suggest an increased risk of CVD after low dose radiation exposure, there is hardly knowledge about the underlying biological mechanisms. So far, experimental findings question the abovementioned hypotheses for low dose radiation exposure. For example, whereas it is assumed that high and moderate dose exposure accelerates the development of age-related atherosclerosis, Mitchel and coworkers have demonstrated that low dose exposure of mice has protective effects on atherosclerosis development and progression [97].

Furthermore, there is evidence that radiation-induced pro-inflammatory signaling holds not true for low dose irradiation. Indeed, no induction of ICAM-1 and E-selectin was observed up to 24 h after exposure to 0.3 Gy and 1 Gy, and was even decreased 4 h after irradiation [105]. This results in a decreased mononuclear cell adhesion onto the endothelium [105, 111]. There is also clinical evidence for anti-inflammatory responses of low dose radiation exposure in individuals who experience inflammatory diseases. Indeed, for decades, low dose

radiotherapy has been used for the treatment of benign inflammatory diseases [112, 113]. However, due to the debate regarding possible cancer and non-cancer risks of low dose radiation exposure, the use of low dose radiotherapy has become out of fashion nowadays [114].

Overall, it seems that effects of low dose radiation on the cardiovascular system differ to those of high dose radiation. Further research is essential to elucidate the low dose effects on the cardiovascular system, and the impact on CVD risk. This is, however, not straightforward due to the subtlety of low dose effects and the, most likely, little impact on clinical outcome. Besides the integration of epidemiology and biology, as mentioned above, pure radiobiological studies are needed. These include mechanistic studies in animal models and *in vitro* studies focused on the elucidation of molecular signaling pathways. In these studies attention should be paid, not only to dose, but also to dose-rate, fractionated exposures and radiation quality.

1.4 Endothelium as a critical target in radiation-related cardiovascular disease

1.4.1 Endothelium is the safeguard of normal vascular functioning

The endothelium is a single layer of cells that lines the interior of the vascular system and has thus a strategic position between the blood and the surrounding tissues. Endothelial cells are involved in a wide range of physiological processes, such as the regulation of vascular tone, vascular permeability, blood coagulation/fibrinolysis and inflammation, which are needed to maintain proper vascular functioning (Figure 8) [115]. Endothelial dysfunction has been observed in patients with atherosclerosis and in patients that exhibit CVD risk factors such as smoking, dyslipidaemia, obesitas, and diabetes mellitus [116], and is considered one of the first indicators of future cardiovascular morbidity and mortality [117]. It should be noted that the endothelium is also needed for angiogenesis, the process of forming new blood vessels from existing vessels [118].

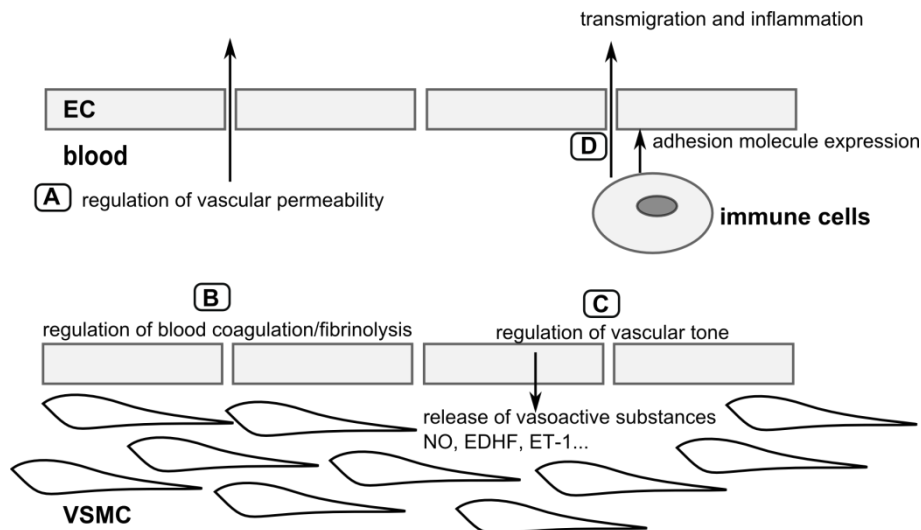


Figure 8: Overview of the major physiological functions of the arterial endothelium. **A.** The endothelium forms a selective barrier regulating the solute flux and fluid permeability between the blood and surrounding tissues [117]. **B.** The formation of a thrombus or blood clot is referred to as coagulation and the breakdown of a thrombus is referred to as fibrinolysis. Normal endothelium has anti-thrombotic and pro-fibrinolysis properties, and actively represses platelet adhesion and aggregation. Vessel damage or exposure to pro-inflammatory molecules will shift the balance towards more pro-thrombotic/anti-fibrinolysis actions [119, 120]. **C.** To regulate vascular tone, the endothelium releases various vasodilatory factors such as NO and EDHF, or vasoconstrictive factors such as ET-1 which will modify VSMC function [121]. **D.** In the case of inflammation, endothelial

permeability will be increased. Endothelial cells will also recruit immune cells via the expression of adhesion molecules, and mediate their transmigration towards the inner vascular wall [120]. Figure based on [115]. ECs: endothelial cells, VSMC: vascular smooth muscle cells, NO: nitric oxide, EDHF: endothelium-derived hyperpolarizing factor, ET-1: endothelin 1.

The endothelium displays phenotypical and functional heterogeneity depending on the vascular bed and tissue it is situated in [122, 123]. The major function of arteries and veins is the conduit of blood through the body. Capillaries, on the other hand, are the major exchange vessels and the capillary endothelium is thus very thin and usually fenestrated to ensure optimal diffusion of oxygen and nutrients between the blood and underlying tissue [123]. Arterial endothelial cells are sensible to disturbed flow at branching points and curvatures in the arterial system, which are, consequently, 'hotspots' for inflammation, coagulation and atherosclerosis [123]. A healthy arterial endothelium mediates vasodilatation and actively suppresses thrombosis, vascular inflammation and inhibits vascular smooth muscle cell proliferation and migration [124].

Nitric oxide (NO) is a key signaling molecule produced by endothelial cells [125]. NO is produced by the enzyme NO synthase (NOS) through the conversion of L-arginine to L-citrulline. Four isoforms of NOS exist: neuronal NOS (nNOS), inducible NOS (iNOS), endothelial NOS (eNOS) and mitochondrial NOS (mNOS) [125]. Production of NO by eNOS is stimulated by shear stress and compounds such as acetylcholine, arachidonic acid, bradykinin, thrombin, and 5-hydroxytryptamine [116, 126]. Besides being the most potent vasodilator, NO has anti-inflammatory and anti-atherosclerotic actions. It inhibits, amongst others, leukocyte adhesion, vascular smooth muscle cell proliferation and limits platelet adhesion and aggregation [116]. Reduced NO bioactivity, due to an imbalance between its synthesis and breakdown or due to an impaired response of vascular smooth muscle cells, is associated with endothelial dysfunction and it will render the blood vessel prone to vasoconstriction. Furthermore, it will promote inflammation, thrombosis and the proliferation of vascular smooth muscle cells [116, 125].

1.4.2 Endothelial dysfunction: molecular and cellular mechanisms

CVD risk factors associated with endothelial dysfunction include hypertension, smoking, dyslipidaemia, and aging. A common underlying cellular mechanism leading to endothelial

dysfunction is oxidative stress [127]. Oxidative stress is defined as an imbalance between the generation of reactive oxygen species (ROS) (Figure 9) and the activity of enzymatic and non-enzymatic antioxidant systems [128]. At physiological levels, ROS are important signaling molecules but at higher concentrations, ROS causes cell injury by oxidative damage to DNA, lipids and proteins, and may result in cell death [129]. Besides cellular damage, oxidative stress leads to a decrease in NO bioavailability, premature senescence and mitochondrial dysfunction in endothelial cells.

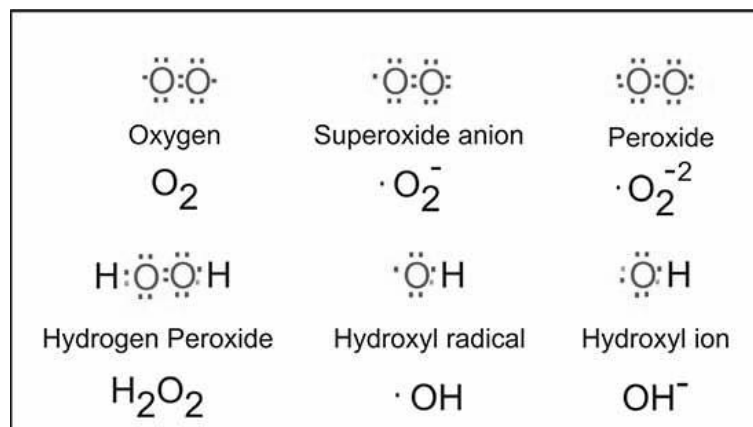


Figure 9: Electron structures of common ROS. Below each structure, its name and chemical formula are given. • represents an unpaired electron [130].

1.4.2.1 Decreased NO bioavailability

When there is overproduction of superoxide radicals ($\cdot\text{O}_2^-$), it interacts with NO to form the reactive nitrogen species (RNS) peroxynitrite (ONOO^-) which decomposes to form the harmful ROS hydroxyl radical ($\cdot\text{OH}$) and nitrogen dioxide radical ($\text{NO}_2\cdot$) [129]. NO levels are reduced because superoxide and NO react with each other three times faster than superoxide would react with superoxide dismutase (SOD), the major antioxidant enzyme that regulates superoxide levels [131]. Besides the cellular injury induced by $\cdot\text{OH}$ and $\text{NO}_2\cdot$, peroxynitrite can lead to eNOS uncoupling. In this phenomenon, eNOS will produce superoxide at the expense of NO [132]. The enzyme requires tetrahydrobiopterin for the formation of NO. Peroxynitrite oxidises tetrahydrobiopterin to its inactive form causing in this way eNOS uncoupling. Other ROS such as hydrogen peroxide can also cause eNOS uncoupling. Thus, in a situation of oxidative stress, eNOS loses its function as an essential regulator for proper

cardiovascular functioning and becomes a superoxide producing enzyme. This creates a vicious circle, further aggravating oxidative stress [127].

1.4.2.2 Premature senescence

Vascular ageing predisposes to CVD, even in the absence of other risk factors [133]. At the cellular level, vascular ageing is related to senescence of endothelial cells [134]. Endothelial senescence is associated with increased ROS production, decreased NO availability and increased production of pro-inflammatory molecules thus favoring an atherosclerotic endothelium [135]. There is *in vivo* evidence for the presence of senescent endothelium in atherosclerotic lesions. Markers of senescence such as senescence-associated β -galactosidase (SA- β -gal) activity and telomere shortening have been used to identify senescent endothelial cells in atherosclerotic lesions [136]. Using SA- β -gal activity as a marker, the presence of senescent endothelial cells was observed in atherosclerotic lesions in human aorta and coronary arteries [137, 138]. Examination of telomere length of endothelial cells revealed that those originating from diseased portions of arteries had shorter telomeres compared to those from healthy parts [139].

Senescence has been described for the first time by Hayflick and colleagues in 1965 who observed proliferation arrest of fibroblasts after a certain period in culture [140]. Later it has been discovered that this was due to the attrition of telomeres, and is referred to as replicative senescence. Telomeres are specialized structures at the 3' end of chromosomes existing of non-coding double-stranded repeats of guanine-rich DNA sequences (TTAGGG) [141]. The presence of telomeres ensure that the stability and integrity of the genome is maintained [142]. During DNA replication, DNA polymerases cannot copy all bases in the 3' end which makes that this end is not replicated completely. As a consequence, telomere length decreases gradually with each replication and eventually leads to telomere uncapping, which is a disruption of the protective cap at the end of a telomere. This seems to be sensed as DNA damage by the cell and induces a DNA damage response, which can initiate senescence [143].

On the molecular level, senescence is established and maintained by the p53 and p16-retinoblastoma protein (pRB) pathways [144] (Figure 10). The DNA damage response will mainly engage the p53 pathway, although secondary engagement of the p16-pRB pathway has been reported as well.

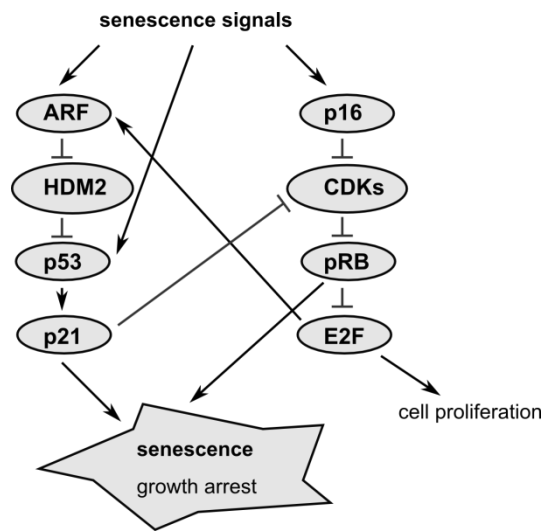


Figure 10: Simplified overview of two major senescence-inducing molecular pathways, the p53 and the p16-pRB pathway. Both pathways seem to act reciprocally. When p53 is active, it will induce the expression of p21, a CDK inhibitor. CDKs phosphorylate pRB leading to its inactivation. Thus, p53 induces senescence mainly through pRB activation via p21. p16 is also a known CDK inhibitor that prevents pRB phosphorylation and inactivation. pRB activates senescence by suppressing E2F, a transcription factor that stimulates the expression of genes needed for cell proliferation. E2F can also induce ARF expression, which negatively regulates HDM2. p53 is negatively regulated by HDM2. Figure adapted from [144]. pRB = retinoblastoma protein, CDK = cyclin-dependent kinase, E2F = E2F transcription factor, ARF = ADP-ribosylation factor, HDM2 = E3-ubiquitin-protein ligase

Senescence can also occur independently of telomere shortening, which is then referred to as stress-induced premature senescence. Indeed, various stresses such as lack of nutrients and growth factors, chromatin perturbations, improper cell contacts or oxidative stress can activate the intracellular senescence cascade prematurely [143]. In particular, oxidative stress is of importance and induces or accelerates senescence on many levels. For instance, oxidative stress has been demonstrated to accelerate telomere shortening in endothelial cells [145]. Furthermore, ROS induce DNA damage initiating a DNA damage response with engagement of p53 as a consequence [146]. NO availability, which has been shown to inhibit senescence in endothelial cells, is decreased by ROS [147]. Finally, ROS-related mitochondrial dysfunction has been suggested to be associated with endothelial senescence [135].

1.4.2.3 Mitochondrial dysfunction

Mitochondria are considered the powerhouse of the cell as they produce adenosine-triphosphate (ATP), the ultimate cellular fuel, by a process called oxidative phosphorylation [148]. In this process, electrons are shuttled within the respiratory transport chain on the inner mitochondrial membrane through four complexes, I (NADH dehydrogenase), II (succinate dehydrogenase), III (cytochrome c oxidoreductase) and IV (cytochrome c oxidase). In the final step, when the electrons are transferred, molecular oxygen is reduced to water at complex IV. As a consequence, a proton gradient is established along the respiratory transport chain which leads to the conversion of adenosine-diphosphate (ADP) to ATP. As a byproduct of the respiratory chain, ROS are formed, making mitochondria the major source of endogenous ROS [148, 149]. Lately, mitochondria have been recognized not only to be responsible for energy generation but also to be involved in other cellular processes [150]. In endothelial cells, these include the regulation of cellular calcium levels for signal transduction, sensing blood oxygen levels, production of NO, the activation of apoptosis, i.e. cellular death, or the induction of senescence [151, 152].

Mitochondria are not only a major source, but also a critical target of ROS. Many CVD risk factors can affect endothelial mitochondria via various mechanisms resulting in an increased ROS production [153]. Excessive mitochondrial ROS production will cause damage to the mitochondrial proteins, membranes and DNA, resulting in even more ROS production. In this vicious circle, mitochondrial dysfunction is further enhanced [154].

The mitochondrial DNA (mtDNA) is a particular vulnerable radiation target due to its location close to the respiratory transport chain, the major source of endogenous ROS. Furthermore, it lacks protective histones, it has a limited repair capacity and it has a high exon to intron ratio [155]. The mtDNA is a 16 kb circular double stranded genome that codes for 13 proteins that are part of the electron transport chain and for mitochondrial-specific rRNAs and tRNAs [156] (Figure 11).

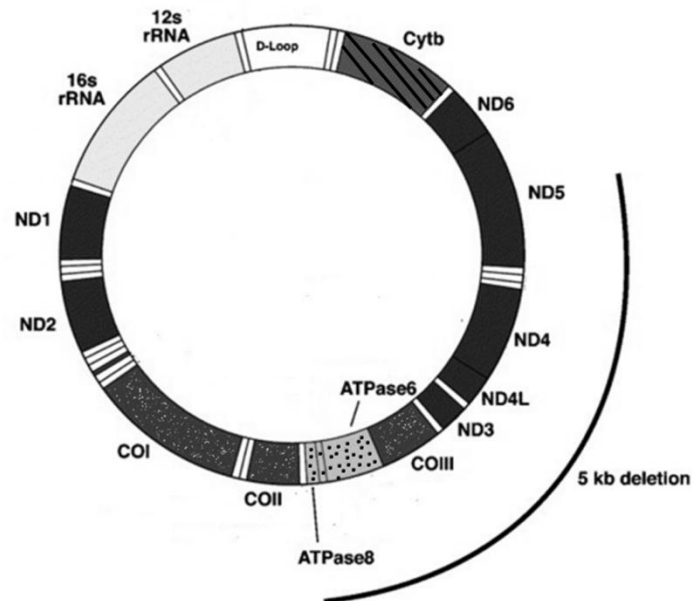


Figure 11: Schematic overview of the human mitochondrial genome. The coloured blocks represent the 22 tRNA genes (white), two ribosomal RNA genes (light grey) and genes encoding for 13 polypeptides that are part of the respiratory transport chain: complex I (dark grey), complex III (crosshatched), complex IV (white dotted) and ATP synthetase (black dotted). The position of the common deletion (5 kb deletion) is indicated as well. Figure adapted from [157].

Since mtDNA codes for components of the electron chain, mutations in these genes may lead to impairment of oxidative phosphorylation which may further increase ROS production which in turn will even generate more mitochondrial and cellular damage [33]. Damage to the mitochondrial genome, and in particular the common deletion (CD), has also been observed in atherosclerotic lesions [158, 159]. The CD is a deletion of a site of 4977 bp that is flanked by two 13 bp direct repeats [160]. It is proposed that DNA damage between these repeats results in inappropriate pairing during mtDNA replication causing the deletion. In this way the lesion is amplified during mtDNA replication which makes it a very useful marker for even very low levels of damage.

1.4.3 *In vitro* endothelial models

The recognition of the endothelium as a central regulator of the cardiovascular system has led to a boom in endothelium-related research. One of the milestones was the first successful isolation and subsequent cultivation and characterization of endothelial cells *in vitro*, in the 1970s [122]. Jaffe and colleagues and Gimbrone and colleagues reported independently the

isolation of endothelial cells from human umbilical veins (HUVEC – human umbilical vein endothelial cells) [161, 162]. Since then many studies have relied on the use of HUVEC since they are relatively easy to obtain. Although originating from large vessels, HUVEC are unique since they exhibit endothelial properties that are intermediate between those of large vessels (e.g. the aorta) and those of the microvasculature [163]. EA.hy926 cells, which are an immortalized derivative from HUVEC, are commonly used as well [164]. Both HUVEC and EA.hy926 cells were used in this PhD project. A more extensive discussion of their characteristics can be found in chapter three.

It should be noted that *in vitro* endothelial cell models are not limited to HUVEC and EA.hy926 cells. Endothelial cells may be isolated from other sources in the human body as well, such as the dermal microvasculature, coronary arteries and the pulmonary vasculature. However, these are usually not easy to obtain and at best only a small amount of material will be available [165]. In addition, these primary cell cultures cannot be kept in long-term cultures as they start to lose their endothelial cell characteristics. Therefore, immortalized derivatives of these primary cells have been established; like EA.hy926 cells are a derivative from HUVEC. Immortalized cells are characterized by their ability to overcome senescence and can be kept in culture for long times [166]. These immortalized derivatives, however, also exhibit tumor cell characteristics [167]. For instance, immortalized human coronary artery endothelial cells (transfected with human telomerase reverse transcriptase (hTERT)) showed 40% of aneuploidy at low passage number and 100% of aneuploidy at high passage number [167].

Of course, *in vitro* endothelial models, although useful, are not fully representative for the *in vivo* situation. Yet, advances have been made such as the development of co-culture models where endothelial cells are cultured with vascular smooth muscle cells to study the atherosclerotic process [168, 169]. Also, 3-D cultures, where endothelial cells are grown in a sort of matrix allowing the formation of tubule-like structures are more and more used to study angiogenesis [170, 171]. A recent review has described in detail the use of these co-culture and 3-D culture models in radiation research [172]. For practical and time-related reasons we decided, however, to focus on traditional single layer culture of endothelial cells.

1.4.4 The effect of ionizing radiation on the endothelium

Gaining insight into the endothelial response to ionizing radiation exposure is not only of importance for understanding the development of radiation-related CVD, but also for optimizing cancer treatment. For instance, adverse reactions in the surrounding healthy tissue of the tumor are related to the radiation-response of the microvasculature in the tissue of concern. Also, tumor growth is highly dependent on abundant blood supply which is maintained by a rich vascular network [173]. The tumor vasculature has thus received attention as a potential target in radiotherapy [174]. Understanding the effects of radiotherapy on tumor endothelium can improve treatment regimes. Since tumor endothelium differs in many aspects to normal endothelium [175], this is not in the scope of this PhD research.

The interest of this PhD lies in the characterization of the endothelium radiation response, in particular to low doses, in the context of radiation-related CVD. Below, an overview is given of classical cellular radiation effects and how these may affect endothelial functioning. Next, the impact of ionizing radiation on mitochondrial function and on senescence is discussed. Finally, attention is paid to the contribution of new technologies such as high throughput transcriptomic profiling which allow a better understanding of the underlying molecular signaling pathways.

1.4.4.1 DNA-targeted effects

Ionizing radiation is known to induce a wide range of DNA lesions, such as base damage, DNA cross links, single strand breaks and double strand breaks (DSB), in a direct manner but also indirectly through the formation of ROS [176, 177]. Upon DNA damage, a DNA damage response is initiated and the cells will activate cell cycle checkpoints which can slow down or stop cell cycle progression [178]. This gives cells the time to repair the damaged DNA or prevents division when chromosomes are damaged or incompletely replicated. If the cells fail to repair the DNA, they can go into apoptosis [179].

In particular, DSB will lead to a high lethality of the affected cells [180]. At the site of DSB damage, the histone H2AX is phosphorylated (referred to as γ -H2AX) by kinases such as ataxia telangiectasia mutated (ATM) and ataxia telangiectasia and Rad3-related protein (ATR) resulting in the formation of γ -H2AX foci [176]. These foci will recruit DNA repair proteins to the DSB sites. It has been shown that there is a 1:1 relationship between the

amount of DSB and the γ -H2AX foci formed [181]. Visualization and quantification of γ -H2AX foci has become standard in assessing radiation-induced DNA damage.

Irreparable DSB can cause cellular apoptosis, or premature senescence (described below). Endothelial apoptosis has implications on both the micro- and macrovasculature. Namely, endothelial cell death in the microvasculature leads to a decrease in capillary density. Also, endothelial apoptosis has been related to the development of atherosclerosis [182, 183] as it may compromise regulation of vascular tone, and increase the proliferation and migration of VSMC [184]. Furthermore, thrombosis, the major complication of atherosclerosis, can be triggered by endothelial cell death [183]. It should be noted that radiation-induced endothelial cell apoptosis is not solely a consequence of DNA damage. Indeed, ionizing radiation can act on the cellular membrane of endothelial cells as well, generating ceramide which can induce apoptosis [185].

Whereas high doses are known to induce apoptosis in endothelial cells [186], less is known about the effect of low doses. There are indications that, regarding apoptosis, endothelial cells display a non-linear dose relationship. Rödel and coworker have demonstrated a discontinuous induction of apoptosis with a relative maximum at 0.3 and 3 Gy and a relative minimum at 0.5 Gy, in endothelial cells activated with TNF- α [187]. Another study, showed no increase in apoptotic endothelial cells after exposure to 0.2 Gy, but only after exposure to 5 Gy [188].

1.4.4.2 Radiation-induced mitochondrial dysfunction

There is a lot of interest in radiation-induced mitochondrial dysfunction seeing the implications it has on CVD [148]. Mitochondrial dysfunction is closely related to oxidative stress, being both a target and source of ROS. Initially, ionizing radiation causes the formation of water radiolysis products including hydroxyl radicals ($\cdot\text{OH}$), hydroperoxyl radicals ($\text{HO}_2\cdot$) and hydrogen peroxide (H_2O_2). These are unstable and disappear within less than 10^{-3} seconds, except for H_2O_2 [189]. However, following irradiation, oxidative stress is observed after longer time periods due to an increase in the endogenous cellular production of ROS [190]. Mitochondria are believed to be the major source of these radiation-induced secondary ROS, although other sources may contribute as well. For instance, Leach and coworkers have demonstrated that, between 1 and 10 Gy, the amount of ROS producing cells increased with

the dose, which they suggested was dependent on radiation-induced propagation of mitochondrial permeability transition⁶ via a Ca^{2+} -dependent mechanism [192].

Since mitochondria, and in particular mtDNA, are also a critical target of ROS, measures of mtDNA damage has been used to determine deleterious effects of ionizing radiation. Increased accumulation of the CD following exposure to ionizing radiation has been detected in various studies [160, 193, 194]. The measurement of CD by quantitative real-time polymerase chain reaction (PCR) has been proposed as a sensitive marker to detect low levels of oxidative damage to the mtDNA [160]. An increased accumulation of the CD was observed in several human fibroblast cell lines, after exposure to doses as low as 0.1 Gy [194]. Interestingly, increased accumulation of the CD was also observed in bystander cells, i.e. cells that were cultured in conditioned medium coming from 0.1 Gy irradiated cells.

However, whether low doses of ionizing radiation have an impact on mitochondrial function is not fully resolved yet. For instance, an *in vivo* study by Barjaktarovic and coworkers investigated the effects of 0.2 and 2 Gy irradiation on cardiac mitochondria [195]. Four weeks after exposure, cardiac mitochondria were isolated from C57BL/6N mice and subjected to proteomic and functional analysis. Whereas with 2 Gy both functional impairment of mitochondria and alterations in the mitochondrial proteome were observed, only a few alterations in the mitochondrial proteome and no effect on mitochondrial function was observed with 0.2 Gy.

1.4.4.3 Radiation-induced premature senescence

Ionizing radiation is a well-known stressor that induces premature senescence in cells (Figure 10). The culprit is most likely severe irreparable radiation-induced DSB [196], but also radiation-induced accelerated telomere attrition has been suggested [197]. Also, oxidative stress is a major player in radiation-induced senescence and is involved in both radiation-induced DNA damage and accelerated telomere attrition [145, 197].

In several *in vitro* studies, it has been demonstrated that ionizing radiation induces endothelial cell senescence, mainly with exposure to higher radiation doses [198-201]. Most studies confirm that radiation-induced premature endothelial senescence is implemented by

⁶ The mitochondrial permeability transition occurs when the mitochondria open permeability pores, present in the inner mitochondrial membrane, as such increasing the permeability to ions and solutes with a mass up to about 1500 Da. Opening of the mitochondrial permeability pores is associated with the loss of mitochondrial membrane potential which is known to induce the formation of ROS [191].

engagement of the classical DNA damage response pathways, similar to replicative senescence [198, 199, 202]. For instance, Kim and coworkers observed that exposure to 4 Gy lead to a senescent phenotype in endothelial cells. An increased formation of γ -H2AX foci and consequent activation of the DNA damage response was measured, as indicated by up-regulation of p53 and p21 and down-regulation of cyclins and Rb phosphorylation [203].

An interesting study was carried out to examine the effect of chronic low dose rate (LDR) irradiation (1.4, 2.4 and 4.1 mGy/h) [204, 205]. Endothelial cells were exposed for one, three and six weeks, to see whether chronic LDR radiation changes the onset of replicative senescence, as measured by SA- β -gal activity and proliferation rate. Their findings are indicative of a threshold dose rate for the induction of premature senescence. Exposure to 1.4 mGy/h did not accelerate the onset of senescence, whereas exposure to 2.4 mGy/h and 4.1 mGy/h did. Remarkably, a senescent profile was observed when the accumulated doses received by the cells reached 4 Gy. Proteomic analysis revealed a role for radiation-induced oxidative stress and DNA damage, resulting in the induction of the p53/p21 pathway [204]. Also, a role for the PI3K/Akt/mTOR pathway was suggested [205]. In the current PhD project, the gene expression profile of these chronic irradiated endothelial cells was analyzed by means of high throughput transcriptomic profiling.

1.4.5 High throughput transcriptomic profiling

Evaluation of the subtle cellular effects of low doses of ionizing radiation is challenging. The cellular radiation response involves an intricate network of signaling pathways, governed by radiation-induced changes in gene expression [206]. Traditionally, changes in gene expression are determined by means of quantitative PCR. Since the 1990s, high throughput technologies have been developed in which the entire transcriptome can be analyzed in one go [207]. One such technology is DNA microarray which consists of a collection of individual oligonucleotide probes fixed to a solid surface [208]. These probes represent specific mRNA sequences and upon hybridization of complementary sample mRNA, the relative mRNA expression of a sample can be quantified. These new high throughput technologies are very useful as they allow a global monitoring of the complex cellular radiation response, and have thus been extensively used in radiobiology since its initial development [209]. For example, microarray technology was used to monitor the transcriptional response of endothelial cells exposed to low doses of ionizing radiation (0.02 – 0.2 Gy) [210]. Overall, they revealed

radiation-induced up-regulated expression of genes such as antioxidants (e.g. superoxide dismutase 1), heat shock proteins (e.g. HSPA8 and HSPCB), and coagulation-related genes (e.g. SERPINE1 and thrombin receptor F2R). Also, endothelin 1, an important vasoconstrictor, was up-regulated at all doses. Another study (mentioned in 1.4.3.3) has used microarray technology to investigate gene expression changes related to radiation-induced senescence (4 Gy) in endothelial cells [203]. Genes that were differentially expressed in their study were mainly related to DNA damage response and immune responses.

1.4.5.1 Microarray data analysis

Usually, microarray results are focused on single genes that are differentially expressed based on an arbitrary cut-off in terms of fold change (FC) or significance. Although this approach can reveal interesting information, the drawback is that the interaction between different genes is not taken into account. As such, single-gene analysis may miss important effects on pathways. Indeed, cellular processes often affect sets of genes acting in concert. In this way, there may be genes that are not considered important according to the pre-determined cut-offs in single gene-analysis, but that can still lead, together, to a significant change in a signaling pathway [211]. As an answer to this issue, other statistical methods for analysis of microarray data have been developed [212]. For example, Gene Set Enrichment Analysis (GSEA) is commonly used for additional analysis of microarray results [213, 214]. This method considers all of the genes in an experiment, and not only those above an arbitrary cut-off in terms of fold change or significance. In essence, GSEA ranks all the genes according to their differential expression between two conditions (e.g. irradiated versus control), after which it calculates to which extent a gene set is represented at the top or bottom of the gene ranking. The gene sets are defined based on prior biological knowledge: e.g. published information about biochemical pathways or coexpression in previous experiments [211].

Chapter 2: Thesis aims

Traditionally, cancer is considered the main health issue associated with exposure to low dose ionizing radiation. Epidemiological findings suggest that non-cancer diseases, and in particular cardiovascular disease (CVD), may be of concern as well. However, these epidemiological studies lack statistical power to evidence an increased risk of CVD following exposure to radiation doses < 0.5 Gy. Complementary radiobiological research is needed to clarify the dose-risk relationship for CVD in this low dose region.

In this PhD, it was intended to contribute to the elucidation of the underlying cellular and biological mechanisms of radiation-related CVD, with a focus on low (≤ 0.5 Gy) doses of X-rays. Since the endothelium is essential for normal vascular functioning, we chose to study the low dose radiation response of the endothelium. We used the primary human umbilical vein endothelial cells (HUVEC) and the thereof derived immortalized endothelial cell line EA.hy926 as *in vitro* endothelial cell models. In the first part of the PhD, the effects of acute low dose radiation exposure and in the second part, the effects of chronic low dose rate radiation exposure were studied.

Both HUVEC and EA.hy926 cells are commonly used in endothelial research. However, their radiation response is not fully known and it is most likely that it will differ. Therefore, we evaluated and compared, in chapter three, the response of HUVEC and EA.hy926 cells following acute radiation exposure, with a focus on low doses. For this, various well-defined endpoints were investigated including DNA damage and repair, cell cycle and apoptosis. Furthermore, we determined intracellular reactive oxygen species (ROS) levels in both HUVEC and EA.hy926 cells, in chapter four. Oxidative stress, defined as an imbalance between ROS and antioxidant defenses, is a well-known underlying factor leading to endothelial dysfunction. It is thus of interest to know whether low doses of radiation have an influence on intracellular ROS levels. Since intracellular ROS levels are closely related to mitochondrial function, it was also aimed to evaluate the effect of ionizing radiation on the mitochondrion. Optimization experiments were carried out to assess mitochondrial DNA (mtDNA), which is a vulnerable target of ionizing radiation.

In the second part, a study, in collaboration with the University of Stockholm, in the context of the European Network of Excellence DoReMi (Low Dose Research towards Multidisciplinary Integration, grant agreement 249689; 2010-2016), was carried out to investigate the effects of chronic low dose rate (LDR) γ -irradiation on HUVEC. It was observed that chronic LDR irradiation induces premature senescence which is of interest since

this is one of the underlying cellular mechanisms proposed to contribute to the development of CVD. Using microarray technology, genome-wide gene expression profiling was performed to get more insight in the underlying molecular pathways by which ionizing radiation induces premature senescence.

On the long-term, it is aimed to contribute with this PhD research to an improved assessment of CVD risk following exposure to acute and chronic low dose radiation. In particular, it is aimed to find selective biomarkers that can be used to assess cardiovascular effects in humans exposed to radiation. These biomarkers can be integrated into epidemiological studies that will be carried out to improve risk assessment. Furthermore, they can be used for risk reducing strategies such as exposure monitoring, individual risk characterization and the development of countermeasures.

**Chapter 3: Differential response to acute low dose
radiation in primary and immortalized endothelial
cells**

Modified from: Rombouts C., Aerts A., Beck M., De Vos W., Van Oostveldt P., Benotmane R., Baatout S. *Differential response to acute low dose radiation in primary and immortalized endothelial cells.* International Journal of Radiation Biology. 2013 Oct;89(10):841-50. doi: 10.3109/09553002.2013.806831.

3.1 Abstract

The low dose radiation response of primary human umbilical vein endothelial cells (HUVEC) and the immortalized derivative, the EA.hy926 cell line, was evaluated and compared. DNA damage and repair, cell cycle progression, apoptosis and cellular morphology in HUVEC and EA.hy926 were evaluated after exposure to low (≤ 0.5 Gy), intermediate (2 Gy) and high doses (5 Gy) of acute X-rays. Subtle, but significant, increases in DNA double strand breaks (DSB) were observed in HUVEC and EA.hy926 30 min after low dose irradiation (0.05 Gy). Compared to high dose irradiation (2 Gy), relatively more DSB/Gy were formed after low dose irradiation. Also, we observed a dose-dependent increase in apoptotic cells, down to 0.5 Gy in HUVEC and 0.1 Gy in EA.hy926 cells. Furthermore, radiation induced significantly more apoptosis in EA.hy926 compared to HUVEC. In conclusion, we demonstrated for the first time that acute low doses of X-rays induce DNA damage and apoptosis in endothelial cells. Our results point to a non-linear dose-response relationship for DSB formation in endothelial cells. Furthermore, the observed difference in radiation-induced apoptosis points to a higher radiosensitivity of EA.hy926 compared to HUVEC, which should be taken into account when using these cells as models for studying the endothelium radiation response.

3.2 Introduction

High radiation doses (> 5 Gy) are known to increase the risk of CVD [41]. In recent years, epidemiological data support the fact that lower radiation doses could increase the risk of CVD as well and this after much longer intervals than previously expected [215]. However for radiation doses below 0.5 Gy, these epidemiological findings are not persuasive and a better understanding of the underlying biological and molecular mechanisms is needed [53, 215]. The possible existence of a low dose risk of CVD would challenge the current radiation protection system which is based on the assumption that for non-cancer effects there is a threshold of low dose radiation below which no significant effects are observed.

It is proposed that the endothelium, the thin layer of cells that line the interior surface of the vascular system and the heart, is a critical target in ionizing radiation-related CVD [41]. The endothelium is a highly active organ system that is constantly sensing and responding to changes in the extracellular environment to maintain a normal functioning of the vascular system [120]. Endothelial dysfunction is known to be a major player in the development and progression of CVD, and in particular atherosclerosis [124, 216]. High doses of ionizing radiation are known to disturb normal functioning of the endothelium by inducing a pro-inflammatory state and inducing loss of endothelial cells [41, 217, 218]. The effects of low doses of ionizing radiation on the endothelium are only partially understood. However, the available evidence suggests that the low dose response is not a simple linear extrapolation from the high dose response. For example, low doses of ionizing radiation seem to have anti-inflammatory actions as demonstrated *in vitro* by an inhibition of leukocyte adhesion to activated endothelial cells that have been irradiated [105]. Further research, as presented in this study, is thus essential for a comprehensive understanding of the endothelium response in the low dose region, and in particular below 0.5 Gy.

There is a wide range of primary endothelial cells or immortalized endothelial cell lines available for use as *in vitro* models to study cellular and molecular changes of the endothelium upon low dose irradiation. The use of immortalized endothelial cell lines offer several advantages compared to their primary counterparts. First, the use of endothelial primary cultures is compromised by their limited lifespan and the change of endothelial characteristics during long-term culture [167]. Immortalized cell lines, on the other hand, grow faster and are easier to handle [219]. Second, experiments with primary cells obtained from different donors cannot be compared since their results may differ [220]. Immortalized

cell lines are well characterized and are proven useful in the development of standardized experimental set-ups yielding reproducible results. Nevertheless, immortalized cell lines may substantially differ from the *in vivo* situation in important aspects, due to activation of oncogenes or deactivation of tumor suppressor genes [221].

Two commonly used endothelial cell types are the primary human umbilical vein endothelial cells (HUVEC) and the EA.hy926 cell line, an immortalized derivative from a HUVEC culture. HUVEC were first isolated in 1973 by Jaffe and coworkers, which started a new area of vascular biology research acknowledging endothelial cells as important regulators of normal vascular functioning [161]. Since then, HUVEC are widely isolated and used as *in vitro* models of the endothelium. EA.hy926 is a well-established endothelial cell line derived from HUVEC. EA.hy926 was created by fusing HUVEC with human lung carcinoma cells (A549/8) [164]. The cell line has been shown to maintain, during long-term culture, endothelial characteristics such as expression of von Willebrand factor, thrombomodulin production, prostacyclin synthesis and the release of platelet-activating factor, tissue plasminogen activator and plasminogen activator inhibitor type-1 [164]. Furthermore, EA.hy926 cells have retained the capacity to form tube-like structures when cultured in Matrigel [222, 223]. However, due to the carcinoma background, these cells also have additional features that may interfere with their endothelial origin. For example, a whole genome comparative study between EA.hy926 with HUVEC indicates that more genes are constitutively expressed in EA.hy926 cells than HUVEC [224]. Assessment of endothelial phenotypical characteristics revealed a significantly higher expression of thrombomodulin and significantly higher protein C activation in EA.hy926 cells compared to HUVEC [224]. Furthermore, Claise and coworkers reported that EA.hy926 cells are more sensitive than HUVEC to the cytotoxic effects of oxidized low density lipoprotein which was associated with significantly lower activities of superoxide dismutase, catalase and selenium-glutathione peroxidase [225]. Also differences between HUVEC and EA.hy926 regarding induced expression of certain molecules important for leukocyte/endothelium interactions such as E-selectin and vascular cell adhesion molecule 1 were shown [226]. These studies seem to suggest that EA.hy926 cells are not always a suitable alternative for HUVEC depending on the aim of the research. Bearing this in mind, we compared HUVEC and EA.hy926 cells for their use in low dose radiation research.

On the cellular level, DNA is a critical target of ionizing radiation and can be damaged both in a direct and in an indirect manner. Indirect damage occurs as a result of the interaction of

DNA with reactive oxygen species that are formed in the cell following radiation exposure [177]. Subsequent cellular responses to DNA damage include gene expression changes that elicit cell cycle arrest, DNA repair and (if repair fails) apoptosis [227]. A study of these endpoints is thus essential to better understand the endothelium response towards low dose radiation. Hence we compared the radiation effects, with a particular focus on lower doses of X-rays (0.05 – 0.5 Gy), in HUVEC and EA.hy926 cells with respect to abovementioned endpoints.

3.3 Material and methods

3.3.1 Cell culture and irradiation

EA.hy926 cells (ATCC, Molsheim Cedex, France) were grown in Dulbecco's Modified Eagle Medium (DMEM) supplemented with 10% fetal bovine serum (FBS) and 1% penicillin/streptomycin (pen/strep). HUVEC (Human Umbilical Vein Endothelial Cells, ATCC) were cultivated in Medium 200 supplemented with 10 ml Low Serum Growth Supplement (LSGS) and 1% pen/strep. All cell culture supplies were purchased from Invitrogen NV/SA (Ghent, Belgium). Cell cultures were regularly tested for mycoplasma using the LookOut® Mycoplasma PCR Detection Kit (Sigma-Aldrich Co. LLC, Diegem, Belgium). Under the microscope, the cell cultures exhibited a cobblestone pattern, representative for endothelial cells. For cell cycle, apoptosis and cell morphology analysis, EA.hy926 cells were plated in T25 flasks with a density of 500,000 cells 24 h prior to X-irradiation. HUVEC were plated in T25 flasks with a density of 100,000 cells 5 days prior to X-irradiation. Medium was refreshed every two days. Cell cultures were subconfluent (i.e. a cell density of 80%) at the time of X-irradiation. Irradiation was performed with a series of X-ray doses (0.05, 0.1, 0.5 and 5 Gy) at a dose rate of 0.25 Gy/min from a Pantak HF420 RX machine (Tungsten target, 250 kV, 15 mA, 1.2 mm Al inherent and 1 mm Cu additional filtration) (Branford, Connecticut, USA). For all experiments the passage number ranged between 10 and 20 for EA.hy926 cells, and between 5 and 7 for HUVEC. The population doubling time (PDT) was defined with I, the number of cells seeded, F, the number of cells obtained, and T, the incubation time which was 2 days for EA.hy926 cells and 1 week for HUVEC:

$$PDT = 2T * \ln 2 / \ln\left(\frac{F}{I}\right)$$

The population doubling time was on average 7 h for EA.hy926 cells and 25 h for HUVEC.

3.3.2 Immunocytochemistry for phosphorylated H2AX histone (γ -H2AX) analysis

EA.hy926 cells and HUVEC were plated onto glass coverslips in 4-well plates with a density of 50,000 and 35,000 cells per coverslip, respectively, and grown to confluence. X-irradiation was then performed with a series of doses (0.05, 0.1, 0.25, 0.5 and 2 Gy). At various time points after irradiation (30 min, 2 h and 24 h), cells were fixed in 4% paraformaldehyde (Merck KGaA, Darmstadt, Germany) in phosphate-buffered saline (PBS) (Invitrogen NV/SA) (pH 7.4) for 10 min at room temperature. Afterwards cells were washed with PBS and permeabilized in 0.25% Triton (Sigma-Aldrich Co. LLC) in PBS for 5 min. Subsequently, cells were probed with mouse anti- γ -H2AX antibody (ab18311, Abcam, Cambridge, UK) (1:300 dilution) and incubated overnight at 4°C. The next day cells were washed with PBS and stained with goat anti-mouse fluorescein isothiocyanate (FITC)-labeled antibody (Sigma-Aldrich Co. LLC) (1:300 dilution) for 1 h at 37°C. Both antibody dilutions were prepared in 3% bovine serum albumin (BSA) (Sigma-Aldrich Co. LLC) in PBS. Following this, three washing steps were performed with PBS and two with MilliQ after which the coverslips were mounted on a microscopic slide with Vectashield containing 4',6-diamidino-2-phenylindole (DAPI) (Vector Laboratories, Brussels, Belgium).

3.3.3 Automated fluorescence microscopy and image analysis

A fully automated inverted fluorescence microscope (Nikon, TE2000-E, Nikon Instruments, Paris, France), equipped with motorized XYZ stage, emission and excitation filter wheels, shutters and a triple dichroic mirror (436/514/604) was used (UGent). Samples were magnified with a 40X Plan Fluor oil objective (numerical aperture 1.3) and images were acquired with an Andor Ixon EMCCD camera. For each coverslip, a mosaic of 25 fields was acquired with a lateral spacing of 190 μ m between fields (corresponding to the size of the field of view) and each field was acquired as a z-stack of 5 planes axially separated by 1 μ m. Images were analyzed with ImageJ software [228] using the INSCYDE toolbox (available from <http://www.limid.ugent.be/downloads>) [229]. This toolbox uses pre-defined algorithms to segment nuclei and γ -H2AX spots in the DAPI and FITC channel, respectively. Only those spots that are present inside a nucleus are included in the calculation of γ -H2AX spot number. Furthermore, spot occupancy, which reflects the area of the nucleus that is covered with spots, is calculated. A manual check-up of the analysed images has been performed to exclude errors

in the segmentation process. On average 250 nuclei for HUVEC and 800 nuclei for EA.hy926 cells were analyzed per sample and 2 biological replicates were screened per condition.

3.3.4 Cell cycle analysis

Cells were trypsinized 24 h or 48 h after X-irradiation (0.1, 0.5 and 5 Gy), washed with PBS and then fixed with ethanol (80%) for minimum 1 h at 4°C. Afterwards, cells were washed with PBS and stained with propidium iodide (PI) solution (50 µg/ml PI + 1% RNase A) (Sigma-Aldrich Co. LLC) for 45 min at 37°C. PI fluorescence of a minimum of 10,000 cells was measured by flow cytometry (Coulter Epics XL-MCL, Beckman Coulter, Suarlée, Belgium). Cells in G0/G1, S and G2/M phase were determined after filtering for doublets and aggregates. First, the peak that represents G0/G1 phase (n) was decided based on the intensity of the PI signal. Next, the G2/M phase ($2n$) was identified as being two times the mean intensity of the PI signal of the G0/G1 peak. The S-phase relates to the intensity signal between the two peaks (G0/G1 and G2/M). Finally, sub G1 cells were identified as cells with a DNA content situated between half the mean value of G1 phase and the minimum value of G1 phase.

3.3.5 Annexin-V/PI costaining for apoptosis analysis

Cells were collected by trypsinization 24 h, 48 h and 72 h after X-irradiation (0.1, 0.5 and 5 Gy). To include cells that already have died and detached, the medium was collected as well. Next, cells were stained with FITC-labeled Annexin-V and PI using the Annexin V-FITC Apoptosis Detection Kit (eBioscience, Vienna, Austria) according to the manufacturer's instructions. Fluorescence of a minimum of 10,000 cells was measured by flow cytometry (Coulter Epics XL-MCL, Beckman Coulter). The mean percentages of living (Annexin-V negative, PI negative), apoptotic (Annexin-V positive, PI negative) and non-apoptotic dead (Annexin-V positive, PI positive) cells were calculated. The gating was set to have around 5 % of apoptotic cells in control cells. This percentage was chosen based on previous experience in the lab.

3.3.6 Cytospin and May-Grünwald Giemsa staining for determination of cell morphology

Cells were trypsinized 24 h after X-irradiation (0.1, 0.5 and 5 Gy). Next, 250,000 cells were resuspended in 1 ml cold PBS containing 10% FBS and after centrifugation washed in 1 ml cold PBS containing 10% FBS. Cell pellets were diluted in 1 ml cold PBS containing 1% FBS and 100 μ l of these cell suspensions were cytospinned on a glass slide prior to May-Grünwald Giemsa staining. Cells (n=400-700) were then counted from each of the 3 technical replicates prepared for each dose and scored for normality, the presence of polynuclei, DNA fragmentation, nuclear bodies and the absence of a cellular membrane. Cell size was measured as well using a home-written script for ImageJ software (GiemsaSegmentation macro, available from www.limid.ugent.be/downloads) [230].

3.3.7 Statistical analysis

Analysis of γ -H2AX spot count data was performed using Kruskal-Wallis and *post-hoc* test according to Chan and Walmsley [231]. Cell cycle and apoptosis data were analyzed by three-way analysis of variance (ANOVA) with dose, time point and cell type as independent variables. For cytospin data analysis, two-way ANOVA, with dose and cell type as independent variables, was performed. Sidak *post-hoc* test was used for determining statistical significance of dose and cell type. All analyses were performed using SPSS software package version 19 (IBM Corp., New York, USA). For all tests, a value of $p < 0.05$ was considered statistically significant.

3.4 Results

3.4.1 Acute low dose X-irradiation causes DNA damage in HUVEC and EA.hy926 cells

Ionizing irradiation induces double strand breaks (DSB) which can be visualized microscopically by immunofluorescent staining of phosphorylated H2AX histones (γ -H2AX), that specifically localize around the site of the break (Figure 12).

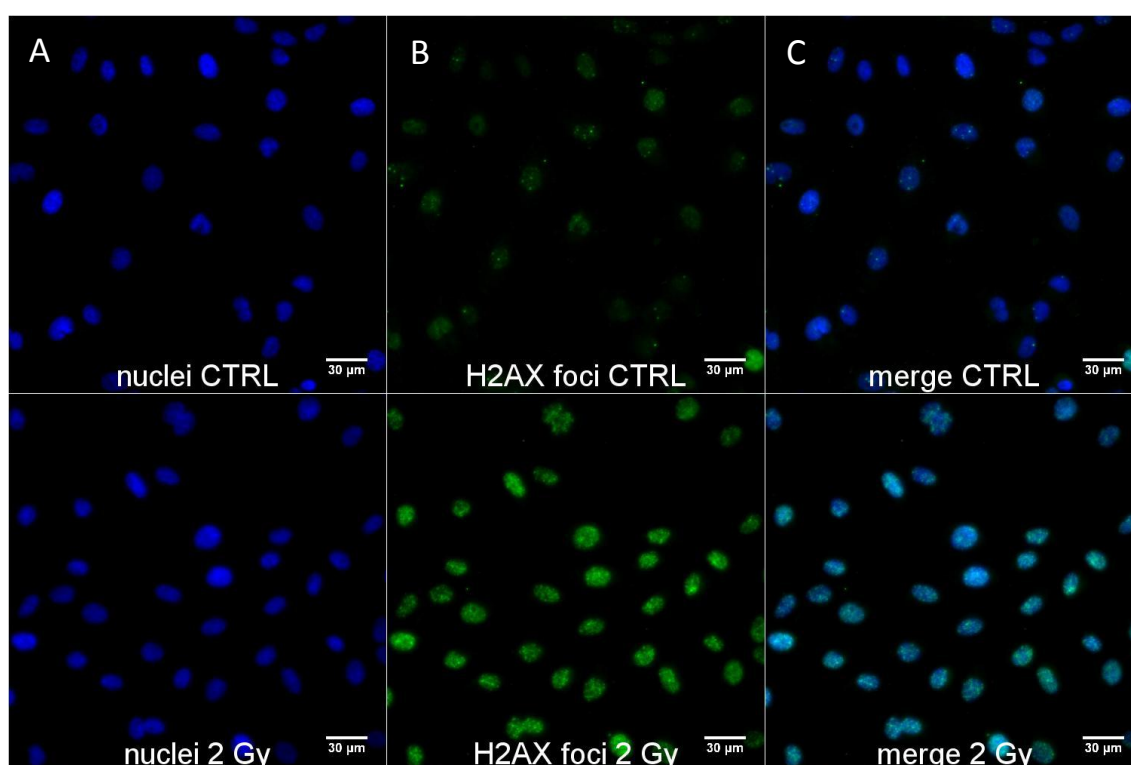


Figure 12: Detection of DSB by immunostaining of γ -H2AX spots followed by fluorescence microscopy. Representative fluorescence microscopic images (40X, oil) of EA.hy926 cells in control conditions (top panels) and irradiated with 2 Gy (bottom panels). Cells were fixed 30 min after exposure. **A.** Nuclei are stained with DAPI (blue). **B.** γ -H2AX spots are visualized with γ -H2AX antibody coupled with FITC (green). **C.** Merged images of DAPI and FITC channel for quantification of the number of γ -H2AX spots per nucleus.

We quantified the number of γ -H2AX spots in the nucleus by automated image analysis at several time points (30 min, 2 h and 24 h) after acute X-irradiation (0.05, 0.1, 0.25, 0.5 and 2 Gy). A significant dose-dependent increase in spot number was observed 30 min and 2 h post

irradiation (p.i.) in both HUVEC and EA.hy926 cells (Figure 13). Comparing spot numbers in HUVEC and EA.hy926 cells reveals that more γ -H2AX spots are formed in EA.hy926 cells (e.g. a median of 37 spots in EA.hy926 cells versus 23 spots in HUVEC 30 min p.i. with 2 Gy). Spot occupancy, which reflects the percentage of the area of the nucleus that is covered with spots [229] tends to follow a similar pattern as spot number, both in HUVEC and EA.hy926 cells, 30 min and 24 h p.i. (Figure 14).

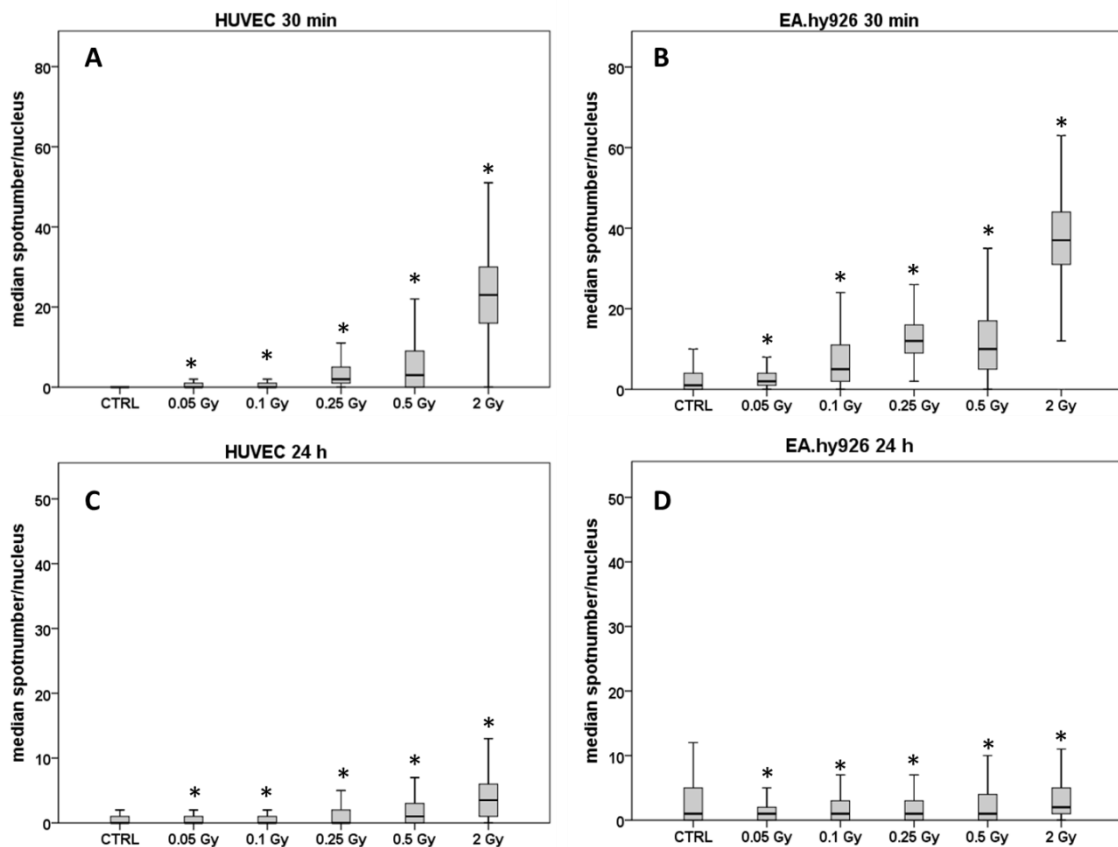


Figure 13: Quantification of γ -H2AX spot number. Boxplots representing median γ -H2AX spot number per nucleus vs. irradiation dose in HUVEC and EA.hy926 cells 30 min (A, B) and 24 h (C, D) after exposure to a range of acute X-ray doses (0.05, 0.1, 0.25, 0.5 and 2 Gy). The box boundaries represent the upper and lower quartiles and the thick black line within represents the median. Extreme outliers were removed. ImageJ software was used to count the number of nuclei and foci in each nucleus. In total, around 250 nuclei for HUVEC and 800 nuclei for EA.hy926 cells were scored and the mean and median of foci per nucleus was calculated. Kruskal-Wallis analysis and *post-hoc* test according to Chan and Walmsley were performed in SPSS with * = p<0.05 (versus control cells).

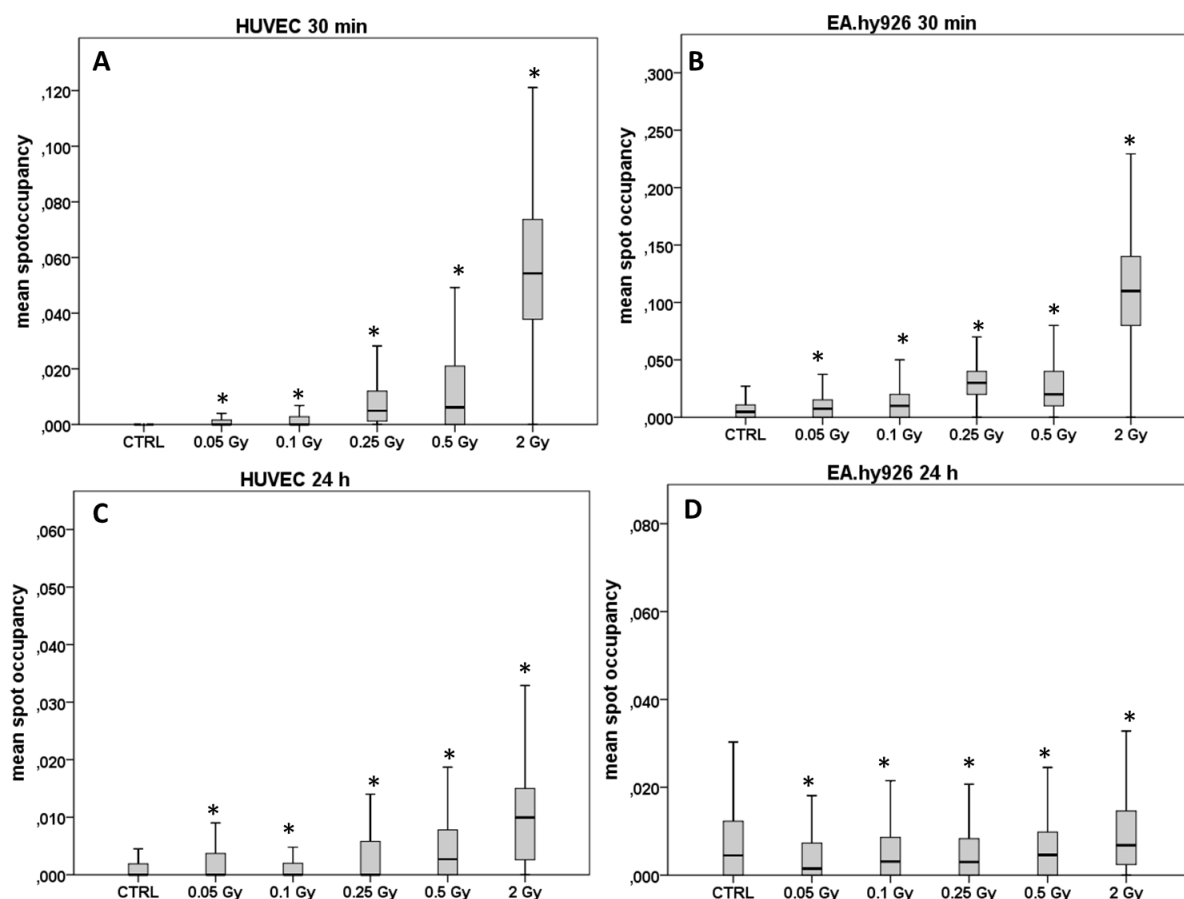


Figure 14: Quantification of γ -H2AX spot occupancy. Boxplots representing mean spot occupancy per nucleus vs. irradiation dose in HUVEC and EA.hy926 cells 30 min (A, B) and 24 h (C, D) after exposure to a range of acute X-ray doses (0.05, 0.1, 0.25, 0.5 and 2 Gy). The box boundaries represent the upper and lower quartiles and the thick black line within represents the median. Extreme outliers were removed. ImageJ software was used to determine the spot occupancy, i.e. the fraction of the nucleus that is covered in spots (%). In total, around 250 nuclei for HUVEC and 800 nuclei for EA.hy926 cells were scored. Kruskal-Wallis analysis and post-hoc test according to Chan and Walmsley were performed in SPSS with * = $p < 0.05$ (versus control cells).

Follow-up in time shows that the decrease in spot number tends to differ between irradiated HUVEC and EA.hy926 cells (Figure 15). In irradiated HUVEC the maximum in spot number was observed at 30 min for all doses, which decreased after 2 h and 24 h. Interestingly, in EA.hy926 cells irradiated with 0.05 and 0.5 Gy, the maximum in spot number was observed after 2 h instead of 30 min. For control cells, however, a similar curve was followed in both cell lines with a slight increase in spot number observed after 24 h compared to 30 min and 2 h.

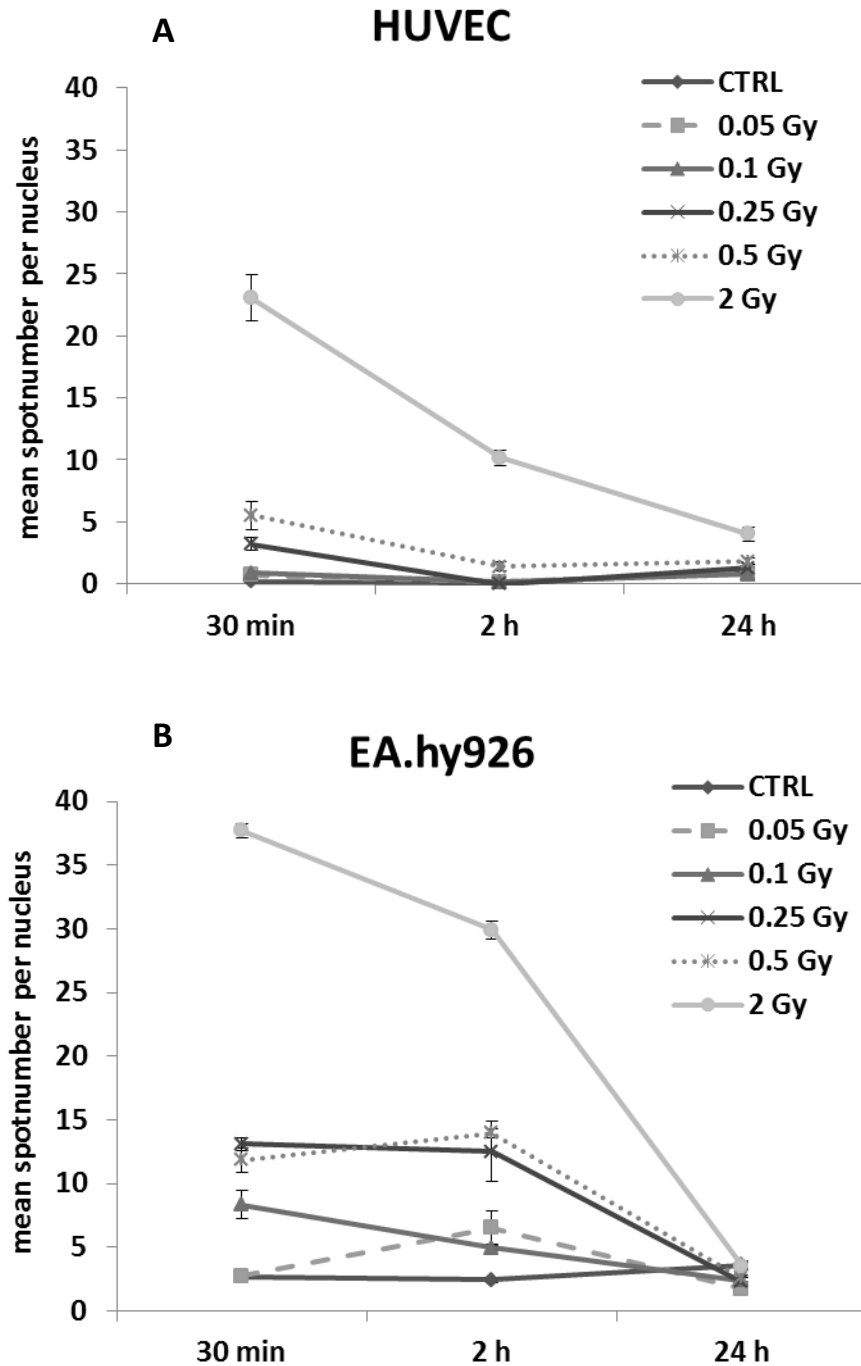


Figure 15: Dissappearance of γ -H2AX spot number over time. Graphical overview of mean γ -H2AX spot number per nucleus for HUVEC (A) and EA.hy926 cells (B), 30 min, 2 h and 24 h after exposure to a range of acute X-ray doses (0.05, 0.1, 0.25, 0.5 and 2 Gy). Error bars represent ± 2 standard error of the mean (SEM).

3.4.2 Acute X-irradiation induces cell cycle arrest in HUVEC and EA.hy926 cells

Radiation-induced changes in cell cycle were analyzed by flow cytometry 24 h and 48 h after acute X-irradiation (0.1, 0.5 and 5 Gy) using PI staining. Following high dose irradiation (5 Gy), the cell cycle distribution shifted towards a significant decreased percentage of cells in G1/G0 and S phase and a significant increased percentage in G2/M phase in both HUVEC and EA.hy926 cells at both tested time points (Figure 16). These findings indicate a persistent arrest in G2 phase which was more pronounced in EA.hy926 cells compared to HUVEC (non-significant). For example, the ratio 5 Gy/control of the percentages of G2/M cells was 1.8 for EA.hy926 cells compared to 1.3 for HUVEC, 24 h after irradiation. At lower doses, the typical cell cycle distribution observed after exposure to 5 Gy was less clear. Nevertheless, a subtle, but significant, decrease in the amount of cells in S-phase 24 h p.i. for 0.1 and 0.5 Gy and 48 h p.i. for 0.5 Gy was observed in EA.hy926 cells.

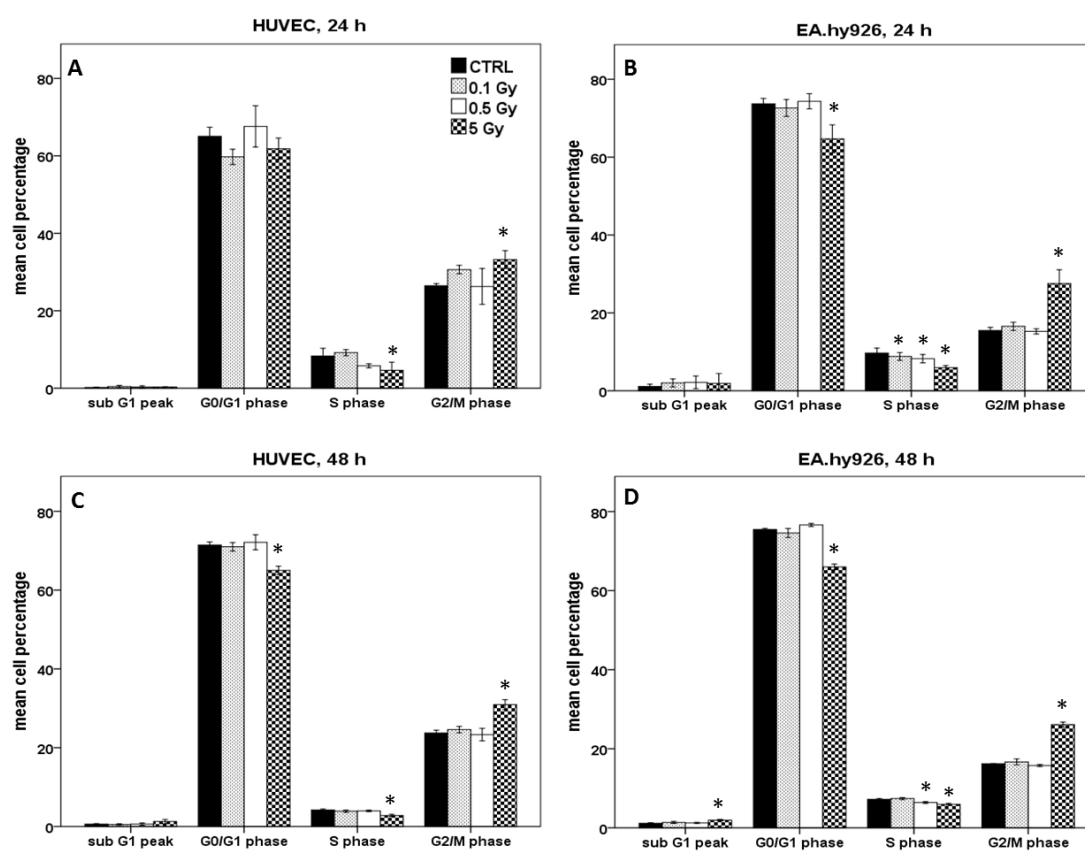


Figure 16: Cell cycle distribution assessed by PI staining and flow cytometry. Bar graphs representing percentages of cells per cell cycle phase in HUVEC (A, C) and EA.hy926 cells (B, D) 24 h and 48 h after

exposure to 0.1, 0.5 and 5 Gy. Bars represent an average of three biological replicates. Three-way ANOVA with Sidak *post-hoc* test was performed in SPSS with * = $p < 0.05$ (versus control cells). Error bars represent ± 2 SEM.

In addition, a trend towards an increase in sub G1 peak, which we assume to represent the apoptotic fraction, was seen with all doses after 24 h in EA.hy926 cells. A significant increase in sub G1 peak was observed with 5 Gy after 48 h in EA.hy926 cells. This was confirmed by the Annexin-V/PI assay for apoptosis detection (see section 3.4.3). It has been reported that when apoptotic cells are fixed in ethanol, which induces pores in the membrane, small size fragments of DNA can then leave the cells during staining in an aqueous solution. Moreover the shedding of apoptotic bodies which contain fragments of nuclear DNA, contribute to the loss of DNA content of apoptotic cells [232]. Due to this DNA loss, and since a high percentage of cells are in G1 phase, apoptotic cells that have a deficit in DNA content can be visualized as a 'sub G1 peak' upon DNA staining.

3.4.3 Acute low dose X-irradiation induces apoptosis in HUVEC and EA.hy926 cells

Annexin-V/PI co-staining was used to determine the percentage of living, apoptotic and non-apoptotic dead cells 24 h, 48 h and 72 h after exposure to a range of acute X-ray doses (0.1, 0.5 and 5 Gy). Overall, a dose-dependent increase in apoptotic cells was observed (Figure 17) that was significant for doses as low as 0.1 Gy for EA.hy926 cells and as low as 0.5 Gy for HUVEC 48 h after exposure. The results show also that a significant higher percentage of EA.hy926 cells underwent apoptosis following radiation exposure (0.5 and 5 Gy) compared to HUVEC. For example, the ratio 0.5 Gy/control of the percentage of apoptotic cells was 2.1 for EA.hy926 cells compared to 1.2 for HUVEC, and the ratio 5 Gy/control was 2.4 for EA.hy926 cells compared to 1.2 for HUVEC, 48 hours after irradiation. Interestingly, in EA.hy926 cells a drop in apoptosis was seen after 72 h, in particular for the lower doses (0.1 and 0.5 Gy), opposed to HUVEC where there is still an increase in apoptosis at that time point (non-significant).

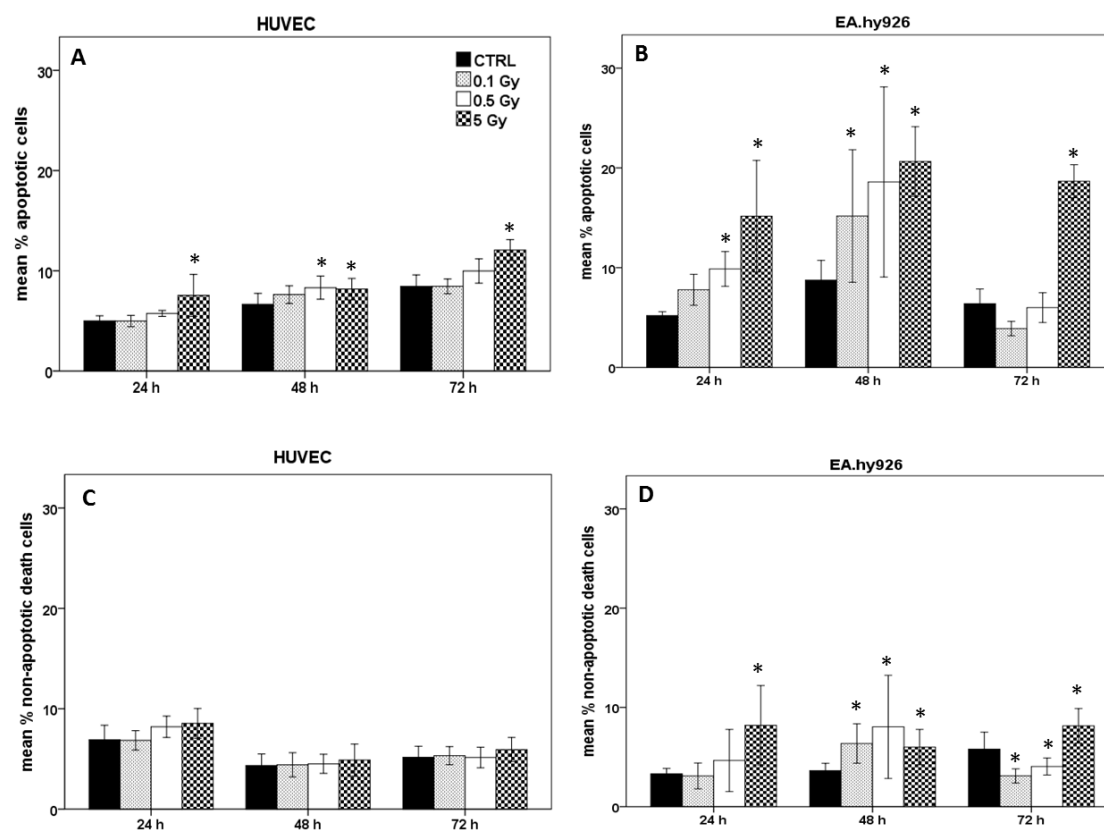


Figure 17: Apoptosis assessed by the Annexin-V/PI assay and flow cytometry. Bar graph representing percentage of apoptotic cells (Annexin-V positive, PI negative) and non-apoptotic dead cells (Annexin-V positive, PI positive) as measured by flow cytometry and Annexin-V/PI costaining in HUVEC (A, C) and EA.hy926 cells (B, D) 24 h, 48 h and 72 h after exposure to 0.1, 0.5 and 5 Gy. Bars represent an average of three biological replicates. Three-way ANOVA with Sidak *post-hoc* test was performed in SPSS with * = $p < 0.05$ (versus control cells). Error bars represent ± 2 SEM.

The dose-response relationship for cells that had died in a non-apoptotic manner was less clear. In EA.hy926 cells exposure to 5 Gy significantly increased the percentage of non-apoptotic dead cells at all time points tested. For the lower doses (0.1 and 0.5 Gy) a significant increase of non-apoptotic dead cells was observed after 48 h which decreased at 72 h. The latter observation is in accordance with the trend observed for apoptotic cells. In HUVEC, no relevant differences in the percentages of non-apoptotic cells were observed between control and irradiated cells, although a small increase 24 h after exposure to 0.5 and 5 Gy seem to have occurred.

3.4.4 Acute X-irradiation induces morphological changes in HUVEC and EA.hy926 cells

Cytospin followed by May-Grünwald Giemsa staining was performed on HUVEC and EA.hy926 cells 24 h after exposure to 0.1, 0.5 and 5 Gy in order to study radiation-induced morphological changes. Cell size was assessed quantitatively using ImageJ software with the home-written Giemsa Segmentation macro (www.limid.ugent.be/downloads). In addition, both HUVEC and EA.hy926 cells were scored manually for other morphological parameters that are indicative of cellular damage or death: polynuclei, DNA fragmentation, cells lacking a cellular membrane, presence of nuclear bodies and of polynuclei (Figure 18).

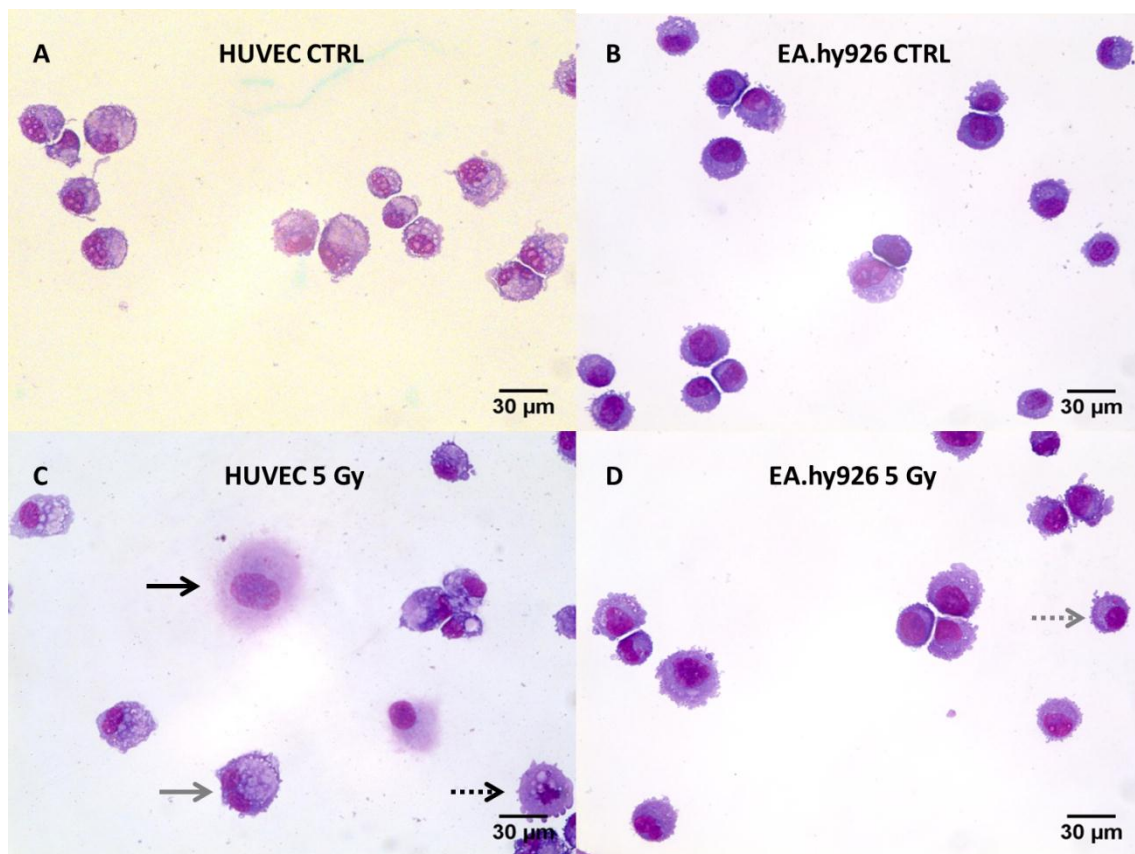


Figure 18: Morphological analysis of HUVEC and EA.hy926 cells. Representative microscopic pictures (40X) of May-Grünwald Giemsa stained slides performed on cytopspinned HUVEC (A, C) and EA.hy926 cells (B, D) 24 h after exposure to 5 Gy and in control conditions. Cells were manually scored for polynuclei (grey arrow), DNA fragmentation (dashed black arrow), nuclear bodies (dashed grey arrow) and cells without membrane (black arrow). Automated image analysis using ImageJ software was used for cell size quantification. Quantitative data are summarized in Table 2.

For both HUVEC and EA.hy926 cells, a significant increase in cell size was observed 24 h after exposure to 5 Gy (Table 2). Comparing both cell lines, it was observed that this increase in cell size after exposure to 5 Gy was larger in HUVEC (ratio 5 Gy/control 1.16) than in EA.hy926 cells (ratio 5 Gy/control 1.10) (non-significant). Evaluation of other morphological parameters revealed that there tends to be more normal HUVEC (91.7 %) compared to normal EA.hy926 cells (83.5 %) after exposure to 5 Gy. However, following exposure to lower doses, the percentage of normal cells inclines towards similarity in both cell lines. After 0.5 Gy, a significant rise in cells that lack a cellular membrane was observed in HUVEC. Next, we observed that the presence of polynuclei tends to increase with radiation dose in both HUVEC and EA.hy926 cells. Furthermore, a significantly increased number of cells containing nuclear bodies was observed in EA.hy926 cells after exposure to 5 Gy. Lastly, it was noticed that DNA fragmentation tends to occur more frequently in EA.hy926 cells compared to HUVEC in both control and irradiated conditions.

	cell size (μm)	polynuclei (%)	DNA fragmentation (%)	cells lacking membrane (%)	nuclear bodies (%)	normal cells (%)
EA.hy926						
CTRL	81.3 \pm 0.6	1.2 \pm 0.5	1.2 \pm 0.5	1.0 \pm 0.4	0.6 \pm 0.4	95.9 \pm 0.9
0.1 Gy	81.2 \pm 0.5	2.6 \pm 0.8	1.2 \pm 0.5	1.1 \pm 0.6	1.7 \pm 0.6	93.4 \pm 1.4
0.5 Gy	82.2 \pm 0.5	2.2 \pm 0.5	2.4 \pm 0.4	2.2 \pm 0.6	0.6 \pm 0.2	92.5 \pm 0.8
5 Gy	89.0* \pm 0.7	4.1 \pm 1.0	2.1 \pm 0.9	1.7 \pm 0.6	8.7* \pm 1.2	83.5* \pm 2.2
HUVEC						
CTRL	93.3 \pm 1.1	1.7 \pm 0.6	0.6 \pm 0.4	1.4 \pm 0.9	1.0 \pm 0.5	95.4 \pm 1.4
0.1 Gy	84.8* \pm 1.0	2.6 \pm 0.8	0.3 \pm 0.2	1.4 \pm 0.9	0.7 \pm 0.4	95.1 \pm 1.0
0.5 Gy	95.4 \pm 1.5	3.5 \pm 0.9	0.0 \pm 0.0	5.5* \pm 1.0	0.8 \pm 0.4	90.3 \pm 1.6
5 Gy	107.9* \pm 1.5	4.7 \pm 0.8	0.4 \pm 0.3	1.9 \pm 0.7	1.4 \pm 0.5	91.7 \pm 1.3

Table 2: Morphological analysis of HUVEC and EA.hy926 cells. Overview of morphological changes evaluated in HUVEC and EA.hy926 cells 24 h after exposure to a range of acute X-ray doses (0.1, 0.5 and 5 Gy). Automated image analysis using ImageJ software was used for cell size quantification. Other features were assessed manually. On average between 400 and 700 cells were evaluated per condition, spread over three technical replicates. Values represent the mean of three technical replicates \pm SEM. Two-way ANOVA with Sidak *post-hoc* test was performed in SPSS with *= $p < 0.05$ (versus control cells). A visual representation is given in Figure 17.

3.5 Discussion

Epidemiological studies indicate an increased risk of CVD following the exposure to lower doses of ionizing radiation, although uncertainty exists below 0.5 Gy [53, 215]. Therefore, to enable an accurate risk assessment in the low dose range (< 0.5 Gy), an understanding of the underlying biological and molecular mechanisms is needed. Both radiation-induced acceleration of age-related atherosclerosis and microvascular damage are hypothesized to underlie radiation-related CVD morbidity [43]. Given the important role of endothelium dysfunction in the development of CVD, the endothelium is considered a critical target in radiation-related CVD [124, 216]. *In vitro* research using endothelial cell cultures is thus useful to better understand the radiation response of the endothelium. However, the choice of the endothelial cell type for *in vitro* studies should be well considered since their characteristics may differ [122, 233-235].

In this study, the radiation response, with a focus on the low dose range (0.05 – 0.5 Gy), of two commonly used endothelial cell types, the primary HUVEC and the thereof derived immortalized EA.hy926 was evaluated. HUVEC was chosen since it is considered as a good general model of the endothelium, displaying characteristics of both micro- and microvasculature [165] and its derivate, EA.hy926, was chosen for its ease of use. To our good knowledge, this is the first direct comparison made in the low dose range of ionizing radiation between HUVEC and the thereof derived EA.hy926 regarding DNA damage, cell cycle, apoptosis and morphology.

In both HUVEC and EA.hy926 cells, we observed 30 min after exposure a significant increase in DSB, as represented by γ -H2AX spot number, down to the lowest dose tested (0.05 Gy). The observed increase in DSB was not proportional to the dose, but relatively higher with the lower doses tested. This was more pronounced in EA.hy926 cells (e.g. 55 spots/Gy after 0.05 Gy vs 19 spots/Gy after 2 Gy) compared to HUVEC (e.g. 14 spots/Gy after 0.05 Gy vs 12 spots/Gy after 2 Gy). A non-linear relationship with dose has also been demonstrated by Neumaier and coworkers [236]. Although these authors used a different experimental approach, they also observed that the relative spot number (per Gy) is much smaller at higher than at lower doses. They explain this by the fact that at higher doses multiple nearby DSB (1 to 2 μ m apart) can rapidly cluster into repair centers, which are visualized as one spot. Consequently, this implies that average spot size is larger with high doses compared to low doses. The size of individual spots is not calculated by the INSCYDE

toolbox that we used for this analysis, but the parameter 'spot occupancy' can be used as an alternative measure [229]. This parameter reflects the area of the nuclei that is covered by γ -H2AX spots and gives thus an indirect indication for the size of the spots. Since we observed a similar dose-response curve for spot occupancy as for spot number, the influence of clustered DSB was most likely rather subtle. An alternative explanation may be that low radiation doses induce a global chromatin reorganization that is associated with the formation of γ -H2AX foci, but which do not necessarily reflect a higher amount of DNA damage [237]. Therefore, the observed non-linear relationship with dose for γ -H2AX spot number does not necessarily reflect a non-linear relationship with dose for DSB.

The disappearance of γ -H2AX spots in irradiated cells with time, as observed in our study, represents effective DSB repair [238]. Remarkably, 24 h after exposure, we observed less spots in cells irradiated with lower doses (0.05 - 0.5 Gy for EA.hy926 cells and 0.05 - 0.1 Gy for HUVEC) compared to control cells. This may be explained by the observation that spot number inclined to be higher in control cells at 24 h compared to control cells at 30 min. With higher doses (2 Gy for EA.hy926 cells and 0.25 - 2 Gy for HUVEC), the spot number remained still elevated compared to controls 24 h after exposure. In a study by Kraemer and coworkers, elevated spot number in EA.hy926 cells was observed as well 24 h after exposure to 2.5 Gy [239]. This may indicate that with more extensive DNA damage, repair is slower or that unrepaired DSB remain present. It has been suggested that slower repair with higher doses reflects the presence of more complex breaks and the possibility of more DSB clustered in one repair center, as explained above [236].

Following DNA damage, a DNA damage response is activated, with p53 as a major regulator, leading to cell cycle arrest until the damage is repaired or until cells undergo apoptosis [183, 240]. Exposure to 5 Gy induced significant accumulation of cells in G2/M phase in both HUVEC and EA.hy926 after 24 h, which tends to be more pronounced in EA.hy926 cells. Likewise, morphological analysis of murine fibroblasts has shown that the cell area increased 24 h after exposure to 5 Gy, concomitantly to a G2/M phase arrest [241]. In our study, this effect was slightly more pronounced in HUVEC compared to EA.hy926 cells. We observed that the significant accumulation of cells in G2/M phase after exposure to 5 Gy was coupled to a decrease of cells in G0/G1 and S phase. This typical cell cycle distribution was also observed, in other studies, HUVEC 24 h after exposure to 3 Gy [174] and in EA.hy926 cells 24 h after exposure to 2.5 Gy [239]. With the lower doses used in our study, this typical cell cycle distribution was less clear.

It has been reported that the accumulation of cells in G2/M phase assayed with PI staining represents cells that were irradiated in G1 or S phase and that were subsequently arrested in their progression from G2 into mitosis [242, 243]. Cells irradiated in G1 phase will quickly repair the induced DNA damage by the error-prone non-homologous DNA end-joining (NHEJ) that is known to predominate in G1 phase [176]. Remaining DNA damage, however, could then lead to a G2-arrest where the error-free homologous recombination (HR) takes care of repair [241]. Indeed, analysis of γ -H2AX spot number has shown that with higher doses, a small number of DSB remains present at 24 h in both EA.hy926 cells and HUVEC in our study.

Next, we evaluated the induction of apoptosis following low dose radiation exposure. Apoptosis, having both proadhesive and procoagulant properties in endothelial cells, is regarded as an important determinant in atherosclerosis progression [244]. Membrane blebs from apoptotic endothelial cells contain biologically active oxidized phospholipids that induce monocyte adhesion to the endothelium [245]. Moreover, thrombus formation is favored due to the exposure of phosphatidylserine, which has procoagulant properties, on the surface of apoptotic endothelial cells [246]. Overall, we observed a dose-dependent increase in apoptotic cells, down to 0.5 Gy in HUVEC and 0.1 Gy in EA.hy926 cells. In contrast, a study by Pluder and coworkers showed no increase in apoptotic EA.hy926 cells after exposure to 0.2 Gy, but only after exposure to 5 Gy [188]. It should be noted that they measured caspase-3 activity as an indicator of apoptosis, whereas we used the Annexin-V/PI assay. It may be that after low dose irradiation, apoptosis is induced in a caspase-3 independent manner, or that the Annexin-V/PI assay is more sensitive than the caspase-3 assay. It is worth mentioning that preliminary data in our lab regarding flow cytometric assessment of caspase-3 activity in EA.hy926 cells showed an absence of caspase-3 activation. This finding may point to a caspase-3 independent induction of apoptosis in EA.hy926 cells, although further research is required. In the study by Pluder and coworkers, sub G1 analysis indicated an increase in sub G1 peak only following exposure to 5 Gy [188], which is in accordance to our observations. Sub G1 analysis may underestimate the total number of apoptotic cells since apoptotic cells in S and G2 phase will not be visualized through this assay [232]. On the other hand, it has been reported that the sub G1 peak may overestimate the number of apoptotic cells since the DNA content of apoptotic bodies or chromatin fragments can be misclassified as single apoptotic cells [247].

Finally, we have evaluated several morphological characteristics related to cell damage and death. Loss of endothelial cells, through apoptosis but also in a non-apoptotic manner (necrosis, autophagy, mitotic catastrophe), will compromise the integrity and function of the endothelium [148, 248]. For example, necrosis is known to be involved in atherosclerosis progression by causing massive inflammation following the loss of intracellular contents [249-251]. By means of Annexin-V/PI staining we showed that in HUVEC the percentage of cells died in a non-apoptotic manner 24 h after irradiation was more or less similar to that of cells died through apoptosis. In EA.hy926 cells, on the other hand, more apoptotic cells than non-apoptotic dead cells were observed 24 h after irradiation. It should be noted that there is no consensus regarding the definition of Annexin-V positive and PI positive cells, as they have also been regarded as late apoptotic cells [252, 253]. Morphological analysis indicated a significant increase in damaged or death cells after exposure to 5 Gy in both HUVEC and EA.hy926 cells. Furthermore, 24 h after exposure to 0.5 Gy, a significant rise in cells lacking a cellular membrane, which may represent necrotic cells [250], has been observed with HUVEC, but not with EA.hy926 cells. Also, a significantly increase in nuclear bodies, indicative of mitotic catastrophe [249], was observed in EA.hy926 cells after exposure to 5 Gy, but not in HUVEC. It should be noted that these characteristics only give an indication of the cellular process ultimately leading to the cell's death, and require a molecular validation. This is in particular needed since a rather heterogeneous mixture of the assessed morphological characteristics was observed. Overall, our findings indicate that radiation-induced endothelial cell death is not limited to apoptosis.

Comparing the radiation response of HUVEC and EA.hy926 cells, a larger radiosensitivity of the latter was revealed. A smaller number of γ -H2AX spots tend to be formed in HUVEC compared to EA.hy926 cells. In this regard, it has been reported that transformed cells frequently have high endogenous spot numbers due to their genomic instability [238, 254] which may well explain the higher spot number found in control and irradiated conditions for the immortalized EA.hy926 cells compared to the primary HUVEC. Also, EA.hy926 cells have weaker enzymatic antioxidant defenses compared to HUVEC [225]. This renders EA.hy926 cells less protected against radiation-induced reactive oxygen species (ROS) formation and thus more susceptible to indirect DNA damage. In addition, the disappearance of spot number over time was not similar in both cell lines. Whereas in HUVEC a plateau of maximum spot number was observed after 30 min, this seemed to be only between 30 min and 2 h for lower doses (< 2 Gy) in EA.hy926 cells suggesting slower DNA repair in the

latter. Subsequent cell cycle arrest in G2/M phase was inclined to be more pronounced in EA.hy926 cells compared to HUVEC. Furthermore, significantly more apoptosis was induced in EA.hy926 cells compared to HUVEC 24 h and 48 h following exposure to 0.5 and 5 Gy. In this context, we observed also that DNA fragmentation, a morphological characteristic of apoptosis, tends to occur more in EA.hy926 cells compared to HUVEC. It has been reported that radiosensitive tissues have a high basal level of p53 mRNA and are more prone to induce apoptosis following radiation exposure [255]. Gene expression profiling performed by Boerma and coworkers has showed a higher basal TP53 expression in EA.hy926 cells compared to HUVEC [224]. Other possible molecules that could influence the difference in radiation-induced apoptosis between HUVEC and EA.hy926 are caspases, traditionally considered as the central executors of apoptosis [256]. As mentioned above, preliminary data suggest that apoptosis is induced in a caspase-3 independent manner in EA.hy926 cells. It would be interesting to investigate whether this is also the case for HUVEC. Furthermore, it would be of interest to investigate molecular players that are involved in radiation-induced necrosis, autophagy or mitotic catastrophe.

One could reason that all parameters should be identical between the two cell cultures to make an unbiased comparison. In our study, it was chosen to use culture conditions which were not identical between HUVEC and EA.hy926 but optimal for each cell type. Indeed, using culture conditions that are not adapted to the specific needs of a cell can have unfavorable consequences (e.g. more easily increase in apoptosis) as such biasing the comparison. On the other hand, an effect of differing culture conditions cannot be excluded. For instance, it has been observed previously that the percentage of FBS influences the amount of apoptosis induced by lectins in MCF-7 breast cancer cells; lectins induced less apoptosis in cell cultures with high FBS concentration (20 %) opposed to low FBS concentration (1 %) [257]. This finding suggests that FBS may also influence the effect of ionizing radiation on the induction of apoptosis. It would thus be useful to investigate the effect of FBS concentration on radiation-induced endothelial cell apoptosis.

3.6 Conclusion

The low dose acute radiation response of primary endothelial cells (HUVEC) and the thereof derived immortalized endothelial cell line (EA.hy926) with regard to DNA damage, apoptosis, cell cycle and morphological changes was studied and compared between the two cell lines. We observed that DNA damage was induced in both HUVEC and EA.hy926 cells following exposure to doses as low as 0.05 Gy. This low dose radiation-induced DNA damage was repaired after 24 h without a significant arrest of cell cycle progression. Even though cell cycle progression was not arrested, apoptosis was induced after exposure to doses as low as 0.1 Gy in EA.hy926 cells and 0.5 Gy in HUVEC. Comparing HUVEC and EA.hy926 cells, we observed a greater radiosensitivity of the latter, mainly with respect to the induction of apoptosis. The differences in radiosensitivity of EA.hy926 cells and HUVEC should be taken into account when studying the radiation response of the endothelium. Moreover, it is advised to include multiple endothelial cell models. Seeing also the important role of endothelial cell apoptosis in atherosclerosis, our finding also indicates that the use of either HUVEC or EA.hy926 cells may in particular influence *in vitro* research regarding radiation-related atherosclerosis. Finally, our results regarding the formation of DSB show that at low doses a relatively higher number of DSB is formed compared to high doses. This may imply a non-linear dose response relationship for DSB formation in endothelial cells supporting thus the notion that the low dose endothelium response is not a simple linear extrapolation from the high dose response. However, practical limitations inherent to the γ -H2AX assay that question the 1:1 relationship between a DSB and a γ -H2AX spot cannot be excluded. Further research is required to resolve this matter as it will have major implications on the assessment of low dose risk.

3.7 Acknowledgements

In the context of the Low Dose Research towards Multidisciplinary Integration (DoReMi) network of excellence, we would like to thank Prof. Sisko Salomaa, Dr. Jean-Rene Jourdain, Prof. Mats Harms-Ringdahl and Dr. Siamak Haghdoost. This study was funded by the EU FP7 DoReMi NoE agreement 249689 on 'low dose research towards multidisciplinary integration'(SCK•CEN), as well as the Hercules Foundation (project AUGÉ/013) (De Vos W.). Rombouts C. is supported by a doctoral SCK-CEN/Ghent University grant. The HUVEC

Low dose radiation response in endothelial cells

cell line was kindly donated by the University of Stockholm. Special thanks to Dr. Pieter Monsieur for the statistical support.

**Chapter 4: Oxidative stress and mitochondrial DNA
damage in endothelial cells following acute low
dose radiation exposure**

4.1 Abstract

Based on epidemiological findings it is not clear whether radiation doses below < 0.5 Gy increase the risk of cardiovascular diseases (CVD), thus further biological research is needed. The endothelium is believed to be a critical target in the development of radiation-related CVD. The major cause of endothelial dysfunction is oxidative stress, which is closely related to mitochondrial function. Moreover, mitochondrial dysfunction is linked to processes such as apoptosis, senescence and inflammation, which are involved in the development of CVD. We hypothesize that low radiation doses (< 0.5 Gy) will induce oxidative stress and alter mitochondrial function in endothelial cells, which may ultimately lead to the development and progression of CVD. The primary human umbilical vein endothelial cells (HUVEC) and the thereof derived immortalized cell line EA.hy926 were used to assess intracellular reactive oxygen species (ROS) levels 30 min after exposure to acute low (< 0.5 Gy) and high doses (5 Gy) of X-irradiation. Intracellular ROS levels were evaluated using the fluorometric CM-H₂DCFDA assay. No clear dose-response relationship was observed for intracellular ROS levels with low dose radiation (< 0.5 Gy). Furthermore, intracellular ROS levels were higher in EA.hy926 cells compared to HUVEC. In the latter, intracellular ROS levels tend to be below background levels. Next, we have carried out optimization experiments for the evaluation of mitochondrial DNA (mtDNA) damage. To this end, we developed PCR protocols for the assessment of the accumulation of a 4977 bp deletion (common deletion), a sensitive marker for mtDNA damage. It should be noted that this chapter represents preliminary work which will be continued in our lab. The results are thus not submitted to peer-reviewed journals.

4.2 Introduction

Epidemiological findings are inconclusive about whether there is an elevated risk of cardiovascular disease (CVD) after exposure to low doses of ionizing radiation (< 0.5 Gy). For an accurate risk assessment, insight in the underlying biological and molecular mechanisms is required including an understanding of the endothelial radiation response [41].

Oxidative stress, an imbalance between reactive oxygen species (ROS) and antioxidant defenses, plays a major role in endothelial dysfunction, and in the onset and progression of atherosclerosis [129, 258]. For example, it will impair vasodilatation by decreasing nitric oxide (NO) bioavailability, the most potent vasodilator [125]. Indeed, super oxide radicals ($O_2^{\cdot-}$) interact with NO to form the unstable and harmful peroxynitrite ($ONOO^{\cdot-}$), a reactive nitrogen species (RNS). This can lead to a state of so-called 'nitrosative' stress [259]. It has been observed in a number of studies that impaired NO-dependent vasodilatation is associated with atherosclerosis [115]. Besides impaired vasodilatation, oxidative stress has been associated with increased endothelial permeability and increased leukocyte adhesion onto the endothelium [132], which is a critical step in the development of atherosclerosis [260]. On the molecular level, oxidative stress is characterized by oxidative damage to macromolecules such as DNA, proteins and lipids. Furthermore, it alters the cellular redox state as such modulating the activity of diverse intracellular molecules and signaling pathways [128, 261]. For instance, alterations in the redox state of protein cysteinyl residues cause changes in protein conformation and function. Also, ROS have an impact on gene expression via modulation of transcription factors such as nuclear factor kappaB (NF- κ B), activator protein 1 (AP-1) and the peroxisome proliferator-activated receptor (PPAR) family of transcriptional activators [261] determining cellular outcome. For example, NF- κ B is known to be involved in the regulation of inflammation, stress responses, apoptosis and the expression of cytokines and cell adhesion molecules [262]. All these processes are known to play an important role in the development and progression of atherosclerosis.

Cellular exposure to ionizing radiation results in the formation of ROS that last a matter of milliseconds [263]. Radiation-induced ROS, with the majority being hydroxyl radicals, will cause immediate oxidative damage to nearby macromolecules (DNA, proteins and lipids), as such contributing to the biological effects of ionizing radiation. However, it has been calculated that the amount of ROS generated by ionizing radiation is relatively small

compared to endogenously produced ROS [264]. Consequently, it can be argued whether low dose radiation-induced ROS will have a significant impact on cellular outcome. Though, there are indications that low-level ionizing events are 'amplified'. Indeed, experimental findings pointed to a cellular 'amplification' of radiation-induced ROS/RNS since much more ROS/RNS was detected as could be accounted for with the primary ionizing events [265-267]. The exact mechanisms are not yet resolved but there is an important role for RNS such as NO. Whereas radiation-induced ROS are the initiators, NO and derivatives are believed to be the effectors activating signal transduction pathways, defining cellular outcome such as apoptosis or senescence [259].

Mitochondria are also considered to play a key role in the amplification of ROS/RNS. Indeed, it has been demonstrated that ionizing radiation can promote mitochondrial ROS production [190, 192, 268-270]. The mechanisms by which ionizing radiation increases mitochondrial ROS production are not yet fully understood. It is hypothesized that the mtDNA is a critical radiation target that is involved in the amplification of intracellular ROS levels. The mtDNA is a sensitive target of ionizing radiation for various reasons including lack of protective histones, high exon to intron ratio and limited repair capacity [155]. The mtDNA contains genes that, amongst others, code for polypeptides involved in the electron transport chain [148]. Electrons are transferred through the electron transport chain ultimately leading to the production of ATP, a process called oxidative phosphorylation. During this process, electrons can also react with oxygen or other electron acceptors, and generate free radicals [149]. Damage to the mtDNA can thus result in the dysfunction of the electron transport chain followed by an enhanced leakage of ROS (in particular superoxide anion radicals) [271]. Superoxide, on its turn, can further damage the mtDNA and can diffuse to nearby mitochondria (passively or by yet unknown active pathways) amplifying mitochondrial damage in the cell resulting in further superoxide production [272]. In this way a situation of persistent mitochondrial dysfunction is created. Interestingly, it is observed that cells respond to mtDNA damage by increasing cellular mitochondrial mass or by synthesizing new mtDNA [272, 273].

A sensitive measure of mtDNA damage is the assessment of the accumulation of the common deletion (CD). This is a specific mtDNA deletion that spans 4977 bp and is flanked by two 13 bp repeats. DNA damage between these repeats can lead to inappropriate pairing during DNA replication, via a slip-replication mechanism, thus causing the deletion [274, 275]. Presence of the CD is often observed in diseases that involve a premature aging process such as the

Kearns-Sayre syndrome⁷ [277], indicating the important role of mitochondria in the aging process. Atherosclerosis is also an age-related disease in which mitochondrial dysfunction is believed to play an important role. In several studies, an accumulation of the CD has been observed in human atherosclerotic lesions [159, 278]. Assessment of the accumulation of the CD has also been proposed as a sensitive marker for the evaluation of low dose radiation-induced effects. For instance, Schilling-Tóth and coworkers have demonstrated an increase in CD levels 72 h after exposure to doses as low as 0.1 Gy in both primary and immortalized fibroblast cell lines [194].

Seeing the importance of oxidative stress in the development of CVD, we aimed in this study to determine intracellular ROS levels following low dose radiation exposure in endothelial cells. For this, we have established the fluorometric CM-H₂DCFDA assay for the detection of intracellular ROS levels in HUVEC and EA.hy926 cells. Furthermore, it is clear that oxidative stress and mitochondrial dysfunction are interlinked in an additive way, contributing to the development and progression of CVD. To study the effect of low dose radiation exposure on the mitochondria, and in particular the mtDNA, we aimed to detect the CD in EA.hy926 cells following exposure to low doses of ionizing radiation.

⁷ Kearns-Sayre syndrome is a rare metabolic disorder with clinical manifestation of chronic progressive external ophthalmoplegia, bilateral atypical pigmentary retinopathy and cardiac conduction abnormalities. The underlying causes of this disease are spontaneous mtDNA rearrangements [276].

4.3 Material and methods

4.3.1 Cell culture and irradiation

Cell culture and irradiation procedures are as described in 3.3.1. For measurement of intracellular ROS levels, EA.hy926 cells were plated in T175 flasks with a density of 4×10^6 cells 48 h prior to X-irradiation (0.25 ± 0.01 Gy/min, 250 keV, 15mA, 1mm Cu) and HUVEC were plated in T175 flasks with a density of 2×10^6 cells 5 days prior to X-irradiation. Medium was refreshed every two days. For detection of the CD, EA.hy926 cells were plated in T25 flasks with a density of 350,000 cells 24 h prior to X-irradiation.

4.3.2 Fluorometric CM-H₂DCFDA assay for measurement of intracellular ROS levels

CM-H₂DCFDA, a chemically reduced and chloromethylated derivate of 2',7'-dichlorofluorescein (DCF) was used for the measurement of intracellular ROS levels (Figure 19). A 1 mM CM-H₂DCFDA (Invitrogen NV/SA) stock solution was prepared in dimethyl sulfoxide (DMSO) and a 1 μ M CM-H₂DCFDA working solution was freshly prepared in PBS. Before X-irradiation, cells were trypsinized and washed with PBS. For each sample, 300,000 cells were collected in an eppendorf tube and incubated with 200 μ L of the 1 μ M CM-H₂DCFDA working solution, for 30 min at 37°C. After the incubation period, X-irradiation was performed with a series of doses (0.05, 0.1, 0.25, 0.5 and 5 Gy). As a positive control, cells incubated for 1 h with 150 μ M tert-butylhydroperoxide (tBHP, a known inducer of ROS) were included. The cells were transported from the irradiation facility to the lab on ice and DCF fluorescence was measured on the flow cytometer in channel FL1, about 30 min after irradiation. Since it was practically not feasible to include all doses in one experiment, the experiment was repeated several times so that at least three biological replicates for each dose were obtained. For CTRL, 5 Gy and tBHP, six biological replicates were obtained. Two-way analysis of variance (ANOVA) was performed in SPSS software package version 19 (IBM Corp., New York, USA) with dose and cell type as independent variables. Sidak *post-hoc* test was used for determining statistical significance of dose and cell type. A value of $p < 0.05$ was considered statistically significant. Fluorescence data are presented as the mean ratio of DCF fluorescence intensity between control and irradiated samples (control adjusted to 1).

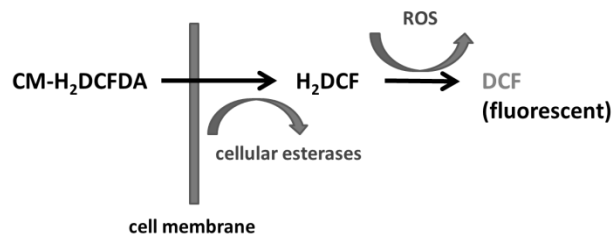


Figure 19: Overview of the CM-H₂DCFDA assay. CM-H₂DCFDA passively diffuses through the cell membrane into cells. Inside the cell its acetate groups are cleaved by intracellular esterases forming H₂DCF. Subsequent oxidation of this product yields a fluorescent adduct, DCF, that is trapped inside the cell and that can be visualized by flow cytometry.

4.3.3 DNA extraction

EA.hy926 cells were trypsinized 72 h after X-irradiation (0.1 and 5 Gy). Furthermore, cells treated for 2 h with 200 μ M H₂O₂ in serum-free medium were included in the experimental set-up. H₂O₂ is a known inducer of mtDNA damage. Cells were washed with PBS and 1×10^6 cells were collected in 200 μ L PBS. Immediately after the collection of cells, DNA extraction was performed with the High Pure PCR Template Preparation Kit (Roche Applied Science, Vilvoorde, Belgium) according to the manufacturer's instructions. DNA quantity was measured using a NanoDrop-2000 spectrophotometer (Thermo Scientific, Erembodegem, Belgium) and the quality was assessed by gel electrophoresis. The extract, containing both nuclear and mitochondrial DNA, was used for PCR analysis without further purification.

4.3.4 PCR detection of the CD

Oligonucleotide sequence of primer pairs F1/R1, F3/R3 and F4/R4 were obtained from Wang and coworkers [193] and primer pair F2/R2 from Santos and coworkers [279] (Figure 20 and Table 3). Their binding sites were checked with the human mtDNA sequence available on MITOMAP [280]. Primers were synthesized by Eurogentec (Eurogentec, Seraing, Belgium).

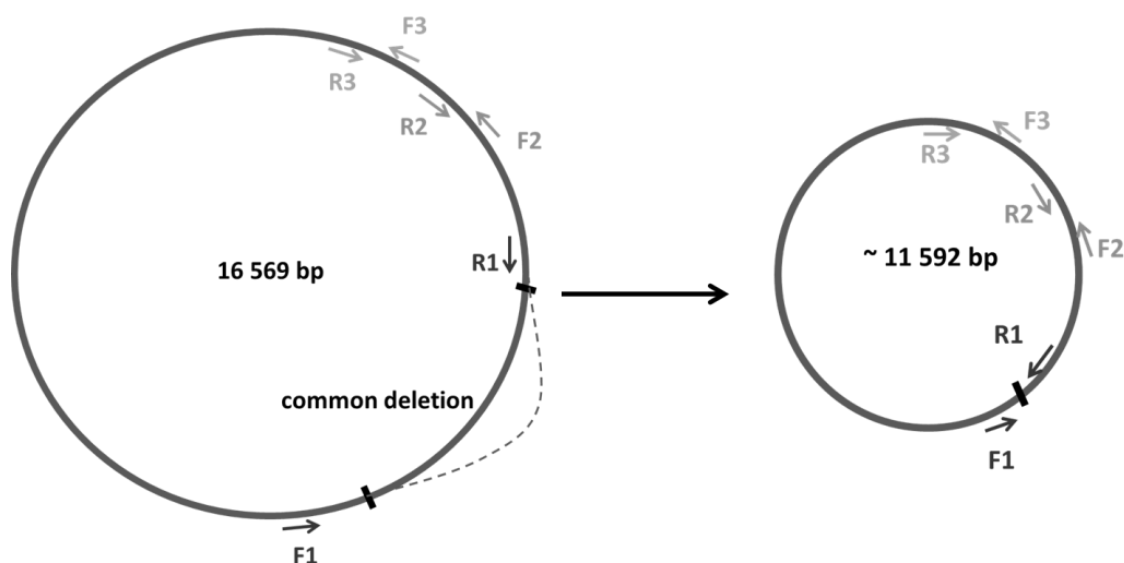


Figure 20: Schematic representation of mtDNA that consists of 16 569 bp. The large circle represents full-length wild-type mtDNA with the region of the CD (4977 bp) situated between the two bars. The smaller circle represents mtDNA after loss of the CD sequence. Primer pair F1/R1 will amplify the region where the CD is situated. Primer pairs F2/R2 and F3/R3 are used as controls for mtDNA copy number since it is not likely for a mutation to occur in these small regions.

name	oligonucleotide sequence		mtDNA position
F1	5'	ATGCCCCACCATAATTACCC	3' NC_012920 : 8389-8408
R1	5'	TCGATGATGTGGTCTTTGGA	3' NC_012920 : 13507-13526
F2	5'	CCCCACAAACCCCATTAATAACCCA	3' NC_012920 : 14620-14645
R2	5'	TTTCATCATGCGGAGATGTTGGATGG	3' NC_012920 : 14816-14841
F3	5'	TATCCGCCATCCATACATT	3' NC_012920 : 15195-15214
R3	5'	GGTGATTCCTAGGGGGTTGT	3' NC_012920 : 15363-15382
name	oligonucleotide sequence (nuclear)		
F4	5'	TTCTACAATGAGCTGCGTGTGG	3'
R4	5'	TCCTACGGAAAACGGCAGAAGA	3'

Table 3: Overview of primer oligonucleotide sequences used for the assessment of mtDNA damage. Primer pair F1/R1 will amplify the region where the CD is situated. Primer pairs F2/R2 (encompasses parts of NADH dehydrogenase subunit 6, mitochondrially encoded tRNA glutamic acid and cytochrome *b* gene) and F3/R3 (encompasses a part of cytochrome *b* gene) are used as controls for mtDNA copy. The mtDNA position of primer pairs F1/R1, F2/R2 and F3/R3 are given. Primer pair F4/R4 amplifies the nuclear β -actin gene.

To detect the CD, two different PCR programs were used with primer pair F1/R1 that flanks the region of the CD: a program with a short extension time that allows formation of a product when the deletion had occurred, and a program with a longer extension time to amplify the

region of the CD without loss of the CD (Table 4). For the assessment of mtDNA copy number, two small mtDNA regions, where mutations rarely occur, are amplified with the use of primer pairs F2/R2 and F3/R3. To normalize the copy number of mtDNA relative to the copy number of nuclear DNA, a primer pair that amplifies the nuclear β -actin gene was used (F4/R4). The PCR mixture contained 40 ng of genomic DNA as template, 1X Taq&Load (mastermix that contains *Taq* DNA polymerase, dNTPs, MgCl₂ and direct loading buffer) (MP Biomedicals, Brussels, Belgium), 0.4 μ M of each primer and RNase free H₂O.

Step	Time	T(°C)
Initial activation step	3 min	94
35 cycles		
<i>denaturation</i>	15 s	94
<i>annealing</i>	30 s	55
<i>extension</i>	6 min / 15 s	72
End of PCR cycle	indefinite	4

Step	Time	T(°C)
Initial activation step	3 min	94
35 cycles		
<i>denaturation</i>	15 s	94
<i>annealing</i>	30 s	57
<i>extension</i>	15 s	72
End of PCR cycle	indefinite	4

Step	Time	T(°C)
Initial activation step	3 min	94
35 cycles		
<i>denaturation</i>	15 s	94
<i>annealing</i>	30 s	50
<i>extension</i>	15 s	72
End of PCR cycle	indefinite	4

Step	Time	T(°C)
Initial activation step	3 min	94
35 cycles		
<i>denaturation</i>	15 s	94
<i>annealing</i>	30 s	50
<i>extension</i>	15 s	72
End of PCR cycle	indefinite	4

Table 4: Overview of the PCR programs used for the assessment of mtDNA damage. For primer pair F1/R1, two different programs were used. One with a long extension time (6 min) to amplify the region of the CD without loss of the CD and one with a short extension time (15 s) that allows the formation of a product when the deletion had occurred.

4.4 Results

4.4.1 Intracellular ROS levels

Optimization experiments pointed out that the most consistent results are obtained when cells are trypsinized and loaded with CM-H₂DCFDA before irradiation takes place. Accumulation of intracellular ROS was evaluated 30 min after exposure to acute low (0.05 – 0.5 Gy) and high (5 Gy) doses of X-rays in HUVEC and EA.hy926 cells (Figure 21). As a positive control, cells incubated for 1 h with 150 μ M tBHP were included in the experimental set-up. Regarding low dose radiation (< 0.5 Gy), no clear dose-response relationship was observed. Overall, EA.hy926 contained more intracellular ROS than HUVEC, which was statistically significant for tBHP. In HUVEC, low doses of radiation tend to reduce intracellular ROS levels.

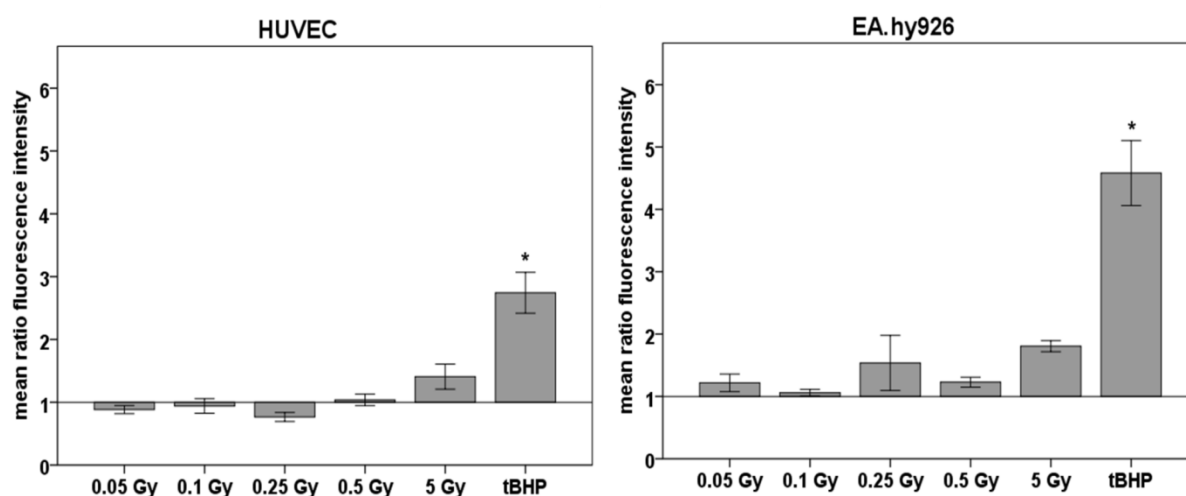


Figure 21: Intracellular ROS levels measured in EA.hy926 cells and HUVEC using the CM-H₂DCFDA assay. Bar graphs represent the mean ratio (CTRL/IR) of fluorescence intensity of intracellular DCF measured by flow cytometry in HUVEC (left panel) and EA.hy926 cells (right panel) 30 min after X-irradiation, or 30 min after 1 h incubation with 150 μ M tBHP. For each condition, data were obtained from at least three biological replicates (measured in different experiments). One-way ANOVA was performed in SPSS. Significance of differences between the control and treated samples was determined using Sidak *post-hoc* test with * = $p < 0.05$ (versus control cells). Error bars represent the standard error (SE) of the mean.

4.4.2 Mitochondrial DNA damage

Amplification of the mtDNA region where the CD is situated (without loss of the CD) using the PCR program with long extension time and primer pair F1/R1 succeeded with high specificity in all experiments (Figure 22). Varying results were obtained for the detection of the loss of the CD using the PCR program with short extension time. Indeed, amplification of the short amplicon (corresponding to the occurrence of the CD) was not always observed when the experiment was repeated. Furthermore, the observed amplicon size (± 250 bp) does not correspond to the expected amplicon size (161 bp). The regions flanked by primer pairs F2/R2 and F3/R3, which will be used to normalize for mtDNA copy number, have been successfully amplified (Figure 23) with high specificity. Amplification of a small fragment of a nuclear reference gene, β -actin (F4/R4) succeeded with high specificity as well.

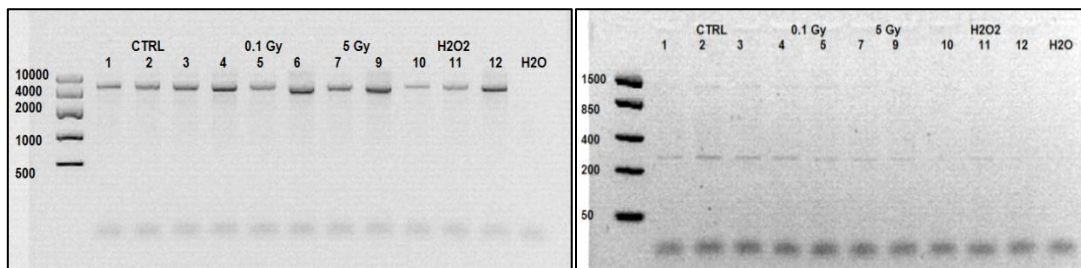


Figure 22: Electrophoresis gels of PCR products obtained after amplification with primer pair F1/R1 for control (lanes 1-3), 0.1 Gy (lanes 4-6), 5 Gy (lanes 7-9) and H₂O₂ treated samples (lanes 10-12) from EA.hy926 cells. On the left panel, PCR was programmed to allow amplification of the whole region without deletion (amplicon size 4960 bp). On the right panel, PCR was programmed to allow amplification to happen only if the deletion had occurred (observed amplicon size ± 250 bp, expected amplicon size 161 bp).

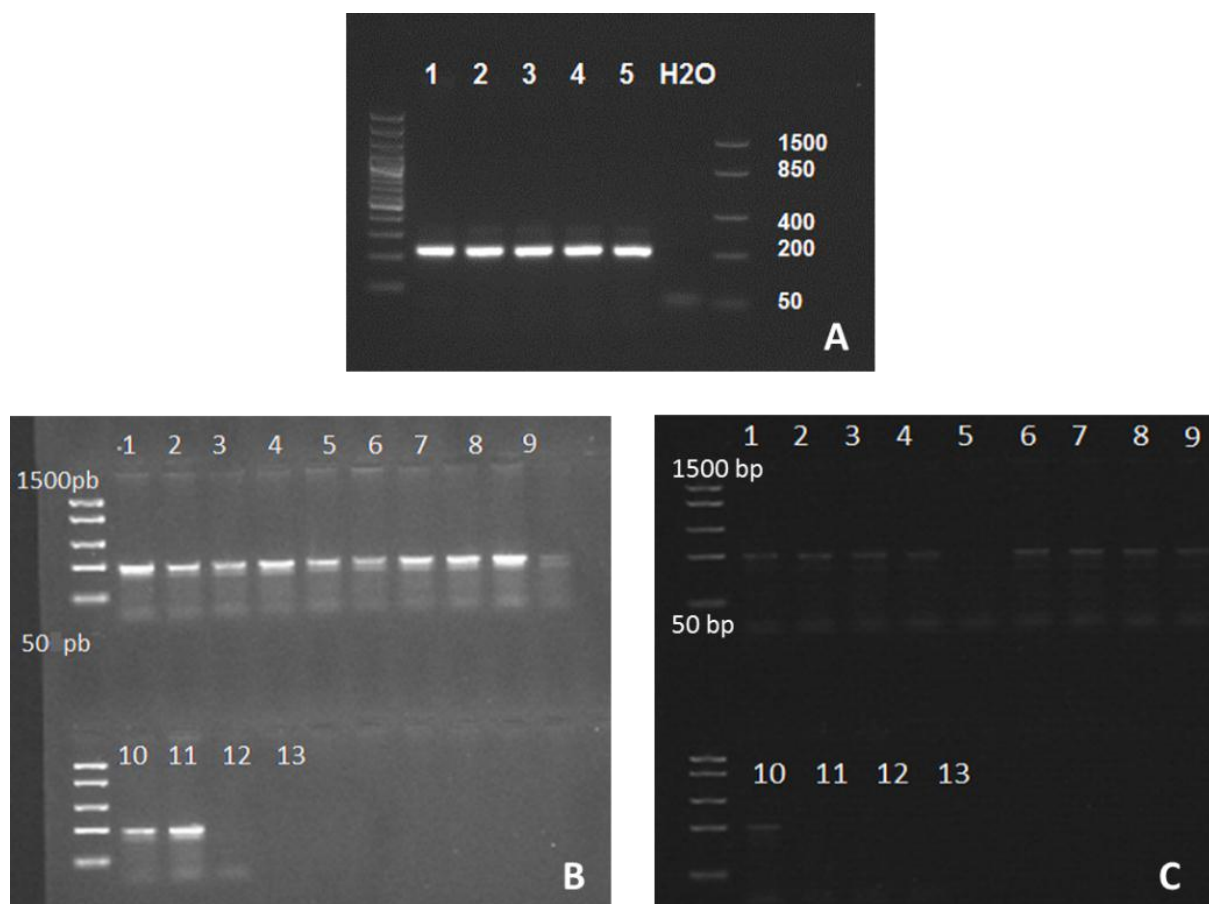


Figure 23: Electrophoresis gels of PCR products obtained after amplification with primers pairs F2/R2, F3/R3 and F4/R4. **A.** primer pair F2/R2 (amplicon size 230 bp) for control (lanes 1, 2 and 4), 5 Gy (lanes 3 and 5) and negative control (H₂O) **B.** primer pair F3/R3 (amplicon size 188 bp) and **C.** primer pair F4/R4 (amplicon size 199 bp) for control (lanes 1-3), 0.1 Gy (lanes 4-6), 5 Gy (lanes 7-9) and H₂O₂ treated samples (lanes 10-12) and with negative control in lane 13 (H₂O).

4.5 Discussion

This chapter presents preliminary data regarding the assessment of oxidative stress and mitochondrial DNA damage in endothelial cells following low dose radiation exposure. Therefore, in the discussion, we will not only discuss the present findings but we will also focus on additional steps to be undertaken for a more complete assessment of radiation-induced oxidative stress and mitochondrial dysfunction.

4.5.1 CM-H₂DCFDA assay for the measurement of intracellular ROS levels

The fluorometric CM-H₂DCFDA assay for the measurement of intracellular ROS levels was optimized. For measurement as soon as possible after irradiation, cells need to be loaded with the dye before irradiation takes place. The optimal loading time was 30 min at 37°C. After the irradiation, the cells were kept on ice. When cells are hit by ionizing radiation, also radiolysis of the water which is present in the buffer where the cells reside will occur. Hydrogen peroxide which is a stable product of radiolysis is capable of entering the cell and can thus also contribute to H₂DCF oxidation, interfering with the measurement of intracellular radiation-induced ROS. By keeping the cells on ice, extracellular hydrogen peroxide will only penetrate into the cells very slowly because of membrane rigidity [281]. Furthermore, since there will always be differences between the samples regarding the time after irradiation they are measured, ROS produced by normal oxidative metabolism can produce artifacts as well. This is, however, minimized by keeping the samples on ice [282].

Intracellular ROS levels were measured 30 minutes after irradiation: due to practical constraints (transport from the irradiation building) it was only possible to measure DCF fluorescence as early as 30 minutes after irradiation. Seeing the complexity of the experimental procedure, the lack of significant results can be explained by the use of a relative low number of replicates. Regarding low dose radiation (< 0.5 Gy), no clear dose-response relationship was observed. In HUVEC, low doses of radiation tend to reduce intracellular ROS levels, although not significant. Overall, EA.hy926 tends to contain more intracellular ROS than HUVEC. This can be explained by the weaker enzymatic antioxidant defense mechanisms in EA.hy926 [225]. Furthermore, the higher level of radiation-induced ROS may be related to our previously observed higher radiosensitivity of EA.hy926 cells compared to HUVEC, in terms of DNA damage and apoptosis [283].

Although the CM-H₂DCFDA assay can be of value, results should be interpreted with caution. For instance, H₂DCFA is directly oxidized by e.g. NO₂[•] and CO₃^{•-} but oxidation by H₂O₂ requires a catalysator [284]. Oxidation of H₂DCFA by H₂O₂ is fast in the presence of peroxidase and of similar catalysts such as cytochrome *c*. This is of importance since cytochrome *c* is released from the mitochondria in the cytosol during apoptosis. Therefore, changes in DCF fluorescence may reflect this phenomenon rather than real changes in intracellular ROS levels. The CM-H₂DCFDA assay was carried out with flow cytometry. However, it would be interesting to perform the experiment using fluorescence microscopy too since this would give a better insight in the cellular distribution of ROS formation. It has been reported that the laser used in both fluorescence microscopy and flow cytometry induces ROS formation. This side effect is more pronounced in fluorescence microscopy compared to flow cytometry [285]. Although, the ROS-inducing effect can neither be excluded in the latter. Therefore, it would be interesting to check the effect of laser intensity on ROS formation. The inclusion of control samples should, however, rule out this side effect in the analysis of our results.

Besides the above mentioned limitations of the CM-H₂DCFDA assay, there may also be a biological explanation for the subtle effects observed following low dose radiation exposure. ROS formed due to the primary ionizing events are known to disappear quickly (in less than 10⁻³ s) and are thus not present anymore after 30 min. On the other hand, it has been shown that these 'primary' ROS can be amplified by the cell [265-267], although it may be that this requires longer time than 30 min. To investigate the long-term effect of radiation exposure on cellular oxidative stress, measurements at longer timepoints after irradiation, e.g. days and weeks, should be carried out. Furthermore, other markers of cellular oxidative stress should be included. For instance, oxidative damage to lipids, proteins and DNA, can be assessed by measuring the levels of 8-isoprostane, p-tyrosine and 8-hydroxydeoxyguanosine, respectively [286, 287]. Furthermore, it is of interest to assess NO levels. First, it is hypothesized that NO concentration will decrease after IR exposure since superoxide is known to inactivate NO. For regulating the vascular tone, endothelial cells produce NO which mediates vascular smooth muscle cell relaxation. Decreased NO availability will impair maintenance of the vascular tone and can thus worsen atherosclerosis-related health symptoms [125]. Next, the interaction of NO with superoxide leads to the formation of peroxynitrite and consequently 3-nitrotyrosine, which is a known marker of nitrative stress [259, 286].

Finally, to investigate further the effect of radiation-induced oxidative stress on cellular endpoints such as DNA damage and the induction of apoptosis or senescence, the use of ROS scavengers in the experimental set-up would be of interest. In this way, one can also elucidate underlying molecular signaling pathways. For instance, Ma and coworkers have revealed a protective role of ferulic acid in radiation-induced (10 Gy) oxidative stress in HUVEC, through upregulation of cellular glutathione (GSH) and nicotinamide adenine dinucleotide phosphate (NAPDH) levels [288]. They reported an involvement of the phosphatidylinositol 3-kinase (PI3K) and extracellular signal regulated kinase (ERK), which were responsible for the translocation of nuclear factor erythroid 2-related factor 2 (Nrf2) to the nucleus where it could bind with anti-oxidant response element (ARE) within the promotor regions of the genes GSH and NAPDH, leading to their up-regulation. Other ROS scavengers that are used in molecular biology to assess oxidative stress are sodium pyruvate, mannitol and manganese(III)-tetrakis(4-benzoic acid)porphyrin [289, 290].

4.5.2 PCR for the assessment of the CD, a marker for mtDNA damage

PCR quantification of the CD, for assessment of radiation-induced mtDNA damage, was worked out. Since the CD is amplified during mtDNA replication, it has been proposed as a sensitive marker for low levels of mtDNA damage, as induced by low dose of ionizing radiation [194]. PCR detection of the CD was inconsistent in our experiments. The presence of the CD was not always observed when the experiment was repeated. In addition, the observed amplicon size was not as expected. This may be because the mtDNA sequence of the cell line EA.hy926 and the primers we used, does not fully correspond to the human mtDNA sequence from MITOMAP [280]. Therefore, it would be good to test the primers on other cell lines as well, such as HUVEC. Furthermore, the PCR product could represent a different mtDNA deletion. For example, Wang and coworkers have identified a novel mtDNA deletion with break points close to that of the CD [193]. For further research in our lab it would be of interest to sequence the full mtDNA from the EA.hy926 cell line which will aid in the development of new primers. Furthermore, sequencing of the mtDNA, before and after exposure to low dose radiation, can reveal radiation-induced point mutations. Another technique that can be used to determine mtDNA damage is restriction fragment length polymorphism. With this technique, the mtDNA is digested into different fragments by restriction enzymes and the resulting restriction fragments are separated according to their length by gel electrophoresis [291].

Besides the induction of mtDNA damage, ionizing radiation-induced amplification of intracellular ROS levels can also be mediated via other mechanisms. For instance, Leach and coworkers have speculated that clinically significant doses of ionizing radiation (1-10 Gy) may amplify mitochondrial ROS/RNS production via a mechanism that involves mitochondrial permeability transition [192]. They proposed that a radiation-induced oxidative event in a mitochondrion initiates the localized release of Ca^{2+} . Adjacent 'non-hit' mitochondria can take up this Ca^{2+} , resulting in transient mitochondrial permeability transition (demonstrated by membrane depolarization) and release of Ca^{2+} . In this way, a single oxidizing event induced by ionizing radiation can be further propagated in the cell. Associated increase in Ca^{2+} release and membrane depolarization can thus enhance ROS/RNS generation. Another mechanism that is proposed to play a role in delayed mitochondrial ROS production is radiation-induced mitochondrial fission, which is associated with an increased expression of the dynamin-like protein DRP1 [292, 293]. This increase in mitochondrial fission was correlated with an impaired function of the respiratory chain, being the cause of the delayed ROS production. It is however, not elucidated how the increase in mitochondrial fission is related to impaired respiratory chain function.

4.6 Conclusion and perspectives

Regarding the assessment of intracellular ROS levels, the CM-H₂DCFDA assay was successfully established. However, considering the limitations of the assay it is advised to include other methods for the assessment of oxidative stress. Furthermore, in a new PhD project, other probes will be used to measure intracellular NO and mitochondrial superoxide levels, to have a better insight in radiation-induced oxidative/nitrosative stress. NO levels following radiation exposure can be assessed using the 4-amino-5-methylamino-2',7'-difluorofluorescein diacetate (DAF-FM diacetate) probe by flow cytometry. In the context of mitochondrial induced amplification of intracellular ROS levels, it is of interest to use the MitoSOX Red probe, which is targeted to the mitochondria and specifically measures mitochondrial superoxide by flow cytometry. Finally, it would be interesting to assess whether ionizing radiation induces amplification of intracellular ROS on the longer term, how it alters redox signaling and its impact on final cellular outcome (e.g. induction of senescence).

Seeing the importance of the mitochondria in the cellular response to radiation, further research in the effects of radiation on mitochondria is required. Besides the assessment of mtDNA damage, knowledge regarding mitochondrial function is needed. Therefore it is planned, in a new PhD project, to assess mitochondrial activity by, amongst others, the measurement of fusion and fission events, the mitochondrial potential, and the production of the TCA cycle (Krebs cyclus) intermediates citrate, succinate and 2-oxoglutarate using validated enzymatic kit protocols.

**Chapter 5: Transcriptomic profiling suggests a role
for IGFBP5 in premature senescence of human
umbilical vein endothelial cells (HUVEC) after
chronic low dose rate irradiation**

Modified from: Rombouts C., Aerts A., Quintens R., Baselet B., El-Saghire H., Harms-Ringdahl M., Haghdoost S., Janssen A., Michaux A., Yentrapalli R., Benotmane R., Baatout S. Transcriptomic profiling suggests a role for IGFBP5 in premature senescence of endothelial cells after chronic low dose rate irradiation. Accepted in International Journal of Radiation Biology.

5.1 Abstract

Ionizing radiation has been recognized to increase the risk of CVD. However, there is no consensus concerning the dose-risk relationship for low radiation doses and a mechanistic understanding of low dose effects is needed. Endothelial senescence is implicated in the development of atherosclerosis, a major cause of CVD morbidity. A European consortium was set-up in which human umbilical vein endothelial cells (HUVEC) were exposed to chronic low dose rate (LDR) radiation (1.4 and 4.1 mGy/h) during one, three and six weeks. It was observed that exposure to 4.1 mGy/h resulted in premature senescence. To gain more insight in the underlying signaling pathways, we analyzed gene expression changes in these cells using microarray technology. The obtained data were analyzed in a dual approach, combining single gene expression analysis and Gene Set Enrichment Analysis. An early stress response was observed after one week of exposure to 4.1 mGy/h which was replaced by a more inflammation-related expression profile after three weeks and onwards. This early stress response may trigger the radiation-induced premature senescence previously observed in HUVEC irradiated with 4.1 mGy/h. A dedicated transcriptomic analysis in our study pointed to the involvement of insulin-like growth factor binding protein 5 (IGFBP5) signaling in radiation-induced premature senescence. Our findings, together with those from the other consortium partners, will be integrated in a systems biology approach to obtain a better mechanistic understanding of chronic LDR radiation-induced premature senescence in HUVEC.

5.2 Introduction

Several epidemiological studies have pointed to an excess risk of cardiovascular diseases (CVD) following radiation exposure [65]. Major sources of information are the Life Span Study (LSS) cohort and the Adult Health Study (AHS) cohort from Japanese atomic bomb survivors, which revealed an excess risk of stroke and heart disease following exposure to lower doses of ionizing radiation [53, 61]. However, there is still considerable uncertainty about the dose-risk relationship, in particular for low (< 0.5 Gy) doses [53]. Recently, a new method of analysis by fitting multiple dose-response models on LSS data has been proposed by Schöllnberger and coworkers to produce more reliable risk estimates. Their findings support a linear non-threshold type of response for mortalities related to CVD in the LSS cohort, with risk estimates consistent with zero risk below 2.2 Gy based on 90% confidence intervals [61]. Regarding cardiovascular risks related to protracted exposures, major sources of information are occupational cohorts and cohorts living in areas with high level background radiation [294]. For example, an excess risk for ischemic heart disease and stroke morbidity was observed among the Chernobyl liquidator cohort [57]. Also, an increasing trend in circulatory disease mortality with dose was revealed by studying the records of the National Dose Registry of Canada (individual dose registries of all occupationally exposed workers in Canada) and the records of male workers at the British Nuclear Fuels plc [56, 295]. A valuable well-established cohort is that of the Mayak nuclear facility workers because information is available for both mortality and morbidity as well as for confounding factors such as smoking and alcohol consumption. The latest analysis of the Mayak worker data revealed an increasing trend in ischemic heart disease incidence with both total external γ -ray dose and internal liver dose [59]. Meta-analysis of all published epidemiological studies suggested a positive association between dose and an excess risk of CVD. However, this could not be statistically evidenced for low doses. The large heterogeneity between the different studies, lack of dosimetry data and/or not eliminating confounding factors hampered a correct evaluation of the dose-risk relationship [10, 38].

To improve the judgment of radiation-related CVD risk it will be crucial to integrate biological knowledge into epidemiological studies, pointing out the necessity of biological research [82]. Fundamental biological research regarding the underlying mechanisms of radiation-related cardiovascular diseases can serve two major goals: (i) identification of suitable biomarkers for use in molecular epidemiological studies, and (ii) identification of

molecular targets that can be used in the development of countermeasures. Genome-wide gene expression profiling has proven to be a useful tool in the quest for biomarkers as well as for the understanding of molecular pathways involved in the radiation response [82, 206].

The endothelium, which constitutes the inner lining of the cardiovascular system, is considered to be a critical target for radiation-related CVD [296]. Endothelial cells are involved in processes such as coagulation, fibrinolysis, vascular tone regulation and inflammation, and are considered safeguards for normal vascular functioning [120]. Consequently, endothelial dysfunction plays a critical role in the development and progression of CVD, and in particular atherosclerosis [124]. Atherosclerosis is a chronic disease of the arterial wall characterized by the formation of a so-called 'plaque' which will impair normal blood flow and can lead to complications such as myocardial infarction and stroke [91]. Aging of the vasculature is a well-known risk factor of atherosclerosis and is associated with impairment of normal endothelial function [147].

There is *in vivo* evidence for the involvement of senescence of endothelial cells in age-related atherosclerosis [137-139, 297]. Senescence is a particular state in which cells enter a permanent form of growth arrest, are incapable of synthesizing DNA and are unresponsive to growth stimuli. Nevertheless, they remain metabolically active [298]. In the case of senescent endothelial cells, this results in a pro-inflammatory, pro-atherosclerotic and pro-thrombotic phenotype [135]. Senescence was observed for the first time by Hayflick and Moorhead as a state in which cells lose their ability to proliferate in culture [140]. This is termed replicative senescence and is due to telomere shortening that occurs during each cell division until a critical length is reached that triggers specific cell signaling pathways [147]. Senescence, however, can also occur in a telomere independent manner following cellular insults causing amongst others intracellular oxidative stress and inflammation. This is called stress-induced senescence and can also be induced following ionizing radiation exposure [196].

It has been hypothesized that chronic low dose rate (LDR) radiation exposure may accelerate the onset of senescence in endothelial cells (personal communication). This radiation-induced premature senescence may indirectly lead to an increased risk of CVD by accelerating the progression of age-related atherosclerosis.

A European consortium to study the response of human umbilical vein endothelial cells (HUVEC) after chronic exposure during one, three or six weeks to γ -radiation (^{137}Cs) at different dose rates, 1.4 mGy/h and 4.1 mGy/h, was set-up (FP7 DoReMi project (task 7.3.),

grant agreement 295823). The long-term goal of this project is to analyse the mechanisms underlying chronic LDR radiation-induced responses in HUVEC in a systems biology approach. The irradiations were carried out at Stockholm University after which the necessary samples were distributed to the partners. Each partner was responsible for a specific endpoint which included proteomics, senescence markers, oxidative stress markers (8-oxo-dG and hMTH1), inflammatory response, capacity to form vascular networks in Matrigel, DNA damage and genomic instability (chromosomal aberration and telomere length). We were responsible for the genome-wide gene expression analysis. Overall, we aimed to gather information about changes in signaling pathways and radiation response mechanisms in HUVEC during chronic LDR γ -irradiation, with a particular focus on radiation-induced premature senescence.

Indeed, consortium partners observed premature senescence in HUVEC after six weeks of exposure to 4.1 mGy/h, but not 1.4 mGy/h (Figure 24). This was determined by a progressive loss of replicative capacity and increased activity of senescence-associated- β -galactosidase (SA- β -gal) [204, 205]. They also carried out proteomic analysis which revealed that several senescence-related pathways were influenced by 4.1 mGy/h, such as cytoskeletal organization, cell-cell communication and adhesion, and inflammation. Furthermore, their proteomic data suggest that chronic radiation-induced DNA damage and oxidative stress resulted in the induction of p53/p21 pathway, ultimately leading to premature senescence [204]. The current chapter is embedded in this European project and gives an overview of the transcriptomic analysis performed on mRNA obtained from the same chronic LDR irradiated HUVEC cultures. The presented results should thus be regarded complementary to two papers which describe the results regarding senescence markers and proteomic changes in these chronic LDR irradiated HUVEC [204, 205]. Moreover, our results together with the results obtained by the other partners will be integrated by modellers, in a systems biology approach, to obtain an understanding of the mechanisms underlying chronic LDR radiation-induced premature senescence.

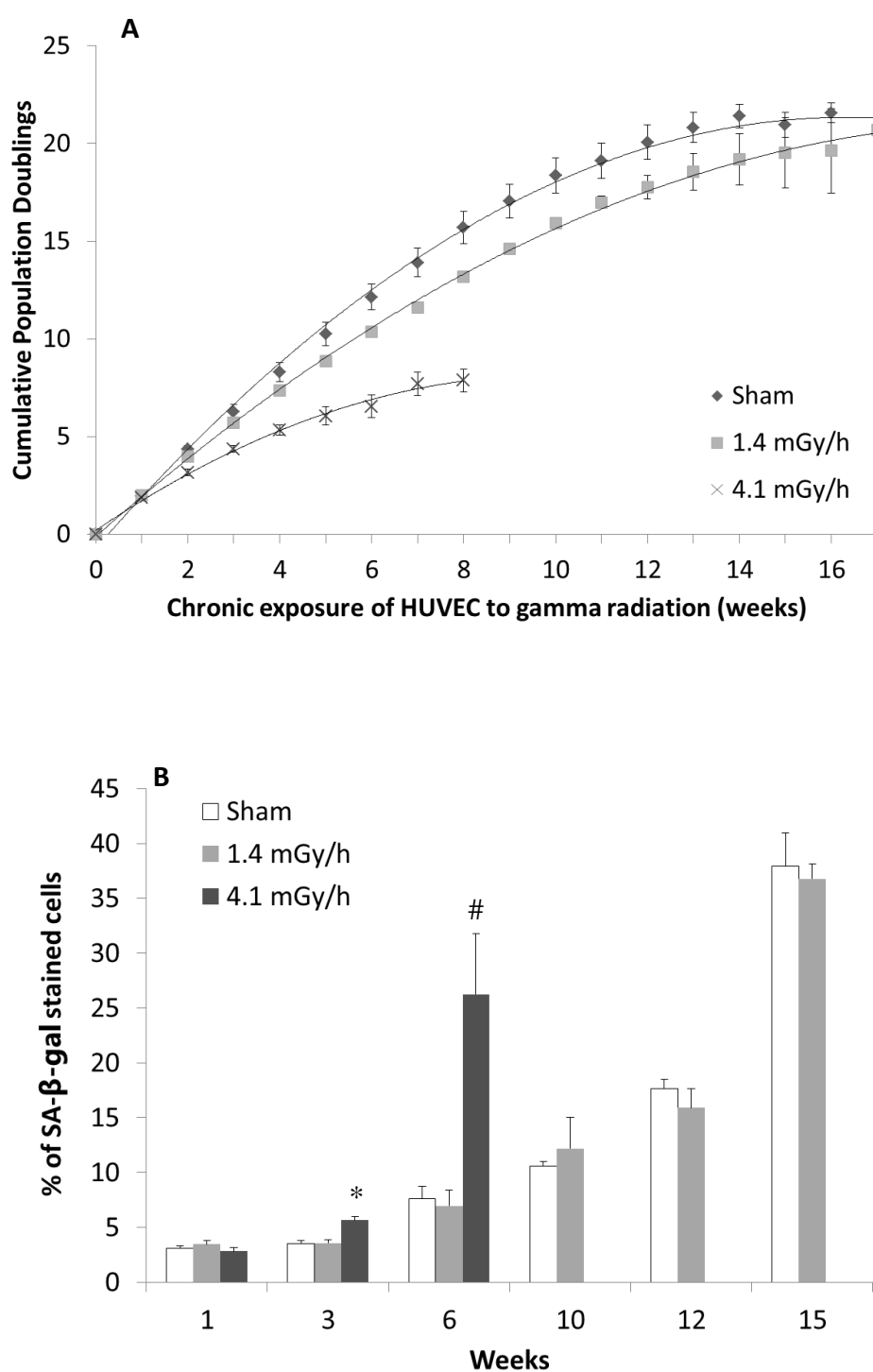


Figure 24: Chronic γ -radiation (^{137}Cs) of HUVEC. **A.** Proliferation rate of HUVEC exposed to different dose rates determined by cumulative population doublings. **B.** Activity of SA- β -gal in HUVEC exposed to different dose rates. Results are the mean value of three independent biological experiments. Results are obtained by the partners at Stockholm University in the EU FP7 DoReMi project. The authors have permitted the use of these figures. * = p-value ≤ 0.01 between sham and 4.1 (week 3) and # = p-value ≤ 0.005 between sham and 4.1 (week 6).

5.3 Materials and methods

5.3.1 Cell culture conditions

Cell culture conditions were as previously described [204]. HUVEC (Invitrogen, Paisley, UK) were obtained from a single donor, and cultures were started from an early passage on (P2). They were cultured in Media 200 (Invitrogen) supplemented with low serum growth supplement containing 2% fetal bovine serum, 1 µg/µl hydrocortisone, 10 ng/ml epidermal growth factor, 10 µg/ml heparin, 100 U/ml penicillin and 0.1 mg/ml streptomycin at 37°C in a 95% air / 5% CO₂ humidified atmosphere. All cell culture media supplements were obtained from Invitrogen. Cells were passaged every seven days (5000 cells/cm²) with culture medium being changed every two days. Accutase (Invitrogen) was used to detach cells during passaging and harvesting of cells.

5.3.2 Chronic gamma radiation exposure

Chronic gamma radiation exposure was performed at Stockholm University as previously described [204]. A cell culture incubator equipped with a ¹³⁷Cs-gamma source was used to expose HUVEC to chronic ionizing radiation (1.4 and 4.1 mGy/h). The cells were irradiated until they lost their proliferative potential. Irradiation was carried out continuously except during the replacement of culture medium and sub-culturing of cells which lasted between 30 minutes and 1 hour. Control cells were grown in an identical incubator, but without exposure to ionizing radiation. The irradiations were performed in triplicate in three separate, subsequent experiments generating three biological replicate samples for each treatment.

5.3.3 RNA extraction

For the two first experiments RNA was extracted at the Helmholtz Zentrum München using the mirVana™ miRNA Isolation Kit (Ambion Inc., Austin, TX, USA). The protocol for total RNA extraction was followed according to the manufacturer's instructions. For the third experiment, RNA was extracted in our lab using the AllPrep DNA/RNA/Protein Mini kit according to manufacturer's instructions (QIAGEN, Hamburg, Germany). RNA quantity was measured using a NanoDrop-2000 spectrophotometer (Thermo Scientific, Erembodegem, Belgium) and the quality was assessed using an Agilent 2100 Bioanalyzer (Agilent

Technologies, Santa Clara, CA, USA). The RNA integrity number (RIN) was at least 8.6 for all samples.

5.3.4 Microarray assay

Microarray assay was performed as previously described [204]. Using the Ambion® WT Expression Kit (Ambion Inc.), cRNA was prepared from cDNA, originally synthesized and purified from 0.25 µg of total RNA following the manufacturer's instructions. Next, cRNA was purified and used for synthesis of 2nd cycle DNA of which 2.75 µg was then used for fragmentation and labeling using the GeneChip® Terminal Labeling Kit (Affymetrix, Santa Clara, CA, USA). Using GeneChip® Hybridization, Wash and Stain Kit (Hybridization module) (Affymetrix), and Hybridization Controls (Affymetrix), fragmented and labeled cDNA was hybridized to Human Gene 1.0 ST Arrays (Affymetrix). After hybridization with rotation for 16 hours at 45°C, arrays were washed and stained using GeneChip® Hybridization, Wash and Stain Kit (Stain module) (Affymetrix) according to the manufacturer's instructions. Finally, arrays were scanned immediately using the Affymetrix GeneChip® Scanner (Affymetrix).

5.3.5 Microarray data analysis

Analysis of microarray data was performed by importing the raw data (CEL-files) in Partek Genomics Suite v6.6 (Partek Incorporated, St. Louis, Mo., USA). In brief, Robust Multi-array Average background correction was applied, data were normalized by Quantile Normalization and probe set summarization was performed by the Median Polish method. Samples were categorized according to following attributes: *time*, *dose rate*, *treatment* (dose rate*time = accumulated dose) and *experiment*. Exon expression data were summarized as gene expression values using the one-step Tukey method. To identify the factors that have the biggest influence on individual gene expression, a 5-way analysis of variance (ANOVA) was run with *experiment*, *scan date*, *dose rate*, *time* and *treatment* as factors. No interactions were included in the ANOVA model. The experimental set-up (most likely the RNA extraction method) had the largest effect on differential gene expression, followed by *scan date*, which we considered as batch effects. Therefore, these batch effects were removed using the Partek Batch Effect Removal tool to create a new gene expression list and the 5-way ANOVA was reran. As a result, the gene expression values were adjusted to what they would have been if

there had been no batch effects. Other signals and noise remained in the data set. Visual assessment by means of Principal Component Analysis (PCA), demonstrated that the batch effects could be effectively removed (Figure 26). After removal of the batch effects, it was observed that *time* had the largest effect on differential gene expression (Figure 25). Comparisons between the different treatments were made by unpaired sample t-tests and genes with an unadjusted p-value below 0.05 and a fold change (FC) below -1.5 or over 1.5 were considered as differentially expressed.

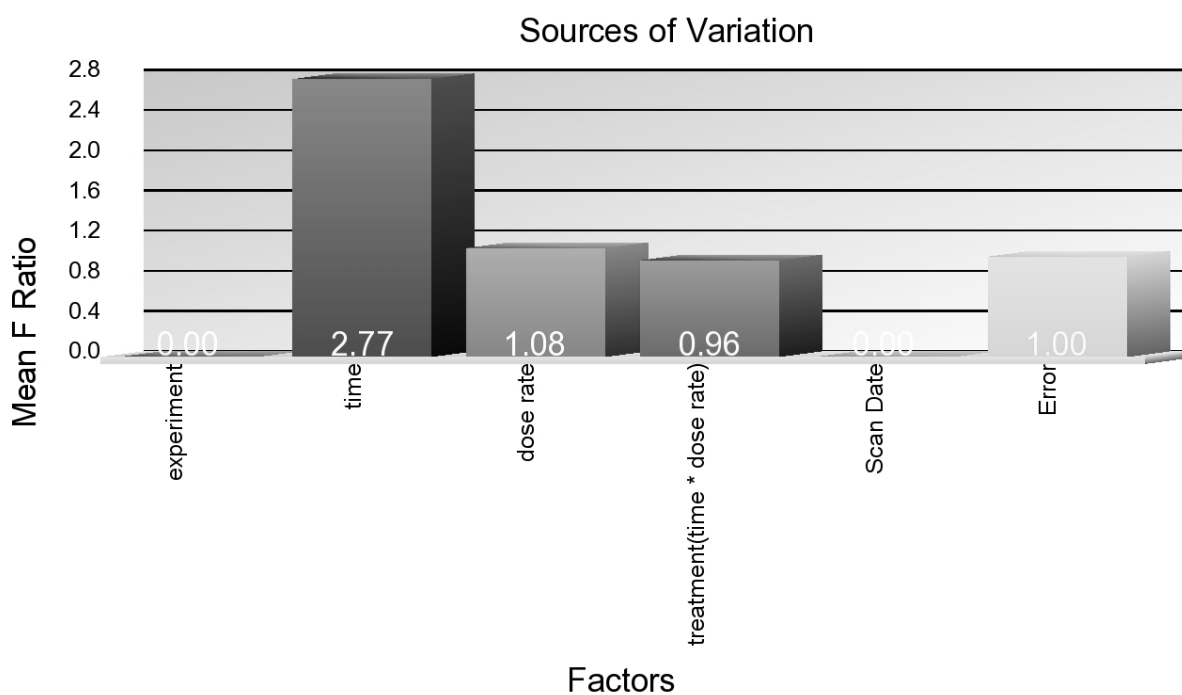


Figure 25: Bar chart of the sources of variation, after batch removal, which gives an overview of the relative contribution of each factor in the 5-way ANOVA. *Time* is the biggest source of variation.

5.3.6 Principal component analysis (PCA)

PCA is a statistical tool that calculates principal components that account for the variability observed in a specific dataset. PCA can be visualized in a graph (Figure 26). Each sphere in the graph represents a sample of our microarray chip. In total 27 samples were included in our experiment. The axes represent the three major principal components which are directed towards increasing variation of the dataset [299]. The spheres are thus spread in the graph based on their variation: i.e. closely located spheres have more similar intensity values across

the probesets on the whole chip (genome) than further away located spheres [300]. Finally, one can attribute a factor to each sphere (in this case *experiment* and *scan date*) as such identifying clustering according to a specific factor. Before removal of the batch effects, the spheres are highly clustered on *experiment* and, to a lesser extent, *scan date* (Figure 26). This clustering has disappeared after removal of the batch effects (*experiment* and *scan date*), indicating an effective removal.

Transcriptomic profiling of endothelial cells exposed to chronic low dose rate irradiation

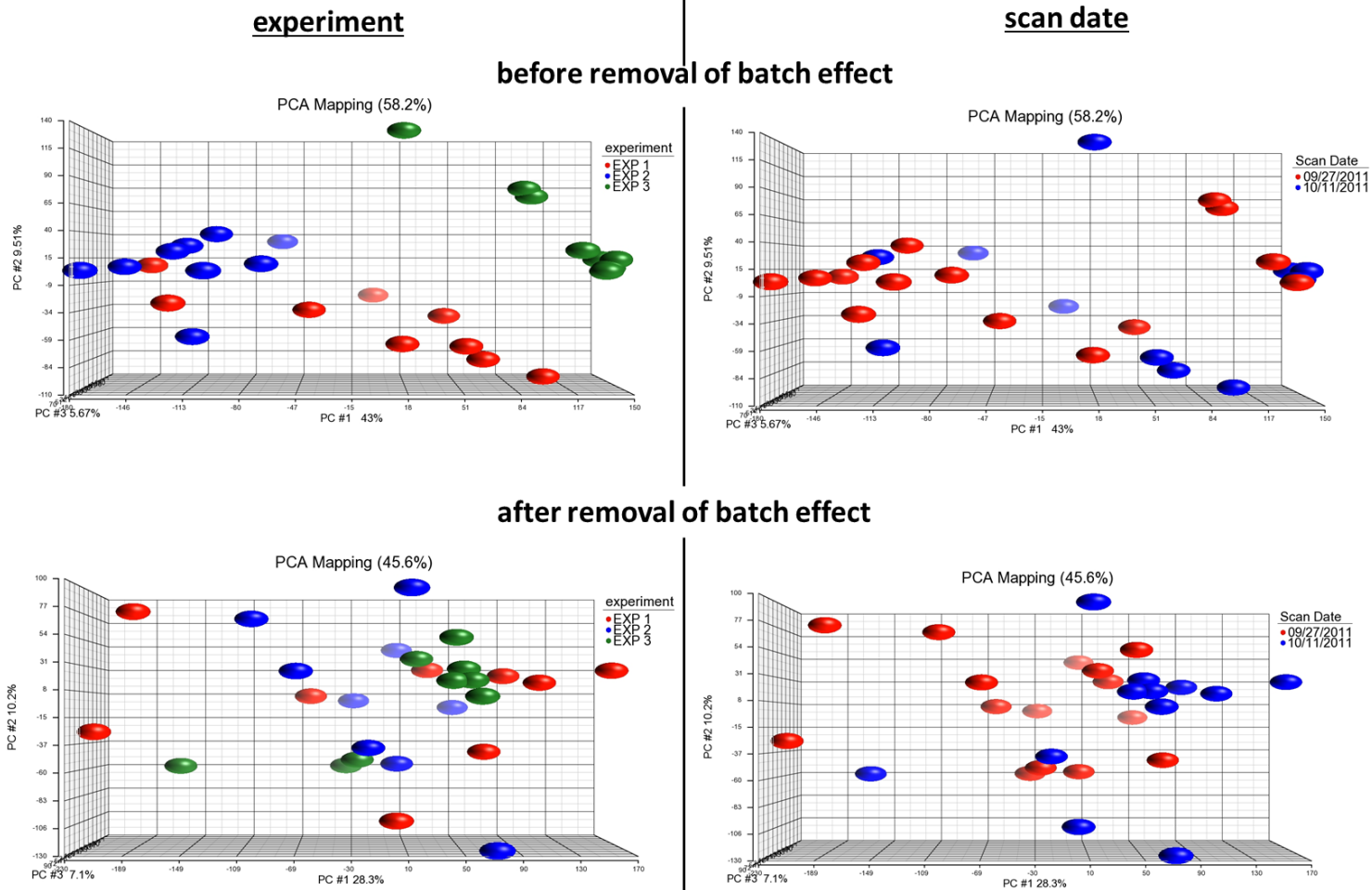


Figure 26: PCA plots which give a visualization of the variation in intensity values across the probesets on the whole chip (genome) between the different samples. In each of the four plots, all samples (27 in total) are represented as separate spheres. The upper plots visualize the variation between the samples before removal of the batch effects (experiment and scan date) and the lower plots represents the variation between the samples after removal of the batch effects. Closely located spheres have a more similar transcriptome than further away located spheres. The spheres are colored by experiment (plots on the left) or scan date (plots on the right).

5.3.7 Analysis of senescence-related differential gene expression

To investigate genes that may be involved in the radiation-induced acceleration of the senescence process, we identified the genes that were differentially expressed between week six and week one (unadjusted p-value < 0.001, no threshold for FC), and in common for control and 4.1 mGy/h irradiated HUVEC. More specifically, we were interested in the genes of which the differential expression between week six and week one were more pronounced in cells irradiated with 4.1 mGy/h compared to control. Therefore, no threshold was set for FC. In this way, genes that are, for example, not differentially expressed between week six and one for control, but that are for 4.1 mGy/h, are included. A more stringent p-value as compared to the one of section 5.3.5 was used ($p < 0.05$). Next, we calculated the ratio between the FC of irradiated genes and the FC of control genes.

$$\text{ratio} = \frac{\text{FC 4.1 mGy/h week 6 vs week 1}}{\text{FC control week 6 vs week 1}}$$

The genes having a ratio that deviate the most from 1 were then considered candidate genes involved in the acceleration of the senescence process. From these genes, insulin-like growth factor binding protein 5 (IGFBP5) was revealed as an important candidate gene. Using a Pearson correlation (in Partek Genomics Suite v6.6), we explored genes of which the expression profile mostly correlated (positively or negatively) with that of IGFBP5.

5.3.8 Gene Set Enrichment Analysis (GSEA)

The microarray data were further analyzed using GSEA to investigate whether predefined gene sets were significantly enriched between control and irradiated cells. GSEA is an analytical method for interpreting gene expression data on the level of gene sets and is used to generate hypotheses for biological interpretation [213]. In essence, GSEA determines whether an a priori defined gene set is overrepresented at the top or the bottom of a ranked list of genes that are found in the expression data set of two phenotypes (in this case irradiated and control cells). Genes are ranked using signal-to-noise ratio. Next, an enrichment score, which reflects the overrepresentation of a given gene set in the ranked list of genes, is calculated based on normalized Kolmogorov-Smirnov statistics [213, 214]. In this study, we kept the default parameters in the GSEA software. Normally, the statistical significance of the normalized enrichment score associated to each gene set is assessed through 1000 random

permutations of the phenotype labels. However, since this study has less than seven samples in each phenotype (only three per treatment), permutations were based on gene sets instead of phenotype labels [301], as is recommended in the GSEA guidelines. Enriched gene sets with a false discovery rate (FDR) value below 0.05 were used for driving further biological interpretation. FDR-value is preferred over p-value for gene sets since it gives the statistical significance of an enriched gene set corrected for gene set size and multiple hypotheses testing [213]. The gene set databases used in our study are Kegg PATHWAY and Gene Ontology Biological Process (GO BP) gene set databases (downloaded from <http://www.broadinstitute.org/gsea/msigdb/index.jsp> (v.4.0)). GSEA results based on GO BP were visualized using Enrichment Map, (downloaded from <http://baderlab.org/Software/EnrichmentMap/>) as a plugin in Cytoscape [302]. Given that Enrichment Map visualization is only useful when using hierarchically organized gene sets like GO [302], GSEA results based on the Kegg PATHWAY database are presented in table format.

5.3.9 Quantitative real-time PCR validation

Expression of IGFBP5 was validated with quantitative real-time PCR using the TaqMan® Gene Expression Assay (catalogue number: Hs00181213_m1) (Applied Biosystems, Foster City, CA, USA) which contains gene-specific primers and a FAMTM (6-carboxyfluorescein) dye-labeled MGB (minor groove binder) probe. For each sample, diluted cDNA originating from the microarray experiment was used and each reaction was ran in technical triplicates using TaqMan® Fast Advanced Master Mix on a 7500 Fast Real-Time PCR system (Applied Biosystems). Cycling conditions were set according to manufacturer's guidelines for a fast 96-well run: hold-step for 20 seconds at 95°C, followed by 40 cycles with 3 seconds at 95°C and 30 seconds at 60°C. Relative expression levels were calculated using the Pfaffl method [303] using ribosomal protein, large, P0 (RPLP0) (catalogue number: Hs99999902_m1) (Applied Biosystems) as reference gene.

5.4 Results

5.4.1 Chronic LDR radiation-induced differential gene expression in HUVEC

Differential gene expression was analyzed after one, three and six weeks (Figure 27 and Table 5) by comparing control cells with irradiated cells. The number of differentially expressed genes (p -value < 0.05 and $|FC| > 1.5$) between control and irradiated cells at each time point was limited (Figure 27) with absolute FC that never exceeded 3-fold, indicating that the transcriptional effects of chronic LDR radiation on HUVEC are rather subtle. Most genes were differentially expressed after one week (46 genes for 1.4 mGy/h, and 58 genes for 4.1 mGy/h). This number dropped after three weeks (3 genes for 1.4 mGy/h, and 2 genes for 4.1 mGy/h) after which it increased again after six weeks (14 genes for 1.4 mGy/h, and 25 genes for 4.1 mGy/h). The highest dose rate (4.1 mGy/h) induced a higher number of differentially expressed genes as opposed to the lowest dose rate (1.4 mGy/h). Six annotated genes that were differentially expressed after one week were in common for both dose rates: epithelial cell adhesion molecule (EPCAM); patched 2 (PTCH2), chromosome 15 open reading frame 51 (C15orf51); ankyrin repeat domain 20B (ANKRD20B); ankyrin repeat domain 20 family, member A12, pseudogene (LOC375010) and RNA, U4 small nuclear 2 (RNU4-2). After three weeks, only one gene was in common for both dose rates: small nucleolar RNA, C/D box 20 (SNORD20), a small nucleolar RNA involved in RNA modification, whereas no genes were in common after six weeks. Remarkably, a large number of genes were not annotated. For these non-annotated genes, transcript ID analysis using the NetAffxTM Analysis Center and USCS Genome Browser was performed. This revealed that these non-annotated genes are mostly small RNAs such as mitochondrial transfer RNA, small cytoplasmic RNA, small nuclear RNA and small nucleolar RNA.

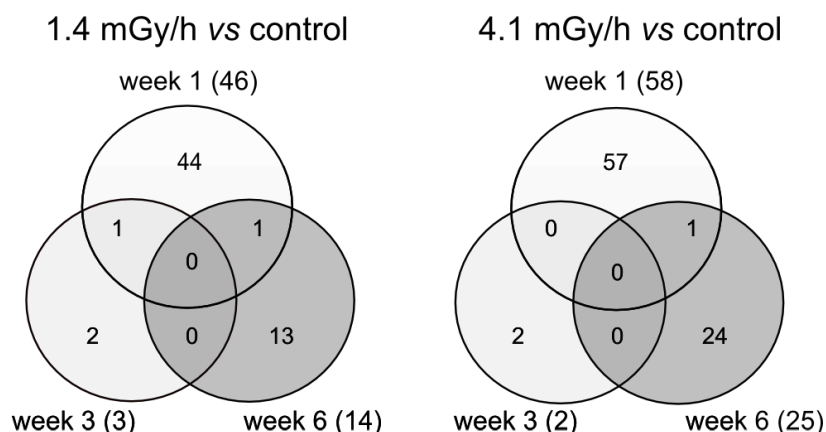


Figure 27: Venn diagrams representing differentially expressed genes (including non-annotated genes) with a p-value < 0.05 and a |FC| > 1.5. Comparisons are made between 1.4 mGy/h and control (left panel) and 4.1 mGy/h and control (right panel) at each time point (week 1, 3 and 6).

WEEK 1			WEEK 3			WEEK 6		
1.4 mGy/h vs CTRL			1.4 mGy/h vs CTRL			1.4 mGy/h vs CTRL		
Gene Symbol	p-value	FC	Gene Symbol	p-value	FC	Gene Symbol	p-value	FC
UGT2B7	4,17E-03	-1.68	SNORD20	0.01	-1.62	PAPPA2	2,10E-04	-1.56
SNORD20	0.01	1.66			PRSS2	1,03E-03	-1.67	
C15orf51	0.01	-1.87			LOC143188	3,06E-03	1.58	
LOC375010	0.02	-1.61			JHDM1D	3,80E-03	-1.54	
ANKRD20B	0.02	-1.55			SNORA62	0.02	1.62	
BAGE2	0.02	-1.81			ND6	0.04	-1.57	
ANKRD20B	0.02	-1.57			GPAM	0.05	-1.58	
GSTM2	0.03	-1.60						
C15orf51	0.03	-1.79						
EPCAM	0.03	-1.57						
ACTR3BP2	0.04	-1.54						
OR4K2	0.04	-1.50						
OR4F16	0.04	-1.84						
RNU4-2	0.05	1.73						
PTCH2	0.05	1.76						
SNORA75	0.05	1.75						

4.1 mGy/h vs CTRL			4.1 mGy/h vs CTRL			4.1 mGy/h vs CTRL		
Gene Symbol	p-value	FC	Gene Symbol	p-value	FC	Gene Symbol	p-value	FC
FERMT3	1,72E-03	1.80	SNORD20	0.02	-1.57	PHGDH	8,47E-05	-2.41
PLIN3	3,82E-03	1.53			AARS	3,50E-04	-1.53	
USP18	3,98E-03	1.59			SELP	4,97E-04	1.55	
VTRNA1-1	0.01	2.34			IFITM1	5,07E-04	-1.59	
SERPIND1	0.01	1.61			HBEGF	6,11E-04	1.64	
CCNA1	0.01	1.52			CHAC1	6,34E-04	-1.64	
EPCAM	0.01	-1.75			PSAT1	1,76E-03	-1.87	
PTCH2	0.01	2.10			LYVE1	0.01	1.65	
UBE2MP1	0.01	1.51			HEY2	0.01	1.55	
EFTUD1	0.02	1.54			IGFBP5	0.01	2.03	
LOC100130876	0.02	-1.57			ID2	0.01	1.56	
C15orf51	0.03	-1.73			CYBRD1	0.01	-1.52	

RNU4ATAC	0.03	1.74	EFNB2	0.01	1.56
RNU5D	0.03	2.69	LOC151760	0.01	1.56
CENPV	0.03	1.53	ASNS	0.01	-1.68
HSD3BP4	0.03	-1.54	PLAT	0.01	2.42
SNORD4A	0.03	1.72	TGFB2	0.02	1.95
GCLM	0.03	1.58	CCDC68	0.02	1.56
RNU5E	0.03	1.56	HIST1H2BK	0.04	1.62
KRT19	0.03	1.58	CST1	0.04	-1.95
ANKRD20B	0.03	-1.50			
LOC375010	0.03	-1.54			
ACOT7	0.04	1.54			
C15orf51	0.04	-1.75			
PLAT	0.04	2.08			
RNU4-2	0.05	1.72			

Table 5: Differentially expressed annotated genes with a p-value < 0.05 and a |FC| > 1.5. Comparisons are made between 1.4 mGy/h and control, and 4.1 mGy/h and control at each time point (week 1, 3 and 6). Genes are ranked according to increasing p-value. Genes in bold are further discussed.

5.4.2 GSEA and Enrichment Map

To evaluate the effect of chronic LDR radiation at the level of pathways, GSEA, using Kegg PATHWAY and GO BP as gene set databases, was performed. For each time point (week 1, 3 and 6), the following comparisons were made: control versus 1.4 mGy/h and control versus 4.1 mGy/h. This allowed the identification of up-regulated (= enriched in irradiated cells) and down-regulated (= enriched in control cells) gene sets in exposed cells at each time point (week 1, 3 and 6). Overall, GSEA results obtained from Kegg PATHWAY and GO BP were highly similar and pointed to the same pathways.

For both dose rates, one week of exposure led to the up-regulation of a large number of gene sets of which the majority was down-regulated after three weeks of exposure (Table 6 and Figure 28). These gene sets are related to classical radiation response processes such as DNA damage response, p53 signaling, apoptosis and cell cycle. Other gene sets are mostly involved in cell metabolism. After three weeks of exposure, only a small number of gene sets, related to cytokine production and adhesion molecules, was up-regulated. Remarkably, most of the genes sets that were up-regulated after one week were down-regulated after three weeks.

Transcriptomic profiling of endothelial cells exposed to chronic low dose rate irradiation

WEEK 1 up-regulated gene sets		
1.4 mGy/h	4.1 mGy/h	common
Basal transcription factors	Alanine aspartate and glutamate metabolism	Acute myeloid leukemia
Glycosaminoglycan biosynthesis keratan sulfate	Biosynthesis of unsaturated fatty acids	Alzheimer's disease
Homologous recombination	Cytosolic DNA sensing pathway	Amino sugar and nucleotide sugar metabolism
Renal cell carcinoma	Fatty acid metabolism	Aminoacyl tRNA biosynthesis
Small cell lung cancer	Glutathione metabolism	Apoptosis
	Glycerophospholipid metabolism	Base excision repair
	Glycosylphosphatidylinositol (GPI)-anchor biosynthesis	Cell cycle
	Insulin signaling pathway	Chronic myeloid leukemia
	Lysosome	Citrate cycle (TCA cycle)
	mTOR signaling pathway	Colorectal cancer
	One carbon pool by folate	DNA replication
	Peroxisome	Epithelial cell signaling in <i>helicobacter pylori</i> infection
	Protein export	Huntington's disease
	Pyruvate metabolism	Inositol phosphate metabolism
	Ribosome	Mismatch repair
	Snare interactions in vesicular transport	N-glycan biosynthesis
	Steroid biosynthesis	Nucleotide excision repair
	<i>Vibrio cholerae</i> infection	Oxidative phosphorylation
		P53 signaling pathway
		Pancreatic cancer
		Parkinson's disease
		Pentose phosphate pathway
		Progesterone mediated oocyte maturation
		Proteasome
		Purine metabolism
		Pyrimidine metabolism
		RNA degradation
		RNA polymerase
		Selenoamino acid metabolism
		Spliceosome
		Systemic lupus erythematosus
		Ubiquitin mediated proteolysis
		Valine leucine and isoleucine degradation
WEEK 1 down-regulated gene sets		
1.4 mGy/h	4.1 mGy/h	common
Drug metabolism cytochrome p450	None	Metabolism of xenobiotics by cytochrome p450
		Neuroactive ligand receptor interaction
		Olfactory transduction
		Steroid hormone biosynthesis
		Taste transduction
WEEK 3 up-regulated gene sets		
1.4 mGy/h	4.1 mGy/h	common

Allograft rejection	ATP-binding cassette (ABC) transporters	Cell adhesion molecules (CAMs)
Autoimmune thyroid disease	Extracellular matrix (ECM)- receptor interaction	Cytokine cytokine receptor interaction
Complement and coagulation cascades		
Graft versus host disease		
Hematopoietic cell lineage		
Intestinal immune network for IgA production		
Linoleic acid metabolism		
Neuroactive ligand receptor interaction		
Olfactory transduction		
Taste transduction		
Type 1 diabetes mellitus		

WEEK 3 down-regulated gene sets

1.4 mGy/h	4.1 mGy/h	common
Alzheimer's disease	Homologous recombination	Aminoacyl tRNA biosynthesis
Amino sugar and nucleotide sugar metabolism	One carbon pool by folate	Base excision repair
Arginine and proline metabolism	Progesterone mediated oocyte maturation	Cell cycle
B-cell receptor signaling pathway	Steroid biosynthesis	Cysteine and methionine metabolism
Basal transcription factors	Systemic lupus erythematosus	DNA replication
Chronic myeloid leukemia		Drug metabolism other enzymes
Citrate cycle (TCA cycle)		Glycine serine and threonine metabolism
Colorectal cancer		Lysine degradation
Endocytosis		Mismatch repair
Fatty acid metabolism		mTOR signaling pathway
Fc gamma receptor-mediated phagocytosis		Nucleotide excision repair
Glutathione metabolism		Oocyte meiosis
Glycosylphosphatidylinositol (GPI)-anchor biosynthesis		Purine metabolism
Histidine metabolism		Pyrimidine metabolism
Huntington's disease		Ribosome
Inositol phosphate metabolism		RNA degradation
Insulin signaling pathway		Spliceosome
Neurotrophin signaling pathway		

WEEK 6 up-regulated gene sets

1.4 mGy/h	4.1 mGy/h	common
None	Hypertrophic cardiomyopathy (HCM)	None

WEEK 6 down-regulated gene sets

1.4 mGy/h	4.1 mGy/h	common
None	Aminoacyl tRNA biosynthesis	None
	DNA replication	
	Glycine serine and threonine metabolism	
	Mismatch repair	
	One carbon pool by folate	

Ribosome
Spliceosome
Systemic lupus erythematosus

Table 6: Overview of up- and down-regulated pathways in irradiated HUVEC (1.4 and 4.1 mGy/h) compared to control conditions, defined by GSEA using Kegg PATHWAY as a gene set database, and with an FDR-value < 0.05. Gene sets are ordered alphabetically. Differentially regulated gene sets that are specific for 1.4 mGy/h are presented in the left column, and differentially regulated gene sets that are specific for 4.1 mGy/h are presented in the middle column. The right column represents differentially regulated gene sets that were in common for both dose rates (1.4 and 4.1 mGy/h).

At week one and three, many up- and down-regulated gene sets were in common for the two dose rates, 1.4 and 4.1 mGy/h, although additional gene sets were enriched in the latter. For example, one week of exposure to 4.1 mGy/h led to the up-regulation of lipid biosynthesis, mammalian target of rapamycin (mTOR) signaling and oxidative stress response (glutathione metabolism). After six weeks of exposure to 4.1 mGy/h, a small number of gene sets, involved in DNA damage response and cell cycle, was down-regulated. No relevant down- or up-regulation was observed after six weeks of exposure to 1.4 mGy/h.

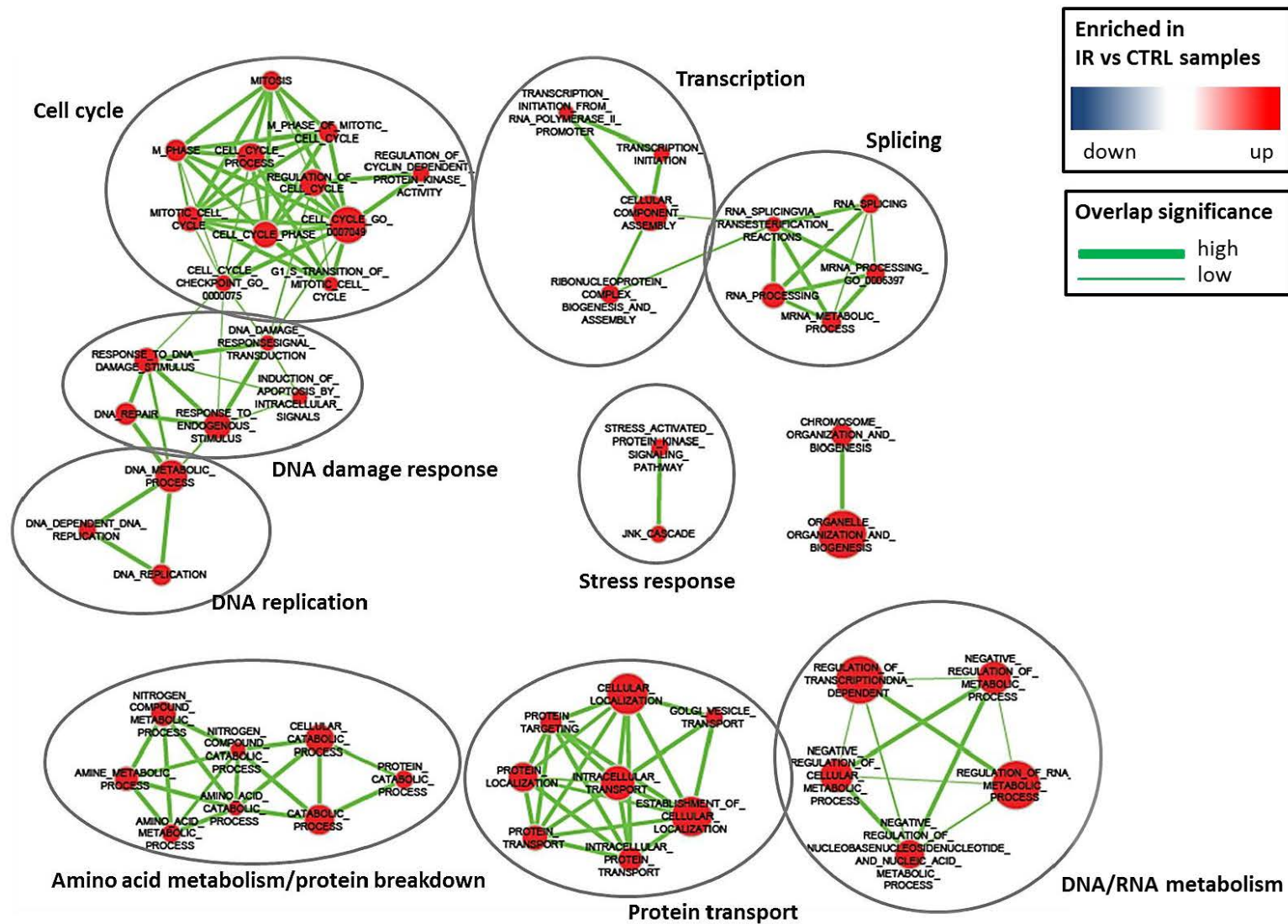


Figure 28 A: Enrichment map for 1.4 mGy/h versus control HUVEC at week one, based on GSEA result for GO BP.

Transcriptomic profiling of endothelial cells exposed to chronic low dose rate irradiation

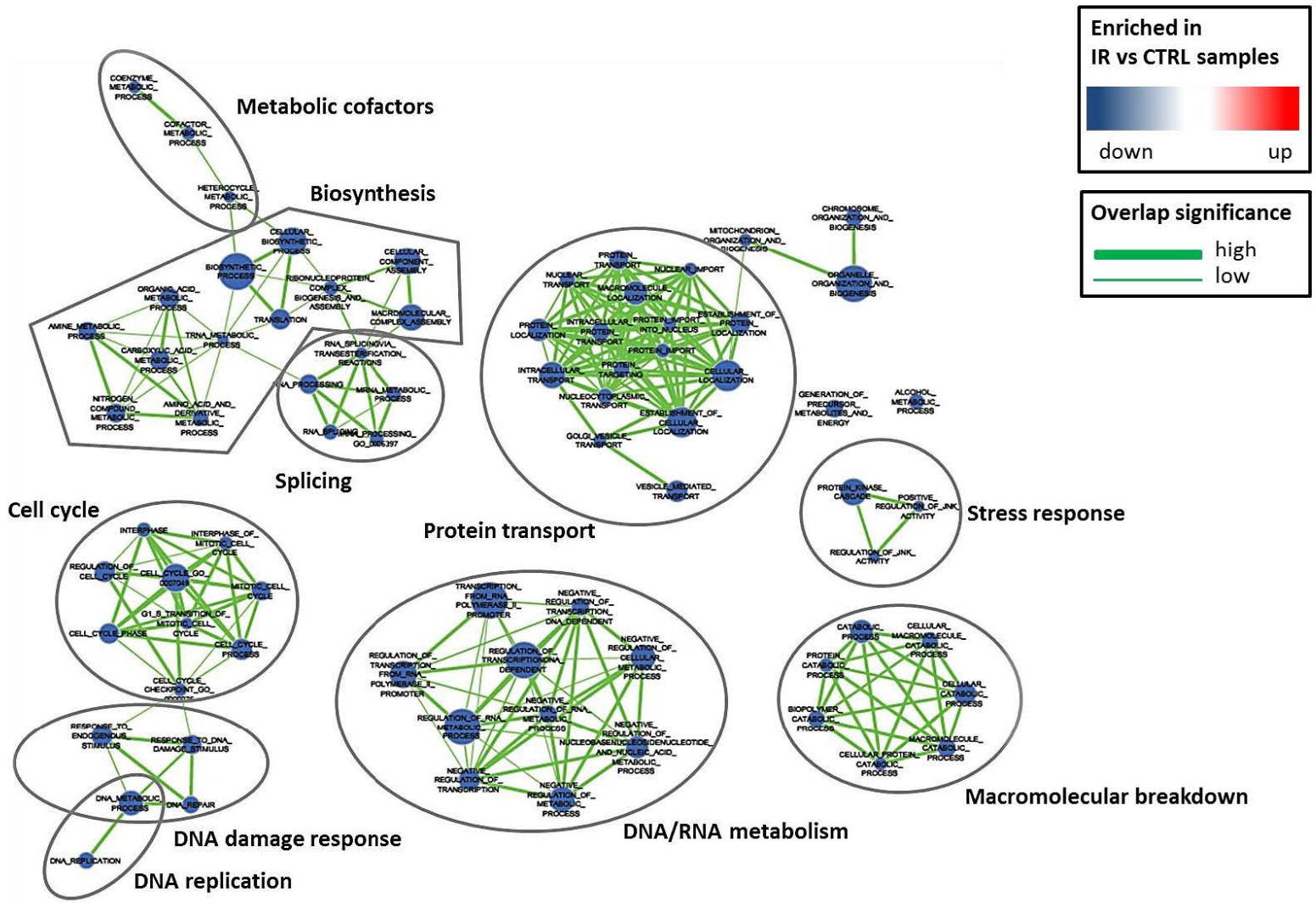


Figure 28 B: Enrichment map for 1.4 mGy/h versus control HUVEC at week three, based on GSEA result for GO BP.

STEROID_
BIOSYNTHETIC_ CELL_DIVISION
PROCESS

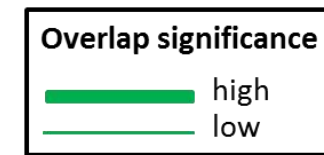
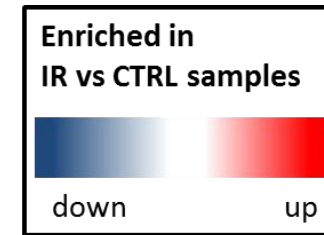


Figure 28 C: Enrichment map for 1.4 mGy/h versus control HUVEC at week six, based on GSEA result for GO BP.

Transcriptomic profiling of endothelial cells exposed to chronic low dose rate irradiation

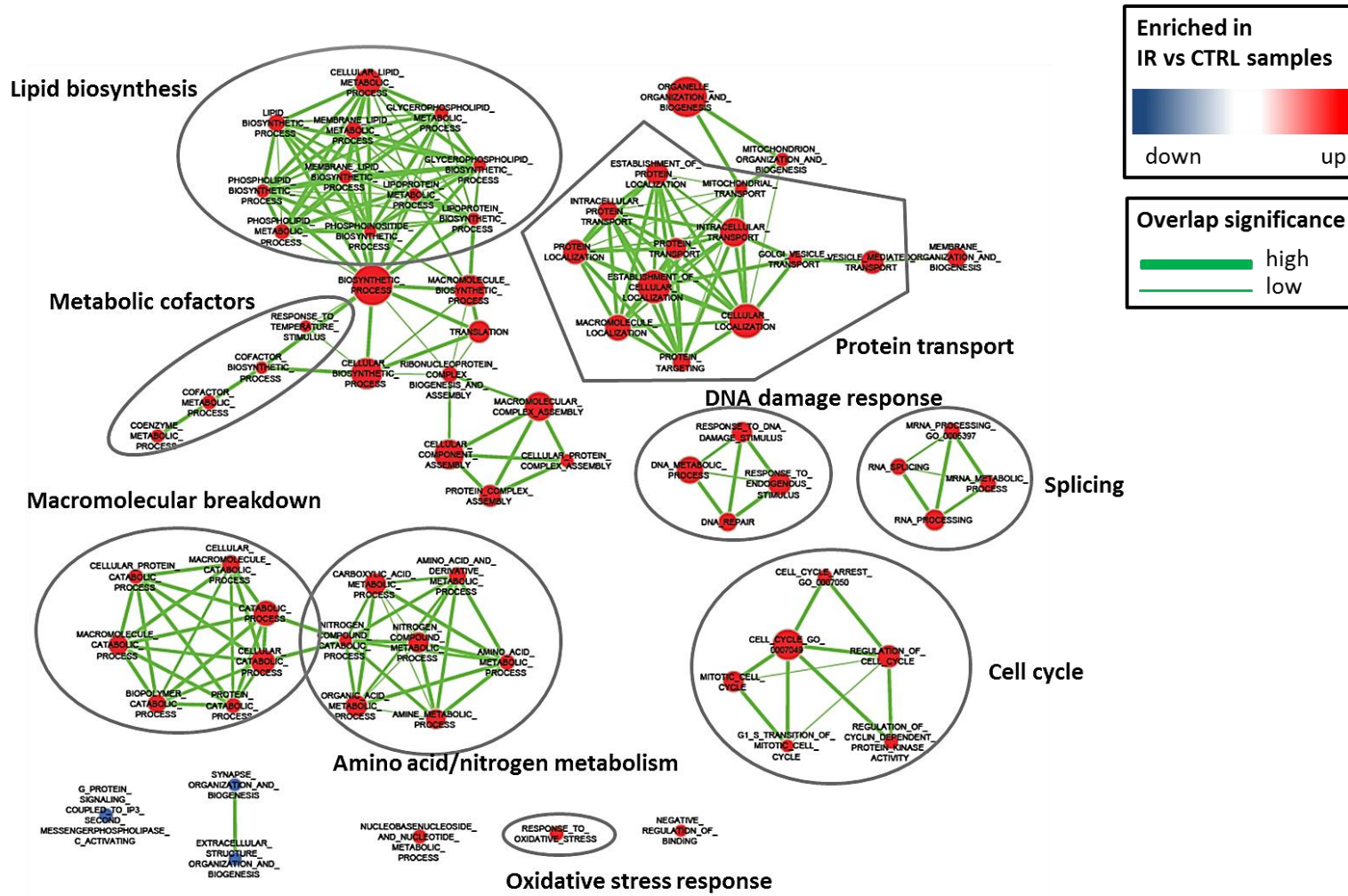


Figure 28 D: Enrichment map for 4.1 mGy/h versus control HUVEC at week one, based on GSEA result for GO BP.

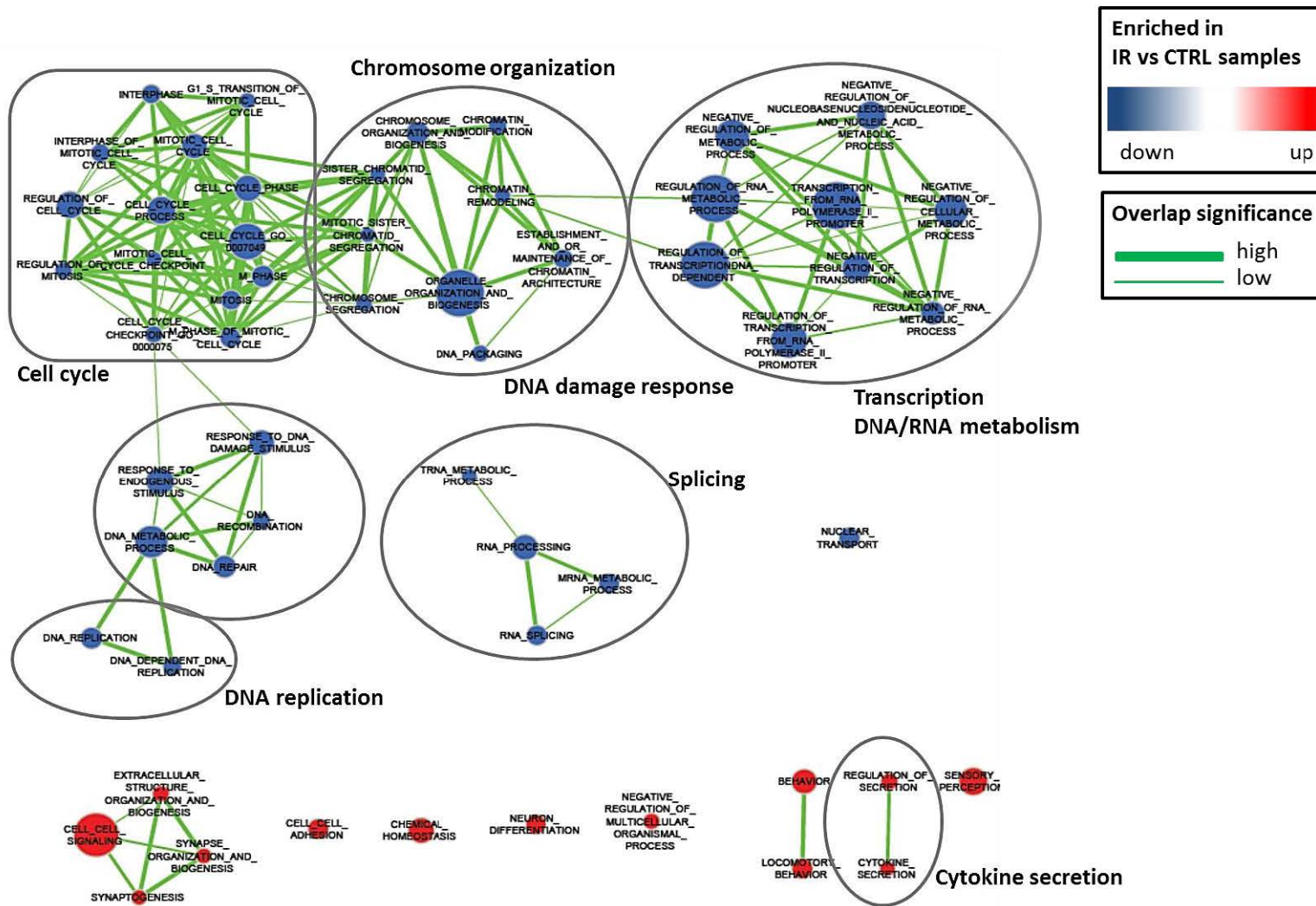


Figure 28 E: Enrichment map for 4.1 mGy/h versus control HUVEC at week three, based on GSEA result for GO BP.

Transcriptomic profiling of endothelial cells exposed to chronic low dose rate irradiation

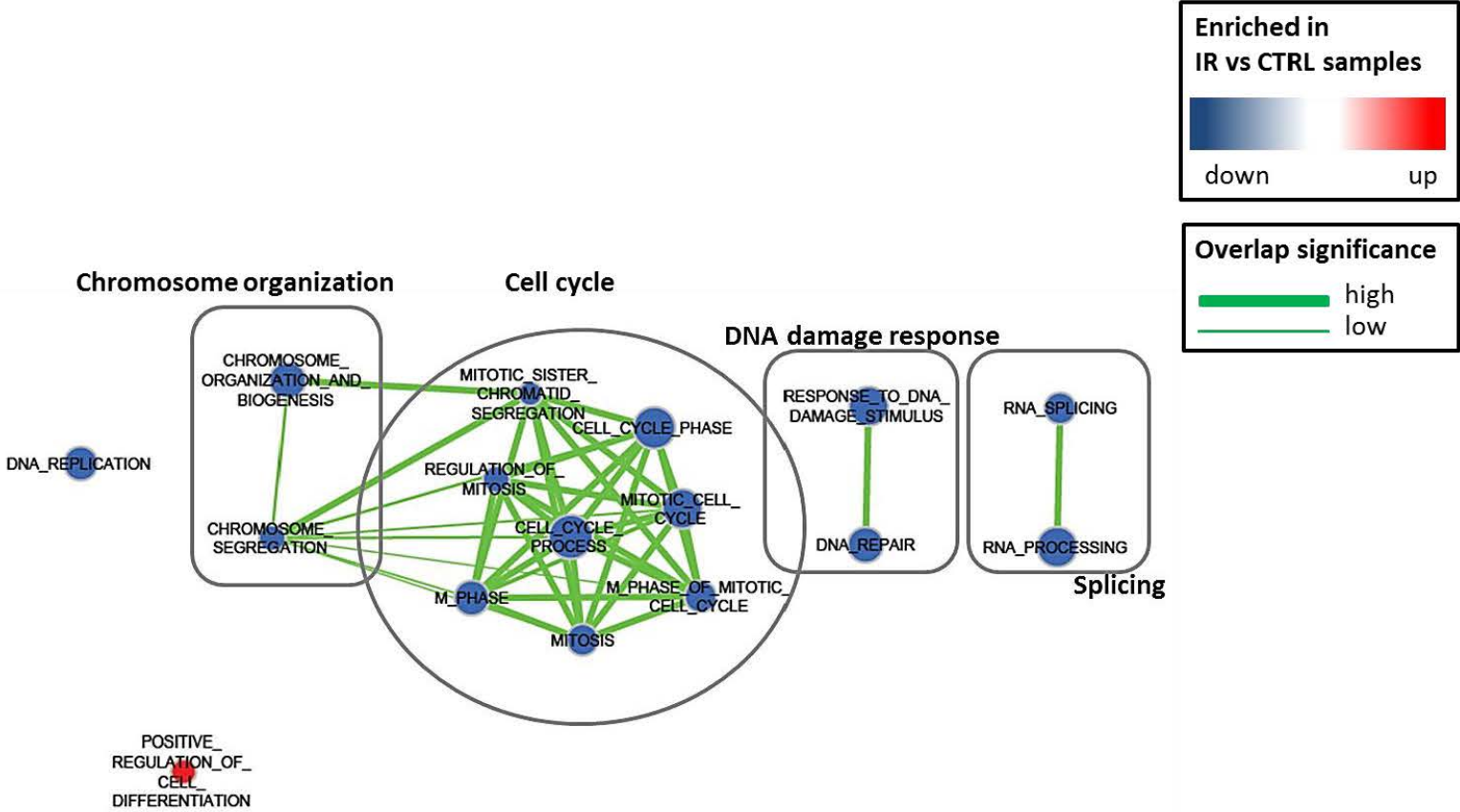


Figure 26 F: Enrichment map for 4.1 mGy/h versus control HUVEC at week six, based on GSEA result for GO BP.

Figure 28: Enrichment Maps for HUVECs exposed to 1.4 mGy/h (A, B, C) and 4.1 mGy/h (D, E, F) at week 1, 3 and 6 based on GSEA results using GO BP. Node size is representative for the number of genes in the respective gene set. Nodes are linked to each other based on the overlap of the number of genes that two gene sets share and is calculated using the overlap coefficient. The thickness of the link corresponds to the degree of overlap. Red nodes represent enriched gene sets in irradiated cells (i.e. upregulated in irradiated HUVECs) whereas blue nodes represent enriched gene sets in control cells (i.e. down-regulated in irradiated HUVECs). Enriched gene sets included in the Enrichment Maps have a FDR value < 0.05 . A cut-off value of 0.5 was chosen for the overlap coefficient. Clusters of functionally related gene-sets were manually circled and assigned a label.

5.4.3 Senescence-related differential gene expression in HUVEC

Assessment of the proliferation rate and SA- β -gal activity of chronic LDR irradiated HUVEC revealed a senescent profile after six weeks of exposure to 4.1 mGy/h [204] (Figure 24). Senescence was only observed after fourteen weeks in control cells, and in cells irradiated with 1.4 mGy/h [205]. This implies that chronic exposure to 4.1 mGy/h induces premature senescence in HUVEC, opposed to natural occurring replicative senescence in control HUVEC. Cells exposed to 1.4 mGy/h also underwent senescence, but at the same week as for control cell. Therefore we consider that 1.4 mGy/h did not induce premature senescence.

The onset of replicative senescence in control cells was already apparent after six weeks as observed by a slight increase in SA- β -gal activity, but without decrease in their proliferation rate. Therefore, to investigate genes that are involved in the acceleration of the senescence process, we identified the genes that were differentially expressed between week six and week one (unadjusted p -value < 0.001 , no threshold for FC). For control cells 124 genes, and for 4.1 mGy/h irradiated samples 167 genes were differentially expressed between week six and week one (Figure 29). Twenty six genes were in common between control and irradiated cells, and are therefore most likely to be important for the senescent phenotype. We speculated that genes which are responsible for accelerating senescence in irradiated cells, would have more pronounced expression changes in irradiated cells compared to controls. Therefore, we calculated the ratio between the FC of irradiated cells and the FC of control cells, for the 26 common genes (Table 8) as explained in the methods section. Genes with a ratio < 0.83 or > 1.20 are presented in Table 8. Genes of interest include IGFBP5 and cystatin SN (CST1), which are further discussed.

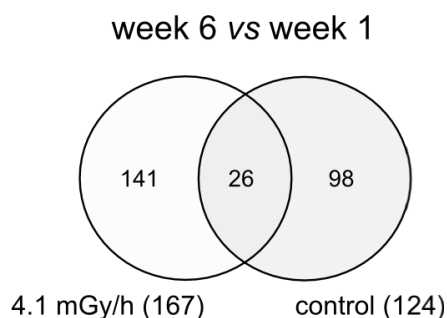


Figure 29: Venn diagram representing differentially expressed genes (including non-annotated genes) between week six and week one for 4.1 mGy/h and control with an unadjusted p-value < 0.001.

Gene Symbol	FC W6 vs W1
ZFHX4	3.40
ABI3BP	2.55
LOC151760	2.37
ZNF717	-2.01
PYGL	-2.10
PHGDH	-2.35
P2RX4	-2.38
PGF	-2.55
TSPAN7	-2.91
RASSF2	-3.11
ZNF737	-3.33

Table 7: Differentially expressed ($p < 0.001$; $|FC| > 2$) annotated genes between week six and week one specific for irradiated cells (4.1 mGy/h). Genes are ranked according to their FC. Genes in bold are further discussed.

Gene Symbol	FC W6 vs W1 _{IRR}	FC W6 vs W1 _{CTRL}	ratio FC _{IRR} /FC _{CTRL}
CST1	21.80	40.49	0.54
FGF5	2.24	1.83	1.23
TGFBI	3.56	2.85	1.25
IGFBP5	9.89	5.09	1.94

Table 8: Gene list created based on the genes that were differentially expressed between week six and week one with a p-value < 0.001 and that were in common between control and irradiated (4.1 mGy/h) HUVEC (overlapping genes in the Venn diagram in Figure 28). The ratio between the FC of irradiated and the FC of control genes was calculated. The genes having a ratio that deviate the most from 1 are considered candidate genes involved in radiation-induced premature senescence. Genes with a ratio < 0.83 or > 1.20 are presented in the table. Genes in bold are further discussed.

From the common genes between control and irradiated cells that were differentially expressed between week six and week one, IGFBP5 was considered a candidate gene involved in radiation-induced premature senescence. Its expression increased over time both in control and irradiated cells, but this induction was more pronounced in irradiated cells. Using quantitative PCR analysis, the expression profile of IGFBP5 was validated (Figure 30). Since IGFBP5 is a well-known regulator of cellular senescence in HUVEC [304, 305], we performed a linear correlation analysis to explore the genes whose expression profile was most similar (positively or negatively) with that of IGFBP5 (Table 9). Genes with a $|R\text{-value}| > 0.88$ are included in Table 9. This analysis revealed several other interesting genes with a similar or reversed expression profile that may be involved in radiation-induced premature senescence, including pirin (PIR), urokinase-type plasminogen activator (PLAU), intercellular adhesion molecule 1 (ICAM1), SMAD specific E3 ubiquitin protein ligase 2 (SMURF2) and a CNOT6L (CCR4-NOT transcription complex, subunit 6-like) pseudogene.

Finally, the genes that were differentially expressed specifically due to radiation exposure (141 genes) are also of interest since they may play a specific role in radiation-induced premature senescence (Table 7). Annotated genes with a p-value below 0.001 and a $|FC| > 2$ are listed in Table V. Genes of interest include ABI family, member 3 (NESH) binding protein (ABI3BP); phosphorylase, glycogen, liver (PYGL) and Ras association (RalGDS/AF-6) domain family member 2 (RASSF2), and are further discussed in the next section.

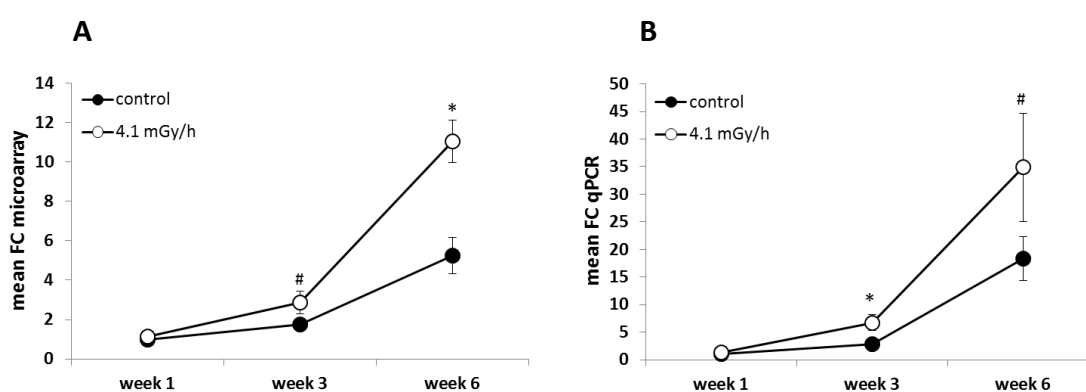


Figure 30: Comparison of Affymetrix Human 1.0 ST arrays data (A) to quantitative real-time PCR (B) for IGFBP5. Fold changes were calculated using control samples at week one as a reference. Error bars represents standard deviations. Statistical T-test was performed in Excel with * = $p < 0.05$ and # = $p < 0.1$ (comparing control and irradiated cells at each week)

Transcriptomic profiling of endothelial cells exposed to chronic low dose rate irradiation

Gene Symbol	R
ICAM1	0.93
PIR	-0.93
SCN8A	0.90
SMURF2	0.89
PLAU	0.89
LAMA3	0.89
AFF3	0.88
CNOT6L	-0.88
ABLIM3	0.88
RN56356	0.88

Table 9: Top-10 genes of which the expression profile was most similar to that of IGFBP5. Genes in bold are further discussed. R = correlation coefficient

5.5 Discussion

An interdisciplinary European study was set-up to evaluate the mechanisms underlying chronic LDR radiation-induced premature senescence in HUVEC. To this end, HUVEC were chronically exposed to two different dose rates (1.4 and 4.1 mGy/h) during one, three and six weeks at Stockholm University after which samples were distributed to all the partners for analysis of specific endpoints. For example, consortium partners have carried out functional assays for the evaluation of senescence (replicative capacity and SA- β -gal-assay). In addition, proteomic changes were assessed [204, 205]. They observed that exposure to 4.1 mGy/h induced premature senescence in HUVEC. In this chapter, we present the data of the genome-wide transcriptomic analysis from the same cells, thus complementing the previously published findings. Moreover, these results, together with the results from the other partners, are being used now by mathematicians, in a systems biology approach, to model the mechanisms that underlie the observed radiation-induced premature senescence in HUVEC.

The traditional approach of gene expression analysis is based on the generation of gene lists consisting of differentially expressed genes that have passed a predefined threshold (p-value, FC) [306]. In this study, our ANOVA model used for differential single gene expression analysis revealed that, after removal of the batch effects, culture time had the biggest influence on differential gene expression followed by dose rate (Figure 25). In order to determine differentially expressed genes in a microarray experiment, an FDR-adjusted p-value is recommended. An FDR-adjusted p-value is corrected for type I errors, also referred to as 'false discovery', which is an error due to false rejection of a null hypothesis that is true. Since single gene analysis tests for differential expression of each of the probes on the chip, it is confronted with the problem of multiple hypothesis testing where type I errors tend to over occur [307]. Ideally, one should thus use an FDR-adjusted p-value, however, using this approach for our data revealed zero differentially expressed genes, most likely due to a too low power. Therefore, it was decided to use an unadjusted p-value (not adjusted for multiple testing), which revealed several differential expressed genes. Seeing the use of unadjusted p-values the results should be interpreted with care since the presence of false discoveries cannot be excluded

Since our study has a low number of replicates ($n = 3$) per condition, the use of more moderated statistical methods such as LIMMA and Significance Analysis of Microarrays (SAM) would have been far more suitable [308]. LIMMA is a package available in R to

analyse microarray data. Its central idea is to fit a linear model to the expression data for each gene [309]. To determine differentially expressed genes LIMMA employs a moderated t-statistic, in which the standard errors have been moderated across all the genes, as opposed to an ordinary t-statistic as used in our study. In SAM, differentially expressed genes are defined by assigning a score to on the basis of its change in gene expression relative to the standard deviation of repeated measurements for that gene [310]. Genes with scores that exceed a certain threshold are considered as differentially expressed. For these genes of interest, an FDR is calculated, based on sample permutations, to define the percentage of genes of interest identified by chance.

Overall, changes in gene expression between control and irradiated cells at the different time points were still rather subtle both in terms of number of differentially expressed genes as in the extent of differential expression (i.e. fold changes). Since we observed subtle differential gene expression, additional analysis was carried out. Indeed, the small changes that we observed at the level of single genes do not necessarily imply that there is no LDR radiation-induced response in HUVEC. It is well known that most biological processes occur through the concerted expression of multiple genes [211]. A modest change in the expression of a group of genes can therefore have greater biological importance than a high change in the expression of a single gene. GSEA is a statistical analysis method that takes this notion into account and focuses on gene sets, groups of genes that share a common biological function, instead of individual genes [213] and has already been proven useful in unraveling the subtle responses induced by low doses of radiation [311].

In this study, we used for GSEA gene set permutation instead of phenotype permutation to assess the statistical significance of the enrichment score, due to the low number of samples per treatment ($n = 3$ for each treatment), as is recommended in the GSEA guidelines (for $n < 7$). In the case of gene set permutation, random gene sets having sizes that match the actual gene sets are created and their enrichment scores are calculated. Next, a null distribution, based on these enrichment scores, is created which is used to determine the significance of the enrichment score of the gene set of interest. Ideally, when you have enough samples ($n > 7$), one should, however, use phenotype permutation which shuffles the phenotype labels across the samples. For each random phenotype the genes are ranked and enrichment scores are calculated for all gene sets. These enrichment scores are used to create the null distribution which is used to determine the significance of the enrichment score of the gene set of interest. The advantage of phenotype permutation is that it does not modify the gene sets, preserving

the correlation between the genes in the dataset and the genes in a gene set. With gene set permutation, on the other hand, the gene-to-gene correlation is not preserved since the genes are randomly shuffled in 'new' gene sets. Since the use of gene set permutation is a less reasonable biological assessment of significance, a more stringent FDR cut-off was used: 5 % instead of 25 % [301]. Although this approach is not ideal, it should be noted that GSEA is a tool that is used to generate biological hypotheses which need to be independently validated later-on (see section 5.5.6).

5.5.1 One week of chronic LDR radiation exposure induces an early stress response

Ionizing radiation is known to induce damage to DNA and other cellular components creating a situation of cellular stress [177]. GSEA indicates that after one week of exposure to both dose rates (1.4 and 4.1 mGy/h) cells reacted to the radiation-induced damage by engaging classical DNA damage response mechanisms such as p53 signaling, cell cycle changes, DNA repair and apoptosis (Table 6, Figure 28). On the level of single genes, two cell cycle related genes were differentially expressed, cyclin A1 (CCNA1) and interferon-induced trans membrane protein (IFITM1). CCNA1 is required for cell proliferation and its expression is normally induced at the entry of the S phase to overcome G1 arrest [312]. In this study, CCNA1 expression was upregulated after one week of exposure to 4.1 mGy/h (FC 1.52). This can be explained as a reaction of chronically irradiated HUVECs to overcome cell cycle arrest. IFITM1 expression is repressed after 6 weeks exposure to 4.1 mGy/h. Induction of IFITM1 has been related to activation of p53 and subsequent inhibition of cell proliferation [313].

To cope with the damage-induced stress situation, energy is needed. This energy is most likely produced by, as GSEA indicated, energy-generating processes such as oxidative phosphorylation, tricarboxylic acid cycle (TCA) cycle and pentose phosphate pathway. Metabolism of amino acids and the breakdown and transport of proteins was up-regulated as well.

Next to these DNA damage response and energy-related processes that were in common for both dose rates, additional pathways were found up-regulated after one week of exposure to 4.1 mGy/h (Table 6, Figure 28). These are involved in, amongst others, lipid metabolism, glutathione metabolism and mTOR signaling, and also point to a stress situation in the cells.

For example, the biosynthesis of fatty acids was up-regulated as was also indicated by single gene analysis (Table 5). Indeed, acyl-CoA thioesterase 7 (ACOT7), which catalyzes the hydrolysis of long-chain acyl-CoA thioesters to free fatty acids and coenzyme A [314] was up-regulated after one week of exposure to 4.1 mGy/h (FC 1.54). Likewise, perilipin 3 (PLIN3) (FC 1.53) was up-regulated, which is, as a carrier protein of free fatty acids, involved in lipid droplet formation, stabilization and functioning [315]. Next, the observed up-regulation of glutathione (GSH) metabolism can be considered as a defense mechanism against radiation-induced oxidative stress since GSH is the predominant antioxidant in cells [316]. Glutamate cysteine ligase modifier subunit (GCLM) plays a role in GSH metabolism by promoting the catalytic properties of GCL, a rate-limiting enzyme in the production of GSH [317]. Expression of GCLM was induced in HUVEC after one week of exposure to 4.1 mGy/h (FC 1.58). It should be noted that lack of GCLM has been shown to induce premature senescence in murine primary fibroblasts probably accompanied by an enhanced level of oxidative stress [317]. Finally, mTOR signaling was up-regulated after one week of exposure to 4.1 mGy/h, which can be considered as a general stress sensor as it gathers the input of a wide range of signals – growth factors, stress, energy status, oxygen, and amino acids – to determine many major processes including energy metabolism, cell growth and proliferation, but also senescence and autophagy [318, 319].

Also, at the protein level, an early stress response was observed in chronic LDR irradiated HUVEC by consortium partners [204]. For instance, "free radical scavenging" was demonstrated to be differentially regulated after one week of exposure to 4.1 mGy/h.

5.5.2 The stress response disappears after three and six weeks of chronic LDR radiation exposure

The stress response observed after one week of exposure to chronic LDR radiation can be considered an early stress response. Indeed, this response observed after one week disappeared after three weeks of exposure. Moreover, GSEA indicated that for both dose rates, most of the DNA damage response pathways, energy-generating processes and stress-related responses were down-regulated after three weeks (Table 6, Figure 28). After six weeks, changes seem to be more dose-rate dependent as opposed to weeks one and three for which most of the enriched pathways were similar between both dose rates. HUVEC that were exposed during six weeks to 1.4 mGy/h did not seem to differ substantially from non-exposed HUVEC as no significantly up- or down-regulated gene sets were observed with

GSEA. Also, with single gene expression analysis, only seven annotated genes were found to be differentially expressed after six weeks of exposure to 1.4 mGy/h (Table 5). Six weeks of exposure to 4.1 mGy/h on the other hand led to down-regulation of gene sets that were mostly related to cell cycle, DNA repair and replication, metabolism of amino acids and aminoacyl tRNA biosynthesis, as was also observed for week three. Furthermore, single gene analysis points to a suppression of amino acid metabolism after six weeks of exposure to 4.1 mGy/h by the down-regulation of phosphoglycerate dehydrogenase (PHGDH) (FC -2.41) and phosphoserine aminotransferase 1 (PSAT1) (FC -1.87), which are key enzymes in the biosynthesis of serine [320, 321]. Another down-regulated gene after six weeks of exposure to 4.1 mGy/h is asparagine synthetase (ASNS) (FC -1.68), which is involved in asparagine biosynthesis [322].

5.5.3 Development of an inflammation-related profile starts after three weeks of exposure to 4.1 mGy/h

According to GSEA, three weeks of exposure to chronic LDR radiation induces an inflammation-related response in HUVEC. Analysis using Kegg PATHWAY database revealed the up-regulation of immune and inflammation-related gene-sets such as cytokine secretion and cell adhesion molecules with both dose rates (Table 6). There were subtle differences between the two dose rates, such as for example additional up-regulation of complement and coagulation cascades with 1.4 mGy/h and additional up-regulation of extracellular matrix receptor (ECM) interaction with 4.1 mGy/h. In contrast to Kegg PATHWAY based analysis, GO BP database based analysis showed cytokine secretion and cell-cell adhesion only to be up-regulated with 4.1 mGy/h (Figure 28).

Also, with single gene analysis, several genes of interest related to inflammation were found to be differentially expressed, although only for 4.1 mGy/h and with the majority being significant after six weeks (Table 5). For example, several up-regulated genes related to the adhesion of leukocytes onto the endothelium, which is an essential step in the initiation of atherosclerosis, were found [323]. Expression of selectin P (SELP), a member of the selectin family of adhesion molecules that initiates leukocyte rolling and interaction of leukocytes with the endothelium [324, 325] was induced over time for 4.1 mGy/h, which was significant after six weeks (FC 1.55). Expression of another gene, ephrin B2 (EFNB2), has been shown to promote atherosclerosis development by enhancing monocyte adhesion to the endothelium and by up-regulating cytokine expression in monocytes [326, 327]. In this study, expression

of EFNB2 tended to decrease over time in non-irradiated cells, whereas in HUVEC exposed to 4.1 mGy/h the expression remained constant over time. Therefore, the expression of EFNB2 was significantly increased in irradiated cells compared to control after six weeks (FC 1.56). Finally, fermitin family member 3 (FERMT3), also known as kindlin 3, is involved in integrin mediated adhesion [328]. Loss of kindlin 3 expression has been associated with decreased adhesion of neutrophils on activated endothelial cells *in vitro* and *in vivo* [329]. After one week of exposure to 4.1 mGy/h FERMT3 expression was increased (FC 1.80). Regarding complement and coagulation cascades, single gene expression analysis is supportive of anti-thrombotic actions as indicated by a significantly increased expression of plasminogen activator tissue-type (PLAT) and serin peptidase inhibitor, clade D, member 1 (SERPIND1; FC 1.61 at week one for 1.4 mGy/h) [330-332]. In particular, PLAT expression is greatly induced over time in HUVEC exposed to 4.1 mGy/h (FC 2.08 at week one, and FC 2.42 at week six).

Overall, based on GSEA and single gene analysis, it seemed that HUVEC exposed to 4.1 mGy/h start to acquire an inflammation-related profile after three weeks onwards. This was also observed on the level of proteins by consortium partners [204]. Ingenuity Pathway Analysis (IPA) analysis revealed "inflammation" and "leukocyte extravasation signaling" to be differentially regulated after three and six weeks, respectively, in HUVEC exposed to 4.1 mGy/h.

5.5.4 Early stress response leads to premature senescence, associated with inflammation, after six weeks of exposure to 4.1 mGy/h

As mentioned before, Yentrapalli and coworkers observed radiation-induced premature senescence, determined by a progressive loss of replicative capacity and an increasing activity of SA- β -gal in HUVEC after six weeks of exposure to 4.1 mGy/h, but not 1.4 mGy/h [204, 205]. A wide range of stressors can induce senescence, usually referred to as stress-induced senescence. Senescent cells have a typical secretory profile, secreting various factors such as pro-inflammatory cytokines, growth factors and their inhibitors, plasminogen activators and their inhibitors, matrix metalloproteinases and fibronectin [196]. Senescence is known to be implicated in various age-related diseases. For instance, vascular ageing, related to senescence of endothelial cells, predisposes to CVD [133, 134]. Endothelial senescence is associated with increased ROS production, decreased NO availability and increased production of pro-inflammatory molecules [144] thus favoring an atherosclerotic endothelium. Various studies

provide *in vivo* evidence for the presence of senescent endothelium in atherosclerotic lesions [137-139]. Since senescence has been associated with the development of CVD, the observation that chronic LDR radiation induces premature senescence in endothelial cells is of particular interest in the search for an understanding of the cellular and molecular mechanisms that underlie an increased radiation-induced risk of CVD.

Using GSEA, we revealed an early stress response in HUVEC exposed to chronic LDR radiation, as pointed out by the activation of DNA damage responses and energy-related processes, and which was more pronounced with 4.1 mGy/h (Figure 28, Table 6). Indeed additional up-regulation of mTOR signaling and glutathione metabolism was observed after one week of exposure to 4.1 mGy/h. The specific engagement of antioxidant defenses such as glutathione in HUVEC exposed for one week to 4.1 mGy/h suggests that these cells have to deal with a greater level of oxidative stress, which is known to cause senescence in the long-term [143, 145]. Also, proteomic analysis by Yentrapalli and coworkers revealed an increase in oxidative stress after one week of exposure to 4.1 mGy/h [204]. Furthermore, they demonstrated a role for mTOR signaling in premature senescence induced by exposure to 2.4 mGy/h [205].

We hypothesize that, overall, this early stress response laid the basis for the induction of premature senescence observed in HUVEC exposed to 4.1 mGy/h. After three weeks of exposure, especially to 4.1 mGy/h, GSEA indicates that this stress response is suppressed and replaced by a more inflammation-related response (Figure 28, Table 6). This inflammatory profile with the secretion of cytokines and expression of cell adhesion molecules is typical for endothelial senescence [146, 196].

Usually, senescence is associated with a sustained DNA damage response due to slow, incomplete or faulty repair [144, 333]. Remarkably, we observed, with GSEA, a down-regulation of DNA damage response after three and six weeks of exposure to 4.1 mGy/h. This is in accordance to a study by Schneider and coworkers who have also observed the induction of senescence together with a suppression of DNA damage response signaling in neural stem cells [334].

5.5.5 Candidate genes involved in radiation-induced premature senescence following exposure to 4.1 mGy/h

To identify genes that may be involved in chronic LDR radiation-induced premature senescence (4.1 mGy/h) we performed a dedicated single gene expression analysis, focusing on genes with a high differential expression between week six and week one.

Three genes with a high differential expression between weeks six and one, and specific in HUVEC exposed to 4.1 mGy/h, are of interest in the context of radiation-induced premature senescence (Table 7). ABI Family, Member 3 (NESH) Binding Protein (ABI3BP) is a binding partner of ABI3 protein, which has been associated with increased senescence in colon and thyroid carcinoma cells [335] and was up-regulated between weeks six and one in irradiated HUVEC (FC 2.55). Phosphorylase, Glycogen, Liver (PYGL) is an enzyme responsible for the phosphorylation of glycogen and depletion of this enzyme leads to accumulation of glycogen. This accumulation causes a situation of oxidative stress and contributes to a p53-dependent induction of senescence in cancer cells [336]. In our study PYGL expression was down-regulated between weeks six and one in irradiated HUVEC (FC -2.10). At last, Ras Association (RalGDS/AF-6) Domain Family Member 2 (RASSF2) was also down-regulated between weeks six and one in irradiated HUVEC (FC -3.11). RASSF2 has been shown to promote apoptosis and cell cycle arrest [230, 337]. Its role in radiation-induced senescence remains a speculation.

Of the genes differentially expressed between week six and week one, and in common between control and irradiated cells, cystatin SN (CST1) and insulin-like growth factor binding protein 5 (IGFBP5) are of interest (Table 8, Figure 29). CST1 expression has been defined as a candidate senescence marker following a study by Keppler and co-workers. They observed an increased expression of CST1 associated with cellular senescence independent of the initial trigger of senescence in normal human fibroblasts [338]. Yet, in our study CST1 expression was more increased in control cells (FC 17.68) compared to cells irradiated with 4.1 mGy/h (FC 8.3).

The expression of IGFBP5 increases between weeks six and one in control cells (FC 3.76), but this change was more pronounced in cells irradiated with 4.1 mGy/h (FC 8.04). Further investigation of the expression profile over time showed that IGFBP5 expression in both control and irradiated cells starts to increase at week three, for both microarray and quantitative real-time PCR analysis (Figure 30). Already at week three, the expression profile

of IGFBP5 in irradiated cells is more pronounced than in control cells, which was in particular apparent in the quantitative real-time PCR results. IGFBP5 encodes for one of the six insulin-like growth factor binding proteins that have a role in insulin-like growth factor (IGF) transport (Figure 31). Although these IGFB proteins are structurally related they each have different cell and tissue type-dependent expression patterns. In general they bind IGF and restrict in this way the bioavailability of this protein [339]. IGF induces an intracellular signaling cascade, which is followed by a wide range of cellular activities. For example, IGF is involved in inhibition of apoptosis and stimulation of cell growth and proliferation [340]. The family of IGFBP genes is known to be involved in senescence, and is believed to be even key regulators [298]. For example, IGFBP3 has been shown to be preferentially expressed in senescent HUVEC expression [341]. Transcriptomic analysis of replicative senescent HUVEC by Shelton and coworkers revealed a highly increased expression of IGFBP5 [304]. A study by Kim and co-workers investigated the role of IGFBP5 in the regulation of senescence in HUVEC. They showed that IGFBP5 accelerates senescence in young HUVECs in a p53-dependent manner [305]. This is in accordance to the proteomic study carried out by consortium partners and who showed an activation of the p53/p21 pathway leading to premature senescence in HUVEC irradiated with 4.1 mGy/h [204]. More specific, immunoblot validation showed an increased expression of total p53, phosphorylated-p53 and p21 protein over time in HUVEC exposed to 4.1 mGy/h [204]. A recent study also showed the up-regulation of IGFBP5 in senescent HUVEC that were exposed to an acute dose of 4 Gy [203] which corresponds to the accumulated dose in our study after six weeks of exposure to 4.1 mGy/h.

Furthermore, we observed that pappalysin 2 (PAPPA2) was decreased after six weeks of exposure to 4.1 mGy/h. PAPPA2 is a known protease of IGFBP5 [342] and its down-regulation may thus lead to higher levels of IGFBP5. Proteomic analysis on chronic LDR irradiated HUVEC suggested earlier that inactivation of the phosphatidylinositol 3-kinase (PI3K)/Akt/mammalian target of rapamycin (mTOR) (PI3K/Akt/mTOR) pathway is involved in the induction of premature senescence [205]. IGFBP5 reduces the bioavailability of IGF, a known activator of the PI3K/AKT pathway. The significant increase in IGFBP5 gene expression over time in exposed HUVEC observed here can be related to inactivation of the PI3K/Akt/mTOR pathway. Thus, both on the level of proteomics and transcriptomics there are indications for the implication of the IGF and the PI3K/AKT/mTOR pathway, and their interplay, in the induction of radiation-induced premature senescence.

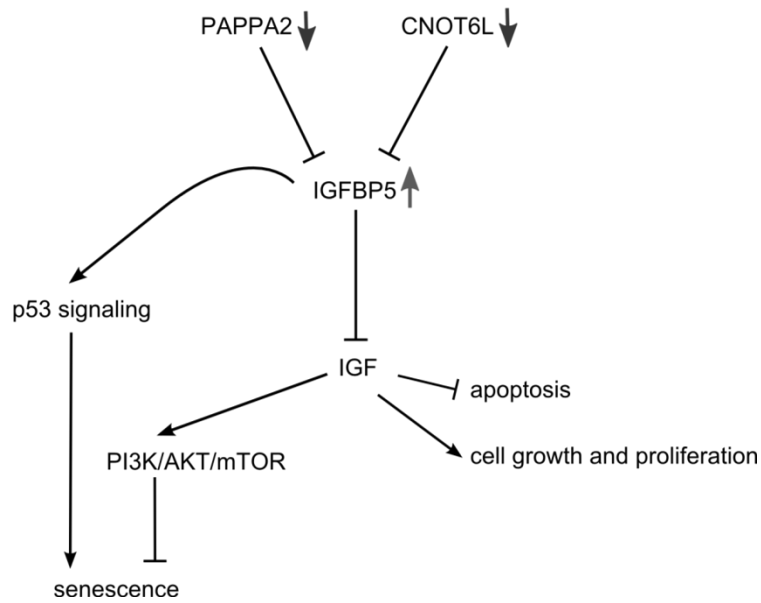


Figure 31: Schematic overview of the possible role of IGFBP5 in radiation-induced premature senescence. Six weeks of exposure to 4.1 mGy/h led to a down-regulated expression of PAPP2 and CNOT6L, which are both demonstrated to decrease IGFBP5 levels [342, 343]. Their down-regulated expression is in accordance with the up-regulation of IGFBP5 observed after six weeks of exposure to 4.1 mGy/h. IGFBP5 may lead to senescence through the p53 signaling pathway [305] or through decreasing IGF availability [339]. p53/p21 signaling has previously been demonstrated to lead to premature senescence in HUVEC exposed to 4.1 mGy/h [204]. IGF signaling is known to inhibit apoptosis and to stimulate cell growth and proliferation. Furthermore, IGF is a known activator of the PI3K/AKT pathway of which the inhibition has been hypothesized to induce premature senescence in HUVEC exposed to chronic LDR radiation [205].

Analysis of genes with similar or reversed expression profiles as IGFBP5 revealed several other interesting genes that may be involved in radiation-induced premature senescence (Table 9). The expression of these genes gradually increases or decreases over time (week one, three and six), and more pronounced in cells irradiated with 4.1 mGy/h. Genes with a correlated expression profile include intracellular adhesion molecule 1 (ICAM1), SMAD Specific E3 Ubiquitin Protein Ligase 2 (SMURF2), urokinase-type plasminogen activator (PLAU), pirin (PIR) and CCR4-NOT Transcription Complex, Subunit 6-Like (CNOT6L). ICAM1, SMURF2 and PLAU have similar expression profiles as IGFBP5 and their increased expression has been associated with senescence in various studies. ICAM1 is well-known to be increased in senescent endothelial cells and is associated with the typical pro-inflammatory profile [304, 344]. SMURF2 expression is increased during telomere shortening in senescent cells and it acts by the activation of p53/p21 and p16/Rb pathways [345, 346]. PLAU is

involved in extracellular matrix degradation as such increasing the bioavailability of growth factors and promoting cell proliferation [347]. PLAU activity is inhibited by plasminogen activator inhibitor-1 (PAI-1). Several studies have revealed that altered regulation of the plasminogen activator system plays a role in the induction of replicative senescence [347]. Both overexpression of PLAU and PAI-1 have been observed in senescent cells [348]. In our study, PLAU expression is increased over time in irradiated HUVEC. Interestingly, it was previously demonstrated that X-rays induces the expression of PLAU [349, 350].

The expression profile of PIR and CNOT6L were the inverse of that of IGFBP5, but also in accordance to the increased senescence observed in HUVEC exposed to 4.1 mGy/h. Down-regulation of PIR expression is observed in senescent melanocytic cells [351] and has also been shown in our study to be down-regulated over time with exposure to 4.1 mGy/h. Regarding CNOT6L, the functional CNOT6L gene showed a similar expression profile as its pseudogene which was also down-regulated over time. CNOT6L has been demonstrated to be a key negative regulator of IGFBP5 as knockdown of this gene in MCF7 cells was associated with increased expression of IGFBP5 [343]. The decreased expression of CNOT6L over time in our study is in accordance with the increased expression of IGFBP5 and can thus be related with increased senescence (Figure 31).

5.5.6 Remarks on the study

The current work is embedded in a European project with different partners all assessing different biological endpoints after chronic LDR of HUVEC. The transcriptomic results presented in this chapter should be regarded as exploratory work. Based on statistical and biological criteria promising targets for further research were defined which include the induction of an early stress response followed by the acquirement of an inflammatory profile upon chronic LDR radiation exposure. These processes are suggested to underlie the chronic LDR radiation-induced premature senescence previously observed within this European project and which was determined by a progressive loss of replicative capacity, an increasing activity of SA- β -gal, and proteomics [204]. Also, a role for IFGBP5 signaling in radiation-induced premature senescence was suggested in our manuscript.

The statistics used for analysis of microarray data faced some limitations which were discussed in detail on page 126-127. The main concerns are the use of unadjusted p-values,

which were not corrected for multiple testing, for single gene analysis, and the use of gene set permutation instead of phenotype permutation for GSEA.

Seeing the statistical limitations of this study (as described in the discussion on p 126-127), independent validation is, however, required. We have performed qPCR analysis of the IFGBP5 gene which constitutes a technical validation since it examines IFGBP5 expression on the mRNA level, like in the microarray. Moreover, it is performed on the same samples used for the microarray. An independent validation requires the use of primary cells from new donors, new samples, other techniques and is in ideal cases performed by other laboratories [307]. As mentioned in the introduction, the gene expression results presented here are part of an interdisciplinary European project which aims, in a systems biology approach, to obtain a better understanding of the molecular mechanisms of chronic LDR radiation-induced premature senescence in HUVEC. Within this project, several functional endpoints were assessed by the different partners including proteomics, senescence markers, oxidative stress markers (8-oxo-dG and hMTH1), inflammatory response, capacity to form vascular networks in Matrigel, DNA damage and genomic instability (chromosomal aberration and telomere length). Although these do not provide a full independent validation since they are performed on the same samples, they are important as they strengthen our findings from the microarray data. In addition, a bioinformatics group at Pavia University will couple the raw proteomics data with the raw transcriptomics data to investigate the overlap and differences between the two levels in a quantitative manner. Finally, it should be remarked that ideally one should start with the exploratory work, as is presented by the transcriptomic analysis, after which the fields of interest should be chosen for further biological research.

5.6 Conclusion

In the context of an interdisciplinary European project, the response of HUVEC to chronic LDR radiation (1.4 and 4.1 mGy/h) was studied, by applying single gene expression analysis combined with GSEA. An early stress response was observed after one week of exposure to 4.1 mGy/h which was replaced by a more inflammation-related expression profile after three weeks and onwards. This early stress response may trigger the radiation-induced premature senescence previously observed in HUVEC irradiated with 4.1 mGy/h. With a dedicated single gene analysis we suggested a role for IGFBP5 signaling in radiation-induced premature senescence. Further biological validation of our findings is, however, required to ascertain our findings. Finally, in a systems biology approach, our findings will be used together with the results from the other partners in the project to come to an understanding of the mechanisms leading to radiation-induced premature senescence, which is suggested to be partially responsible for a radiation-related increased risk of CVD.

5.7 Acknowledgments

This study was funded by the EU FP7 DoReMi (grant agreement 249689) on ‘low dose research towards multidisciplinary integration’, the EU FP7 Procardio project (grant agreement 295823) and by the Federal Agency of Nuclear Control (FANC-AFCN, Belgium), (grant agreement: CO-90-13-3289-00). Harms-Ringdahl M. has received support for these studies from the Swedish Radiation Safety Authority. Rombouts C. is supported by a doctoral SCK•CEN/Ghent University grant. Special thanks to Dr. Pieter Monsieur for the statistical support.

Chapter 6: General discussion and perspectives

Protecting humans and the environment against the hazardous effects of ionizing radiation is the essence of radiation protection. Since the first radiation protection recommendations proposed in 1928, the radiation protection system has evolved steadily, intertwined with the discovery of new sources of radiation exposure and an improved understanding of radiation-related health risks [352]. Epidemiological studies, such as the Life Span Study from the survivors of the atomic bombings in Japan, have raised awareness of possible health effects following exposure to lower doses of ionizing radiation. In particular, an increased risk for cancer was evidenced following exposure to doses above 100 mGy. A milestone in the history of radiation protection is the adoption of the linear non-threshold (LNT) model for the estimation of low dose radiation-related cancer risk (< 100 mGy) [24]. The LNT model, in which no dose is considered absolutely safe, regarding stochastic effects, forms the fundament for current radiation protection standards that are in agreement with the *as low as reasonable achievable* (ALARA) philosophy [353]. The radiobiological rationale of the LNT model relates to the notion that physical energy deposition of ionizing radiation increases carcinogenic risk linearly with increasing dose, with DNA being the critical target. This is referred to as the target theory [354].

The current radiation protection standards, based on the LNT model for cancer induction, are challenged. Experimentally observed responses such as bystander effects, genomic instability and the adaptive response undermine the target theory [29]. It is likely that these responses have implications for the linearity of cancer risk in the low dose region, but it is not clear in which way. Furthermore, epidemiological findings suggest that also non-cancer effects, and in particular cardiovascular effects, are possible health risks related to low dose radiation exposure [215]. However, like for cancer, epidemiological studies lack statistical power to determine CVD risk following low dose radiation exposure (< 0.5 Gy for CVD). If radiation-induced risk of CVD proves to be without a threshold, thus being stochastic in nature instead of deterministic, this would impact current health risk estimations. According to the ICRP, a dose of 0.5 Sv may lead to approximately 1% of exposed individuals developing cardiovascular or cerebrovascular disease, more than 10 years after the exposure, in addition to the 30-50% suffering from disease without being exposed to ionizing radiation [73]. Although relative excess risk may be small, the absolute number of excess cases would be substantial due to the high background rate of CVD [65]. Indeed, current health risk estimation in the low dose region is only based on the stochastic effects, cancer and hereditary disease. Since epidemiology alone will not answer the question whether there exists an excess

risk of CVD following low dose radiation exposure or not, complementary radiobiological research is needed.

Based on the current available experimental evidence, two hypotheses have been formulated for possible biological mechanisms underlying an increased risk of radiation-related CVD, which are not mutually exclusive [43]. The first states that ionizing radiation interacts with the pathogenesis of age-related atherosclerosis, as such accelerating atherosclerosis development. The second states that ionizing radiation increases the lethality of age-related myocardial infarction by decreasing the heart tolerance to acute infarctions due to damage to the microvasculature of the heart. The endothelium, which forms the inner layer of the cardiovascular system, is involved in both hypotheses. Loss of endothelial cells and pro-inflammatory responses are believed to be the underlying cellular and molecular events involved in the development and progression of radiation-related CVD. Nevertheless, it is not certain whether these hypotheses hold true for low doses and low dose rates. For instance, pro-inflammatory responses of the endothelium following exposure to low doses of ionizing radiation (< 1 Gy) were not observed in several *in vitro* experiments [105, 111]. Also, a recent *in vivo* study with ApoE $-/-$ mice has revealed protective effects of low doses (< 0.05 Gy), given at a low dose rate (1 mGy/h), on atherosclerosis development [97].

The aim of this PhD was to investigate the endothelial response to low doses of ionizing radiation using *in vitro* endothelial cell cultures as a model. Although *in vitro* endothelial models are not fully representative for the complex *in vivo* situation, it offers several practical advantages. For instance, *in vitro* experiments are usually cheaper, less time-consuming, and less laborious which makes results relatively easily to obtain. Nevertheless, translation of the obtained results to an *in vivo* situation should be done with care. Furthermore, it is important to choose the endothelial cell model wisely, seeing the considerable heterogeneity in endothelial cells derived from different sites in the vascular tree and from different organs [355]. For our experiments, we have chosen to use the primary human umbilical vein endothelial cells (HUVEC) and the thereof derived immortalized EA.hy926 cells. Although originating from large vessels, HUVEC are unique since they exhibit endothelial properties that are intermediate between those of large vessels (e.g. aorta) and those of the microvasculature [163]. Hence, HUVEC depict a good general endothelial cell model. Furthermore, they are primary cells and thus more related to the *in vivo* situation than an immortalized cell line. However, the use of endothelial primary cultures is compromised by their limited lifespan and the change of endothelial characteristics during long-term culture

[167]. Immortalized cell lines, on the other hand, grow faster and are easier to handle [219], but differ even more from the *in vivo* situation than primary cells. It should be noted that for more specific research such as the investigation of coronary artery disease it is advised to use more appropriate cell models such as human coronary endothelial cells.

In the first part of this PhD, in chapter three, we have observed that the acute radiation response of EA.hy926 cells was more pronounced compared to HUVEC, with respect to the induction of double strand breaks (DSB) and apoptosis. Indeed, radiation exposure induced more DSB, the most lethal DNA lesion, in EA.hy926 cells which also repaired more slowly. Consequently, more EA.hy926 cells underwent apoptosis compared to HUVEC. In addition, investigation of intracellular ROS levels, in chapter four, revealed that these levels appear to be slightly higher in EA.hy926 cells compared to HUVEC. Since 60–70% of radiation-induced DNA damage is estimated to result from indirect actions by ROS [1], the higher level of intracellular ROS in EA.hy926 can be associated to the higher number of DSB formed following irradiation. Furthermore, this finding is in agreement with the previously observed lower anti-oxidant defenses in EA.hy926 cells compared to HUVEC [225]. Overall, our findings indicate that the choice of the *in vitro* endothelial cell model for a specific study can influence the outcome, and it is advised to include more than one cell model. Also, in the work presented here, the inclusion of additional endothelial cell lines such as human coronary artery endothelial cells and human dermal microvascular cells would have strengthened the research carried out. For instance, it is known that microvascular endothelial cells have a larger radiosensitivity than macrovascular endothelial cells [356].

The use of three dimensional (3D) endothelial models is advised as well since they are more related to the *in vivo* situation of endothelial cells as compared to 2D monolayer cultures [172]. Current knowledge regarding ionizing radiation effects on 3D-models is rather sparse and reveals conflicting results as both increased [357-359] and decreased migration of endothelial cells [360, 361] (an essential step in angiogenesis) has been observed following irradiation. Moreover, the role of angiogenesis in CVD is a controversial issue. Stimulation of angiogenesis is regarded as a promising therapy for vascular diseases such as ischemic heart disease and peripheral arterial disease [118]. On the other hand, it has been suggested that angiogenesis of microvessels in an atherosclerotic plaque might contribute to plaque instability and thus rupture [360]. Therefore it is difficult to hypothesize to which extent angiogenesis plays a role in radiation-induced cardiovascular disease and what the effect of radiation on this process is.

In chapter three, we have found important differences between the endothelial response following low (≤ 0.5 Gy) and high (2, 5 Gy) acute dose X-irradiation, with respect to the formation of DSB. Exposure to acute low doses induced proportionally more DSB, 30 min after irradiation, as quantified by the number of γ -H2AX foci, compared to high dose acute exposure. This was most apparent in EA.hy926 cells. In another study at Ghent University, blood samples from pediatric patients with congenital heart disease who underwent cardiac catheterization procedures were taken before and shortly after the procedure, and the number of γ -H2AX foci was quantified [362]. In addition, they assessed γ -H2AX foci in peripheral blood lymphocytes irradiated *in vitro*. Both their *in vivo* and *in vitro* findings indicated a proportionally higher induction of DSB at lower doses. It should, however, be noted that practical reasons inherent to the methodology may be an explanation as well for a proportionally lower number of γ -H2AX foci observed at high doses. Like Neumaier and coworkers have suggested, multiple nearby DSB (1 to 2 μm apart) induced by high dose radiation exposure may rapidly cluster into repair centers, which are visualized as one foci [236]. Nevertheless, evaluation of spot occupancy, which reflects the area of the nucleus covered by spots, indicates that the clustering of DSB at high doses has a rather subtle effect on the observed disproportional induction of DSB.

Follow-up of γ -H2AX foci number over time revealed that, 24 h after irradiation, exposure to high doses (2 Gy) leads to an increased foci number compared to control cells. It is generally assumed that loss of γ -H2AX foci represents effective DNA repair [238], although there are indications that this is limited to low level DNA damage. Indeed, a study by Bouquet and coworkers have revealed that disappearance of γ -H2AX foci is only representative of DSB repair when less than 100-150 foci were induced per nucleus [363]. Since, the highest dose used (2 Gy) only induced an average of 38 foci per nucleus we assume that in our study loss of foci number represents effective DSB repair. Our findings thus indicate that not all DNA damage is repaired following high dose exposure, which consequently leads to increased levels of apoptosis, as evaluated by the Annexin-V/PI assay. Following low dose exposure, on the other hand, most DNA damage seems repaired after 24 h, since the number of γ -H2AX foci is even reduced below background level in control cells. This may be explained by the observation that a slight increase in spot number was observed in control cells at 24 h compared to 30 min. In EA.hy926 cells, DNA repair kinetics seems to be different for lower doses (0.05 and 0.5 Gy), since 2 h after exposure the number of γ -H2AX foci was still increased as opposed to the high dose (2 Gy). Interestingly, in the literature, DNA repair

efficiencies are reported to be lower with very low doses (< 0.05 Gy), most likely reflecting the inability of the cell to induce a DNA damage response with these low levels of DNA damage [364, 365]. However, this phenomenon is observed with doses which were not included in our study and it would be interesting to study the effect of these very low doses (< 0.05 Gy) on DNA repair in endothelial cells.

Furthermore, in chapter three, we observed an increase in apoptosis following exposure to acute doses as low as 0.5 Gy in HUVEC and 0.1 Gy in EA.hy926 cells, although without cell cycle arrest. This finding suggests that acute doses below 0.5 Gy can cause endothelial cell loss, which is known to be involved in the development and progression of radiation-related CVD. For example, endothelial cell loss causes a decrease in capillary density in the heart. In addition, endothelial apoptosis has been related to the development of atherosclerosis [364, 365] as it may compromise regulation of vascular tone, and increase the proliferation and migration of vascular smooth muscle cells (VSMC) [182, 183]. Thrombosis, the major complication of atherosclerosis, can also be triggered by endothelial cell death [184]. Translation of our observed increase in low dose radiation-induced endothelial cell apoptosis to the *in vivo* situation should, however, be done with care. Indeed, the impact of this, rather small, increase in endothelial cell apoptosis on the final health outcome *in vivo* is uncertain.

Besides the classical DNA-targeted effects, we were also interested in the effect of acute low dose X-irradiation on oxidative stress and on the mitochondrion. It has been proposed that the biological effects of low doses are mainly mediated via the induction of oxidative stress, an imbalance between intracellular ROS and antioxidants, rather than direct DNA damage [183]. Also, in the context of CVD, it is most likely that low dose ionizing radiations mediates their effects by creating a state of oxidative stress. The actions of ROS are various and include the induction of cellular damage which can lead to apoptosis and necrosis [366]. For instance, Kumar and coworkers have shown that reduction of ROS levels increased the survival rate of cardiac fibroblasts [367]. Oxidative stress is also a known cause of cellular senescence [129]. Furthermore, ROS can create an inflammatory situation, decrease NO bioavailability, damage the mitochondrion, and cause oxidative modification of circulating low density lipoprotein (LDL) to form the harmful oxLDL. All these processes play a major role in the development and progression of CVD [145, 146].

Using the fluorometric CM-H₂DCFDA assay, we measured intracellular ROS levels in both HUVEC and EA.hy926 cells 30 min after acute X-irradiation, in chapter four. High dose

exposure (5 Gy) increased intracellular ROS levels in both HUVEC and EA.hy926 cells. It has been observed previously that irradiated cells arrested in G2/M phase have higher mitochondrial content, which has been associated with higher intracellular ROS levels [261, 368]. We have also observed a G2/M arrest in both HUVEC and EA.hy926 cells following exposure to 5 Gy, which may be related to the observed increased intracellular ROS levels. For low dose irradiation (≤ 0.5 Gy) we observed no clear dose-relationship for intracellular ROS levels. It should be noted that, due to limitations of the CM-H₂DCFDA assay, additional methodologies for the assessment of oxidative stress should be included as well in future research. For instance, the detection of extracellular 8-oxo-7,8-dihydro-2-deoxyguanosine (8-oxo-dG) has been successfully used for the assessment of oxidative stress after exposure to low doses of ionizing radiation [190]. 8-oxo-7,8-dihydro-2-deoxyguanosine triphosphate (8-oxo-dGTP) is a mutagenic lesion in the DNA and in the nucleotide pool that is induced by ROS. The lesion is removed from the DNA by base excision repair and from the nucleotide pool by the nucleotide sanitization enzyme Human MutT homologue (hMTH1)⁸, and is exported from the intracellular to the extracellular milieu as 8-oxo-dG, where it can be easily detected. Interestingly, in this study it was found that a dose as low as 1 mGy could increase 8-oxo-dG levels in whole blood samples, 1 h after irradiation. They speculated that this low dose, which results in about one hit per cell⁹, could trigger an endogenous stress response leading to an increased ROS production. Another promising tool that can be applied in radiation research to monitor cellular redox changes are genetically encoded fluorescence probes such as redox-sensitive yellow fluorescent proteins (rxYFP), redox-sensitive green fluorescent proteins (roGFPs), and the hydrogen peroxide sensor HyPer [369, 370]. These probes have many advantages including high sensitivity, subcellular targeting and the possibility of live-cell imaging. For instance, roGFP equilibrates with the total thiol pool and can thus be used as an indicator for the glutathione redox state [370]. Also, these probes allow single cell redox measurements which can be of interest in the investigation of bystander effects. As far as we know, these genetically encoded fluorescence probes have not been used yet in ionizing radiation studies, and offers thus an interesting approach for the measurement of radiation-induced oxidative stress.

In our study, we measured intracellular ROS levels 30 min after irradiation. Since it is believed that low dose ionizing radiation may lead to persistent oxidative stress, it would be

⁸ hMTH1 inhibits the incorporation of 8-oxo-dGTP in DNA by hydrolysing it to 8-oxo-dGMP [190].

⁹ The descriptor 'one hit per cell' was originally taken from an article from Feinendegen and coworkers. They defined a hit as the energy deposited by a single radiation (particle) track in a cell [381].

interesting to evaluate intracellular ROS levels longer times (e.g. weeks) after radiation exposure. Furthermore, *in vivo* studies are required as well. The above-mentioned genetically encoded fluorescence probes are a promising step towards measurement of redox status *in vivo* [369, 370]. However, there remain many technical challenges that need to be overcome. For instance, redox-imaging in non-transparent species poses a problem which needs to be overcome first. Solutions can be provided by the use of two-photon imaging or the development of techniques for a chemical conservation of the biosensor redox state of the probe which can then be analyzed in tissue sections [369]. Another way to assess oxidative stress in animal models is the use of biomarkers of oxidative stress such as p-tyrosine, L-DOPA and 8-hydroxydeoxyguanosine in the plasma. Specific markers for nitrative stress, such as 3-nitrotyrosine, can also be used. For instance, using these nitrative stress biomarkers, Kumarathasan and coworkers have revealed persistent nitrative stress in ApoE *-/-* mice three to six months after exposure to acute and chronic irradiation (total doses of 0.5 and 2 Gy) [286]. Finally, one can also investigate oxidative stress by studying the anti-oxidant mechanisms of the cell. For example, measurement of anti-oxidant enzymes such as superoxide dismutase (SOD) and catalase, and the measurement of glutathione levels are frequently used to assess oxidative stress [225].

Mitochondria are proposed to play an important role in the amplification of radiation-induced intracellular ROS levels. Indeed, mitochondria are the major source of endogenously produced ROS, as a byproduct of oxidative phosphorylation, and the total cellular mitochondrial volume (4-25 % depending on the cell) represents a substantial radiation target volume in the cell [287]. In particular, the mitochondrial DNA (mtDNA) is a vulnerable radiation target due to the lack of protective histones and limited DNA repair capacity. Since mtDNA encodes for several components from the electron transport chain, mtDNA damage may lead to impairment of oxidative phosphorylation and as a consequence to an increased ROS production causing even more mitochondrial and cellular damage [192]. We have initiated the development of a PCR-based assay to quantify the common deletion, the most abundant large-scale deletion reported in mtDNA [33]. Next to mtDNA damage assessment, it is of interest to evaluate more in-depth mitochondrial function, and in particular the association between mitochondrial function and ROS production, following low dose radiation exposure. For instance, assessment of the respiratory chain function via the determination of cytochrome *c* (complex IV) and succinate dehydrogenase (complex II) activity after cytoplasmatic exposure to α -particles has revealed a reduced activity which

consequently leads to an increase in ROS levels [193]. Also, the activity of complex I and III was significantly decreased in mice exposed to 2 Gy [293]. Furthermore, the induction of mitochondrial permeability transition has been demonstrated to increase ROS production [195]. The permeability transition occurs when permeability pores of the inner mitochondrial membrane open, as such increasing the permeability to ions and solutes with a mass up to 1500 Da. This is associated with loss of the mitochondrial membrane potential which is known to induce the formation of ROS [192]. With low dose exposure it is unlikely that many mitochondria will undergo a permeability transition as a direct consequence of a primary ionizing event. However, it has been shown that propagation of this mitochondrial permeability transition from one mitochondrion to another is possible and is believed to be mediated via a Ca^{2+} -dependent mechanism [191]. At last, it is of interest to evaluate mitochondrial protein import following low dose radiation exposure. Many mitochondrial proteins are encoded by nuclear DNA and need to be imported for the maintenance and regeneration of mitochondria. Mitochondrial protein import is dependent on the inner mitochondrial membrane potential and a proper functioning of the import machinery. Radiation-induced defects in protein import may amplify oxidative stress and assessment of mitochondrial protein import may thus also be used as a marker for low dose radiation effects [192].

To conclude the first part of this PhD (chapters three and four) where we have evaluated the response of HUVEC and EA.hy926 to acute low dose X-irradiation:

- 1.) Relevant differences between the radiation response of HUVEC and EA.hy926 cells have been found, pointing out the importance of the choice of endothelial cell model for *in vitro* research.**
- 2.) Our findings regarding DSB formation and repair suggest that the low dose response may not be a simple linear extrapolation of the high dose response, although practical limitations of the γ -H2AX assay underlying the observed differences between γ -H2AX foci formation induced by low and high dose radiation cannot be excluded.**
- 3.) Exposure to lower doses (down to 0.05 Gy) led to an increased number of DSB, which was associated with an increase in endothelial cell apoptosis (down to 0.1 Gy).**

Endothelial cell loss is known to be involved in the development and progression of CVD.

4.) Since it is believed that the actions of low dose irradiation are mediated by creating a state of oxidative stress and impacting mitochondrial function, and seeing the importance of these events in the development and progression of CVD, further research should focus on these topics.

Whereas the above described results concern acute low dose radiation exposures, we were also interested in the effects of chronic low dose rate (LDR) radiation exposure. Indeed, the biological effects of ionizing radiation exposure are also dependent on the dose rate by which it is delivered. Experimental animals and humans usually can tolerate higher total doses of chronic LDR irradiation than of acute single doses [273] due to repair of sublethal injury and adaptive reactions on the cellular, tissue and whole body level [371]. For example, it has been strongly suggested that DNA damage is efficiently repaired during chronic LDR irradiation (^{137}Cs , 0.3 mGy/h for 1, 6 and 13 days) in human immortalized fibroblast cells [73]. Nevertheless, some epidemiological cohorts that are chronically exposed to low doses of radiation in their occupation are suggestive of detrimental health effects of chronic low dose radiation exposure. For instance, a significant increasing trend in ischemic heart disease morbidity was observed with increasing total external dose in Mayak nuclear workers [372].

In the second part of this PhD, in chapter five, we have examined the effect of chronic LDR irradiation (^{137}Cs , 1.4 and 4.1 mGy/h) during one, three and six weeks on HUVEC by means of transcriptomic profiling. This study was embedded in a large European interdisciplinary project (FP7 DoReMi project (grant agreement 295823)), which is a feasibility study towards a systems biology approach of LDR radiation response of the endothelium. It was observed at Stockholm University that irradiation at a dose rate of 4.1 mGy/h induces premature senescence in HUVEC [59]. Senescence of endothelial cells is related to vascular aging, which predisposes to CVD. Indeed, endothelial senescence is associated with increased ROS production, decreased NO bioavailability and increased production of pro-inflammatory mediators [204]. Moreover, there is *in vivo* evidence for the presence of senescent endothelium in human atherosclerotic lesions [144]. The final aim of this European interdisciplinary project is the integration of all studied biological endpoints in a specific

model explaining the mechanisms underlying radiation-induced premature senescence in HUVEC.

We were interested in elucidating the underlying mechanisms on the transcriptomic level that could be involved in the previously observed chronic LDR radiation-induced premature senescence in HUVEC. Analysis of single gene expression has revealed a rather subtle response of HUVEC following chronic LDR radiation exposure, as determined by a low number of differentially expressed genes. Moreover, the differentially expressed genes have small fold changes that never exceeded |3|. Amundson and coworkers performed microarray analysis on LDR irradiated human myeloid leukemia cells with wild-type p53 function [373]. They revealed several genes, including GADD45A and CDKN1A, of which differential expression was dose rate dependent. In our study, these genes were not differentially expressed which may be explained by differences in duration of exposure and in total dose received. In the study of Amundson and coworkers total exposure time was in the range of several hours (with highest total dose = 0.5 Gy), as opposed to our study where total exposure time was in the range of weeks (with highest total dose = 4 Gy).

Seeing the subtle effects on the level of single genes, we decided to use a complementary approach for the evaluation of transcriptomic changes in our study: Gene Set Enrichment Analysis (GSEA). GSEA is a statistical analysis method that focuses on gene sets, groups of genes that share a common biological function, instead of individual genes [135, 137, 138]. In essence, this method determines how the members of a given gene set, based on a priori biological knowledge, are distributed among the list of genes ranked according to their differential expression between specific treatments, in this case chronic LDR irradiation versus control. If they tend to occur at the top (or bottom) of this gene list, the gene set is considered to be associated with the specific treatment [213]. The advantage of GSEA is that it takes all genes into account without an arbitrary cut-off. Since most biological processes occur through the concerted expression of multiple genes, a modest change in the expression of a group of genes can have greater biological importance than a high change in the expression of a single gene [213]. The validity of GSEA results is highly dependent on the quality of the gene set databases used. Gene sets are based on a specific biological pathway or process, and genes annotated to that gene set are usually also associated with each other in a meaningful way [211]. In our study, we used the Kegg PATHWAY and Gene Ontology Biological Process (GO BP) gene set databases obtained from the MSigDB website (v4.0). The Kegg PATHWAY database contains gene sets representing a network of gene products

involved in biological processes and pathways. It is curated by humans and constantly updated with the latest information from published literature and is thus considered a good quality database [211]. The biological processes represented in the gene sets of the GO BP database are defined as a chemical or physical transformation and comprises broad (e.g. cell growth and maintenance) and more specific processes (e.g. pyrimidine metabolism) [211, 374]. The GO BP is a commonly used database but care should be taken since the genes in a specific gene set are not necessarily associated with each other in a meaningful way.

Based on single gene analysis and GSEA, we hypothesized that one week of exposure triggered an early stress response which was followed by the acquirement of an inflammatory-related profile after three weeks. In particular, exposure of HUVEC to 4.1 mGy/h led to the engagement of antioxidant mechanisms indicating that these cells had to deal with a greater level of oxidative stress. We suggested that this early stress response led to the observed premature senescence in HUVEC exposed to 4.1 mGy/h. Looking in more detail, we revealed an important role for IGFBP5 in the induction of radiation-induced premature senescence. It has been shown previously that IGFBP5 can induce senescence in HUVEC by engaging the p53 pathway [375]. In addition, another study revealed an increased IGFBP5 expression in HUVEC following acute exposure to 4 Gy, which corresponds to the accumulated dose that HUVEC received after six weeks of exposure to 4.1 mGy/h in our study [305]. In future research, it would be interesting to include HUVEC knock-out for IGFBP5 to determine whether IGFBP5 plays an essential role in radiation-induced premature senescence. Finally, it is also advised to confirm the generated hypotheses (i.e. the induction of an early stress response followed by the acquirement of an inflammatory profile) by means of functional assays, which has already been done partially. Indeed, within the project several biological endpoints such as senescence and inflammatory response are assessed as well by the other partners.

To conclude the second part of this PhD (chapter five) where we investigated the effect of chronic LDR radiation on HUVEC by means of transcriptomic profiling:

1.) Single gene analysis revealed a rather subtle response of chronic LDR irradiation.

2.) GSEA indicated that chronic LDR irradiation induces an early stress response after one week which is replaced by an inflammatory profile after three weeks. These are suggested to underlie the observed premature senescence.

3.) A role for IGFBP5 signaling is suggested for the previously observed premature senescence in HUVEC exposed to 4.1 mGy/h.

This PhD was embedded in the search for a cellular and molecular understanding of low dose radiation effects on the development and progression of CVD. The ultimate goal of this research is an improved assessment of CVD risk related to acute and chronic low dose radiation exposures. Epidemiological studies are limited in their statistical capacity to prove either the absence or presence of an increased risk of CVD following low dose exposure (< 0.5 Gy). The integration of cellular and molecular biomarkers in epidemiological research is a promising way to attain an improved risk assessment [82]. It is, however, challenging to find a reliable, easily measurable and specific biomarker to assess radiation-induced cardiovascular effects in epidemiological cohorts. Understanding of the cellular and molecular mechanisms underlying radiation-induced cardiovascular effects by means of *in vitro* and *in vivo* research will aid in the discovery of such biomarkers.

The results presented in this thesis can be considered as a step forward in the search for biomarkers for radiation-related CVD. In the context of radiation-related CVD, the main interest is to find specific biomarkers that provide an early detection of radiation-induced CVD, before clinical detection, with the possibility for early treatment and prevention [82]. The subtlety of low dose health effects and the multifactorial nature of CVD makes this quest very complex. The ideal biomarker will, most likely, be a mix of several biomarkers. Furthermore, this multi-biomarker should be rather easily obtained (e.g. collection of a blood or DNA sample). Although specific biomarkers were not identified in this work, several fields of research were explored including the assessment of DNA-targeted effects, oxidative stress, mitochondrial dysfunction and senescence, which may provide biomarkers upon further research. Animal studies are needed as they provide a step-forward in the translation of the *in vitro* findings towards the human situation. The use of atherosclerosis prone mice models such as ApoE *-/-* or LDL *-/-* mice have been extensively used to assess the effect of ionizing radiation on the development and progression of atherosclerosis [95, 97, 104, 286]. Ideally, candidate biomarkers should be assessed in humans as well. Recently, the phenomenon of so-

called endothelial microparticles gains more attention. A microparticle is a membrane vesicle that is released by the endothelial cell upon apoptosis or activation (i.e. the acquirement of a pro-inflammatory and pro-thrombotic state) [376]. They can be measured in the plasma by detection of their phospholipid content (mainly phosphatidylserine) and proteins specific for endothelial cells such as E-selectin and vascular endothelial cadherin [377]. The level of these endothelial microparticles has been shown to be elevated in coronary artery disease, diabetes, hypertension, etc. [378]. It is proposed as a surrogate marker for endothelial health, although further research is required to assess their prognostic value for clinical events [376]. If these microparticles are proven to be a good marker for endothelial health, it would be interesting to explore their possible use as biomarker for radiation-related CVD.

Besides improving risk assessment, biomarkers can be used for the implementation of strategies to reduce radiation-induced CVD risk, such as individual risk characterization and the development of countermeasures [82]. These strategies are of particular interest for radiotherapy patients, such as breast cancer patients, who receive a dose to the heart. Also, health practitioners, such as radiologists and interventional cardiologists, may benefit from these risk reducing strategies.

Besides the search for biomarkers, biological research is needed to ascertain the dose-response relationship in the low dose region. Currently the LNT model based on the stochastic effects, cancer and hereditary disease, is employed as basis for risk assessment. Our findings regarding radiation-induced DNA damage may point to a non-linear dose-relationship which questions the LNT model. CVD, which is considered as a deterministic effect, is at the moment not included in low dose risk assessment. Indeed, epidemiological findings are only certain about elevated CVD risk after exposure to doses higher than 0.5 Gy. Up till now, there is not sufficient scientific evidence for a relevant increased risk of CVD following low dose radiation exposure (< 0.5 Gy). And as long as there is not sufficient scientific evidence, the current radiation protection standards (based on stochastic effects) that limit the effective dose exposures of the public and workers, are not adapted. However, one could set equivalent dose limits for specific exposure to the cardiovascular system, like the equivalent dose limits issued by the ICRP for the lens of the eye, skin, hands and feet [379]. These dose limits can be based on the threshold doses for radiation-related CVD determined by epidemiological and radiobiological findings. At last, it should be noted that, although scientific knowledge is crucial for the implementation of radiation protection standards, it also involves a societal, economic and political judgment [380].

To conclude, this PhD aimed to partially unravel the endothelial radiation response using *in vitro* endothelial cell cultures as model. Indeed, the endothelium is considered a critical target in radiation-related CVD. Overall, for all investigated endpoints, a rather subtle response was found in endothelial cells following exposure to low doses of ionizing radiation. It was observed that acute low dose irradiation (0.05 Gy) induces a small, but significant, increase in DNA damage in both HUVEC and EA.hy926 cells which seemed to be fully repaired. In addition, a small, but significant, increase in apoptosis (0.01 Gy) was demonstrated. Furthermore, it was seen, 30 min after exposure, that intracellular ROS levels were not much influenced by acute low doses. Finally, we demonstrated subtle effects of chronic low dose rate (LDR) radiation on differential gene expression in HUVEC. We showed that chronic LDR radiation (4.1 mGy/h) induced premature senescence, in which IGFBP5 signaling seems to play an important role. To fully grasp the impact of these subtle effects on final health outcome, with respect to CVD, further research is required, as discussed throughout the last chapter.

Summary

Humans can be exposed to low doses of ionizing radiation during medical diagnostics and in their occupation. Also, nuclear accidents such as Chernobyl and the recent event in Fukushima form a source of radiation exposure. The implementation of radiation protection guidelines aids in the protection of humans against possible detrimental health effects. Over time, these guidelines have evolved, intertwined with scientific advances made in the understanding of radiation-induced health effects. Nowadays, radiation protection guidelines comply with the '*as low as reasonable achievable*' (ALARA) principle. For low doses of ionizing radiation (< 100 mGy), it is believed that only stochastic effects such as cancer and hereditary disease are of importance. Low dose risk estimations for cancer are based on a linear non-threshold (LNT) extrapolation of high dose risks known from epidemiological studies. Recently, epidemiological findings suggest that also non-cancer diseases, and in particular cardiovascular diseases (CVD), may be a health risk associated with low dose radiation exposure. However, below 0.5 Gy an increased risk of CVD cannot be evidenced by epidemiology and a biological understanding is needed. Indeed, if there proves to be an increased risk of CVD following low dose exposure, it may have considerable impact on current low dose health risk estimates.

The endothelium, which forms the inner lining of the cardiovascular system, is a critical target in the development and progression of radiation-related CVD. The acceleration of age-related atherosclerosis and the increase of the lethality of age-related myocardial infarction, in which endothelial cells play an important role, are hypothesized to underlie an increased CVD risk following high dose exposure. However, it is not known whether these hypotheses hold true for low dose radiation exposure and other mechanisms may play a role. Therefore, in this PhD, the endothelial response to acute low doses of ionizing radiation and to doses delivered at chronic low dose rate were investigated *in vitro*, using two endothelial cell models, primary human umbilical vein endothelial cells (HUVEC) and the immortalized derivate EA.hy926 cells. The different radiation response of HUVEC compared to EA.hy926 cells, observed in this study after acute low dose exposure, point out the importance of the choice of the endothelial cell model for *in vitro* research.

It was observed that acute low dose radiation exposure (0.05 Gy) induced an increase in double strand breaks, the most lethal DNA lesions. This was associated with an increase in apoptosis following exposure to doses down to 0.1 Gy, suggesting a role for endothelial loss in the development and progression of CVD following low dose radiation exposure. Nevertheless, translation of this finding to the *in vivo* situation should be done with care and

in vivo experiments should be performed for confirmation. Next to endothelial cell loss, radiation-induced endothelium dysfunction is proposed to be of importance.

Oxidative stress, an imbalance between intracellular ROS levels and antioxidant defenses, is a well-known cause of endothelial dysfunction. No clear dose-relationship was found between intracellular ROS levels 30 minutes after exposure to acute low dose radiation exposure in HUVEC and EA.hy926 cells. However, it is hypothesized that there exist radiation-induced mechanisms by which the cell 'amplifies' the formation of intracellular ROS on the long-term, in which mitochondria play an essential role. Detection of the common deletion, a sensitive marker of mtDNA damage, aids in the determination of radiation-induced mitochondrial damage and has been optimized for further use in the lab. For future research, it would be of interest to evaluate oxidative stress and mitochondrial function in endothelial cells exposed to low doses of ionizing radiation after longer periods (e.g. weeks).

Whereas above investigations concerned acute low dose radiation exposures, the effects of chronic low dose rate (LDR) radiation exposure on HUVEC were investigated as well. This study was carried out in the context of the FP7 DoReMi project. In this project it was observed that chronic LDR radiation induced premature senescence in HUVEC. Since several studies have observed endothelial senescence in human atherosclerotic lesions, this finding supports the idea that radiation-induced premature senescence contributes to the development and progression of CVD. In this PhD, transcriptomic profiling was carried out to investigate the underlying pathways of radiation-induced premature senescence. Gene Set Enrichment Analysis revealed that chronic LDR radiation induced an early stress response after one week, followed by the acquirement of an inflammatory profile after three weeks. We suggested that this early stress response laid the basis for the induction of premature senescence. A more detailed single gene analysis has suggested a role for insulin growth factor binding protein 5 (IGFBP5) signaling in radiation-induced premature senescence.

In conclusion, this PhD was embedded in the search for an understanding of the cellular and molecular mechanisms underlying the effects of low dose radiation exposure on the development and progression of CVD. The ultimate goal is an improved assessment of CVD risk related to acute and chronic low dose radiation exposures. In particular, it is aimed to find specific biomarkers for radiation-related cardiovascular effects for use in molecular epidemiological studies and for risk reducing strategies such as individual risk characterization and the development of countermeasures. These risk reducing strategies will

be of particular interest for radiotherapy patients and occupational workers, who receive a certain dose to the cardiovascular system.

Samenvatting

Mensen kunnen blootgesteld worden aan lage dosis ioniserende straling tijdens diagnostische procedures in de geneeskunde en tijdens specifieke beroepsactiviteiten. Nucleaire ongevallen zoals in Tsjernobyl, en de recente gebeurtenis in Fukushima kunnen eveneens leiden tot blootstelling aan straling. Om mensen te beschermen tegen ongewenste blootstelling aan straling zijn er bepaalde richtlijnen opgesteld. Deze richtlijnen zijn sterk geevoelend in de tijd en worden beïnvloed door de alsmaar betere kennis van de schadelijke gezondheidseffecten van ioniserende straling. De huidige richtlijnen hanteren het '*as low as reasonable achievable*' (ALARA) principe. Momenteel wordt aangenomen dat voor lage dosis straling (< 100 mGy) enkel stochastische effecten, zoals kanker en genetisch overdraagbare aandoeningen, van belang zijn. Om het risico op kanker na blootstelling aan lage dosis straling in te schatten gebruikt men een lineaire extrapolatie, zonder drempelwaarde, van het risico na blootstelling aan hoge dosis straling. Deze laatste is gekend uit epidemiologische studies. Recent hebben epidemiologische studies echter aangewezen dat ook andere ziekten, en vooral cardiovasculaire aandoeningen, een mogelijk gezondheidsrisico vormen na blootstelling aan lage dosis straling. Echter, voor dosissen lager dan 0.5 Gy is het statistisch niet haalbaar om een significant verhoogd risico vast te stellen in epidemiologische studies. Radiobiologisch onderzoek is daarom nodig om een mogelijk risico op cardiovasculaire aandoeningen na blootstelling aan lage dosis straling vast te stellen of eventueel uit te sluiten. Als er een verhoogd risico blijkt te zijn, zal dit een belangrijke impact hebben op de huidige inschatting van gezondheidsrisico's verbonden aan lage dosis straling.

Het endotheel, dat de binnenkant van het cardiovasculaire systeem bekleedt, speelt een belangrijke rol in het ontstaan en de verdere ontwikkeling van cardiovasculaire aandoeningen. Een verhoogd risico op cardiovasculaire aandoeningen na hoge dosis bestraling is het gevolg van een versnelling van ouderdoms-gerelateerde atherosclerose en van een verhoogde letaliteit van ouderdoms-gerelateerde hartinfarcten. In beide processen speelt het endotheel een belangrijke rol. Het is echter niet geweten of dezelfde processen betrokken zijn bij de effecten van lage dosis bestraling. Daarom onderzochten we in dit PhD project de respons van het endotheel *in vitro* na blootstelling aan acute lage dosis straling of aan dosissen gegeven aan chronische laag dosistempo met behulp van twee endotheelcel modellen: de primaire humane endotheelcellen afkomstig van de venen in de navelstreng (HUVEC) en de daarvan geïmmortalizeerde cellijn EA.hy926. We toonden aan dat de respons na bestraling met een acute lage dosis verschilt tussen HUVEC en EA.hy926, wat wijst op het belang van het type endotheelcel model voor *in vitro* onderzoek.

We toonden aan dat acute lage dosis straling (0.5 Gy) het aantal dubbelstrengige DNA breuken, de meest lethale DNA schade, verhoogde. Dit was geassocieerd met een verhoging in apoptosis na bestraling met dosissen tot 0.1 Gy. Deze bevinding suggereert een rol voor het verlies van endotheelcellen in het ontstaan en de verdere ontwikkeling van cardiovasculaire aandoeningen na lage dosis bestraling. Het belang van deze bevindingen moet echter bevestigd worden met *in vivo* onderzoek. Naast het verlies van endotheelcellen, is er een belangrijke rol weggelegd voor dysfunctie van het endotheel.

Oxidatieve stress, gekarakteriseerd door een verstoord evenwicht tussen het intracellulaire peil van reactieve zuurstofverbindingen (ROS) en anti-oxidatieve afweermechanismen, is een belangrijke oorzaak van dysfunctie van endotheelcellen. We hebben geen duidelijk verband gevonden tussen stralingsdosis en de waarden van intracellulaire ROS, 30 minuten na bestraling van HUVEC en EA.hy926 cellen. Desondanks wordt verondersteld dat door straling op langere termijn het niveau van intracellulaire ROS wordt verhoogd via bepaalde mechanismen van amplificatie waarbij de mitochondriën een belangrijke rol spelen. In deze context hebben we de ons gericht op detectie van de 'common deletion', een gevoelige merker om schade aan het mitochondriaal DNA vast te stellen, en deze geoptimaliseerd voor verder gebruik. Voor toekomstig onderzoek zou het interessant zijn om in endotheelcellen oxidatieve stress in meer detail te bestuderen, en te bepalen hoe en in welke mate de mitochondriale functie wordt verstoord, en dit langere perioden (bv. weken) na bestraling met lage dosissen.

Naast acute lage dosis straling, zijn ook de effecten van chronisch lage dosis straling, gegeven aan een laag dosistempo, bestudeerd in HUVEC. Deze studie maakt onderdeel uit van het FP7 DoReMi project. In dit project heeft men waargenomen dat lage dosis chronische bestraling prematuur senescentie induceert in HUVEC. Aangezien in verscheidene studies senescentie van het endotheel is aangetoond in humane atherosclerotische laesies, wijst deze bevinding op een mogelijk mechanisme waarmee lage dosis straling kan bijdragen tot de ontwikkeling van cardiovasculaire aandoeningen. In dit PhD project hebben we het transcriptoom van deze chronisch bestraalde HUVEC geanalyseerd om onderliggende moleculaire signaaltransductiewegen bloot te leggen. Met behulp van Gene Set Enrichment Analysis hebben we aangetoond dat lage dosistempo chronische bestraling een vroege stress respons initieert in HUVEC na een week, gevolgd door een inflammatoire reactie na drie weken. Dit wordt verondersteld aan de basis te liggen van de voordien waargenomen premature senescentie. Door een doorgedreven genexpressie analyse konden we een sleutelrol suggereren

voor "insulin growth factor binding protein 5" (IGFBP5) en IGFBP5-gerelateerde signaaltransductiewegen in premature senescentie.

Om te besluiten, deze PhD maakt deel uit van de zoektocht naar een beter begrip van de cellulaire en moleculaire mechanismen die aan de basis liggen van de effecten van lage dosis straling op de ontwikkeling van cardiovasculaire aandoeningen. Het uiteindelijke doel is om tot een verbeterde beoordeling te komen van het risico op cardiovasculaire aandoeningen na blootstelling aan acute en chronische lage dosissen straling. In het bijzonder wil men specifieke biomerkers vinden voor gebruik in moleculaire epidemiologische studies en voor de ontwikkeling van strategieën om het risico op cardiovasculaire aandoeningen te verminderen. Bijvoorbeeld, door characterisatie van het individuele risico en de ontwikkeling van tegenmaatregelen. Deze strategieën zouden dan kunnen toegepast worden om onder andere radiotherapie patiënten, radiologen en interventionele cardiologen te beschermen tegen een ongewenst risico op cardiovasculaire aandoeningen.

References

1. Hall, E.J. and Giaccia, A.J., *Radiobiology for the Radiologist* 2012: Lippincott Williams & Wilkins.
2. Martin, A., Harbison, S., Beach, K., Cole, P., *An Introduction to Radiation Protection* 2012: CRC Press.
3. L'Annunziata, M.F., *Radioactivity: Introduction and History: Introduction and History* 2007: Elsevier.
4. Kudriashov, I.B. and Kudriashov, Y.B., *Radiation Biophysics (Ionizing Radiations)* 2008: Nova Publishers.
5. Orecchia, R., Krengli, M., Jereczek-Fossa, B.A., Franzetti, S., Gerards, J.P., *Clinical and research validity of hadrontherapy with ion beams*. *Critical Reviews in Oncology/Hematology*, 2004. **51**(2): p. 81-90.
6. Maalouf, M., Durante, M., and Foray, N., *Biological effects of space radiation on human cells: history, advances and outcomes*. *Journal of Radiation Research*, 2011. **52**(2): p. 126-146.
7. Grupen, C., *Introduction to Radiation Protection: Practical Knowledge for Handling Radioactive Sources*. 2010: Springer.
8. Einstein, A.J., *Effects of radiation exposure from cardiac imaging: how good are the data?* *Journal of the American College of Cardiology*, 2012. **59**: p. 553-565.
9. Einstein, A.J. and J. Knuuti, *Cardiac imaging: does radiation matter?* *European Heart Journal*, 2012. **33**(5): p. 573-578.
10. Advisory Group on Ionising Radiation (AGIR). *Circulatory disease risk. Report of the independent Advisory Group on Ionising Radiation*. 2010: Health Protection Agency.
11. Committee to assess Health Risks from Exposure to Low Levels of Ionizing Radiation Research, National Research Council, *Health risks from exposure to low levels of ionizing radiation: BEIR VII - Phase 2*. 2006, National Academy of Sciences.
12. Caufield, C., *Multiple Exposures: Chronicles of the Radiation Age* Vol. 5. 1989: University of Chicago Press.
13. Walker, J.S., *Permissible dose: A history of Radiation Protection in the Twentieth Century* 2000.
14. Hacker, B.C., *The Dragon's Tail: A History of Radiation Safety in the Manhattan Project, 1942-1946* 1987.
15. UNSCEAR, *Report of the United Nations Scientific Committee on the Effects of Atomic Radiation 1958* 1958.
16. Burgan, M., *Hiroshima: Birth of the Nuclear Age* 2009: Marshall Cavendish.
17. Burlakova, E.B. and V.I. Naidich, *The Effects of Low Dose Radiation: New Aspects of Radiobiological Research Prompted by the Chernobyl Nuclear Disaster* 2004: CRC Press.
18. Stabin, M.G., *Radiation Protection and Dosimetry: An Introduction to Health Physics* 2007: Springer.
19. Hendry, J.H., *Radiation biology and radiation protection*. *Annals of the ICRP*. **41**: p. 64-71.
20. Wrixon, A.D., *New recommendations from the International Commission on Radiological Protection--a review*. *Physics in Medicine and Biology*, 2008. **53**: p. R41-60.
21. UNSCEAR, *Biological mechanisms of radiation actions at low doses. A white paper to guide the Scientific Committee's future programme of work*. 2012.
22. ICRP, *The 2007 Recommendations of the ICRP*, in *ICRP Publication 103*. 2007.
23. UNSCEAR, *Report of the United Nations Scientific Committee on the Effects of Atomic Radiation 2010* 2010.

24. Brenner, D.J., et al., *Cancer risks attributable to low doses of ionizing radiation: assessing what we really know*. Proceedings of the National Academy of Sciences of the United States of America, 2003. **100**(24): p. 13761-13766.
25. Martin, C.J., Sutton, C.J., West, C.M. and Wright, E.G., *The radiobiology/radiation protection interface in healthcare*. Journal of radiological protection: official journal of the Society for Radiological Protection, 2009. **29**: p. A1-A20.
26. Martin, C.J., *The LNT model provides the best approach for practical implementation of radiation protection*. The British journal of radiology, 2005. **78**: p. 14-16.
27. Wall, B.F., Kendall, G.M., Edwards, A.A., Bouffler, S., Muirhead, C.R. and Meara, J.R., *What are the risks from medical X-rays and other low dose radiation?* The British journal of radiology, 2006. **79**: p. 285-294.
28. Suzuki, K. and S. Yamashita, *Low-dose radiation exposure and carcinogenesis*. Japanese Journal of Clinical Oncology, 2012. **42**: p. 563-568.
29. Kadhim, M., Salomaa, S., Wright, E., Hildebrandt, G., Belyakov, O.V., Prise, K.M. and Little M.P., *Non-targeted effects of ionising radiation-Implications for low dose risk*. Mutation Research, 2013. **752**: p. 84-98.
30. Hei, T.K., Zhou, H., Chai, Y. Ponnaiya, B. and Ivanov V.N., *Radiation induced non-targeted response: mechanism and potential clinical implications*. Current Molecular Pharmacology, 2011. **4**(2): p. 96-105.
31. Morgan, W.F. and W.J. Bair, *Issues in low dose radiation biology: the controversy continues. A perspective*. Radiation Research, 2013. **179**(5): p. 501-510.
32. Morgan, W.F., *Non-targeted and delayed effects of exposure to ionizing radiation: I. Radiation-induced genomic instability and bystander effects in vitro*. Radiation Research, 2003. **159**(5): p. 567-580.
33. Kim, G.J., K. Chandrasekaran, and W.F. Morgan, *Mitochondrial dysfunction, persistently elevated levels of reactive oxygen species and radiation-induced genomic instability: a review*. Mutagenesis, 2006. **21**(6): p. 361-367.
34. Matsumoto, H., Hamada, N., Takahashi, A., Kobayashi, Y. and Ohnisi, T., *Vanguards of paradigm shift in radiation biology: radiation-induced adaptive and bystander responses*. Journal of Radiation Research, 2007. **48**(2): p. 97-106.
35. Little, M.P., *Do non-targeted effects increase or decrease low dose risk in relation to the linear-non-threshold (LNT) model?* Mutation Research, 2010. **687**: p. 17-27.
36. Prise, K.M., M. Folkard, and B.D. Michael, *A review of the bystander effect and its implications for low-dose exposure*. Radiation Protection Dosimetry, 2003. **104**(4): p. 347-355.
37. Hildebrandt, G., *Non-cancer diseases and non-targeted effects*. Mutation Research, 2010. **687**(1-2): p. 73-77.
38. Little, M.P., Azizova, T. V., Bazyka, D., Bouffler, S. D., Cardis, E., Chekin, S., Chumak, V. V., Cucinotta, F. A., de Vathaire, F., Hall, P., Harrison, J. D., Hildebrandt, G., Ivanov, V., Kashcheev, V. V., Klymenko, S. V., Kreuzer, M., Laurent, O., Ozasa, K., Schneider, T., Tapio, S., Taylor, A. M., Tzoulaki, I., Vandoolaeghe, W. L., Wakeford, R., Zablotska, L. B., Zhang, W. and Lipshultz, S. E., *Systematic review and meta-analysis of circulatory disease from exposure to low-level ionizing radiation and estimates of potential population mortality risks*. Environmental Health Perspectives, 2012. **120**(11): p. 1503-1511.
39. Stewart, J.R. and L.F. Fajardo, *Radiation-induced heart disease. Clinical and experimental aspects*. Radiologic Clinics of North America, 1971. **9**(3): p. 511-531.
40. Stewart, F.A., *Mechanisms and dose-response relationships for radiation-induced cardiovascular disease*. Annals of the ICRP, 2012. **41**(3-4): p. 72-79.

41. Schultz-Hector, S. and K.R. Trott, *Radiation-induced cardiovascular diseases: is the epidemiologic evidence compatible with the radiobiologic data?* International Journal of Radiation Oncology, Biology, Physics, 2007. **67**(1): p. 10-18.
42. Clarke, M., Collins, R., Darby, S., Davies, C., Elphinstone, P., Evans, E., Godwin, J., Gray, R., Hicks, C., James, S., MacKinnon, E., McGale, P., McHugh, T., Peto, R., Taylor, C. and Wang, Y., *Effects of radiotherapy and of differences in the extent of surgery for early breast cancer on local recurrence and 15-year survival: an overview of the randomised trials.* Lancet, 2005. **366**(9503): p. 2087-2106.
43. Darby, S.C., Cutter, D. J., Boerma, M., Constine, L. S., Fajardo, L. F., Kodama, K., Mabuchi, K., Marks, L. B., Mettler, F. A., Pierce, L. J., Trott, K. R., Yeh, E. T. and Shore, R. E., *Radiation-related heart disease: current knowledge and future prospects.* International Journal of Radiation Oncology, Biology, Physics, 2010. **76**(3): p. 656-665.
44. Darby, S.C., McGale, P., Taylor, C. W. and Peto, R., *Long-term mortality from heart disease and lung cancer after radiotherapy for early breast cancer: prospective cohort study of about 300,000 women in US SEER cancer registries.* Lancet Oncology, 2005. **6**(8): p. 557-565.
45. McGale, P., Darby, S. C., Hall, P., Adolfsson, J., Bengtsson, N. O., Bennet, A. M., Fornander, T., Gigante, B., Jensen, M. B., Peto, R., Rahimi, K., Taylor, C. W. and Ewertz, M., *Incidence of heart disease in 35,000 women treated with radiotherapy for breast cancer in Denmark and Sweden.* Radiotherapy and Oncology, 2011. **100**(2): p. 167-175.
46. Carr, Z.A., Land, C. E., Kleinerman, R. A., Weinstock, R. W., Stovall, M., Griem, M. L. and Mabuchi, K., *Coronary heart disease after radiotherapy for peptic ulcer disease.* International Journal of Radiation Oncology, Biology, Physics, 2005. **61**(3): p. 842-850.
47. Trott, K.R., *The pathology and the pathogenesis of late radiation-induced heart diseases after low and high radiation doses.* Paper based on a key note lecture given at the European Society of Radiation Research Annual Meeting in Vietri in October 2011 (personal communication)..
48. Ozasa, K., Shimizu, Y., Sakata, R., Sugiyama, H., Grant, E. J., Soda, M., Kasagi, F. and Suyama, A., *Risk of cancer and non-cancer diseases in the atomic bomb survivors.* Radiation Protection Dosimetry, 2011. **146**(1-3): p. 272-275.
49. Radiation Effects Research Foundation, 2007 [cited; Available from: http://www.rerf.jp/glossary_e/ds02.htm.]
50. Takahashi, I., Abbott, R. D., Ohshita, T., Takahashi, T., Ozasa, K., Akahoshi, M., Fujiwara, S., Kodama, K. and Matsumoto, M., *A prospective follow-up study of the association of radiation exposure with fatal and non-fatal stroke among atomic bomb survivors in Hiroshima and Nagasaki (1980-2003).* BMJ Open, 2012. **2**(1): p. e000654.
51. Preston, D.L., Shimizu, Y., Pierce, D. A., Suyama, A. and Mabuchi, K., *Studies of mortality of atomic bomb survivors. Report 13: Solid cancer and noncancer disease mortality: 1950-1997.* Radiation Research, 2003. **160**(4): p. 381-407.
52. Shimizu, Y., Pierce, D. A., Preston, D. L. and Mabuchi, K., *Studies of the mortality of atomic bomb survivors. Report 12, part II. Noncancer mortality: 1950-1990.* Radiation Research, 1999. **152**(4): p. 374-389.
53. Shimizu, Y., Kodama, K., Nishi, N., Kasagi, F., Suyama, A., Soda, M., Grant, E. J., Sugiyama, H., Sakata, R., Moriwaki, H., Hayashi, M., Konda, M. and Shore, R. E., *Radiation exposure and circulatory disease risk: Hiroshima and Nagasaki atomic bomb survivor data, 1950-2003.* BMJ, 2010. **340**: p. b5349.

54. Vrijheid, M., Cardis, E., Ashmore, P., Auvinen, A., Bae, J. M., Engels, H., Gilbert, E., Gulis, G., Habib, R., Howe, G., Kurtinaitis, J., Malker, H., Muirhead, C., Richardson, D., Rodriguez-Artalejo, F., Rogel, A., Schubauer-Berigan, M., Tardy, H., Telle-Lamberton, M., Usel, M. and Veress, K., *Mortality from diseases other than cancer following low doses of ionizing radiation: results from the 15-Country Study of nuclear industry workers*. International Journal of Epidemiology, 2007. **36**(5): p. 1126-1135.
55. Muirhead, C.R., J.A. O'Hagan, R.G. Haylock, M.A. Phillipson, T. Willcock, G.L. Berridge, and W. Zhang, *Mortality and cancer incidence following occupational radiation exposure: third analysis of the National Registry for Radiation Workers*. British Journal of Cancer, 2009. **100**(1): p. 206-212.
56. Ashmore, J.P., D. Krewski, J.M. Zielinski, H. Jiang, R. Semenciw, and P.R. Band, *First analysis of mortality and occupational radiation exposure based on the National Dose Registry of Canada*. American Journal of Epidemiology, 1998. **148**(6): p. 564-574.
57. Ivanov, V.K., M.A. Maksoutov, S.Y. Chekin, A.V. Petrov, A.P. Biryukov, Z.G. Kruglova, V.A. Matyash, A.F. Tsyb, K.G. Manton, and J.S. Kravchenko, *The risk of radiation-induced cerebrovascular disease in Chernobyl emergency workers*. Health Physics, 2006. **90**(3): p. 199-207.
58. Azizova, T.V., R.D. Day, N. Wald, C.R. Muirhead, J.A. O'Hagan, M.V. Sumina, Z.D. Belyaeva, M.B. Druzhinina, Teplyakov, II, N.G. Semenikhina, L.A. Stetsenko, E.S. Grigoryeva, L.N. Krupenina, and E.V. Vlasenko, *The "clinic" medical-dosimetric database of Mayak production association workers: structure, characteristics and prospects of utilization*. Health Physics, 2008. **94**(5): p. 449-458.
59. Azizova, T.V., C.R. Muirhead, M.B. Druzhinina, E.S. Grigoryeva, E.V. Vlasenko, M.V. Sumina, J.A. O'Hagan, W. Zhang, R.G. Haylock, and N. Hunter, *Cardiovascular diseases in the cohort of workers first employed at Mayak PA in 1948-1958*. Radiation Research, 2010. **174**(2): p. 155-168.
60. Azizova, T.V., C.R. Muirhead, M.B. Moseeva, E.S. Grigoryeva, E.V. Vlasenko, N. Hunter, R.G. Haylock, and J.A. O'Hagan, *Ischemic heart disease in nuclear workers first employed at the Mayak PA in 1948-1972*. Health Physics, 2012. **103**(1): p. 3-14.
61. Schollnberger, H., J.C. Kaiser, P. Jacob, and L. Walsh, *Dose-responses from multi-model inference for the non-cancer disease mortality of atomic bomb survivors*. Radiation and Environmental Biophysics, 2012. **51**(2): p. 165-178.
62. European Commission: Working Party on Research Implications on Health and Safety, Standards of the Article 31 Group of Experts, *Radiation Protection No 158, in EU Scientific Seminar 2008 "Emerging evidence for radiation induced circulatory diseases"* 2008.
63. UNSCEAR, *UNSCEAR 2006 report: Volume I, Annex B: epidemiological evaluation of cardiovascular diseases and other non-cancer diseases*. 2006.
64. Montgomery, J.E. and J.R. Brown, *Metabolic biomarkers for predicting cardiovascular disease*. Journal of Vascular Health and Risk Management, 2013. **9**: p. 37-45.
65. Borghini, A., E.A. Luca Gianicolo, E. Picano, and M.G. Andreassi, *Ionizing radiation and atherosclerosis: Current knowledge and future challenges*. Atherosclerosis, 2013. **230**(1): p. 40-47.
66. Seddon, B., A. Cook, L. Gothard, E. Salmon, K. Latus, S.R. Underwood, and J. Yarnold, *Detection of defects in myocardial perfusion imaging in patients with early breast cancer treated with radiotherapy*. Radiotherapy and Oncology, 2002. **64**(1): p. 53-63.

67. Chung, E., J.R. Corbett, J.M. Moran, K.A. Griffith, R.B. Marsh, M. Feng, R. Jagsi, M.L. Kessler, E.C. Ficaro, and L.J. Pierce, *Is there a dose-response relationship for heart disease with low-dose radiation therapy?* International Journal of Radiation Oncology, Biology, Physics, 2013. **85**(4): p. 959-964.
68. Januzzi, J.L., Jr., *Natriuretic peptide testing: a window into the diagnosis and prognosis of heart failure.* Cleveland Clinic Journal of Medicine, 2006. **73**(2): p. 149-152, 155-147.
69. Palazzuoli, A., M. Gallotta, I. Quatrini, and R. Nuti, *Natriuretic peptides (BNP and NT-proBNP): measurement and relevance in heart failure.* Journal of Vascular Health and Risk Management, 2010. **6**: p. 411-418.
70. Sabatine, M.S., D.A. Morrow, J.A. de Lemos, T. Omland, S. Sloan, P. Jarolim, S.D. Solomon, M.A. Pfeffer, and E. Braunwald, *Evaluation of multiple biomarkers of cardiovascular stress for risk prediction and guiding medical therapy in patients with stable coronary disease.* Circulation, 2012. **125**(2): p. 233-240.
71. D'Errico, M.P., L. Grimaldi, M.F. Petruzzelli, E.A. Gianicolo, F. Tramacere, A. Monetti, R. Placella, G. Pili, M.G. Andreassi, R. Sicari, E. Picano, and M. Portaluri, *N-terminal pro-B-type natriuretic peptide plasma levels as a potential biomarker for cardiac damage after radiotherapy in patients with left-sided breast cancer.* International Journal of Radiation Oncology, Biology, Physics, 2012. **82**(2): p. e239-246.
72. Julian Preston, R., J.D. Boice Jr, A. Bertrand Brill, R. Chakraborty, R. Conolly, F. Owen Hoffman, R.W. Hornung, D.C. Kocher, C.E. Land, R.E. Shore, and G.E. Woloschak, *Uncertainties in estimating health risks associated with exposure to ionising radiation.* Journal of radiological protection : official journal of the Society for Radiological Protection, 2013. **33**: p. 573-588.
73. ICRP, *ICRP Statement on Tissue Reactions and Early and Late Effects of Radiation in Normal Tissues and Organs – Threshold Doses for Tissue Reactions in a Radiation Protection Context, ICRP publication 118, in Ann. ICRP 41.* 2012.
74. Hall, E.J. and D.J. Brenner, *Cancer risks from diagnostic radiology.* British Journal of Radiology, 2008. **81**(965): p. 362-378.
75. UNSCEAR, *Sources and effects of ionizing radiation. Annex A: medical radiation exposures.* 2008.
76. Shapiro, B.P., P.J. Mergo, D.F. Snipelisky, B. Kantor, and T.C. Gerber, *Radiation dose in cardiac imaging: how should it affect clinical decisions?* American Journal of Roentgenology, 2013. **200**(3): p. 508-514.
77. Miller, J.A., E. Raichlin, E.E. Williamson, R.B. McCully, P.A. Pellikka, D.O. Hodge, T.D. Miller, R.J. Gibbons, and P.A. Araoz, *Evaluation of coronary CTA Appropriateness Criteria in an academic medical center.* Journal of the American College of Radiology, 2010. **7**(2): p. 125-131.
78. Hendel, R.C., M. Cerqueira, P.S. Douglas, K.C. Caruth, J.M. Allen, N.C. Jensen, W. Pan, R. Brindis, and M. Wolk, *A multicenter assessment of the use of single-photon emission computed tomography myocardial perfusion imaging with appropriateness criteria.* Journal of the American College of Cardiology, 2010. **55**(2): p. 156-162.
79. Paterick, T.E., M.F. Jan, Z.R. Paterick, A.J. Tajik, and T.C. Gerber, *Cardiac imaging modalities with ionizing radiation: the role of informed consent.* JACC: Cardiovascular Imaging 2012. **5**(6): p. 634-640.
80. Picano, E. and E. Vano, *The radiation issue in cardiology: the time for action is now.* Cardiovascular Ultrasound, 2011. **9**: p. 35.

81. Halliburton, S.S. and P. Schoenhagen, *Cardiovascular imaging with computed tomography: responsible steps to balancing diagnostic yield and radiation exposure*. JACC: Cardiovascular Imaging, 2010. **3**(5): p. 536-540.
82. Pernot, E., J. Hall, S. Baatout, M.A. Benotmane, E. Blanchardon, S. Bouffler, H. El Saghire, M. Gomolka, A. Guertler, M. Harms-Ringdahl, P. Jeggo, M. Kreuzer, D. Laurier, C. Lindholm, R. Mkacher, R. Quintens, K. Rothkamm, L. Sabatier, S. Tapio, F. de Vathaire, and E. Cardis, *Ionizing radiation biomarkers for potential use in epidemiological studies*. Mutation Research, 2012. **751**(2): p. 258-286.
83. Adams, M.J., P.H. Hardenbergh, L.S. Constine, and S.E. Lipshultz, *Radiation-associated cardiovascular disease*. Critical Reviews in Oncology/Hematology, 2003. **45**(1): p. 55-75.
84. Adams, M.J., S.E. Lipshultz, C. Schwartz, L.F. Fajardo, V. Coen, and L.S. Constine, *Radiation-associated cardiovascular disease: manifestations and management*. Seminars in Radiation Oncology, 2003. **13**(3): p. 346-356.
85. Schultz-Hector, S., *Heart*, in *Radiopathology of Organs and Tissues*, E. Eberhard Scherer, C. Streffer, and K.R. Trott, Editors. 1991.
86. Fajardo, L.F. and J.R. Stewart, *Experimental radiation-induced heart disease. I. Light microscopic studies*. American Journal of Pathology, 1970. **59**(2): p. 299-316.
87. Gavin, P.R. and E.L. Gillette, *Radiation response of the canine cardiovascular system*. Radiation Research, 1982. **90**(3): p. 489-500.
88. Lauk, S., Z. Kiszal, J. Buschmann, and K.R. Trott, *Radiation-induced heart disease in rats*. International Journal of Radiation Oncology, Biology, Physics, 1985. **11**(4): p. 801-808.
89. Lusis, A.J., *Atherosclerosis*. Nature, 2000. **407**(6801): p. 233-241.
90. Virmani, R., F.D. Kolodgie, A.P. Burke, A.V. Finn, H.K. Gold, T.N. Tulenko, S.P. Wrenn, and J. Narula, *Atherosclerotic plaque progression and vulnerability to rupture: angiogenesis as a source of intraplaque hemorrhage*. Arteriosclerosis, Thrombosis, and Vascular Biology, 2005. **25**(10): p. 2054-2061.
91. Libby, P., P.M. Ridker, and G.K. Hansson, *Progress and challenges in translating the biology of atherosclerosis*. Nature, 2011. **473**(7347): p. 317-325.
92. Zadelaar, S., R. Kleemann, L. Verschuren, J. de Vries-Van der Weij, J. van der Hoorn, H.M. Princen, and T. Kooistra, *Mouse models for atherosclerosis and pharmaceutical modifiers*. Arteriosclerosis, Thrombosis, and Vascular Biology, 2007. **27**(8): p. 1706-1721.
93. Ohashi, R., H. Mu, Q. Yao, and C. Chen, *Cellular and molecular mechanisms of atherosclerosis with mouse models*. Trends in Cardiovascular Medicine, 2004. **14**(5): p. 187-190.
94. Stewart, F.A., S. Heeneman, J. Te Poele, J. Kruse, N.S. Russell, M. Gijbels, and M. Daemen, *Ionizing radiation accelerates the development of atherosclerotic lesions in ApoE^{-/-} mice and predisposes to an inflammatory plaque phenotype prone to hemorrhage*. American Journal of Pathology, 2006. **168**(2): p. 649-658.
95. Gabriels, K., S. Hoving, I. Seemann, N.L. Visser, M.J. Gijbels, J.F. Pol, M.J. Daemen, F.A. Stewart, and S. Heeneman, *Local heart irradiation of ApoE^{-/-} mice induces microvascular and endocardial damage and accelerates coronary atherosclerosis*. Radiotherapy and Oncology, 2012. **105**(3): p. 358-364.
96. Hoving, S., S. Heeneman, M.J. Gijbels, J.A. te Poele, N.S. Russell, M.J. Daemen, and F.A. Stewart, *Single-dose and fractionated irradiation promote initiation and progression of atherosclerosis and induce an inflammatory plaque phenotype in ApoE^{-/-} mice*. International Journal of Radiation Oncology, Biology, Physics, 2008. **71**(3): p. 848-857.

97. Mitchel, R.E., M. Hasu, M. Bugden, H. Wyatt, M.P. Little, A. Gola, G. Hildebrandt, N.D. Priest, and S.C. Whitman, *Low-dose radiation exposure and atherosclerosis in ApoE(-)/(-) mice*. Radiation Research, 2011. **175**(5): p. 665-676.
98. Mitchel, R.E., M. Hasu, M. Bugden, H. Wyatt, G. Hildebrandt, Y.X. Chen, N.D. Priest, and S.C. Whitman, *Low-dose radiation exposure and protection against atherosclerosis in ApoE(-/-) mice: the influence of P53 heterozygosity*. Radiation Research, 2013. **179**(2): p. 190-199.
99. Jeon, Y.H., S.G. Kraus, T. Jowsey, and N.J. Glasgow, *The experience of living with chronic heart failure: a narrative review of qualitative studies*. BMC Health Services Research, 2010. **10**: p. 77.
100. Lauk, S., *Endothelial alkaline phosphatase activity loss as an early stage in the development of radiation-induced heart disease in rats*. Radiation Research, 1987. **110**(1): p. 118-128.
101. Schultz-Hector, S., *Radiation-induced heart disease: review of experimental data on dose response and pathogenesis*. International Journal of Radiation Biology, 1992. **61**(2): p. 149-160.
102. Franken, N.A., J.A. Camps, F.J. van Ravels, A. van der Laarse, E.K. Pauwels, and J. Wondergem, *Comparison of in vivo cardiac function with ex vivo cardiac performance of the rat heart after thoracic irradiation*. British Journal of Radiology, 1997. **70**(838): p. 1004-1009.
103. Seemann, I., K. Gabriels, N.L. Visser, S. Hoving, J.A. te Poele, J.F. Pol, M.J. Gijbels, B.J. Janssen, F.W. van Leeuwen, M.J. Daemen, S. Heeneman, and F.A. Stewart, *Irradiation induced modest changes in murine cardiac function despite progressive structural damage to the myocardium and microvasculature*. Radiotherapy and Oncology, 2012. **103**(2): p. 143-150.
104. Monceau, V., L. Meziani, C. Strup-Perrot, E. Morel, M. Schmidt, J. Haagen, B. Escoubet, W. Dorr, and M.C. Vozenin, *Enhanced sensitivity to low dose irradiation of ApoE-/- mice mediated by early pro-inflammatory profile and delayed activation of the TGFbeta1 cascade involved in fibrogenesis*. PLoS One, 2013. **8**(2): p. e57052.
105. Hildebrandt, G., L. Maggiorella, F. Rodel, V. Rodel, D. Willis, and K.R. Trott, *Mononuclear cell adhesion and cell adhesion molecule liberation after X-irradiation of activated endothelial cells in vitro*. International Journal of Radiation Biology, 2002. **78**(4): p. 315-325.
106. Hallahan, D.E., S. Virudachalam, and J. Kuchibhotla, *Nuclear factor kappaB dominant negative genetic constructs inhibit X-ray induction of cell adhesion molecules in the vascular endothelium*. Cancer Research, 1998. **58**(23): p. 5484-5488.
107. Van Der Meeren, A., C. Squiban, P. Gourmelon, H. Lafont, and M.H. Gaugler, *Differential regulation by IL-4 and IL-10 of radiation-induced IL-6 and IL-8 production and ICAM-1 expression by human endothelial cells*. Cytokine, 1999. **11**(11): p. 831-838.
108. Milliat, F., A. Francois, M. Isoir, E. Deutsch, R. Tamarat, G. Tarlet, A. Atfi, P. Validire, J. Bourhis, J.C. Sabourin, and M. Benderitter, *Influence of endothelial cells on vascular smooth muscle cells phenotype after irradiation: implication in radiation-induced vascular damages*. American Journal of Pathology, 2006. **169**(4): p. 1484-1495.
109. Hayashi, T., Y. Morishita, R. Khattree, M. Misumi, K. Sasaki, I. Hayashi, K. Yoshida, J. Kajimura, S. Kyoizumi, K. Imai, Y. Kusunoki, and K. Nakachi, *Evaluation of systemic markers of inflammation in atomic-bomb survivors with special reference to radiation and age effects*. FASEB Journal, 2012. **26**(11): p. 4765-4773.

110. Wang, J., H. Zheng, X. Ou, L.M. Fink, and M. Hauer-Jensen, *Deficiency of microvascular thrombomodulin and up-regulation of protease-activated receptor-1 in irradiated rat intestine: possible link between endothelial dysfunction and chronic radiation fibrosis*. American Journal of Pathology, 2002. **160**(6): p. 2063-2072.
111. Kern, P.M., L. Keilholz, C. Forster, R. Hallmann, M. Herrmann, and M.H. Seegenschmiedt, *Low-dose radiotherapy selectively reduces adhesion of peripheral blood mononuclear cells to endothelium in vitro*. Radiotherapy and Oncology, 2000. **54**(3): p. 273-282.
112. Trott, K.R. and F. Kamprad, *Radiobiological mechanisms of anti-inflammatory radiotherapy*. Radiotherapy and Oncology, 1999. **51**(3): p. 197-203.
113. Seegenschmiedt, M.H., A. Katalinic, H.B. Makoski, W. Haase, G. Gademann, and E. Hassenstein, *Radiotherapy of benign diseases: a pattern of care study in Germany*. Strahlentherapie und Onkologie, 1999. **175**(11): p. 541-547.
114. Rodel, F., L. Keilholz, M. Herrmann, R. Sauer, and G. Hildebrandt, *Radiobiological mechanisms in inflammatory diseases of low-dose radiation therapy*. International Journal of Radiation Biology, 2007. **83**(6): p. 357-366.
115. Hirase, T. and K. Node, *Endothelial dysfunction as a cellular mechanism for vascular failure*. American Journal of Physiology - Heart and Circulatory Physiology, 2012. **302**(3): p. H499-505.
116. Flammer, A.J. and T.F. Luscher, *Three decades of endothelium research: from the detection of nitric oxide to the everyday implementation of endothelial function measurements in cardiovascular diseases*. Swiss Medical Weekly 2010. **140**: p. w13122.
117. Triggle, C.R., S.M. Samuel, S. Ravishankar, I. Marei, G. Arunachalam, and H. Ding, *The endothelium: influencing vascular smooth muscle in many ways*. Canadian Journal of Physiology and Pharmacology, 2012. **90**(6): p. 713-738.
118. Tomanek, R.J. and G.C. Schatteman, *Angiogenesis: new insights and therapeutic potential*. Anatomical Record, 2000. **261**(3): p. 126-135.
119. van Hinsbergh, V.W., *Endothelium--role in regulation of coagulation and inflammation*. Seminars in Immunopathology, 2012. **34**(1): p. 93-106.
120. Michiels, C., *Endothelial cell functions*. Journal of Cellular Physiology, 2003. **196**(3): p. 430-443.
121. Sandoo, A., J.J. van Zanten, G.S. Metsios, D. Carroll, and G.D. Kitas, *The endothelium and its role in regulating vascular tone*. Open Cardiovascular Medicine Journal, 2010. **4**: p. 302-312.
122. Aird, W.C., *Phenotypic heterogeneity of the endothelium: I. Structure, function, and mechanisms*. Circulation Research, 2007. **100**(2): p. 158-173.
123. Aird, W.C., *Phenotypic heterogeneity of the endothelium: II. Representative vascular beds*. Circulation Research, 2007. **100**(2): p. 174-190.
124. Landmesser, U., B. Hornig, and H. Drexler, *Endothelial function: a critical determinant in atherosclerosis?* Circulation, 2004. **109**(21 Suppl 1): p. II27-33.
125. Levine, A.B., D. Punihale, and T.B. Levine, *Characterization of the role of nitric oxide and its clinical applications*. Cardiology, 2012. **122**(1): p. 55-68.
126. Khazaei, M., F. Moien-Afshari, and I. Laher, *Vascular endothelial function in health and diseases*. Pathophysiology, 2008. **15**(1): p. 49-67.
127. Mudau, M., A. Genis, A. Lochner, and H. Strijdom, *Endothelial dysfunction: the early predictor of atherosclerosis*. The Cardiovascular Journal of Africa, 2012. **23**(4): p. 222-231.
128. Shah, A.M. and K.M. Channon, *Free radicals and redox signalling in cardiovascular disease*. Heart, 2004. **90**(5): p. 486-487.

129. Lum, H. and K.A. Roebuck, *Oxidant stress and endothelial cell dysfunction*. American Journal of Physiology - Cell Physiology 2001. **280**(4): p. C719-741.
130. Held, P. *An introduction to reactive oxygen species: measurement of ROS in cells*. 2010 [cited; Available from: <http://www.biotek.com/resources/articles/reactive-oxygen-species.html>.]
131. Bahorun, T., M.A. Soobrattee, V. Luximon-Ramma, and O.I. Aruoma, *Free radicals and antioxidants in cardiovascular health and disease*. International Journal of Medical Update, 2006. **1**(2): p. 25-41.
132. Cai, H. and D.G. Harrison, *Endothelial dysfunction in cardiovascular diseases: the role of oxidant stress*. Circulation Research, 2000. **87**(10): p. 840-844.
133. Ungvari, Z., G. Kaley, R. de Cabo, W.E. Sonntag, and A. Csiszar, *Mechanisms of vascular aging: new perspectives*. Journals of Gerontology. Series A, Biological Sciences and Medical Sciences, 2010. **65**(10): p. 1028-1041.
134. Voghel, G., N. Thorin-Trescases, N. Farhat, A. Nguyen, L. Villeneuve, A.M. Mamarbachi, A. Fortier, L.P. Perrault, M. Carrier, and E. Thorin, *Cellular senescence in endothelial cells from atherosclerotic patients is accelerated by oxidative stress associated with cardiovascular risk factors*. Mechanisms of Ageing and Development, 2007. **128**(11-12): p. 662-671.
135. Erusalimsky, J.D., *Vascular endothelial senescence: from mechanisms to pathophysiology*. Journal of Applied Physiology, 2009. **106**(1): p. 326-332.
136. Erusalimsky, J.D. and C. Skene, *Mechanisms of endothelial senescence*. Experimental Physiology, 2009. **94**(3): p. 299-304.
137. Minamoto, T., H. Miyauchi, T. Yoshida, Y. Ishida, H. Yoshida, and I. Komuro, *Endothelial cell senescence in human atherosclerosis: role of telomere in endothelial dysfunction*. Circulation, 2002. **105**(13): p. 1541-1544.
138. Vasile, E., Y. Tomita, L.F. Brown, O. Kocher, and H.F. Dvorak, *Differential expression of thymosin beta-10 by early passage and senescent vascular endothelium is modulated by VPF/VEGF: evidence for senescent endothelial cells in vivo at sites of atherosclerosis*. FASEB Journal, 2001. **15**(2): p. 458-466.
139. Ogami, M., Y. Ikura, M. Ohsawa, T. Matsuo, S. Kayo, N. Yoshimi, E. Hai, N. Shirai, S. Ehara, R. Komatsu, T. Naruko, and M. Ueda, *Telomere shortening in human coronary artery diseases*. Arteriosclerosis, Thrombosis, and Vascular Biology, 2004. **24**(3): p. 546-550.
140. Hayflick, L., *The Limited in Vitro Lifetime of Human Diploid Cell Strains*. Experimental Cell Research, 1965. **37**: p. 614-636.
141. Zhu, H., M. Belcher, and P. van der Harst, *Healthy aging and disease: role for telomere biology?* Clinical Science, 2011. **120**(10): p. 427-440.
142. Gomez, D.E., R.G. Armando, H.G. Farina, P.L. Menna, C.S. Cerrudo, P.D. Ghiringhelli, and D.F. Alonso, *Telomere structure and telomerase in health and disease (review)*. International Journal of Oncology, 2012. **41**(5): p. 1561-1569.
143. Ben-Porath, I. and R.A. Weinberg, *The signals and pathways activating cellular senescence*. International Journal of Biochemistry and Cell Biology, 2005. **37**(5): p. 961-976.
144. Campisi, J. and F. d'Adda di Fagagna, *Cellular senescence: when bad things happen to good cells*. Nature Reviews Molecular Cell Biology, 2007. **8**(9): p. 729-740.
145. Kurz, D.J., S. Decary, Y. Hong, E. Trivier, A. Akhmedov, and J.D. Erusalimsky, *Chronic oxidative stress compromises telomere integrity and accelerates the onset of senescence in human endothelial cells*. Journal of Cell Science, 2004. **117**(Pt 11): p. 2417-2426.

146. Minamino, T. and I. Komuro, *Vascular cell senescence: contribution to atherosclerosis*. Circulation Research, 2007. **100**(1): p. 15-26.
147. El Assar, M., J. Angulo, S. Vallejo, C. Peiro, C.F. Sanchez-Ferrer, and L. Rodriguez-Manas, *Mechanisms involved in the aging-induced vascular dysfunction*. Frontiers in Physiology, 2012. **3**: p. 132.
148. Yu, E., J. Mercer, and M. Bennett, *Mitochondria in vascular disease*. Cardiovascular Research, 2012. **95**(2): p. 173-182.
149. Balaban, R.S., S. Nemoto, and T. Finkel, *Mitochondria, oxidants, and aging*. Cell, 2005. **120**(4): p. 483-495.
150. Frohman, M.A., *Mitochondria as integrators of signal transduction and energy production in cardiac physiology and disease*. Journal of Molecular Medicine (Berl), 2010. **88**(10): p. 967-970.
151. Davidson, S.M. and M.R. Duchon, *Endothelial mitochondria: contributing to vascular function and disease*. Circulation Research, 2007. **100**(8): p. 1128-1141.
152. Gutierrez, J., S.W. Ballinger, V.M. Darley-Usmar, and A. Landar, *Free radicals, mitochondria, and oxidized lipids: the emerging role in signal transduction in vascular cells*. Circulation Research, 2006. **99**(9): p. 924-932.
153. Zhang, D.X. and D.D. Gutterman, *Mitochondrial reactive oxygen species-mediated signaling in endothelial cells*. American Journal of Physiology - Heart and Circulatory Physiology, 2007. **292**(5): p. H2023-2031.
154. Puddu, P., G.M. Puddu, E. Cravero, S. De Pascalis, and A. Muscari, *The emerging role of cardiovascular risk factor-induced mitochondrial dysfunction in atherogenesis*. Journal of Biomedical Science, 2009. **16**: p. 112.
155. Yakes, F.M. and B. Van Houten, *Mitochondrial DNA damage is more extensive and persists longer than nuclear DNA damage in human cells following oxidative stress*. Proceedings of the National Academy of Sciences of the United States of America, 1997. **94**(2): p. 514-519.
156. Edwards, J.G., *Quantification of mitochondrial DNA (mtDNA) damage and error rates by real-time QPCR*. Mitochondrion, 2009. **9**(1): p. 31-35.
157. Mandavilli, B.S., J.H. Santos, and B. Van Houten, *Mitochondrial DNA repair and aging*. Mutation Research, 2002. **509**(1-2): p. 127-151.
158. Ballinger, S.W., C. Patterson, C.A. Knight-Lozano, D.L. Burow, C.A. Conklin, Z. Hu, J. Reuf, C. Horaist, R. Lebovitz, G.C. Hunter, K. McIntyre, and M.S. Runge, *Mitochondrial integrity and function in atherogenesis*. Circulation, 2002. **106**(5): p. 544-549.
159. Bogliolo, M., A. Izzotti, S. De Flora, C. Carli, A. Abbondandolo, and P. Degan, *Detection of the '4977 bp' mitochondrial DNA deletion in human atherosclerotic lesions*. Mutagenesis, 1999. **14**(1): p. 77-82.
160. Prithivirajasingh, S., M.D. Story, S.A. Bergh, F.B. Geara, K.K. Ang, S.M. Ismail, C.W. Stevens, T.A. Buchholz, and W.A. Brock, *Accumulation of the common mitochondrial DNA deletion induced by ionizing radiation*. FEBS Letters, 2004. **571**(1-3): p. 227-232.
161. Jaffe, E.A., R.L. Nachman, C.G. Becker, and C.R. Minick, *Culture of human endothelial cells derived from umbilical veins. Identification by morphologic and immunologic criteria*. Journal of Clinical Investigation, 1973. **52**(11): p. 2745-2756.
162. Gimbrone, M.A., Jr., R.S. Cotran, and J. Folkman, *Human vascular endothelial cells in culture. Growth and DNA synthesis*. Journal of Cell Biology, 1974. **60**(3): p. 673-684.
163. Bicknell, R., *Endothelial cell culture* Handbooks in practical animal cell biology. 1996.

164. Edgell, C.J., C.C. McDonald, and J.B. Graham, *Permanent cell line expressing human factor VIII-related antigen established by hybridization*. Proceedings of the National Academy of Sciences of the United States of America, 1983. **80**(12): p. 3734-3737.
165. van Leeuwen, E.B.M., *Isolation, immortalization and characterisation of human endothelial cells*. 1999
166. Dickson, M.A., W.C. Hahn, Y. Ino, V. Ronfard, J.Y. Wu, R.A. Weinberg, D.N. Louis, F.P. Li, and J.G. Rheinwald, *Human keratinocytes that express hTERT and also bypass a p16(INK4a)-enforced mechanism that limits life span become immortal yet retain normal growth and differentiation characteristics*. Molecular and Cellular Biology, 2000. **20**(4): p. 1436-1447.
167. Bouis, D., G.A. Hospers, C. Meijer, G. Molema, and N.H. Mulder, *Endothelium in vitro: a review of human vascular endothelial cell lines for blood vessel-related research*. Angiogenesis, 2001. **4**(2): p. 91-102.
168. Wallace, C.S. and G.A. Truskey, *Direct-contact co-culture between smooth muscle and endothelial cells inhibits TNF-alpha-mediated endothelial cell activation*. American Journal of Physiology - Heart and Circulatory Physiology, 2010. **299**(2): p. H338-346.
169. Rainger, G.E. and G.B. Nash, *Cellular pathology of atherosclerosis: smooth muscle cells prime cocultured endothelial cells for enhanced leukocyte adhesion*. Circulation Research, 2001. **88**(6): p. 615-622.
170. Dietrich, F. and P.I. Lelkes, *Fine-tuning of a three-dimensional microcarrier-based angiogenesis assay for the analysis of endothelial-mesenchymal cell co-cultures in fibrin and collagen gels*. Angiogenesis, 2006. **9**(3): p. 111-125.
171. Vernon, R.B. and E.H. Sage, *A novel, quantitative model for study of endothelial cell migration and sprout formation within three-dimensional collagen matrices*. Microvascular Research, 1999. **57**(2): p. 118-133.
172. Acheva, A., A. Aerts, S. Baatout, C. Rombouts, S. Salomaa, K. Manda, G. Hildebrandt, and M. Kämäräinen, *Human 3-D tissue models in radiation biology – current status and future perspectives*. International Journal of Radiation Research, 2013. **Accepted and in press**.
173. Goel, S., D.G. Duda, L. Xu, L.L. Munn, Y. Boucher, D. Fukumura, and R.K. Jain, *Normalization of the vasculature for treatment of cancer and other diseases*. Physiological Reviews, 2011. **91**(3): p. 1071-1121.
174. Zhang, H.P., K. Takayama, B. Su, X.D. Jiao, R. Li, and J.J. Wang, *Effect of sunitinib combined with ionizing radiation on endothelial cells*. Journal of Radiation Research, 2011. **52**(1): p. 1-8.
175. Dudley, A.C., *Tumor endothelial cells*. Cold Spring Harbor Perspectives in Medicine, 2012. **2**(3): p. a006536.
176. Jeggo, P. and M. Lobrich, *Radiation-induced DNA damage responses*. Radiation Protection Dosimetry, 2006. **122**(1-4): p. 124-127.
177. Bolus, N.E., *Basic review of radiation biology and terminology*. Journal of Nuclear Medicine Technology, 2001. **29**(2): p. 67-73; test 76-67.
178. Norbury, C.J. and I.D. Hickson, *Cellular responses to DNA damage*. Annual Review of Pharmacology and Toxicology, 2001. **41**: p. 367-401.
179. Clarke, P.R. and L.A. Allan, *Cell-cycle control in the face of damage--a matter of life or death*. Trends in Cell Biology, 2009. **19**(3): p. 89-98.
180. Dikomey, E., J. Dahm-Daphi, I. Brammer, R. Martensen, and B. Kaina, *Correlation between cellular radiosensitivity and non-repaired double-strand breaks studied in nine mammalian cell lines*. International Journal of Radiation Biology, 1998. **73**(3): p. 269-278.

181. Kuo, L.J. and L.X. Yang, *Gamma-H2AX - a novel biomarker for DNA double-strand breaks*. In Vivo, 2008. **22**(3): p. 305-309.
182. Stoneman, V.E. and M.R. Bennett, *Role of apoptosis in atherosclerosis and its therapeutic implications*. Clinical Science, 2004. **107**(4): p. 343-354.
183. Mercer, J., M. Mahmoudi, and M. Bennett, *DNA damage, p53, apoptosis and vascular disease*. Mutation Research, 2007. **621**(1-2): p. 75-86.
184. Choy, J.C., D.J. Granville, D.W. Hunt, and B.M. McManus, *Endothelial cell apoptosis: biochemical characteristics and potential implications for atherosclerosis*. Journal of Molecular and Cellular Cardiology, 2001. **33**(9): p. 1673-1690.
185. Haimovitz-Friedman, A., C.C. Kan, D. Ehleiter, R.S. Persaud, M. McLoughlin, Z. Fuks, and R.N. Kolesnick, *Ionizing radiation acts on cellular membranes to generate ceramide and initiate apoptosis*. Journal of Experimental Medicine, 1994. **180**(2): p. 525-535.
186. Langley, R.E., E.A. Bump, S.G. Quartuccio, D. Medeiros, and S.J. Braunhut, *Radiation-induced apoptosis in microvascular endothelial cells*. British Journal of Cancer, 1997. **75**(5): p. 666-672.
187. Rodel, F., B. Frey, G. Capalbo, U. Gaipl, L. Keilholz, R. Voll, G. Hildebrandt, and C. Rodel, *Discontinuous induction of X-linked inhibitor of apoptosis in EA.hy.926 endothelial cells is linked to NF-kappaB activation and mediates the anti-inflammatory properties of low-dose ionising-radiation*. Radiotherapy and Oncology, 2010. **97**(2): p. 346-351.
188. Pluder, F., Z. Barjaktarovic, O. Azimzadeh, S. Mortl, A. Kramer, S. Steininger, H. Sarioglu, D. Leszczynski, R. Nylund, A. Hakanen, A. Sriharshan, M.J. Atkinson, and S. Tapio, *Low-dose irradiation causes rapid alterations to the proteome of the human endothelial cell line EA.hy926*. Radiation and Environmental Biophysics, 2011. **50**(1): p. 155-166.
189. Riley, P.A., *Free radicals in biology: oxidative stress and the effects of ionizing radiation*. International Journal of Radiation Biology, 1994. **65**(1): p. 27-33.
190. Yamamori, T., H. Yasui, M. Yamazumi, Y. Wada, Y. Nakamura, H. Nakamura, and O. Inanami, *Ionizing radiation induces mitochondrial reactive oxygen species production accompanied by upregulation of mitochondrial electron transport chain function and mitochondrial content under control of the cell cycle checkpoint*. Free Radical Biology and Medicine, 2012. **53**(2): p. 260-270.
191. Bernardi, P., *The mitochondrial permeability transition pore: a mystery solved?* Frontiers in Physiology, 2013. **4**: p. 95.
192. Leach, J.K., G. Van Tuyle, P.S. Lin, R. Schmidt-Ullrich, and R.B. Mikkelsen, *Ionizing radiation-induced, mitochondria-dependent generation of reactive oxygen/nitrogen*. Cancer Research, 2001. **61**(10): p. 3894-3901.
193. Wang, L., Y. Kuwahara, L. Li, T. Baba, R.W. Shin, Y. Ohkubo, K. Ono, and M. Fukumoto, *Analysis of Common Deletion (CD) and a novel deletion of mitochondrial DNA induced by ionizing radiation*. International Journal of Radiation Biology, 2007. **83**(7): p. 433-442.
194. Schilling-Toth, B., N. Sandor, E. Kis, M. Kadhim, G. Safrany, and H. Hegyesi, *Analysis of the common deletions in the mitochondrial DNA is a sensitive biomarker detecting direct and non-targeted cellular effects of low dose ionizing radiation*. Mutation Research, 2011. **716**(1-2): p. 33-39.
195. Barjaktarovic, Z., D. Schmaltz, A. Shyla, O. Azimzadeh, S. Schulz, J. Haagen, W. Dorr, H. Sarioglu, A. Schafer, M.J. Atkinson, H. Zischka, and S. Tapio, *Radiation-induced signaling results in mitochondrial impairment in mouse heart at 4 weeks after exposure to X-rays*. PLoS One, 2011. **6**(12): p. e27811.

196. Vavrova, J. and M. Rezacova, *The importance of senescence in ionizing radiation-induced tumour suppression*. *Folia Biologica*, 2011. **57**(2): p. 41-46.
197. Sabatino, L., E. Picano, and M.G. Andreassi, *Telomere shortening and ionizing radiation: a possible role in vascular dysfunction?* *International Journal of Radiation Biology*, 2012. **88**(11): p. 830-839.
198. Oh, C.W., E.A. Bump, J.S. Kim, D. Janigro, and M.R. Mayberg, *Induction of a senescence-like phenotype in bovine aortic endothelial cells by ionizing radiation*. *Radiation Research*, 2001. **156**(3): p. 232-240.
199. Panganiban, R.A., O. Mungunsukh, and R.M. Day, *X-irradiation induces ER stress, apoptosis, and senescence in pulmonary artery endothelial cells*. *International Journal of Radiation Biology*, 2013. **89**(8): p. 656-667.
200. Igarashi, K., I. Sakimoto, K. Kataoka, K. Ohta, and M. Miura, *Radiation-induced senescence-like phenotype in proliferating and plateau-phase vascular endothelial cells*. *Experimental Cell Research*, 2007. **313**(15): p. 3326-3336.
201. Kim, K.S., J.E. Kim, K.J. Choi, S. Bae, and D.H. Kim, *Characterization of DNA damage-induced cellular senescence by ionizing radiation in endothelial cells*. *International Journal of Radiation Biology*, 2014. **90**(1): p. 71-80.
202. Suzuki, K., I. Mori, Y. Nakayama, M. Miyakoda, S. Kodama, and M. Watanabe, *Radiation-induced senescence-like growth arrest requires TP53 function but not telomere shortening*. *Radiation Research*, 2001. **155**(1 Pt 2): p. 248-253.
203. Kim, K.S., J.E. Kim, K.J. Choi, S. Bae, and D.H. Kim, *Characterization of DNA damage-induced cellular senescence by ionizing radiation in endothelial cells*. *International Journal of Radiation Biology*, 2014. **90**(1): p. 71-80.
204. Yentrapalli, R., O. Azimzadeh, Z. Barjaktarovic, H. Sarioglu, A. Wojcik, M. Harms-Ringdahl, M.J. Atkinson, S. Haghdoost, and S. Tapio, *Quantitative proteomic analysis reveals induction of premature senescence in human umbilical vein endothelial cells exposed to chronic low-dose rate gamma-radiation*. *Proteomics*, 2013. **13**(7): p. 1096-1107.
205. Yentrapalli, R., O. Azimzadeh, A. Sriharshan, K. Malinowsky, J. Merl, A. Wojcik, M. Harms-Ringdahl, M.J. Atkinson, K.-F. Becker, S. Haghdoost, and S. Tapio, *The PI3K/Akt/mTOR Pathway Is Implicated in the Premature Senescence of Primary Human Endothelial Cells Exposed to Chronic Radiation*. *PLoS ONE*, 2013. **8**(8): p. e70024.
206. Amundson, S.A., *Functional genomics in radiation biology: a gateway to cellular systems-level studies*. *Radiation and Environmental Biophysics*, 2008. **47**(1): p. 25-31.
207. Snyder, A.R. and W.F. Morgan, *Gene expression profiling after irradiation: clues to understanding acute and persistent responses?* *Cancer and Metastasis Reviews*, 2004. **23**(3-4): p. 259-268.
208. Loven, J., D.A. Orlando, A.A. Sigova, C.Y. Lin, P.B. Rahl, C.B. Burge, D.L. Levens, T.I. Lee, and R.A. Young, *Revisiting global gene expression analysis*. *Cell*, 2012. **151**(3): p. 476-482.
209. Roy, L., G. Gruel, and A. Vaurijoux, *Cell response to ionising radiation analysed by gene expression patterns*. *Annali dell Istituto Superiore di Sanita*, 2009. **45**(3): p. 272-277.
210. Lanza, V., V. Pretazzoli, G. Olivieri, G. Pascarella, A. Panconesi, and R. Negri, *Transcriptional response of human umbilical vein endothelial cells to low doses of ionizing radiation*. *Journal of Radiation Research*, 2005. **46**(2): p. 265-276.
211. Wu, M.C. and X. Lin, *Prior biological knowledge-based approaches for the analysis of genome-wide expression profiles using gene sets and pathways*. *Statistical Methods in Medical Research*, 2009. **18**(6): p. 577-593.

212. Hung, J.H., T.H. Yang, Z. Hu, Z. Weng, and C. DeLisi, *Gene set enrichment analysis: performance evaluation and usage guidelines*. Briefings in Bioinformatics, 2012. **13**(3): p. 281-291.
213. Subramanian, A., P. Tamayo, V.K. Mootha, S. Mukherjee, B.L. Ebert, M.A. Gillette, A. Paulovich, S.L. Pomeroy, T.R. Golub, E.S. Lander, and J.P. Mesirov, *Gene set enrichment analysis: a knowledge-based approach for interpreting genome-wide expression profiles*. Proceedings of the National Academy of Sciences of the United States of America, 2005. **102**(43): p. 15545-15550.
214. Mootha, V.K., C.M. Lindgren, K.F. Eriksson, A. Subramanian, S. Sihag, J. Lehar, P. Puigserver, E. Carlsson, M. Ridderstrale, E. Laurila, N. Houstis, M.J. Daly, N. Patterson, J.P. Mesirov, T.R. Golub, P. Tamayo, B. Spiegelman, E.S. Lander, J.N. Hirschhorn, D. Altshuler, and L.C. Groop, *PGC-1alpha-responsive genes involved in oxidative phosphorylation are coordinately downregulated in human diabetes*. Nature Genetics, 2003. **34**(3): p. 267-273.
215. Little, M.P., E.J. Tawn, I. Tzoulaki, R. Wakeford, G. Hildebrandt, F. Paris, S. Tapio, and P. Elliott, *Review and meta-analysis of epidemiological associations between low/moderate doses of ionizing radiation and circulatory disease risks, and their possible mechanisms*. Radiation and Environmental Biophysics, 2010. **49**(2): p. 139-153.
216. Versari, D., E. Daghini, A. Viridis, L. Ghiadoni, and S. Taddei, *Endothelial dysfunction as a target for prevention of cardiovascular disease*. Diabetes Care, 2009. **32 Suppl 2**: p. S314-321.
217. Gaugler, M.H., *A unifying system: does the vascular endothelium have a role to play in multi-organ failure following radiation exposure?* British Journal of Radiology Supplements, 2005. **27**: p. 100-105.
218. Wang, J., M. Boerma, Q. Fu, and M. Hauer-Jensen, *Significance of endothelial dysfunction in the pathogenesis of early and delayed radiation enteropathy*. World Journal of Gastroenterology, 2007. **13**(22): p. 3047-3055.
219. Karbach, S., T. Jansen, S. Horke, T. Heeren, A. Scholz, M. Coldewey, A. Karpi, M. Hausding, S. Kroller-Schon, M. Oelze, T. Munzel, and A. Daiber, *Hyperglycemia and oxidative stress in cultured endothelial cells--a comparison of primary endothelial cells with an immortalized endothelial cell line*. Journal of Diabetes and Its Complications, 2012. **26**(3): p. 155-162.
220. Watson, C.A., L. Camera-Benson, R. Palmer-Crocker, and J.S. Pober, *Variability among human umbilical vein endothelial cultures*. Science, 1995. **268**(5209): p. 447-448.
221. Pan, C., C. Kumar, S. Bohl, U. Klingmueller, and M. Mann, *Comparative proteomic phenotyping of cell lines and primary cells to assess preservation of cell type-specific functions*. Molecular & Cellular Proteomics 2009. **8**(3): p. 443-450.
222. Bauer, J., M. Margolis, C. Schreiner, C.J. Edgell, J. Azizkhan, E. Lazarowski, and R.L. Juliano, *In vitro model of angiogenesis using a human endothelium-derived permanent cell line: contributions of induced gene expression, G-proteins, and integrins*. Journal of Cellular Physiology, 1992. **153**(3): p. 437-449.
223. Aranda, E. and G.I. Owen, *A semi-quantitative assay to screen for angiogenic compounds and compounds with angiogenic potential using the EA.hy926 endothelial cell line*. Biological Research, 2009. **42**(3): p. 377-389.
224. Boerma, M., G.R. Burton, J. Wang, L.M. Fink, R.E. McGehee Jr., and M. Hauer-Jensen, *Comparative expression profiling in primary and immortalized endothelial cells: changes in gene expression in response to hydroxy methylglutaryl-coenzyme A reductase inhibition*. Blood Coagulation and Fibrinolysis, 2006. **17**: p. 173-180.

225. Claise, C., J. Chalas, M. Edeas, A. Abella, Y. Khalfoun, D. Laurent, and A. Lindenbaum, *Comparison of oxidized low-density lipoprotein toxicity on EA.hy 926 cells and human vein endothelial cells: influence of antioxidant systems*. Cellular and Molecular Life Sciences, 1997. **53**(2): p. 156-161.
226. Lidington, E.A., D.L. Moyes, A.M. McCormack, and M.L. Rose, *A comparison of primary endothelial cells and endothelial cell lines for studies of immune interactions*. Transplant Immunology, 1999. **7**(4): p. 239-246.
227. Tichy, A., J. Vavrova, J. Pejchal, and M. Rezacova, *Ataxia-telangiectasia mutated kinase (ATM) as a central regulator of radiation-induced DNA damage response*. Acta Medica (Hradec Kralove), 2010. **53**(1): p. 13-17.
228. Schneider, C.A., W.S. Rasband, and K.W. Eliceiri, *NIH Image to ImageJ: 25 years of image analysis*. Nature Methods, 2012. **9**(7): p. 671-675.
229. De Vos, W.H., L. Van Neste, B. Dieriks, G.H. Joss, and P. Van Oostveldt, *High content image cytometry in the context of subnuclear organization*. Cytometry Part A, 2010. **77**(1): p. 64-75.
230. Vos, M.D., C.A. Ellis, C. Elam, A.S. Ulku, B.J. Taylor, and G.J. Clark, *RASSF2 is a novel K-Ras-specific effector and potential tumor suppressor*. Journal of Biological Chemistry, 2003. **278**(30): p. 28045-28051.
231. Chan, Y. and R.P. Walmsley, *Learning and understanding the Kruskal-Wallis one-way analysis-of-variance-by-ranks test for differences among three or more independent groups*. Physical Therapy, 1997. **77**(12): p. 1755-1762.
232. Huang, X., H.D. Halicka, F. Traganos, T. Tanaka, A. Kurose, and Z. Darzynkiewicz, *Cytometric assessment of DNA damage in relation to cell cycle phase and apoptosis*. Cell Proliferation, 2005. **38**(4): p. 223-243.
233. Luu, N.T., M. Rahman, P.C. Stone, G.E. Rainger, and G.B. Nash, *Responses of endothelial cells from different vessels to inflammatory cytokines and shear stress: evidence for the pliability of endothelial phenotype*. Journal of Vascular Research, 2010. **47**(5): p. 451-461.
234. Chi, J.T., H.Y. Chang, G. Haraldsen, F.L. Jahnsen, O.G. Troyanskaya, D.S. Chang, Z. Wang, S.G. Rockson, M. van de Rijn, D. Botstein, and P.O. Brown, *Endothelial cell diversity revealed by global expression profiling*. Proceedings of the National Academy of Sciences of the United States of America, 2003. **100**(19): p. 10623-10628.
235. Stevens, T., R. Rosenberg, W. Aird, T. Quertermous, F.L. Johnson, J.G. Garcia, R.P. Hebbel, R.M. Tuder, and S. Garfinkel, *NHLBI workshop report: endothelial cell phenotypes in heart, lung, and blood diseases*. American Journal of Physiology - Cell Physiology, 2001. **281**(5): p. C1422-1433.
236. Neumaier, T., J. Swenson, C. Pham, A. Polyzos, A.T. Lo, P. Yang, J. Dyball, A. Asaithamby, D.J. Chen, M.J. Bissell, S. Thalhammer, and S.V. Costes, *Evidence for formation of DNA repair centers and dose-response nonlinearity in human cells*. Proceedings of the National Academy of Sciences of the United States of America, 2012. **109**(2): p. 443-448.
237. Costes, S.V., I. Chiolo, J.M. Pluth, M.H. Barcellos-Hoff, and B. Jakob, *Spatiotemporal characterization of ionizing radiation induced DNA damage foci and their relation to chromatin organization*. Mutation Research, 2010. **704**(1-3): p. 78-87.
238. Lobrich, M., A. Shibata, A. Beucher, A. Fisher, M. Ensminger, A.A. Goodarzi, O. Barton, and P.A. Jeggo, *gammaH2AX foci analysis for monitoring DNA double-strand break repair: strengths, limitations and optimization*. Cell Cycle, 2010. **9**(4): p. 662-669.

239. Kraemer, A., N. Anastasov, M. Angermeier, K. Winkler, M.J. Atkinson, and S. Moertl, *MicroRNA-mediated processes are essential for the cellular radiation response*. Radiation Research, 2011. **176**(5): p. 575-586.
240. Shrivastav, M., L.P. De Haro, and J.A. Nickoloff, *Regulation of DNA double-strand break repair pathway choice*. Cell Research, 2008. **18**(1): p. 134-147.
241. Beck, M., M. Moreels, P. Jacquet, P. Van Oostveldt, W.H. De Vos, and S. Baatout, *X-irradiation induces cell death in fetal fibroblasts*. International Journal of Molecular Medicine, 2012. **30**(1): p. 114-118.
242. Xu, B., S.T. Kim, D.S. Lim, and M.B. Kastan, *Two molecularly distinct G(2)/M checkpoints are induced by ionizing irradiation*. Molecular and Cellular Biology, 2002. **22**(4): p. 1049-1059.
243. Fernet, M., F. Megnin-Chanet, J. Hall, and V. Favaudon, *Control of the G2/M checkpoints after exposure to low doses of ionising radiation: implications for hyper-radiosensitivity*. DNA Repair (Amst), 2010. **9**(1): p. 48-57.
244. Tricot, O., Z. Mallat, C. Heymes, J. Belmin, G. Leseche, and A. Tedgui, *Relation between endothelial cell apoptosis and blood flow direction in human atherosclerotic plaques*. Circulation, 2000. **101**(21): p. 2450-2453.
245. Lesauskaite, V., L. Ivanoviene, and A. Valanciute, *Programmed cellular death and atherogenesis: from molecular mechanisms to clinical aspects*. Medicina (Kaunas), 2003. **39**(6): p. 529-534.
246. Mallat, Z. and A. Tedgui, *Apoptosis in the vasculature: mechanisms and functional importance*. British Journal of Pharmacology, 2000. **130**(5): p. 947-962.
247. Darzynkiewicz, Z., E. Bedner, F. Traganos, and T. Murakami, *Critical aspects in the analysis of apoptosis and necrosis*. Human Cell, 1998. **11**(1): p. 3-12.
248. Asai, K., R.K. Kudej, Y.T. Shen, G.P. Yang, G. Takagi, A.B. Kudej, Y.J. Geng, N. Sato, J.B. Nazareno, D.E. Vatner, F. Natividad, S.P. Bishop, and S.F. Vatner, *Peripheral vascular endothelial dysfunction and apoptosis in old monkeys*. Arteriosclerosis, Thrombosis, and Vascular Biology, 2000. **20**(6): p. 1493-1499.
249. Golden, E.B., I. Pellicciotta, S. Demaria, M.H. Barcellos-Hoff, and S.C. Formenti, *The convergence of radiation and immunogenic cell death signaling pathways*. Frontiers in Oncology, 2012. **2**: p. 88.
250. Ziegler, U. and P. Groscurth, *Morphological features of cell death*. News in Physiological Sciences, 2004. **19**: p. 124-128.
251. Libby, P., P.M. Ridker, and A. Maseri, *Inflammation and atherosclerosis*. Circulation, 2002. **105**(9): p. 1135-1143.
252. Juan, W.S., H.W. Lin, Y.H. Chen, H.Y. Chen, Y.C. Hung, S.H. Tai, S.Y. Huang, T.Y. Chen, and E.J. Lee, *Optimal Percoll concentration facilitates flow cytometric analysis for annexin V/propidium iodine-stained ischemic brain tissues*. Cytometry Part A, 2012. **81**(5): p. 400-408.
253. Bacso, Z., R.B. Everson, and J.F. Eliason, *The DNA of annexin V-binding apoptotic cells is highly fragmented*. Cancer Research, 2000. **60**(16): p. 4623-4628.
254. Firsanov, D.V., L.V. Solovjeva, and M.P. Svetlova, *H2AX phosphorylation at the sites of DNA double-strand breaks in cultivated mammalian cells and tissues*. Clinical Epigenetics, 2011. **2**(2): p. 283-297.
255. Eriksson, D. and T. Stigbrand, *Radiation-induced cell death mechanisms*. Tumour Biology, 2010. **31**(4): p. 363-372.
256. Granville, D.J., J.R. Shaw, S. Leong, C.M.Carthy, P. Margaron, D.W. Hunt, and B.M. McManus, *Release of cytochrome c, Bax migration, Bid cleavage, and activation of caspases 2, 3, 6, 7, 8, and 9 during endothelial cell apoptosis*. American Journal of Pathology, 1999. **155**(4): p. 1021-1025.

257. Faheina-Martins, G.V., A.L. da Silveira, M.V. Ramos, L.F. Marques-Santos, and D.A. Araujo, *Influence of fetal bovine serum on cytotoxic and genotoxic effects of lectins in MCF-7 cells*. Journal of Biochemical and Molecular Toxicology, 2011. **25**(5): p. 290-296.
258. Kondo, T., M. Hirose, and K. Kageyama, *Roles of oxidative stress and redox regulation in atherosclerosis*. Journal of atherosclerosis and thrombosis, 2009. **16**(5): p. 532-538.
259. Mikkelsen, R.B. and P. Wardman, *Biological chemistry of reactive oxygen and nitrogen and radiation-induced signal transduction mechanisms*. Oncogene, 2003. **22**(37): p. 5734-5754.
260. Galkina, E. and K. Ley, *Immune and inflammatory mechanisms of atherosclerosis (*)*. Annual Review of Immunology, 2009. **27**: p. 165-197.
261. Elahi, M.M., Y.X. Kong, and B.M. Matata, *Oxidative stress as a mediator of cardiovascular disease*. Oxidative Medicine and Cellular Longevity, 2009. **2**(5): p. 259-269.
262. Baeuerle, P.A. and T. Henkel, *Function and activation of NF-kappa B in the immune system*. Annual Review of Immunology, 1994. **12**: p. 141-179.
263. Spitz, D.R., E.I. Azzam, J.J. Li, and D. Gius, *Metabolic oxidation/reduction reactions and cellular responses to ionizing radiation: a unifying concept in stress response biology*. Cancer and Metastasis Reviews, 2004. **23**(3-4): p. 311-322.
264. Ward, J.F., *DNA damage as the cause of ionizing radiation-induced gene activation*. Radiation Research, 1994. **138**(1 Suppl): p. S85-88.
265. Clutton, S.M., K.M. Townsend, C. Walker, J.D. Ansell, and E.G. Wright, *Radiation-induced genomic instability and persisting oxidative stress in primary bone marrow cultures*. Carcinogenesis, 1996. **17**(8): p. 1633-1639.
266. Narayanan, P.K., E.H. Goodwin, and B.E. Lehnert, *Alpha particles initiate biological production of superoxide anions and hydrogen peroxide in human cells*. Cancer Research, 1997. **57**(18): p. 3963-3971.
267. Morales, A., M. Miranda, A. Sanchez-Reyes, A. Biete, and J.C. Fernandez-Checa, *Oxidative damage of mitochondrial and nuclear DNA induced by ionizing radiation in human hepatoblastoma cells*. International Journal of Radiation Oncology, Biology, Physics, 1998. **42**(1): p. 191-203.
268. Pham, N.A. and D.W. Hedley, *Respiratory chain-generated oxidative stress following treatment of leukemic blasts with DNA-damaging agents*. Experimental Cell Research, 2001. **264**(2): p. 345-352.
269. Ogura, A., S. Oowada, Y. Kon, A. Hirayama, H. Yasui, S. Meike, S. Kobayashi, M. Kuwabara, and O. Inanami, *Redox regulation in radiation-induced cytochrome c release from mitochondria of human lung carcinoma A549 cells*. Cancer Letters, 2009. **277**(1): p. 64-71.
270. Tulard, A., F. Hoffschir, F.H. de Boisferon, C. Luccioni, and A. Bravard, *Persistent oxidative stress after ionizing radiation is involved in inherited radiosensitivity*. Free Radical Biology and Medicine, 2003. **35**(1): p. 68-77.
271. Yoneda, M., K. Katsumata, M. Hayakawa, M. Tanaka, and T. Ozawa, *Oxygen stress induces an apoptotic cell death associated with fragmentation of mitochondrial genome*. Biochemical and Biophysical Research Communications, 1995. **209**(2): p. 723-729.
272. Kam, W.W. and R.B. Banati, *Effects of ionizing radiation on mitochondria*. Free Radical Biology and Medicine, 2013. **65C**: p. 607-619.
273. Azzam, E.I., J.P. Jay-Gerin, and D. Pain, *Ionizing radiation-induced metabolic oxidative stress and prolonged cell injury*. Cancer Letters, 2012. **327**(1-2): p. 48-60.

274. Shoffner, J.M., M.T. Lott, A.S. Voljavec, S.A. Soueidan, D.A. Costigan, and D.C. Wallace, *Spontaneous Kearns-Sayre/chronic external ophthalmoplegia plus syndrome associated with a mitochondrial DNA deletion: a slip-replication model and metabolic therapy*. Proceedings of the National Academy of Sciences of the United States of America, 1989. **86**(20): p. 7952-7956.
275. Cortopassi, G.A., D. Shibata, N.W. Soong, and N. Arnheim, *A pattern of accumulation of a somatic deletion of mitochondrial DNA in aging human tissues*. Proceedings of the National Academy of Sciences of the United States of America, 1992. **89**(16): p. 7370-7374.
276. Obara-Moszynska, M., J. Maceluch, W. Bobkowski, A. Baszko, O. Jaremba, M.R. Krawczynski, and M. Niedziela, *A novel mitochondrial DNA deletion in a patient with Kearns-Sayre syndrome: a late-onset of the fatal cardiac conduction deficit and cardiomyopathy accompanying long-term rGH treatment*. BMC Pediatrics, 2013. **13**: p. 27.
277. Reichmann, H., F. Degoul, R. Gold, B. Meurers, U.P. Ketelsen, J. Hartmann, C. Marsac, and P. Lestienne, *Histological, enzymatic and mitochondrial DNA studies in patients with Kearns-Sayre syndrome and chronic progressive external ophthalmoplegia*. European Neurology, 1991. **31**(2): p. 108-113.
278. Botto, N., S. Berti, S. Manfredi, A. Al-Jabri, C. Federici, A. Clerico, E. Ciofini, A. Biagini, and M.G. Andreassi, *Detection of mtDNA with 4977 bp deletion in blood cells and atherosclerotic lesions of patients with coronary artery disease*. Mutation Research, 2005. **570**(1): p. 81-88.
279. Santos, J.H., J.N. Meyer, B.S. Mandavilli, and B. Van Houten, *Quantitative PCR-based measurement of nuclear and mitochondrial DNA damage and repair in mammalian cells*. Methods in Molecular Biology, 2006. **314**: p. 183-199.
280. *MITOMAP: A Human Mitochondrial Genome Database*. 2013 [cited; Available from: <http://www.mitomap.org/>.]
281. Korystov, Y.N., *About the role of extracellular radiation-induced oxidants in cell oxidative stress at irradiation determined with the dichlorofluorescein assay*. Radiation Research, 2008. **170**(3): p. 407-408.
282. Hafer, K., K.S. Iwamoto, and R.H. Schiestl, *Refinement of the dichlorofluorescein assay for flow cytometric measurement of reactive oxygen species in irradiated and bystander cell populations*. Radiation Research, 2008. **169**(4): p. 460-468.
283. Rombouts, C., A. Aerts, M. Beck, W.H. De Vos, P. Van Oostveldt, B.M. Abderrafi, and S. Baatout, *Differential response to acute low dose radiation in primary and immortalized endothelial cells*. International Journal of Radiation Biology, 2013. **89**(10): p. 841-850.
284. Wardman, P., *Use of the dichlorofluorescein assay to measure "reactive oxygen species"*. Radiation Research, 2008. **170**(3): p. 406-407.
285. Mukhopadhyay, P., M. Rajesh, K. Yoshihiro, G. Hasko, and P. Pacher, *Simple quantitative detection of mitochondrial superoxide production in live cells*. Biochemical and Biophysical Research Communications, 2007. **358**(1): p. 203-208.
286. Kumarathanan, P., R. Vincent, E. Blais, A. Saravanamuthu, P. Gupta, H. Wyatt, R. Mitchel, M. Hannan, A. Trivedi, and S. Whitman, *Cardiovascular changes in atherosclerotic ApoE-deficient mice exposed to Co60 (gamma) radiation*. PLoS One. 2013. **8**(6): p. e65486.
287. Sangsuwan, T. and S. Haghdoost, *The nucleotide pool, a target for low-dose gamma-ray-induced oxidative stress*. Radiation Research, 2008. **170**(6): p. 776-783.
288. Ma, Z.C., Q. Hong, Y.G. Wang, H.L. Tan, C.R. Xiao, Q.D. Liang, B.L. Zhang, and Y. Gao, *Ferulic acid protects human umbilical vein endothelial cells from radiation*

- induced oxidative stress by phosphatidylinositol 3-kinase and extracellular signal-regulated kinase pathways*. *Biological and Pharmaceutical Bulletin*, 2010. **33**(1): p. 29-34.
289. Franco, R., M.I. Panayiotidis, and J.A. Cidlowski, *Glutathione depletion is necessary for apoptosis in lymphoid cells independent of reactive oxygen species formation*. *Journal of Biology & Chemistry*, 2007. **282**(42): p. 30452-30465.
290. Bleeke, T., H. Zhang, N. Madamanchi, C. Patterson, and J.E. Faber, *Catecholamine-induced vascular wall growth is dependent on generation of reactive oxygen species*. *Circulation Research*, 2004. **94**(1): p. 37-45.
291. Ota, M., H. Fukushima, J.K. Kulski, and H. Inoko, *Single nucleotide polymorphism detection by polymerase chain reaction-restriction fragment length polymorphism*. *Nature Protocols*, 2007. **2**(11): p. 2857-2864.
292. Kobashigawa, S., K. Suzuki, and S. Yamashita, *Ionizing radiation accelerates Drp1-dependent mitochondrial fission, which involves delayed mitochondrial reactive oxygen species production in normal human fibroblast-like cells*. *Biochemical and Biophysical Research Communications*, 2011. **414**(4): p. 795-800.
293. Zhang, B., M.M. Davidson, H. Zhou, C. Wang, W.F. Walker, and T.K. Hei, *Cytoplasmic Irradiation Results in Mitochondrial Dysfunction and DRP1-Dependent Mitochondrial Fission*. *Cancer Research*, 2013. **73**(22): p. 6700-6710.
294. Hendry, J.H., S.L. Simon, A. Wojcik, M. Sohrabi, W. Burkart, E. Cardis, D. Laurier, M. Tirmarche, and I. Hayata, *Human exposure to high natural background radiation: what can it teach us about radiation risks?* *Journal of Radiological Protection*, 2009. **29**(2A): p. A29-42.
295. McGeoghegan, D., K. Binks, M. Gillies, S. Jones, and S. Whaley, *The non-cancer mortality experience of male workers at British Nuclear Fuels plc, 1946-2005*. *International Journal of Epidemiology*, 2008. **37**(3): p. 506-518.
296. Baker, J.E., J.E. Moulder, and J.W. Hopewell, *Radiation as a risk factor for cardiovascular disease*. *Antioxidants & Redox Signaling*, 2011. **15**(7): p. 1945-1956.
297. Wang, J.C. and M. Bennett, *Aging and atherosclerosis: mechanisms, functional consequences, and potential therapeutics for cellular senescence*. *Circulation Research*, 2012. **111**(2): p. 245-259.
298. Fridman, A.L. and M.A. Tainsky, *Critical pathways in cellular senescence and immortalization revealed by gene expression profiling*. *Oncogene*, 2008. **27**(46): p. 5975-5987.
299. Wass, J.A., *A quick introduction to genomics software: Partek Genomics Suite could see much wider future distribution*, in *Scientific Computing*. 2006.
300. Mao, R., X. Wang, E.L. Spitznagel, Jr., L.P. Frelin, J.C. Ting, H. Ding, J.W. Kim, I. Ruczinski, T.J. Downey, and J. Pevsner, *Primary and secondary transcriptional effects in the developing human Down syndrome brain and heart*. *Genome Biology* 2005. **6**(13): p. R107.
301. Technology, B.I.M.I.o., *Gene Set Enrichment Analysis: User guide*. 2010.
302. Merico, D., R. Isserlin, O. Stueker, A. Emili, and G.D. Bader, *Enrichment map: a network-based method for gene-set enrichment visualization and interpretation*. *PLoS One*, 2010. **5**(11): p. e13984.
303. Pfaffl, M.W., *A new mathematical model for relative quantification in real-time RT-PCR*. *Nucleic Acids Research*, 2001. **29**(9): p. 6.
304. Shelton, D.N., E. Chang, P.S. Whittier, D. Choi, and W.D. Funk, *Microarray analysis of replicative senescence*. *Current Biology*, 1999. **9**(17): p. 939-945.
305. Kim, K.S., Y.B. Seu, S.H. Baek, M.J. Kim, K.J. Kim, J.H. Kim, and J.R. Kim, *Induction of cellular senescence by insulin-like growth factor binding protein-5*

- through a p53-dependent mechanism. *Molecular Biology of the Cell*, 2007. **18**(11): p. 4543-4552.
306. Jiang, Z. and R. Gentleman, *Extensions to gene set enrichment*. *Bioinformatics*, 2007. **23**(3): p. 306-313.
307. Goeman, J.J. and A. Solari, *Tutorial in biostatistics: multiple hypothesis testing in genomics*. *Statistics in Medicine*, 2014.
308. Mensaert, K., S. Denil, G. Trooskens, W. Van Criekinge, O. Thas, and T. De Meyer, *Next-generation technologies and data analytical approaches for epigenomics*. *Environmental and Molecular Mutagenesis*, 2013. **55**(3): p. 155-170.
309. Smyth, G.K., *limma: Linear Models for Microarray Data*, in *Bioinformatics and Computational Biology Solutions Using R and Bioconductor*, R. Gentleman, et al., Editors. 2006.
310. Tusher, V.G., R. Tibshirani, and G. Chu, *Significance analysis of microarrays applied to the ionizing radiation response*. *Proceedings of the National Academy of Sciences of the United States of America*, 2001. **98**(9): p. 5116-5121.
311. El-Saghire, H., H. Thierens, P. Monsieurs, A. Michaux, C. Vandevoorde, and S. Baatout, *Gene set enrichment analysis highlights different gene expression profiles in whole blood samples X-irradiated with low and high doses*. *International Journal of Radiation Biology*, 2013. **89**(8): p. 628-638.
312. Spyridopoulos, I., P. Mayer, K.S. Shook, D.I. Axel, R. Viebahn, and K.R. Karsch, *Loss of cyclin A and G1-cell cycle arrest are a prerequisite of ceramide-induced toxicity in human arterial endothelial cells*. *Cardiovascular Research*, 2001. **50**(1): p. 97-107.
313. Yang, G., Y. Xu, X. Chen, and G. Hu, *IFITM1 plays an essential role in the antiproliferative action of interferon-gamma*. *Oncogene*, 2007. **26**(4): p. 594-603.
314. Fujita, M., A. Momose, T. Ohtomo, A. Nishinosono, K. Tanonaka, H. Toyoda, M. Morikawa, and J. Yamada, *Upregulation of fatty acyl-CoA thioesterases in the heart and skeletal muscle of rats fed a high-fat diet*. *Biological and Pharmaceutical Bulletin*, 2011. **34**(1): p. 87-91.
315. Buers, I., O. Hofnagel, A. Ruebel, N.J. Severs, and H. Robenek, *Lipid droplet associated proteins: an emerging role in atherogenesis*. *Histology and Histopathology*, 2011. **26**(5): p. 631-642.
316. Sies, H., *Glutathione and its role in cellular functions*. *Free Radical Biology and Medicine*, 1999. **27**(9-10): p. 916-921.
317. Chen, Y., E. Johansson, Y. Fan, H.G. Shertzer, V. Vasiliou, D.W. Nebert, and T.P. Dalton, *Early onset senescence occurs when fibroblasts lack the glutamate-cysteine ligase modifier subunit*. *Free Radical Biology and Medicine*, 2009. **47**(4): p. 410-418.
318. Hay, N. and N. Sonenberg, *Upstream and downstream of mTOR*. *Genes and Development*, 2004. **18**(16): p. 1926-1945.
319. Laplante, M. and D.M. Sabatini, *mTOR signaling in growth control and disease*. *Cell*, 2012. **149**(2): p. 274-293.
320. Baek, J.Y., D.Y. Jun, D. Taub, and Y.H. Kim, *Characterization of human phosphoserine aminotransferase involved in the phosphorylated pathway of L-serine biosynthesis*. *Biochemical Journal*, 2003. **373**(Pt 1): p. 191-200.
321. Furuya, S., K. Yoshida, Y. Kawakami, J.H. Yang, T. Sayano, N. Azuma, H. Tanaka, S. Kuhara, and Y. Hirabayashi, *Inactivation of the 3-phosphoglycerate dehydrogenase gene in mice: changes in gene expression and associated regulatory networks resulting from serine deficiency*. *Functional and Integrative Genomics*, 2008. **8**(3): p. 235-249.

322. Hermanova, I., M. Zaliova, J. Trka, and J. Starkova, *Low expression of asparagine synthetase in lymphoid blasts precludes its role in sensitivity to L-asparaginase*. *Experimental Hematology*, 2012. **40**(8): p. 657-665.
323. Libby, P., *Inflammation and cardiovascular disease mechanisms*. *American Journal of Clinical Nutrition*, 2006. **83**(2): p. 456S-460S.
324. Molenaar, T.J., J. Twisk, S.A. de Haas, N. Peterse, B.J. Vogelaar, S.H. van Leeuwen, I.N. Michon, T.J. van Berkel, J. Kuiper, and E.A. Biessen, *P-selectin as a candidate target in atherosclerosis*. *Biochemical Pharmacology*, 2003. **66**(5): p. 859-866.
325. Volcik, K.A., D. Catellier, A.R. Folsom, N. Matijevic, B. Wasserman, and E. Boerwinkle, *SELP and SELPLG genetic variation is associated with cell surface measures of SELP and SELPLG: the Atherosclerosis Risk in Communities Carotid MRI Study*. *Clinical Chemistry*, 2009. **55**(6): p. 1076-1082.
326. Braun, J., S.C. Hoffmann, A. Feldner, T. Ludwig, R. Henning, M. Hecker, and T. Korff, *Endothelial cell ephrinB2-dependent activation of monocytes in arteriosclerosis*. *Arteriosclerosis, Thrombosis, and Vascular Biology*, 2011. **31**(2): p. 297-305.
327. Abengozar, M.A., S. de Frutos, S. Ferreira, J. Soriano, M. Perez-Martinez, D. Olmeda, M. Marenchino, M. Canamero, S. Ortega, D. Megias, A. Rodriguez, and J.L. Martinez-Torrecuadrada, *Blocking ephrinB2 with highly specific antibodies inhibits angiogenesis, lymphangiogenesis, and tumor growth*. *Blood*, 2012. **119**(19): p. 4565-4576.
328. Robert, P., M. Canault, C. Farnarier, A. Nurden, C. Grosdidier, V. Barlogis, P. Bongrand, A. Pierres, H. Chambost, and M.C. Alessi, *A novel leukocyte adhesion deficiency III variant: kindlin-3 deficiency results in integrin- and nonintegrin-related defects in different steps of leukocyte adhesion*. *Journal of Immunology*, 2011. **186**(9): p. 5273-5283.
329. Moser, M., M. Bauer, S. Schmid, R. Ruppert, S. Schmidt, M. Sixt, H.V. Wang, M. Sperandio, and R. Fassler, *Kindlin-3 is required for beta2 integrin-mediated leukocyte adhesion to endothelial cells*. *Nature Medicine*, 2009. **15**(3): p. 300-305.
330. Ladenvall, P., S. Nilsson, K. Jood, A. Rosengren, C. Blomstrand, and C. Jern, *Genetic variation at the human tissue-type plasminogen activator (tPA) locus: haplotypes and analysis of association to plasma levels of tPA*. *European Journal of Human Genetics*, 2003. **11**(8): p. 603-610.
331. Vicente, C.P., L. He, and D.M. Tollefsen, *Accelerated atherogenesis and neointima formation in heparin cofactor II deficient mice*. *Blood*, 2007. **110**(13): p. 4261-4267.
332. Aihara, K., *Heparin cofactor II attenuates vascular remodeling in humans and mice*. *Circulation Journal* 2010. **74**(8): p. 1518-1523.
333. Jackson, S.P. and J. Bartek, *The DNA-damage response in human biology and disease*. *Nature*, 2009. **461**(7267): p. 1071-1078.
334. Schneider, L.P., S.; Favaro, R.; Pisata, F.; Roncaglia, P.; Testa, G.; Nicolis, S.K.; Finocchiaro, G.; d'Adda di Fagagna, F., *DNA damage in mammalian neural stem cells leads to astrocytic differentiation mediated by BMP2 signaling through JAK-STAT*. *Stem Cell Reports*, 2013. **1**: p. 123-138.
335. Latini, F.R., J.P. Hemerly, B.C. Freitas, G. Oler, G.J. Riggins, and J.M. Cerutti, *ABI3 ectopic expression reduces in vitro and in vivo cell growth properties while inducing senescence*. *BMC Cancer*, 2011. **11**: p. 11.
336. Favaro, E., K. Bensaad, M.G. Chong, D.A. Tennant, D.J. Ferguson, C. Snell, G. Steers, H. Turley, J.L. Li, U.L. Gunther, F.M. Buffa, A. McIntyre, and A.L. Harris, *Glucose utilization via glycogen phosphorylase sustains proliferation and prevents premature senescence in cancer cells*. *Cell Metabolism*, 2012. **16**(6): p. 751-764.

337. Donninger, H., L. Hesson, M. Vos, K. Beebe, L. Gordon, D. Sidransky, J.W. Liu, T. Schlegel, S. Payne, A. Hartmann, F. Latif, and G.J. Clark, *The Ras effector RASSF2 controls the PAR-4 tumor suppressor*. *Molecular and Cellular Biology*, 2010. **30**(11): p. 2608-2620.
338. Keppler, D., J. Zhang, T. Bihani, and A.W. Lin, *Novel expression of CST1 as candidate senescence marker*. *Journals of Gerontology. Series A, Biological Sciences and Medical Sciences*, 2011. **66**(7): p. 723-731.
339. Beattie, J., G.J. Allan, J.D. Lochrie, and D.J. Flint, *Insulin-like growth factor-binding protein-5 (IGFBP-5): a critical member of the IGF axis*. *Biochemical Journal*, 2006. **395**(1): p. 1-19.
340. Zhan, M. and Z.C. Han, *Phosphatidylinositide 3-kinase/AKT in radiation responses*. *Histology and Histopathology*, 2004. **19**(3): p. 915-923.
341. Grillari, J., O. Hohenwarter, R.M. Grabherr, and H. Katinger, *Subtractive hybridization of mRNA from early passage and senescent endothelial cells*. *Experimental Gerontology*, 2000. **35**(2): p. 187-197.
342. Yan, X., R.C. Baxter, and S.M. Firth, *Involvement of pregnancy-associated plasma protein-A2 in insulin-like growth factor (IGF) binding protein-5 proteolysis during pregnancy: a potential mechanism for increasing IGF bioavailability*. *Journal of Clinical Endocrinology and Metabolism*, 2010. **95**(3): p. 1412-1420.
343. Mittal, S., A. Aslam, R. Doidge, R. Medica, and G.S. Winkler, *The Ccr4a (CNOT6) and Ccr4b (CNOT6L) deadenylase subunits of the human Ccr4-Not complex contribute to the prevention of cell death and senescence*. *Molecular Biology of the Cell*, 2011. **22**(6): p. 748-758.
344. Kletsas, D., H. Pratsinis, G. Mariatos, P. Zacharatos, and V.G. Gorgoulis, *The proinflammatory phenotype of senescent cells: the p53-mediated ICAM-1 expression*. *Annals of the New York Academy of Sciences*, 2004. **1019**: p. 330-332.
345. Zhang, H. and S.N. Cohen, *Smurf2 up-regulation activates telomere-dependent senescence*. *Genes and Development*, 2004. **18**(24): p. 3028-3040.
346. Kong, Y., H. Cui, and H. Zhang, *Smurf2-mediated ubiquitination and degradation of Id1 regulates p16 expression during senescence*. *Aging Cell*, 2011. **10**(6): p. 1038-1046.
347. Kortlever, R.M. and R. Bernards, *Senescence, wound healing and cancer: the PAI-1 connection*. *Cell Cycle*, 2006. **5**(23): p. 2697-2703.
348. West, M.D., J.W. Shay, W.E. Wright, and M.H. Linskens, *Altered expression of plasminogen activator and plasminogen activator inhibitor during cellular senescence*. *Experimental Gerontology*, 1996. **31**(1-2): p. 175-193.
349. Boothman, D.A., M. Wang, and S.W. Lee, *Induction of tissue-type plasminogen activator by ionizing radiation in human malignant melanoma cells*. *Cancer Research*, 1991. **51**(20): p. 5587-5595.
350. Uchida, N., K. Takahashi, T. Kasai, T. Ishida, and H.C. Kwaan, *The concomitant augmentation of urokinase-type plasminogen activator and collagenase-like proteinase activities in X-ray irradiated cells of a human metastatic carcinomatous line*. *Thrombosis Research*, 1994. **74**(6): p. 565-576.
351. Licciulli, S., C. Luise, G. Scafetta, M. Capra, G. Giardina, P. Nuciforo, S. Bosari, G. Viale, G. Mazzarol, C. Tonelli, L. Lanfrancone, and M. Alcalay, *Pirin inhibits cellular senescence in melanocytic cells*. *American Journal of Pathology*, 2011. **178**(5): p. 2397-2406.
352. Boyd, M.A., *A regulatory perspective on whether the system of radiation protection is fit for purpose*. *Annals of the ICRP*, 2012. **41**(3-4): p. 57-63.

353. West, C.M., C.J. Martin, D.G. Sutton, and E.G. Wright, *21st L H Gray Conference: the radiobiology/radiation protection interface*. British Journal of Radiology, 2009. **82**(977): p. 353-362.
354. Averbek, D., *Does scientific evidence support a change from the LNT model for low-dose radiation risk extrapolation?* Health Physics, 2009. **97**(5): p. 493-504.
355. Staton, C.A., M.W. Reed, and N.J. Brown, *A critical analysis of current in vitro and in vivo angiogenesis assays*. International Journal of Experimental Pathology, 2009. **90**(3): p. 195-221.
356. Rubin, D.B., *The radiation biology of the vascular endothelium*. 1998: CRC Press LLC.
357. Sonveaux, P., A. Brouet, X. Havaux, V. Gregoire, C. Dessy, J.L. Balligand, and O. Feron, *Irradiation-induced angiogenesis through the up-regulation of the nitric oxide pathway: implications for tumor radiotherapy*. Cancer Research, 2003. **63**(5): p. 1012-1019.
358. Annabi, B., Y.T. Lee, C. Martel, A. Pilorget, J.P. Bahary, and R. Beliveau, *Radiation induced-tubulogenesis in endothelial cells is antagonized by the antiangiogenic properties of green tea polyphenol (-) epigallocatechin-3-gallate*. Cancer Biology and Therapy, 2003. **2**(6): p. 642-649.
359. Sofia Vala, I., L.R. Martins, N. Imaizumi, R.J. Nunes, J. Rino, F. Kuonen, L.M. Carvalho, C. Ruegg, I.M. Grillo, J.T. Barata, M. Mareel, and S.C. Santos, *Low doses of ionizing radiation promote tumor growth and metastasis by enhancing angiogenesis*. PLoS One. **5**(6): p. e11222.
360. Khurana, R., M. Simons, J.F. Martin, and I.C. Zachary, *Role of angiogenesis in cardiovascular disease: a critical appraisal*. Circulation, 2005. **112**(12): p. 1813-1824.
361. Imaizumi, N., Y. Monnier, M. Hegi, R.O. Mirimanoff, and C. Ruegg, *Radiotherapy suppresses angiogenesis in mice through TGF-betaRI/ALK5-dependent inhibition of endothelial cell sprouting*. PLoS One, 2010. **5**(6): p. e11084.
362. Beels, L., K. Bacher, D. De Wolf, J. Werbrouck, and H. Thierens, *gamma-H2AX foci as a biomarker for patient X-ray exposure in pediatric cardiac catheterization: are we underestimating radiation risks?* Circulation, 2009. **120**(19): p. 1903-1909.
363. Bouquet, F., C. Muller, and B. Salles, *The loss of gammaH2AX signal is a marker of DNA double strand breaks repair only at low levels of DNA damage*. Cell Cycle, 2006. **5**(10): p. 1116-1122.
364. Beels, L., J. Werbrouck, and H. Thierens, *Dose response and repair kinetics of gamma-H2AX foci induced by in vitro irradiation of whole blood and T-lymphocytes with X- and gamma-radiation*. International Journal of Radiation Biology, 2010. **86**(9): p. 760-768.
365. Grudzenski, S., A. Raths, S. Conrad, C.E. Rube, and M. Lobrich, *Inducible response required for repair of low-dose radiation damage in human fibroblasts*. Proceedings of the National Academy of Sciences of the United States of America, 2010. **107**(32): p. 14205-14210.
366. Schofield, P. and J. Garcia-Bernardo, *Chapter 22: Radiation, oxidative stress and senescence; the vascular endothelial cell as a common target*, in *Multiple stressors: A Challenge for the Future*, C. Mothersill, Editor. 2007, Springer. p. 325-334.
367. Kumar, S. and S. Gupta, *Thymosin beta 4 prevents oxidative stress by targeting antioxidant and anti-apoptotic genes in cardiac fibroblasts*. PLoS One, 2011. **6**(10): p. e26912.

368. Lee, R., M. Margaritis, K.M. Channon, and C. Antoniades, *Evaluating oxidative stress in human cardiovascular disease: methodological aspects and considerations*. Current Medicinal Chemistry, 2012. **19**(16): p. 2504-2520.
369. Meyer, A.J. and T.P. Dick, *Fluorescent protein-based redox probes*. Antioxidants & Redox Signaling, 2010. **13**(5): p. 621-650.
370. Lukyanov, K.A. and V.V. Belousov, *Genetically encoded fluorescent redox sensors*. Biochimica et Biophysica Acta, 2013. **1840**(2): p. 745-756.
371. Fliedner, T.M., D. Graessle, C. Paulsen, and K. Reimers, *Structure and function of bone marrow hemopoiesis: mechanisms of response to ionizing radiation exposure*. Cancer Biotherapy & Radiopharmaceuticals, 2002. **17**(4): p. 405-426.
372. Ishizaki, K., Y. Hayashi, H. Nakamura, Y. Yasui, K. Komatsu, and A. Tachibana, *No induction of p53 phosphorylation and few focus formation of phosphorylated H2AX suggest efficient repair of DNA damage during chronic low-dose-rate irradiation in human cells*. Journal of Radiation Research, 2004. **45**(4): p. 521-525.
373. Amundson, S.A., R.A. Lee, C.A. Koch-Paiz, M.L. Bittner, P. Meltzer, J.M. Trent, and A.J. Fornace Jr., *Differential responses of stress genes to low dose-rate gamma irradiation*. Molecular Cancer Research, 2003. **1**: p. 445-452.
374. Aoki-Kinoshita, K.F. and M. Kanehisa, *Gene annotation and pathway mapping in KEGG*. Methods in Molecular Biology, 2007. **396**: p. 71-91.
375. Ashburner, M., C.A. Ball, J.A. Blake, D. Botstein, H. Butler, J.M. Cherry, A.P. Davis, K. Dolinski, S.S. Dwight, J.T. Eppig, M.A. Harris, D.P. Hill, L. Issel-Tarver, A. Kasarskis, S. Lewis, J.C. Matese, J.E. Richardson, M. Ringwald, G.M. Rubin, and G. Sherlock, *Gene ontology: tool for the unification of biology. The Gene Ontology Consortium*. Nature Genetics, 2000. **25**(1): p. 25-29.
376. Dignat-George, F. and C.M. Boulanger, *The many faces of endothelial microparticles*. Arteriosclerosis, Thrombosis, and Vascular Biology, 2011. **31**(1): p. 27-33.
377. Chironi, G.N., C.M. Boulanger, A. Simon, F. Dignat-George, J.M. Freyssinet, and A. Tedgui, *Endothelial microparticles in diseases*. Cell and Tissue Research, 2009. **335**(1): p. 143-151.
378. Horstman, L.L., W. Jy, J.J. Jimenez, and Y.S. Ahn, *Endothelial microparticles as markers of endothelial dysfunction*. Frontiers in Bioscience, 2004. **9**: p. 1118-1135.
379. Foffa, I., M. Cresci, and M.G. Andreassi, *Health risk and biological effects of cardiac ionising imaging: from epidemiology to genes*. International Journal of Environmental Research and Public Health, 2009. **6**(6): p. 1882-1893.
380. Wrixon, A.D., *New ICRP recommendations*. Journal of radiological protection : official journal of the Society for Radiological Protection, 2008. **28**: p. 161-168.
381. Feinendegen, L.E., M. Pollycove, and C.A. Sondhaus, *Responses to low doses of ionizing radiation in biological systems*. Nonlinearity in Biology, Toxicology and Medicine, 2004. **2**(3): p. 143-171.

Acknowledgments

Here we are, staring at a blank page to write the last part of the thesis, the acknowledgements, which implies I have made it through the PhD. I can honestly say that I never thought to come this far. The fact that I did is thanks to many people for which I want to express my gratitude. Seeing the number of people, I apologize by forehand if I would have forgotten someone.

It all started four years ago during my internship in Southampton when I decided to apply for the PhD position available at the Radiobiology Unit in SCK•CEN in collaboration with Ghent University. I still remember my first visit to the lab where I was warmly welcomed by **Prof. Dr. Sarah Baatout**, who would become my promoter later on. Her enthusiasm and dedication struck me from the very first moment. I found out later that she had, in particular, the magical power to make my many moments of doubt disappear. I am deeply grateful that she had accepted me in the lab as her PhD student. Also, I would like to offer my special thanks to **Dr. An Aerts**, my mentor. Throughout my PhD she has supported me in all the aspects of the PhD work going from the conception of the experiments until the oral and written communication of the results. I would like to thank the members of the thesis committee, **Prof. Dr. Ir. Pascal Boeckx, Prof. Dr. Ir. Tom Van De Wiele, Prof. Dr. Luc Leybaert, Prof. Dr. Ir. Sofie Bekaert, Prof. Dr. Ir. Tim De Meyer, Prof. Dr. Dietrich Averbeck** and **Prof. Dr. Jan Philippé** for their much appreciated constructive comments which have improved greatly the thesis.

From Ghent University I would like to thank **Prof. Dr. Patrick Van Oostveldt** to accept me as a PhD student and for his kind advices throughout the thesis. **Prof. Dr. Winnok De Vos** needs to be thanked for sharing his enormous microscopic knowledge and for his constructive comments of my written work, which were highly appreciated. I should not forget to thank **Sofie De Schynkel** without whom the university would have remained a big administrative labyrinth. Crossing the Belgian borders, I would like to thank the collaborators of the European project in which this PhD was partly embedded, in particular **Prof. Dr. Mats Harms-Ringdahl, Dr. Siamak Haghdoost** and **Dr. Ramesh Yentrapalli**. Not only they have provided much help and assistance in the experiments but they have also provided a pleasant two-week course at Stockholm University.

Returning inside the Belgian borders, back to Mol, I thank my co-mentor **Dr. Rafi Benotmane** for his advices and comments throughout the years. The older generation, **Dr. Louis de Saint-Georges** and **Dr. Paul Jacquet**, are highly appreciated for insightful discussions. Other researchers that deserve great thanks are **Dr. Roel Quintens** and **Dr.**

Pieter Monsieurs to make transcriptomic profiling and statistics less frightening. Also thanks to **Dr. Marjan Moreels** with whom conferences were a nice experience.

Of course, I would have never succeeded this PhD work without all the support from the lab colleagues in SCK•CEN. My first steps in the lab were guided by two ancient PhD students, **Dr. Michael Beck** and **Dr. Khalil Ardat**, who taught me all the little tricks to successfully carry out my experiments. Their kindness made me feel soon at home at the Radiobiology Unit. Furthermore, I am grateful that they were not reluctant to share their great knowledge with me, which has helped me a lot in the conception and interpretation of my results. A great thanks also to **Kevin Tabury** with whom I shared the 'aquarium' office since the beginning. Sadly he decided to leave our office in my last year to get a real office. Not only he was a great support in the lab but more importantly he became a good friend. His big smile was always a great start of the day! **Hanène Badri**, with whom I have spent a nice time in the office, also moved to another desk. Fortunately, the other 'aquarium' residents, **Sandra Condori Catachura** and **Joachim Vandecraen**, stayed and kept the office a very pleasant place to arrive in the morning.

I started my PhD at the same time as **Annelies Suetens**. Although we studied at the same university, we were not aware that we were starting a PhD at the same lab. This was a great surprise which even got better since we became not only colleagues but also friends. We went through the ups and downs of the PhD life together and I could not have imagined a better partner in crime to experience all these moments with. Thanks for being there all these years. At the moments she has started the dreaded writing process as well and I want to wish her all the luck for the last steps! Special thanks to **Hussein El Saghire** who guided me through the complex world of microarrays. Besides this guidance, I appreciated all the nice discussions we had together. Mentioning microarray would be impossible without thanking **Arlette Michaux** and **Ann Janssen** who have helped me a lot with those. Also, I appreciate greatly **Mieke Neefs**, **Liselotte Leysen** and **Jasmine Buset** who make the lab run smoothly.

Thanks to the other PhD students with whom I had a pleasant time: **Marlies Gijs**, **Tom Verbiest** and **Tine Verreet**. Hopefully we will meet soon in Oxford! Also, **Dr. Kristel Mijndonckx**, **Dr. Nada Samari**, **Dr. Giuseppe Pani**, **Matthias D'Huyvetter**, and **Ellina Macaeva** were a delight to have around. All the best for the new arrivals in the lab: **Bjorn Baselet**, **Bo Byloos** and **Merel Van Walleghem**.

Special thanks to **Roel Dillen** who always responded with a smile to my many demands to change tiny details on my posters and cover page.

Of course there is more to life than just work. Therefore I would like to thank all the people who have made my time at Mol unforgettable. A brief stay in the dormitories has resulted in many nice encounters and special friends including **Graham** and **Kerry** (and little **Tyla** ☺). Finishing the PhD would not have been possible without my family. Knowing that you have a warm place to come home to is priceless! Good luck also to my sister **Caroline** since she has decided to follow my footsteps and start a PhD herself. **Jef**, you know what is waiting for you ☺. Special thanks to my friends for providing the necessary distraction: **Caroline Huyskens**, **Manon Engelen** and all the "Ladies at the date" (**Julie**, **Katrien**, **Annelies**, **Evelyn**, **Elise**, **Katia**, **Carolien**, **Nathalie**, **Stéphanie** and **Britt**). Although I'm not in Belgium anymore and I miss you all in France, I know that you will always be there! Finally, we can say that SCK•CEN is indirectly responsible for my encounter with **Grégoire** for which I'm ever grateful. Grégoire, merci pour ton support et ton amour! J'espère qu'on aura une belle vie ensemble!

Curriculum Vitae

Personal details

Last name: Rombouts

First name: Charlotte

Email: romboutscharlotte@gmail.com

Birth date: 03/08/1987

Nationality: Belgian

Education

2010-2014 PhD in Applied Biological Sciences (SCK•CEN – UGent)

2008-2010 Master's degree in Biomedical Sciences (University of Antwerp, Belgium)

2005-2008 Bachelor's degree in Biomedical Sciences (University of Antwerp, Belgium)

1999-2005 Latijn-Wetenschappen (Sint-Lievenscollege, Antwerp, Belgium)

Research

- Molecular and cellular radiobiology: investigation of the endothelium response to low doses of ionizing radiation using fluorescence microscopy, flow cytometry and microarray. Radiobiology Unit, SCK•CEN (Prof. Sarah Baatout) and Department for Molecular Biotechnology (Prof. Patrick Van Oostveldt). This research was carried out to obtain the degree of PhD.
- Investigation of the role of varying lipids in total parenteral nutrition on fatty acid composition of PBMCs and plasma phospholipids and immune responses in healthy volunteers using gas chromatography and flow cytometry. Research performed in the context of an Erasmus internship at the Human Institute of Nutrition, University of Southampton (UK) (Prof. Dr. Philip Calder). This research was carried out to obtain the Master degree in Biomedical Sciences.

Awards

- ERRS travel award to participate in the 14th International congress of Radiation Research, Warsaw, Poland, 28/08-01/09/2011
- ERRS Young Investigator award to participate in the 40th Annual Meeting of the European Radiation Research society in Dublin, Ireland, 1-5/09/2013

Publication list

Peer-reviewed international articles

- **Rombouts C.**, Aerts A., Beck M., De Vos W., Van Oostveldt P., Benotmane R., Baatout S. *Differential response to acute low dose radiation in primary and immortalized endothelial cells*. International Journal of Radiation Biology. 2013 Oct;89(10):841-50.

- Versleijen MW., Roelofs HM., **Rombouts C.**, Hermans PW., Noakes PS., Calder PC., Wanten GJ. *Short-term infusion of a fish oil-based lipid emulsion modulates fatty acid status, but not immune function or (anti)oxidant balance: a randomized cross-over study.* European Journal of Clinical Investigations. 2012 Mar;42(3):290-302
- Acheva A., Aerts A., **Rombouts C.**, Baatout S., Salomaa S., Manda K., Hildebrandt G., Kämäräinen M. *Human 3-D tissue models in radiation biology: current status and future perspectives.* International Journal of Radiation Research. In press.
- Beck M., **Rombouts C.**, Moreels M., Aerts A., Quintens R., Tabury K., Michaux A., Janssen A., Neefs M., Ernst E., Dieriks B., Lee R., De Vos WH., Lambert C., Van Oostveldt P., Baatout S. *Modulation of gene expression of endothelial cells in response to high LET nickel irradiation.* International Journal of Molecular Medicine. In press.
- **Rombouts C.**, Aerts A., Quintens R., Harms-Ringdahl M., Haghdoost S., Janssen A., Michaux A., Yentrapalli R., Benotmane R., Baatout S. *Transcriptomic profiling suggests a role for IGFBP5 in premature senescence of endothelial cells after chronic low dose rate irradiation.* International Journal of Radiation Biology. In press.

National articles

- **Rombouts C.**, Aerts A., Beck M., De Vos W., Vanmarcke H., Van Oostveldt P., Benotmane R., Baatout S. *Low dose radiation response in endothelial cells as biological model for radiation-related cardiovascular risks.* Annalen van de Belgische Vereniging voor Stralingsbescherming - Annales de l'Association Belge de Radioprotection, 2013 Dec;38(3):289-298.

Oral presentations

- **Rombouts C.**, Aerts A., Moreno Talavera N., Van Oostveldt P., Benotmane R., Baatout S. *Oxidative stress and mitochondrial DNA damage in endothelial cells after low dose ionizing radiation exposure.* ERR 2013, Dublin, Ireland, 1-5/09/2013
- **Rombouts C.**, Aerts A., Harms-Ringdahl M., Haghdoost S., Janssen A., Michaux A., Yentrapalli R., Quintens R., de Saint-Georges L., Benotmane R., Baatout S. *Chronic low dose rate γ -irradiation of HUVECs: a high throughput gene expression analysis.* DoReMi 2nd periodic meeting, Paris, France, 22-24/01/2013
- Beck M., **Rombouts C.**, Moreels M., Aerts A., Quintens R., Tabury K., Michaux A., Janssen A., Neefs M., Ernst E., Diericks B., De Vos W., Lambert C., Van Oostveldt P., Baatout S. *Modulation of gene expression of endothelial cells in response to high and low LET irradiation.* 1st BHTC in vitro workshop, Brussels, Belgium, 25/10/2012
- **Rombouts C.**, Aerts A., Beck M., De Vos W., Van Oostveldt P., Benotmane R., Baatout S. *Characterization of the cellular response of the endothelial cell lines, HUVEC and EA.hy926, following exposure to low dose acute X-irradiation.* 39th Annual Meeting of the European Radiation Research Society. Vietri sul Mare, Italy, 15-19/10/2012
- **Rombouts C.** *Cardiovascular effects related to low doses of radiation.* Day of the PhD's, Mol, Belgium, 27/04/2012
- **Rombouts C.** *The endothelium response to low doses of radiation.* Seminars in Radiobiology, Mol, Belgium, 6/02/2012
- **Rombouts C.**, Aerts A., Beck M., Tabury K., De Vos W., Benotmane M.A., Van Oostveldt P., Baatout S. *DoReMi task 7.3: SCK•CEN contribution on "Feasibility study towards a systems*

biology approach of radiation response of the endothelium". DoReMi 1st periodic meeting, Brussels, Belgium, 05/07/2011

- **Rombouts C.**, Aerts A. *Comparison of the immortalized endothelial cell line EA.hy926 with primary HUVEC*. Seminars in Radiobiology, Mol, Belgium, 24/01/2011

Poster presentations

- **Rombouts C.**, Aerts A., Beck M., De Vos W., Talavera Moreno N., Benotmane R., Van Oostveldt P., Baatout S. *Cardiovascular risk related to low doses of ionizing radiation: the endothelial response*. PhD Day, Mol, Belgium, 23/10/2013
- **Rombouts C.**, Aerts A., Harms-Ringdahl M., Haghdoost S., Janssen A., Michaux A., Yentrapalli R., Quintens R., Benotmane R., Baatout S. *Chronic low dose rate γ -irradiation induces premature senescence in Primary Human Umbilical Vein Endothelial Cells (HUVEC): high throughput gene expression profiling*. Fifth International MELODI Workshop, Brussels, Belgium, 07-10/10/2013
- **Rombouts C.**, Aerts A., Moreno Talavera N., Van Oostveldt P., Benotmane R., Baatout S. *Oxidative stress and mitochondrial DNA damage in endothelial cells after low dose ionizing radiation exposure*. ERR 2013, Dublin, Ireland, 1-5/09/2013
- Beck M., **Rombouts C.**, Moreels M., Aerts A., Quintens R., Tabury K., Michaux A., Janssen A., Neefs M., Ernst E., Diericks B., Lee R., De Vos W., Lambert C., Van Oostveldt P., Baatout S. *Modulation of gene expression of endothelial cells in response to high-LET nickel irradiation*. 19th IAA Humans in Space Symposium 2013. Keulen, Germany, 7-12/07/2013
- Beck M., **Rombouts C.**, Moreels M., Aerts A., Quintens R., Tabury K., Michaux A., Janssen A., Neefs M., Ernst E., Diericks B., Lee R., De Vos W., Lambert C., Van Oostveldt P., Baatout S. *Modulation of gene expression of endothelial cells in response to high-LET nickel irradiation*. HITSRS2013, Chiba, Japan, 15/05/2013
- **Rombouts C.**, Aerts A., Beck M., Tabury K., De Vos W., Benotmane R., Van Oostveldt P., Baatout S. *Comparison of the low dose ionizing radiation response of the primary Human Umbilical Vein Endothelial Cells (HUVEC) and the immortalized endothelial cell line EA.hy926*. International Symposium on the occasion of the 50th anniversary of the Belgian Association for Radiological Protection, Brussels, Belgium, 8-10/04/2013
- **Rombouts C.**, Aerts A., Harms-Ringdahl M., Haghdoost S., Janssen A., Michaux A., Yentrapalli R., Quintens R., de Saint-Georges L., Benotmane R., Baatout S. *Transcriptomic analysis after chronic low dose rate γ -irradiation of primary Human Umbilical Vein Endothelial Cells (HUVECs)*. International Symposium on the occasion of the 50th anniversary of the Belgian Association for Radiological Protection, Brussels, Belgium, 8-10/04/2013
- **Rombouts C.**, Aerts A., Beck M., De Vos W., Benotmane R., Van Oostveldt P., Baatout S. *The endothelium response to low dose ionizing radiation*. DoReMi 2nd Periodic Meeting, Paris, France, 22-24/01/2013
- **Rombouts C.**, Aerts A., Harms-Ringdahl M., Haghdoost S., Janssen A., Michaux A., Yentrapalli R., Quintens R., de Saint-Georges L., Benotmane R., Baatout S. *Chronic low dose rate γ -irradiation of Human Umbilical Vein Endothelial Cells: a high throughput gene expression analysis*. 39th Annual Meeting of the European Radiation Research Society, Vietri sul Mare, Italy, 15-19/10/2012

- **Rombouts C.**, Aerts A., Beck M., Tabury K., De Vos W., Benotmane R., Van Oostveldt P., Baatout S. *The endothelium response to low dose ionizing radiation*. MELODI-2012, Helsinki, Finland, 12-14/09/2012
- **Rombouts C.**, Aerts A., Beck M., Tabury K., De Vos W., Benotmane R., Van Oostveldt P., Baatout S. *Assessment of DNA damage, apoptosis and cell cycle changes in endothelial cells after low dose X-irradiation*. Association for Radiation Research Annual Conference, Brunel, United Kingdom, 25-27/06/2012
- **Rombouts C.**, Aerts A., Beck M., Tabury K., De Vos W., Benotmane R., Van Oostveldt P., Baatout S. *The endothelium response to low dose ionizing radiation*. Radiation Science in the Netherlands, 2nd Symposium, Noordwijkerhout, Netherlands, 19-20/04/2012
- **Rombouts C.**, Aerts A., Beck M., Tabury K., De Vos W., Benotmane R., Van Oostveldt P., Baatout S. *Low dose research on cardiovascular risks at SCK•CEN*. Third MELODI Workshop, Rome, Italy, 2-4/11/2011
- **Rombouts C.**, Aerts A., Beck M., Tabury K., De Vos W., Benotmane R., Van Oostveldt P., Baatout S. *Non-cancer effects (and in particular cardiovascular effects) related to low doses of radiation*. PhD day, Mol, Belgium, 06/10/2011
- **Rombouts C.**, Aerts A., Beck M., Tabury T., De Vos W., Benotmane R., Van Oostveldt P., Baatout S. *Assessment of DNA damage, apoptosis and cell cycle changes in HUVECs and EA.hy926 cells after low dose X-irradiation*. 14th International congress of radiation research, Warsaw, Poland, 28/08-01/09/2011
- **Rombouts C.**, Aerts A., Beck M., Tabury K., De Vos W., Benotmane M.A., Van Oostveldt P., Baatout S. *DoReMi task 7.3: SCK•CEN contribution on "Feasibility study towards a systems biology approach of radiation response of the endothelium"*. DoReMi 1st periodic meeting, Brussels, Belgium, 05/07/2011
- **Rombouts C.**, Aerts A., Beck M., Tabury K., De Vos W., Benotmane M.A., Van Oostveldt P., Baatout S. *Biological and molecular mechanisms of vascular damage after low dose X-irradiation*. CARDIORISK symposium, Munich, Germany, 07/06/2011

Contribution to contract reports

- **Rombouts C.**, Aerts A., Quintens R., Michaux A., Janssen A., Tabury K., Beck M., Benotmane R., Baatout S. *Feasibility study towards a systems biology approach of radiation response of the endothelium. DoReMi Task 7.3: Work performed by SCK•CEN from January 2011 to December 2012*. 19/12/2012
- **Rombouts C.**, Aerts A., Quintens R., Michaux A., Tabury K., Beck M., Benotmane R., Baatout S. *Feasibility study towards a systems biology approach of radiation response of the endothelium. Report Task 7.3.: Work performed by SCK•CEN from January 2010 to December 2011*. 19/12/2011
- Baatout S., Abouelaradat K., Aerts A., Benotmane M.A., Derradji H., el-Saghire H., Jacquet P., Quintens R., **Rombouts C.**, Beck M., de Saint-Georges L., Impens N., Monsieurs P., Samari N. *FP7 EU DoReMi annual activity report 2011*. 24/07/2011
- Baatout S., Benotmane M.A., Abouelaradat K., Aerts A., Beck M., de Saint-Georges L., Derradji H., Jacquet P., Monsieurs P., Quintens R., **Rombouts C.**, Samari N. *FP7 EU DoReMi annual activity report 2010*. 29/01/2011

Courses followed

- European Master CELOD course (Cellular effects of low doses and low-dose rates with focus on DNA damage and stress response), Stockholm, Sweden, 28/03 – 08/04/2011
- Cursus Stralingsbescherming, International school for Radiation Protection, SCK•CEN, Mol, Belgium, 18-23/10/2010

Follow-up of student

- Talavera Moreno N. *Radiation-induced cardiovascular risks: Cardiovascular effects related to low doses of ionizing radiation; endothelial response after low dose X-ray radiation, focusing on oxidative stress and mitochondrial DNA damage*. UGent and ETSIAM (UPV, Valencia, Spain), 2012, Master thesis of Biotechnology

Languages

- Dutch: mother tongue
- English: fluently written and spoken
- French: good